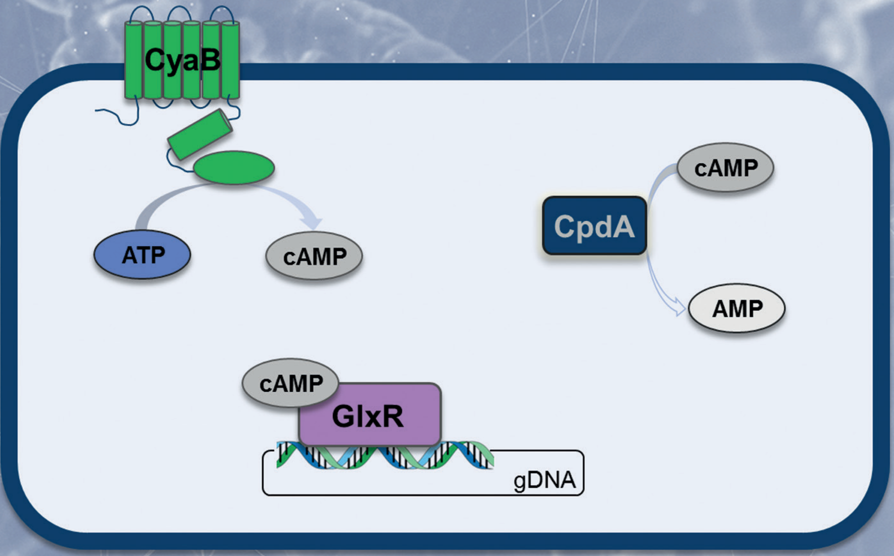

Studies on the cAMP-responsive regulatory network of *Corynebacterium glutamicum*

Natalie Wolf

Schlüsseltechnologien / Key Technologies
Band / Volume 278
ISBN 978-3-95806-736-3

Mitglied der Helmholtz-Gemeinschaft

JÜLICH
Forschungszentrum

Schriften des Forschungszentrums Jülich
Reihe Schlüsseltechnologien / Key Technologies Band / Volume 278

Forschungszentrum Jülich GmbH
Institut für Bio- und Geowissenschaften (IBG)
Biotechnologie (IBG-1)

Studies on the cAMP-responsive regulatory network of *Corynebacterium glutamicum*

Natalie Wolf

Schriften des Forschungszentrums Jülich
Reihe Schlüsseltechnologien / Key Technologies Band / Volume 278

ISSN 1866-1807 ISBN 978-3-95806-736-3

Bibliografische Information der Deutschen Nationalbibliothek.
Die Deutsche Nationalbibliothek verzeichnet diese Publikation in der
Deutschen Nationalbibliografie; detaillierte Bibliografische Daten
sind im Internet über http://dnb.d-nb.de abrufbar.

Herausgeber und Vertrieb: Forschungszentrum Jülich GmbH
Zentralbibliothek, Verlag
52425 Jülich
Tel.: +49 2461 61-5368
Fax: +49 2461 61-6103
zb-publikation@fz-juelich.de
www.fz-juelich.de/zb

Umschlaggestaltung: Grafische Medien, Forschungszentrum Jülich GmbH

Druck: Grafische Medien, Forschungszentrum Jülich GmbH

Schriften des Forschungszentrums Jülich
Reihe Schlüsseltechnologien / Key Technologies, Band / Volume 278

D 61 (Diss. Düsseldorf, Univ., 2023)

ISSN 1866-1807
ISBN 978-3-95806-736-3

Vollständig frei verfügbar über das Publikationsportal des Forschungszentrums Jülich (JuSER)
unter www.fz-juelich.de/zb/openaccess.

Results described in this dissertation have been published in the following original publication or are described in a manuscript that will be submitted for publication:

Wolf N., Bussmann M., Koch-Koerfges A., Katcharava N., Schulte J., Polen T., Hartl J., Vorholt J.A., Baumgart M. and Bott M. (2020). Molecular basis of growth inhibition by acetate of an adenylate cyclase-deficient mutant of *Corynebacterium glutamicum. Front Microbiol 11*(87). doi: 10.3389/fmicb.2020.00087

Wolf N., Lehmann L., Filipchyk A., Polen T., Bussmann M., Baumgart M. and Bott M. (2023). Comparison of *in vivo* GlxR binding in *Corynebacterium glutamicum* ATCC 13032 and the adenylate cyclase deletion mutant Δ*cyaB* using ChAP-Seq*. To be submitted.*

Table of contents

Summary

Cyclic adenosine monophosphate (cAMP) is one of the best studied signalling molecules. In prokaryotes, the molecule was shown to be involved in numerous processes, such as metabolism, motility, and virulence. In the Gram-positive actinobacterium *Corynebacterium glutamicum*, cAMP serves as an effector for the global transcriptional regulator GlxR, a homolog of Crp of *Escherichia coli*. Enzymes responsible for the synthesis and degradation of cAMP in *C. glutamicum* are the membrane-bound adenylate cyclase CyaB and the cytoplasmic phosphodiesterase CpdA, respectively. In this study, the consequences of decreased intracellular cAMP levels of a *cyaB* deletion mutant (Δ*cyaB*) were investigated. The main objectives were (i) to characterize the physiological differences between the Δ*cyaB* mutant and the wild-type strain and (ii) to investigate the effects of a low cAMP level on GlxR-DNA interactions *in vivo*. The following results were obtained:

(i) The lack of the adenylate cyclase CyaB led to a growth defect of *C. glutamicum* when acetate was present in the medium. The acetate sensitivity of the Δ*cyaB* mutant could be reversed by plasmid-based *cyaB* expression or supplementation of the medium with cAMP, showing that indeed the low intracellular cAMP level in the Δ*cyaB* mutant was the reason for this acetate sensitivity. The acetate effect was concentration- and pH-dependent, suggesting a link to the uncoupling activity of acetate. In agreement, the Δ*cyaB* mutant displayed an increased sensitivity to the protonophore carbonyl cyanide *m*-chlorophenyl hydrazone (CCCP). The increased uncoupler sensitivity correlated with a lowered membrane potential of acetate-grown Δ*cyaB* cells compared to wild-type cells. Transcriptome analyses and RT-qPCR experiments showed that the genes encoding the cytochrome bc_1-aa_3 supercomplex and the F_1F_O-ATP synthase, previously shown to be activated by GlxR, had a decreased expression in the Δ*cyaB* mutant. Since the cytochrome bc_1-aa_3 supercomplex is the major provider of proton-motive force in *C. glutamicum*, decreased expression of its genes in the Δ*cyaB* mutant was assumed to be mainly responsible for the deficits in energy metabolism and the higher sensitivity to uncouplers. During cultivations of Δ*cyaB* mutant with acetate, a suppressor mutant was identified which had lost the acetate sensitivity. Genome sequence analysis revealed a single mutation in the suppressor strain causing the amino acid exchange Ala131Thr in GlxR. Introduction of this point mutation into the original Δ*cyaB* mutant abolished the growth defect on acetate, supporting the importance of GlxR for the phenotype of the Δ*cyaB* mutant and for the control of energy metabolism.

(ii) The influence of a lowered cAMP level on GlxR-DNA interaction *in vivo* was studied by ChAP-Seq experiments with the wild type and Δ*cyaB* mutant grown either on glucose or on glucose plus acetate. Analysis of the four data sets identified 243 GlxR peaks with an enrichment factor (EF) of ≥3 in at least one data set. *De novo* motif search identified the consensus sequence $TGTGN_8CACA$ in 242 of the GlxR peaks. 141 of these peaks were also reported in previous studies, whereas 102 represent novel binding sites. Remarkably, the majority of the 243 GlxR binding sites were found to be enriched in all four data sets when using an EF ≥1.5 as cutoff. These results show that the strongly diminished or completely absent cAMP level in the Δ*cyaB* mutant reduced GlxR binding, particularly in the presence of acetate, but did not prevent it. This suggests that GlxR binding to its target sites *in vivo* is less dependent on cAMP than GlxR binding *in vitro* and that additional, yet unknown factors might be involved in the control of GlxR-binding to DNA within the cell.

Zusammenfassung

Zyklisches Adenosinmonophosphat (cAMP) ist eines der am besten untersuchten Signalmoleküle. In Prokaryonten ist das Molekül an zahlreichen Prozessen beteiligt, z. B. am Stoffwechsel, an der Motilität und an der Virulenz. Im Gram-positiven Actinobakterium *Corynebacterium glutamicum* dient cAMP als Effektor für den globalen Transkriptionsregulator GlxR, ein Homolog von Crp aus *Escherichia coli*. Die für Synthese und Abbau von cAMP verantwortlichen Enzyme sind in *C. glutamicum* die membrangebundene Adenylatzyklase CyaB bzw. die zytoplasmatische Phosphodiesterase CpdA. In dieser Studie wurden die Folgen eines verminderten intrazellulären cAMP-Spiegels einer *cyaB*-Deletionsmutante (Δ*cyaB*) untersucht. Hauptziele waren (i) die Charakterisierung der physiologischen Unterschiede zwischen der Δ*cyaB*-Mutante und dem Wildtyp-Stamm und (ii) die Untersuchung der Auswirkungen eines niedrigen cAMP-Spiegels auf GlxR-DNA-Interaktionen *in vivo*. Die folgenden Ergebnisse wurden erzielt:

(i) Das Fehlen von CyaB führte zu einem Wachstumsdefekt in Gegenwart von Acetat, der durch plasmidbasierte *cyaB*-Expression oder Supplementierung des Mediums mit cAMP aufgehoben werden konnte. Der Acetat-Effekt war konzentrations- und pH-abhängig, was auf einen Zusammenhang mit der Entkoppleraktivität von Acetat hindeutete. In Übereinstimmung damit besaß die Δ*cyaB*-Mutante eine erhöhte Sensitivität gegenüber dem Protonophor Carbonylcyanid *m*-Chlorphenylhydrazon (CCCP) sowie bei Wachstum in Gegenwart von Acetat ein niedrigeres Membranpotential als der Wildtyp. Transkriptom- und RT-qPCR-Analysen zeigten, dass die Expression der durch GlxR aktivierten Gene für den Cytochrom-bc_1-aa_3-Superkomplex in der Δ*cyaB*-Mutante verringert war. Da der Superkomplex der Hauptlieferant der protonen-motorischen Kraft in *C. glutamicum* ist, wurde eine verringerte Expression seiner Gene als Hauptursache für die Acetat- und Entkoppler-Sensitivität der Δ*cyaB*-Mutante postuliert. Bei der Kultivierung der Δ*cyaB*-Mutante mit Acetat wurde eine Suppressor-Mutante identifiziert, die die Acetat-Empfindlichkeit verloren hatte. Die Genomsequenzanalyse ergab eine einzige Mutation in dem Suppressorstamm, die den Aminosäureaustausch Ala131Thr in GlxR verursachte. Durch Einführung dieser Punktmutation in das Genom der parentalen Δ*cyaB*-Mutante wurde der Wachstumsdefekt auf Acetat wiederhergestellt, was die Bedeutung von GlxR für den Phänotyp der Δ*cyaB*-Mutante und die Kontrolle des Energiestoffwechsels belegt.

(ii) Der Einfluss eines verringerten cAMP-Spiegels auf die GlxR-DNA-Interaktion *in vivo* wurde durch ChAP-Seq-Experimente mit dem Wildtyp und der Δ*cyaB*-Mutante untersucht, die entweder auf Glukose oder auf Glukose plus Acetat kultiviert wurden. Die Analyse der vier Datensätze ergab 243 GlxR-Peaks mit einem Anreicherungsfaktor (AF) von ≥3 in mindestens einem Datensatz. Die *de novo* Motivsuche identifizierte die Konsensussequenz TGTGN$_8$CACA in 242 der GlxR-Peaks. 141 dieser Peaks wurden auch in früheren Studien gefunden, während 102 Peaks neue Bindungsstellen repräsentieren. Bemerkenswert ist, dass die meisten der 243 GlxR-Bindungsstellen in allen vier Datensätzen angereichert waren, wenn ein AF ≥1,5 als Grenzwert verwendet wurde. Die Ergebnisse zeigen, dass der stark verringerte oder völlig fehlende cAMP-Spiegel in der Δ*cyaB*-Mutante die GlxR-Bindung, insbesondere in Gegenwart von Acetat, reduzierte, aber nicht verhinderte. Dies deutet darauf hin, dass die GlxR-Bindung *in vivo* weniger cAMP-abhängig ist als die GlxR-Bindung *in vitro* und dass zusätzliche, noch unbekannte Faktoren an der Kontrolle der GlxR-Bindung an die DNA innerhalb der Zelle beteiligt sein könnten.

Abbreviations

Δ	Deletion
AC	Adenylate cyclase
AMP	Adenosine monophosphate
ATCC	American Type Culture Collection
ATP	Adenosine triphosphate
bp	Base pairs
BHI	Brain heart infusion
cAMP	Cyclic adenosine monophosphate
CCR	Carbon catabolite repression
CCCP	Carbonyl cyanide *m*-chlorophenyl hydrazone
CDW	Cell dry weight
cGMP	Cyclic guanosine monophosphate
ChAP-Seq	Chromatin affinity purification combined with DNA sequencing
CHD	Cyclase homology domain
ChIP-Seq	Chromatin immunoprecipitation combined with DNA sequencing
CRP	cAMP receptor protein
Da	Dalton
EIA	Enzyme immunoassay
ELISA	Enzyme-linked immunosorbent assay
EMSA	Electrophoretic mobility shift assay
HAMP	Histidine kinases, adenylate cyclases, methyl accepting proteins and phosphatases
ITC	Isothermal titration calorimetry
Kan^R	Kanamycin resistant
K_d	Dissociation constant
K_m	Michaelis constant
LB	Lysogeny broth
M	Molar (mol/l)
OD_{600}	Optical density at 600 nm
PDE	Phosphodiesterase
PEP	Phosphoenolpyruvate
(p)ppGpp	Guanosine pentaphosphate/tetraphosphate
PTS	Phosphotransferase system
RT-qPCR	Reverse transcription quantitative PCR
rpm	Revolutions per minute
TLS	Translational start site
TSS	Transcription start site
USP	Universal stress protein
V_{max}	Maximum initial velocity of a reaction (moles/min)
wt	Wild type
w/v	Weight per volume

Further abbreviations not included in this section are according to international standards.

1 Introduction

1.1 The molecule 3’,5’-cyclic adenosine monophosphate (cAMP)

The molecule 3’,5’-cyclic adenosine monophosphate, known as cyclic AMP or cAMP, was simultaneously discovered and described by two groups in 1957. One group was studying the chemical alkaline degradation of adenosine-5’-triphosphate (ATP), while the other studied the role of the hormones glucagon and epinephrine in the gluconeogenesis of the liver (Berthet et al., 1957; Cook et al., 1957; Sutherland & Rall, 1958). The discovery and characterization of cAMP was important for revealing the mechanism of action of hormones. Earl W. Sutherland and co-workers showed that in the course of signal transmission via hormones like adrenaline, cAMP serves as a second messenger within the cell (Berthet et al., 1957). In 1971, this discovery was rewarded with the Nobel Prize in Physiology or Medicine.

The hydrophilic molecule cAMP is an adenine nucleotide with a single phosphate group linked to the 3’- and 5’-hydroxyl groups of ribose. The cyclic nucleotide cAMP is synthesized from ATP with the concomitant release of pyrophosphate. The enzyme which catalyses this reaction is referred to as adenylyl cyclase or adenylate cyclase (AC, EC 4.6.1.1) (Danchin, 1993). The degradation of cAMP is mediated by a 3',5'-cyclic-AMP phosphodiesterase (PDE, EC 3.4.1.55), which catalyses the hydrolytic cleavage of the 3’-phosphoester bond, forming 5’-adenosine monophosphate (AMP) (Richter, 2002) (Figure 1). Today, we know that cAMP occurs in all domains of life, found in animals, plants, fungi, archaea, and bacteria (Blanco et al., 2020; Botsford & Harman, 1992; D'Souza & Heitman, 2001; Kamenetsky et al., 2006). The control of the intracellular cAMP concentration is mostly described to be regulated by the activity of ACs and PDEs, meaning by the adjustment of synthesis or degradation of the cyclic nucleotide (McKnight, 1991; Sassone-Corsi, 2012). Only for few organisms (e.g. *Escherichia coli*) it has been described that the control of the intracellular cAMP levels can be mediated through the transport of cAMP across the membrane (Goldenbaum & Hall, 1979). However, a distinct cAMP transporter has not been described yet.

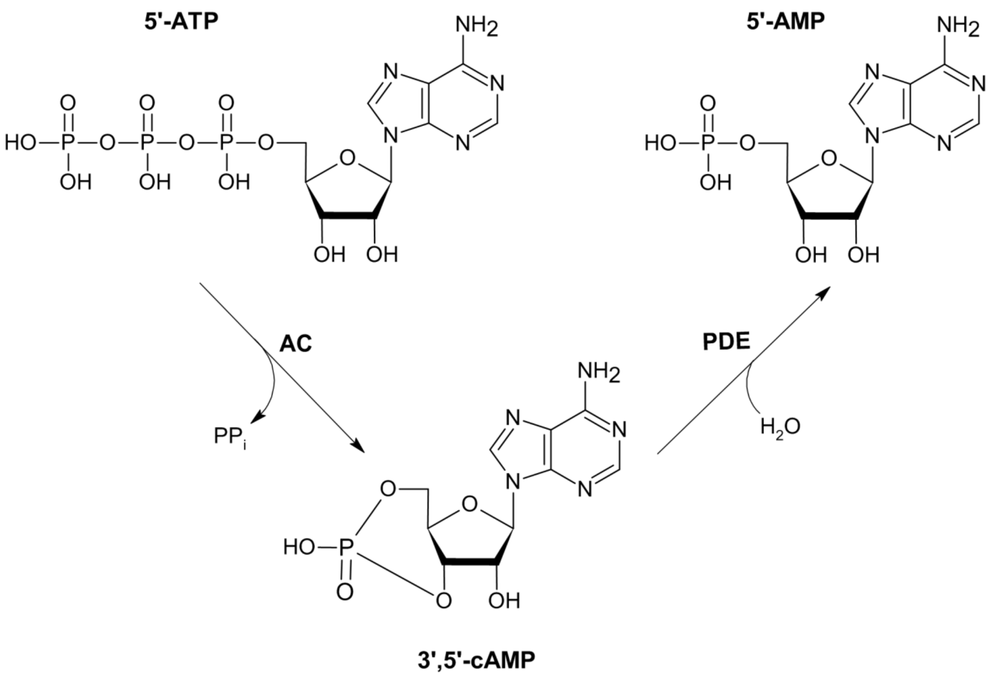

Figure 1: Biosynthesis and degradation of 3',5'-cAMP. The cyclic nucleotide cAMP is synthesized from 5’-ATP through cyclization at the 3’-OH group of the ribose moiety. Enzymes that catalyse this reaction under release of pyrophosphate (PP_i) are called adenylate cyclases (ACs). The cAMP phosphodiesterases (PDEs) catalyse the hydrolytic cleavage of the 3’-phosphoester bond and thereby degrade 3’,5’-cAMP to 5’-AMP. The molecule structures were generated with the program ACD/ChemSketch.

1.1.1 cAMP synthesizing and degrading enzymes

As mentioned above ACs are enzymes that catalyse the synthesis of cAMP from ATP. All ACs described so far are grouped into six classes based on the similarity of their amino acid sequence (Bârzu & Danchin, 1994; Danchin, 1993; Dessauer et al., 2017; Linder & Schultz, 2003). Class I ACs are found in enterobacteria, such as *E. coli*, *Salmonella typhimurium*, or *Yersinia pestis* (Saier et al., 1975). ACs of class II are found, e.g., in the Gram-negative *Bordetella pertussis* and the Gram-positive *Bacillus anthracis.* These pathogens secrete the ACs, which then are activated by the host protein calmodulin and become toxic for the host organism (Arumugham et al., 2018; Dautin et al., 2002; Weiss et al., 1984). An AC grouped into class IV was first identified in *Aeromonas hydrophila* (Sismeiro et al., 1998) and later also reported in *Y. pestis* (Gallagher et al., 2006). Not much is known about the ACs of class V and VI with only one representative found in *Prevotella ruminicola* (Cotta et al., 1998) and

Rhizobium etli (Téllez-Sosa et al., 2002), respectively. In contrast, class III represents a very large group with the structurally and functionally most diverse ACs and representatives in both, eukaryotes and prokaryotes (Bassler et al., 2018). Due to the diverse forms of ACs, class III is divided into four subgroups (IIIa-IIId) based on the primary sequence of the cyclase homology domain (CHD) with its catalytically active sites (Linder & Schultz, 2003). ACs of class III can be either cytosolic or integral membrane enzymes. Mammalian and bacterial ACs of class III are described to be active as homodimers (Linder & Schultz, 2003; Zhang et al., 1997). *In vitro* enzyme activity tests showed that Mn^{2+} or Mg^{2+} ions serve as cofactor in the catalytic centres, which are located at the dimer interface of the CHDs (Kasahara et al., 2001; Linder et al., 2004; Shenoy et al., 2005). The catalytic domains of ACs are often linked with regulatory domains, such as a transmembrane domain or a HAMP domain (found in histidine kinases, adenylate cyclases, methyl accepting proteins, and phosphatases) (Aravind & Ponting, 1999; Linder & Schultz, 2003). A HAMP domain is composed of two amphipathic helices connected by a short linker (Williams & Stewart, 1999); the domain connects the transmembrane domain with the catalytic domain and was shown to play a crucial role in the signal transduction of histidine kinases and ACs (Kishii et al., 2007; Tews et al., 2005). Enzyme tests with truncated ACs from *Mycobacterium tuberculosis* showed that the presence of the HAMP domain had either an inhibitory effect or a highly stimulating effect on the AC activity of the proteins Rv1319c and Rv3645, respectively (Linder et al., 2004).

Phosphodiesterases (PDEs), the enzymes that catalyse the degradation of cAMP, have been grouped in three classes based on their primary structures (Richter, 2002). The PDEs in class I harbour a conserved C-terminal catalytic domain with the motif $H(X)_3H(X)_{25-35}D/E$ (Richter, 2002). All mammalian PDEs belong to the class I PDEs and have been grouped into 11 PDE subfamilies with preferences for cAMP, cGMP, or both cyclic nucleotides (Conti & Beavo, 2007; Francis et al., 2011; Francis et al., 2001; Omori & Kotera, 2007). A small number of class I PDEs are also found in lower eukaryotes such as yeast or amoeba (Sass et al., 1986; Thomason et al., 1999). PDEs of class II share the conserved motif H(X)HLDH and are found in lower eukaryotes and in bacteria (Callahan et al., 1995). Class III harbours mainly PDEs from bacteria, the first one being described in *E. coli* (Imamura et al., 1996). Bioinformatic approaches showed that PDEs from class III are also present in archaea and eukaryotes (Powell et al., 2014). All PDEs have in common that they are active as dimers and have two metal ions in their catalytic centre (Richter, 2002).

1.1.2 Physiological function of cAMP in *E. coli*

In 1965, cAMP in bacteria was first identified in the Gram-negative *E. coli* and since then cAMP and its physiological role was analysed in a variety of other prokaryotic organisms (Botsford & Harman, 1992). In *E. coli* the synthesis of cAMP via an AC has been intensively studied. It was shown that the glucose-specific phosphoenolpyruvate (PEP)-dependent sugar phosphotransferase system (PTS) modulates AC activity. Import of glucose into the cell through the PTS is linked to the dephosphorylation of the substrate-specific enzyme $EIIA^{Glu}$ and in the dephosphorylated state $EIIA^{Glu}$ does not activate AC activity, leading to a low cytoplasmic cAMP concentration. When glucose is absent in the medium, the phosphorylated form of $EIIA^{Glu}$ increases and this form stimulates the activity of the AC, causing an increase of the cAMP level (Bettenbrock et al., 2007; Park et al., 2006). The increased concentration of the signalling molecule cAMP, in turn, influences the transcription of many genes, for example those of the *lac* operon. The respective gene products are involved in the transport and metabolism of the carbon source lactose. The activation of transcription of the *lac* operon is mediated by a cAMP-dependent transcription factor, the cAMP receptor protein (CRP). This mechanism of carbon catabolite repression (CCR) became a paradigm of cAMP-mediated signalling in bacteria (Görke & Stülke, 2008; Kolb et al., 1993). A recent study indicated that in *E. coli* cAMP signalling is responsible for coordinating the expression of catabolic proteins with that of biosynthetic and ribosomal proteins, in dependency of the metabolic demands under different environmental conditions (You et al., 2013).

CRP of *E. coli* (CRP_{Eco}) is the most intensively investigated transcriptional regulator with cAMP as the allosteric effector (Emmer et al., 1970; Gosset et al., 2004). With more than 200 promoters that are putatively under the regulatory control of the cAMP-CRP complex, CRP_{Eco} is classified as a global regulator (Gosset et al., 2004; Mendoza-Vargas et al., 2009; Robison et al., 1998; Zheng et al., 2004). It was shown that the cAMP-CRP complex binds to specific sites within a promoter sequence of a gene and activates or represses the transcription, as a result of enhanced or hindered promoter recognition by the RNA polymerase (Botsford & Harman, 1992; Kolb et al., 1993). CRP_{Eco} is active as a homodimer, each dimer binding a cAMP molecule. Analyses of CRP_{Eco} crystal structures in the presence and absence of cAMP revealed that binding of cAMP leads to notable changes in the tertiary structure and the affinity to its target DNA is significantly increased in the cAMP-CRP complex (Passner et al., 2000; Popovych et al., 2009; Weber & Steitz, 1987).

The prediction, in which cases CRP_{Eco} tends to increase the activity of a promoter, hence, acts as an activator, is described in the 3-Class rules (Lee et al., 2012). In the Class I rule CRP_{Eco} acts as an activator if it binds upstream of the promoter elements -35 and -10 around position -61.5 relative to the transcriptional start site (TSS) (Busby & Ebright, 1997, 1999; Zheng et al., 2004). Enhanced binding of RNA polymerase to the promoter is accomplished through the interaction of CRP with the carboxyl-terminal domain of the α-subunit (αCTD) of RNA polymerase (Benoff et al., 2002). The *lac* promoter is the most prominent example for a CRP-dependent promoter of the Class I rule (de Crombrugghe et al., 1984; Majors, 1975). The Class II rule of CRP_{Eco} states that activation of transcription is possible when the regulator binds around position -41.5 and the binding site overlaps with the -35 element of the promoter (Savery et al., 1998). A CRP-dependent promoter of the Class II rule is, for example, the *galP1* promoter (Attey et al., 1994). The Class III rule describes that if a promotor has two or more CRP-binding sites, the promoter tends to be activated upon cAMP-CRP binding. The Class III rule is also valid if the promoter has one or more CRP binding sites and one or more binding sites for another protein acting as activator. The promoters of *araBAD* and *malK* are prominent examples of such Class III rule promoters (Richet et al., 1991; Zhang & Schleif, 1998).

1.1.3 Physiological function of cAMP in *Mycobacterium* species

In *M. tuberculosis* and the faster growing *Mycobacterium smegmatis*, cAMP plays a role for the pathogenicity of the cells (Lowrie et al., 1979). *M. tuberculosis* possesses 16 different ACs and the intracellular cAMP concentration is considered to be 100-fold higher compared to other bacteria, such as *E. coli* (McCue et al., 2000; Shenoy & Visweswariah, 2006). Macrophages infected with *M. tuberculosis* showed an increase of cytoplasmic cAMP levels, which then led to an intoxication of the host cell. The mycobacterial origin of the cAMP was demonstrated by *M. tuberculosis* cells that were pre-labelled with ^{14}C-glycerol. Furthermore, the mycobacterial AC Rv0386 responsible for the synthesis of the majority of the radiolabelled cAMP was identified by detecting a significant drop in cAMP when using an Rv0386 deletion strain (Agarwal et al., 2009). The secretion of cAMP by *M. tuberculosis* and the resulting increase of the cAMP level in the host cell play an important role in the suppression of the host defence mechanisms inside of macrophages (Bai et al., 2011; Lowrie et al., 1979). In contrast to the 16 described ACs, only two cAMP-degrading enzymes are known in *M. tuberculosis* (Shenoy et al., 2005; Thomson et al., 2020). And although the bacterium seems to regulate the intracellular cAMP level through excretion of cAMP, no distinct cAMP transporter protein was characterized yet.

A cAMP-dependent lysine acetyltransferase (KATmt) (Rv0998) of *M. tuberculosis* was detected, which acetylates catalytically important lysine residues of fatty acyl-CoA synthetases (FadD enzymes) (Nambi et al., 2010; Nambi et al., 2013, 2019). In a search for further cAMP-binding proteins in mycobacteria, the protein Usp (Rv1636) was identified in *M. tuberculosis* as an abundant and specific cAMP-binding protein (Banerjee et al., 2015). Binding of the Rv1636 protein to cAMP was confirmed by cAMP agarose affinity chromatography and verified by isothermal titration calorimetry (ITC). Rv1636 belongs to the family of universal stress proteins (USPs) and carries a USP domain. Members of the USP family were described to be involved in stress responses, because it was shown that their synthesis was induced upon different stress conditions, such as starvation for carbon or phosphate, entry into the stationary phase in rich medium, exposure to heat, or presence of uncouplers inhibiting oxidative phosphorylation (Vollmer & Bark, 2018). The biological function of the cAMP-binding protein Rv1636 has not yet been elucidated. However, it was proposed that cAMP-binding to USPs in mycobacteria is a mechanism for regulation of the intracellular ‘free’ cAMP level and therefore a regulation of the downstream effects of cAMP (Banerjee et al., 2015). In another study, it was shown that Rv1636 of *M. tuberculosis* is in the top twenty of the most abundant proteins of the organism, which also supports the hypothesis that Rv1636 acts as a cAMP reservoir (Schubert et al., 2013).

M. tuberculosis carries a cAMP receptor protein (CRP) that acts as a global transcriptional regulator with its effector cAMP (Stapleton et al., 2010). The faster growing mycobacterium *M. smegmatis* contains two CRP homologues, the major CRP1 protein Msmeg_6189 and its paralog CRP2/Msmeg_0539 (Sharma et al., 2014). Both transcriptional regulators recognize the same DNA consensus sequence, but have different binding affinities for cAMP (K_d 30 µM for Msmeg_6189 and K_d 3 µM for Msmeg_0539) and are probably active under different conditions in response to carbon and energy supply (Aung et al., 2015; Sharma et al., 2014). While Msmeg_0539 was shown to regulate genes involved in transport and catabolism of carbohydrates, Msmeg_6189 was found to play a dominant role for the induction of the *cydAB* operon under hypoxic conditions (Aung et al., 2014; Ko & Oh, 2020).

The *cydAB* genes encode for subunit I and II of the terminal cytochrome *bd* oxidase, which has a high affinity for O_2 and thus its activity is important under oxygen-limiting conditions (Kana et al., 2001).

Apparently, in mycobacteria, cAMP is not only involved in the regulation of gene expression via cAMP-CRP, but also serves as the effector of a cAMP-dependent lysine acetyltransferase, binds to a universal stress protein, and is an important part of host-pathogen interaction due to export of cAMP into host cells (Agarwal et al., 2009; Banerjee et al., 2015; Nambi et al., 2010; Nambi et al., 2013, 2019; Sharma et al., 2014; Stapleton et al., 2010). Thus, cAMP in prokaryotes not only serves as an effector of transcriptional regulators with generally a large regulon, but also has additional functions, which are probably only incompletely known.

1.2 The role of cAMP in *Corynebacterium glutamicum*

The Gram-positive soil bacterium *Corynebacterium glutamicum* was discovered in a screening for natural microbial glutamate producers (Kinoshita et al., 1957; Udaka, 1960). It is a facultative anaerobic bacterium with a GC-content of 53.8% and belongs to the order *Corynebacteriales* within the phylum *Actinomycetota* (Oren & Garrity, 2021). This order also comprises the important human pathogens *Corynebacterium diphtheriae, Mycobacterium leprae*, and *M. tuberculosis* (Gao & Gupta, 2012). The ability of *C. glutamicum* to secrete glutamate into the medium was the starting point for the development of ‘fermentative’ industrial amino acid production, which nowadays is a billion dollar business (Becker & Wittmann, 2012; Wendisch et al., 2016). Over the years, *C. glutamicum* with the generally-regarded-as-safe (GRAS) status became the most important microorganism for the large scale production of the amino acids L-glutamate and L-lysine (Eggeling & Bott, 2015; Leuchtenberger et al., 2005). After genome sequencing of the *C. glutamicum* type strain ATCC13032 by two independent laboratories (Ikeda & Nakagawa, 2003; Kalinowski et al., 2003), rational strain development by metabolic engineering, novel high-throughput screening methods employing single-cell metabolite biosensors, and adaptive laboratory evolution became important tools for *C. glutamicum* strain development (Binder et al., 2012; Eggeling et al., 2015; Inui et al., 2004; Mustafi et al., 2012; Schendzielorz et al., 2014). Since 2003, numerous *C. glutamicum* strains were created for the production of various amino acids (Stolz et al., 2007; Vogt et al., 2014; Vogt et al., 2015) and other industrially relevant compounds such as organic acids (Litsanov, Brocker, et al., 2012; Litsanov, Kabus, et al., 2012; Okino, Noburyu, et al., 2008; Okino, Suda, et al., 2008; Wieschalka et al., 2013), alcohols (Blombach et al., 2011; Inui et al., 2004), carotenoids (Heider et al., 2014; Henke et al., 2016), or phenylpropanoids (Kallscheuer et al., 2016). The biotechnological importance of *C. glutamicum* and its close phylogenetic relationship to pathogenic bacteria fuel the ongoing interest for a deeper understanding of its metabolic and regulatory network.

1.2.1 GlxR – the CRP-like protein of *C. glutamicum*

The first time cAMP was mentioned in connection with *C. glutamicum* was in a publication that identified and characterized a CRP-like protein (Cg0350) that was named GlxR due to its involvement in the regulation of the genes of the glyoxylate pathway (Kim et al., 2004). Based on its amino acid sequence, GlxR belongs to the CRP-FNR family of transcriptional regulators and shows 27% amino acid sequence identity with CRP of *E. coli* and 78% identity with the CRP protein (Rv3676) of *M. tuberculosis* (Kim et al., 2004). Bioinformatic analysis of GlxR with the online tool PFAM (Mistry et al., 2020) showed that GlxR is composed of an N-terminal cNMP-binding domain (PF00027) and a C-terminal HTH_CRP domain (PF13545) (Figure 2). Besides GlxR, the genome of *C. glutamicum* ATCC13032 encodes two other proteins that have one or both of these domains: Cg1327 has a similar domain composition as GlxR, whereas Cg3291 only shares the HTH_CRP domain with GlxR (Figure 2). The functions of Cg1327 and Cg3291 have not yet been studied.

In 2014 the crystal structures of apo-GlxR and holo-GlxR (in complex with cAMP) were solved. Their comparison revealed that the 25 kDa protein undergoes small structural changes upon cAMP-binding, resulting in a 100-fold higher DNA-binding affinity (Townsend et al., 2014). The crystal structure of GlxR in complex with cAMP is displayed in Figure 2 and shows a homodimer with two structurally identical binding sites for cAMP in the centre of the ligand binding pocket close to the dimer interface. The K_d value measured for binding of the first cAMP molecule was 17 µM, whereas the K_d value for binding of the second cAMP molecule was 130 µM (Townsend et al., 2014). The DNA-binding helices are located in the proximity of the C-terminus. In electrophoretic mobility shift assays (EMSAs) DNA binding by GlxR only occurred in the presence of cAMP (Bussmann et al., 2009; Jungwirth et al., 2013; Kim et al., 2004; Kohl et al., 2008; Kohl & Tauch, 2009; Letek et al., 2006).

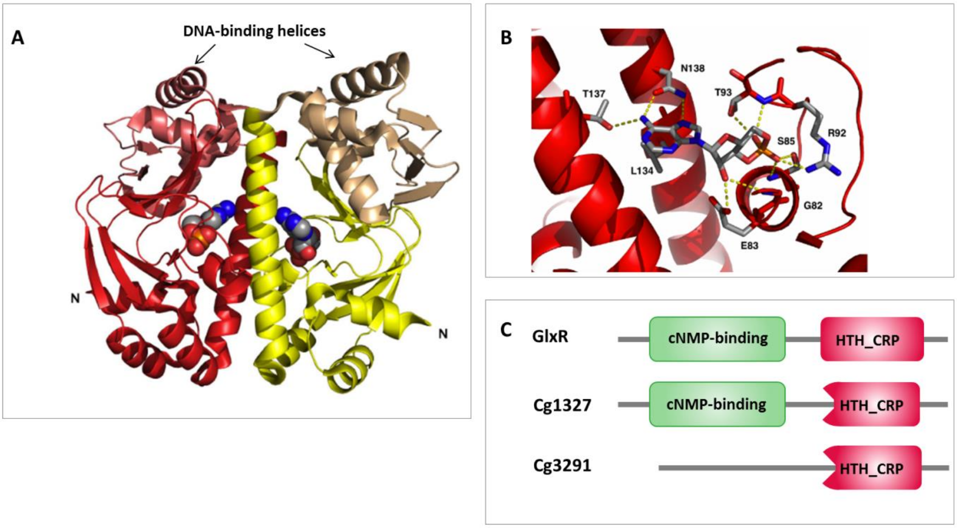

Figure 2: Structure of homodimeric GlxR in complex with cAMP and protein domains of GlxR and its paralogs. (**A**) Ribbon diagram of a GlxR dimer in complex with cAMP. The two protein chains are depicted in red and yellow, with the DNA-binding domains in lighter shade. Each dimer binds one cAMP molecule in the ligand-binding pocket. The ligand cAMP is shown in a ball-and-stick representation (modified after Townsend et al., 2014). (**B**) Close-up of one cAMP-binding site in GlxR. The figure was taken from Townsend et al., 2014. (**C**) Protein domains of GlxR and the related proteins Cg1327 and Cg3291. cNMP-binding domains often are composed of an eight-stranded, antiparallel beta-barrel structure and three alpha-helices. The HTH_CRP domain comprises a DNA-binding helix-turn-helix (HTH) domain.

GlxR stands for the abbreviation glyoxylate pathway regulator, due to the initial finding that this protein represses transcription of the gene *aceB* encoding malate synthase, a key enzyme of the glyoxylate bypass (Kim et al., 2004). In the following years, more and more genes were found to be transcriptionally regulated by GlxR, such as *gntP* and *gntK* (Letek et al., 2006), the *sdhCAB* operon (Bussmann et al., 2009), *gluABCD* (Park et al., 2010), *gltA* (van Ooyen et al., 2011), *narKGHJI* (Nishimura et al., 2011), *pstSCAB* (Panhorst et al., 2011), *atpB*, *ctaCF*, and *ctaD* (Toyoda et al., 2011), or *adhA* and *ald* (Subhadra & Lee, 2013). The use of promoter fusions, quantitative RT-PCR or enzyme assays revealed that GlxR can function as an activator or a repressor. A more global approach to broaden the knowledge about the GlxR regulon was conducted by *in silico* prediction of GlxR binding sites in the genome of *C. glutamicum* ATCC13032 (Kohl & Tauch, 2009). Predictions were verified by showing *in vitro* GlxR-DNA interaction for 138 DNA regions by EMSAs. The GlxR consensus DNA-binding motif identified was 5’-TGTGANNTANNTCACA-3’ and is very similar or identical to the consensus motifs reported in other GlxR studies (Jungwirth et al., 2013; Kohl et al., 2008; Toyoda et al., 2011).

The *in vivo* DNA-binding sites of GlxR were analysed by using ChIP-Seq or ChIP-Chip. Whereas 107 DNA fragments enriched by GlxR were identified by ChIP-Seq using *C. glutamicum* ATCC13032, even 209 GlxR-binding regions could be identified by ChIP-Chip using the closely related strain *C. glutamicum* R (Jungwirth et al., 2013; Toyoda et al., 2011). Due to the large regulon, GlxR is characterized as a master regulator, with its regulatory network interconnecting different cellular functions, such as carbon metabolism and transport, nitrogen and phosphate metabolism, SOS and stress responses, respiration, sulphur homeostasis, and iron homeostasis (Kohl & Tauch, 2009). As GlxR also binds upstream of genes encoding for transcriptional regulators, such as *ramA* and *ramB*, the regulatory network of GlxR goes far beyond the direct regulation of gene transcription (Jungwirth et al., 2013). In case of *ramA,* GlxR acts as a transcriptional activator, whereas RamA and SugR function as repressors for *ramA* transcription (Toyoda et al., 2013). A prediction was made that GlxR probably could influence about 14% of the genes in *C. glutamicum* (Kohl & Tauch, 2009). A mini-review summarizing the function and regulons of transcription factors from *C. glutamicum* presented results that were gained by ChIP-based technologies and contributed to the understanding of the GlxR regulon (Toyoda & Inui, 2016). The authors emphasized that the transcriptional regulation of one gene by several transcription factors increases the possibility of multiple regulatory loops in the regulatory network of *C. glutamicum,* which requires more intensive laboratory work finding the factors that explain how the transcription of a distinct gene is balanced.

A high-throughput approach for the determination of the *in vivo* regulatory role of the transcription factor GlxR would be a comparative gene expression analysis with DNA microarrays or RNA-seq with a mutant lacking the *glxR* (cg0350) gene and the wild type. However, in *C. glutamicum* ATCC13032 several attempts to construct a *glxR* deletion mutant lacking the entire GlxR coding sequence failed (Bussmann, 2009; Kim et al., 2004; Letek et al., 2006). Two groups succeeded to construct *glxR* mutants that lack the *glxR* region encoding the cAMP-binding domain in strain ATCC13032 (Moon et al 2007; Park et al 2010) or nearly the complete *glxR* gene in strain R (Toyoda et al., 2009). However, due to the severe growth defects of these mutants, meaningful global gene expression experiments could not be performed. As *in vivo* data from a *glxR* deletion mutant are missing, the regulatory role of GlxR for a particular gene is often predicted from the location of its binding site within the promoter region.

DNA affinity chromatography experiments with the *glxR* promoter region suggested that *glxR* is itself the target of several transcriptional regulators: The transcriptional regulator AtlR (Cg0146, previously known as SucR or MtlR), a regulator of the DeoR family involved in arabitol metabolism (Laslo et al., 2012; Peng et al., 2011) and the GntR-family regulator GntR3 (Cg2544) activate the transcription of *glxR* (Subhadra et al., 2015), whereas RamB (Cg0444), a transcriptional regulator of the MerR family involved in acetate metabolism, represses the transcription of *glxR* (Subhadra et al., 2015). Furthermore, *glxR* is negatively autoregulated, i.e. GlxR represses transcription of its own gene (Jungwirth et al., 2008; Subhadra et al., 2015). Although *glxR* is subject to complex transcriptional regulation, it was reported to be constitutively expressed during growth in minimal medium with glucose as carbon source (Hong et al., 2014). Furthermore, the mRNA level of *glxR* was similar when cells were cultivated with citrate or a citrate-glucose mixture as carbon source (Polen et al., 2007).

A proteome study that was searching for proteins undergoing lysine acetylation and/or lysine succinylation identified three lysine residues of GlxR in a succinylated form (K59, K155, and K212) (Mizuno et al., 2016). Furthermore, another study showed that the lysine residue K57 of GlxR was found to be covalently linked to the small prokaryotic ubiquitin-like protein Pup (Küberl et al., 2014). As *C. glutamicum* lacks a proteasome, the purpose of GlxR pupylation is not yet known and the fractions of pupylated and succinylated GlxR are unknown. Hong and co-workers reported that the subtilisin-like serine protease SprA interacts with GlxR (Hong et al., 2014). They showed that GlxR was proteolytically cleaved in the presence of purified SprA, however, this cleavage was inhibited if cAMP was present. All in all, the physiological roles of the posttranscriptional modifications of GlxR, especially of pupylation and succinylation, remain elusive and should be studied further, as the results could contribute to a deeper understanding of the activity of the transcriptional regulation of GlxR.

1.2.2 CyaB – the AC of *C. glutamicum*

The only enzyme known to date to be involved in the synthesis of cAMP in *C. glutamicum* is the membrane-bound AC CyaB (Cg0375) (Cha et al., 2020, Bussmann 2009). CyaB is conserved in *Corynebacterium* species and is an ortholog of the AC Rv3645 of *M. tuberculosis* with 43% sequence identity (Bussmann, 2009; Shenoy et al., 2004). In the initial annotation of the *C. glutamicum* genome in 2003 (Kalinowski et al., 2003), a CyaB protein composed of 547 amino acid residues was predicted. The CyaB start codon was later changed (Pfeifer-Sancar et al., 2013), leading to a protein of 508 amino acid residues. The start codon of the latter version corresponds to the one predicted for the CyaB proteins of *Corynebacterium efficiens* and *Corynebacterium diphtheriae* (Figure 3A). Bioinformatic analysis of the CyaB amino acid sequence reveals that this cyclase consists of an N-terminal membrane-integral domain with six transmembrane helices with no signal peptide (Figure 3B) fused to a cytoplasmic HAMP domain followed by the adenylate cyclase catalytic domain (cyclase homology domain, CHD) (Mistry et al., 2020).

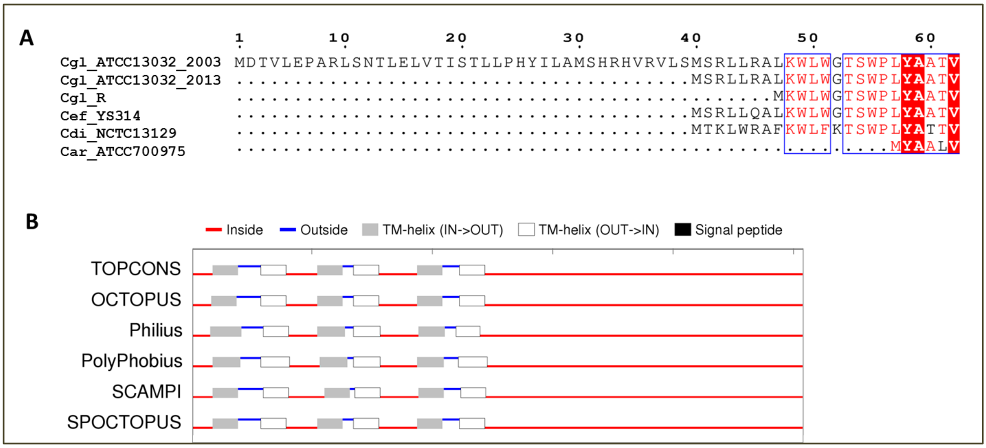

Figure 3: Alignment of the N-terminal regions of the adenylate cyclase CyaB and its homologs and predicted membrane topology of CyaB (Cg0375). (**A**) Amino acid sequence alignment of the N-terminal regions of CyaB from *C. glutamicum* ATCC13032 as predicted by Kalinowski et al., (2003) and by Pfeifer-Sancar et al., (2013), from *C. glutamicum* strain R (Cgl_R), from *C. efficiens* (Cef_YS314), from *C. diphtheriae* (Cdi_NCTC13129), and from *Corynebacterium aurimucosum* (Car_ATCC700975). The alignment was generated with ClustalW (Thompson et al., 1994) and further processed with ESPript 3.0 (Robert & Gouet, 2014). (**B**) Prediction of the membrane topology of CyaB using the webserver TOPCONS (https://topcons.cbr.su.se/)(Tsirigos et al., 2015). All six programs predicted a protein with six transmembrane helices. No signal peptide was detected. The input amino acid sequence of CyaB (Cg0375, 508 amino acid residues) was taken from Pfeifer-Sancar et al., 2013.

According to these predictions, CyaB in the dimeric state contains 12 transmembrane helices. This number is often found in secondary transporters (Henderson, 1993); however, a transport function of the ACs has not been recognized up to now. Furthermore, it is possible that the transmembrane domain of CyaB serves as a sensor for an extracellular or membrane-associated stimulus. While membrane-bound mammalian ACs are known to be activated by G-proteins as a response to extracellular hormone signals (Linder & Schultz, 2003), a stimulus for bacterial membrane-bound ACs has yet to be discovered. Cultivations of *C. glutamicum* Δ*cyaB* with plasmid-based expression of *cyaB* showed that only plasmids coding the entire CyaB protein or an N-terminal truncated variant with a residual 13 aa transmembrane domain followed by the HAMP domain and the catalytic domain were able to abrogate the growth defect of the Δ*cyaB* mutant in the presence of acetate (Katcharava, 2015). Interestingly, a plasmid-based expression of *cyaB* coding for a CyaB variant which is not located in the membrane (only HAMP domain and catalytic domain) was not able to abolish the growth defect.

Although CyaB appears to be the only AC in *C. glutamicum*, the phenotype of a *cyaB* deletion mutant differs strongly from that of the *glxR* mutants described above. Whereas the latter mutants showed severe growth defects, growth of *cyaB*-deficient mutants was found to be comparable to the parental strain when cultivated in minimal medium with carbon sources such as glucose, gluconate, or pyruvate (Bussmann, 2009; Cha et al., 2010). Only when cultivated in the presence of acetate as carbon source, the *cyaB*-deficient mutants showed a light or severe growth defect (Bussmann, 2009; Cha et al., 2010). The reasons for this phenotype were studied in the course of this doctoral thesis.

1.2.3 CpdA – the PDE of *C. glutamicum*

In *C. glutamicum* a PDE converting cAMP to AMP was described only recently (Schulte et al., 2017). This PDE, named CpdA (Cg2761), showed only 15-19% amino acid sequence identity to other known PDEs from bacteria of class II, but contained a sequence motif that is very similar to the one reported to be characteristic of class II PDEs (Richter 2002). In 2020 this CpdA together with a newly described PDE (Rv1339) of *M. tuberculosis* and the PDE YfhI of *Bacillus subtilis* was proposed to be classified in a new PDE group called 'atypical class II PDEs' (Thomson et al., 2022). This atypical class II PDEs have a signature metal-binding motif (T/S)HXHXDH in common, where X is likely to be a hydrophobic or small residue (Thomson et al., 2022). Characterization of the purified corynebacterial CpdA revealed a K_m^{app} value of 2.5 ± 0.3 mM for cAMP and a V_{max}^{app} of 33.6 ± 4.3 µmol min^{1} mg^{1}. The K_m^{app} is more than 30-fold higher compared to the class II PDEs of *Vibrio fischeri* (73 µM) (Callahan et al., 1995) or of *Myxococcus xanthus* (12 µM) (Kimura et al., 2011), but 4-fold lower than the PDE of

Arthrobacter sp. CGMCC 3584 (6.82 mM) (Schulte et al., 2017; Zheng et al., 2013). The V_{max}^{app} value of CpdA (33.6 ± 4.3 µmol min^{1} mg^{1}) is 112-fold lower compared to the V_{max}^{app} of *V. fischeri* (3.7 mmol min^{1} mg^{1}) but almost 500-fold higher than the V_{max}^{app} of *M. xanthus* (67.5 nmol min^{1} mg^{1}) (Callahan et al., 1995; Kimura et al., 2011).

A *cpdA* deletion mutant of *C. glutamicum* showed severe growth defects and reduced growth rates on all carbon sources tested, such as glucose, gluconate, acetate, citrate, or an ethanol-glucose mixture (Schulte et al., 2017). Determination of the intracellular cAMP level revealed a 2-fold higher cAMP level in the Δ*cpdA* mutant compared to the parental strain (50 pmol/mg protein and 27 pmol/mg protein, respectively) (Schulte et al., 2017). This result indicates that CpdA of *C. glutamicum* is a phosphodiesterase with an important role in the control of the cellular cAMP level. In agreement, transcriptome analysis comparing the Δ*cpdA* mutant to the parental *C. glutamicum* strain identified 247 genes with a more than 2-fold altered mRNA level in the Δ*cpdA* mutant. These altered gene expressions probably result from an altered activity of the transcriptional regulator GlxR due to the higher intracellular cAMP level. Indeed, many GlxR-regulated genes showed altered expression levels in the Δ*cpdA* mutant, including genes involved in carbon source transport and metabolism, which could explain the growth defects of the Δ*cpdA* mutant. For example, the Δ*cpdA* mutant showed more than 3-fold reduced mRNA levels of genes involved in the uptake of glucose, sucrose, and citrate (*ptsG*, *ptsI*, *ptsS*, *tctA* and *tctB*) and in the metabolism of acetate, gluconate, L-lactate, and ethanol (*pta*, *ackA*, *gntK*, *lldD*, *adhA* and *ald*). An important finding by Schulte et al. was that *cpdA* expression is transcriptionally activated by GlxR. A model shows that an intracellular increase of cAMP should lead to higher numbers of cAMP-GlxR complexes and thus a transcriptional activation of the *cpdA* expression (Figure 4). Thus, as a consequence the level of CpdA should increase, which then should lead to a lowering of the cellular cAMP level due to the higher degradation rate of cAMP by CpdA. This feedback loop is probably crucial for the regulation of the cellular cAMP level as the 2-fold increase in the level was shown to lead to severe growth defects. Further active phosphodiesterases besides CpdA have not yet been described in *C. glutamicum*.

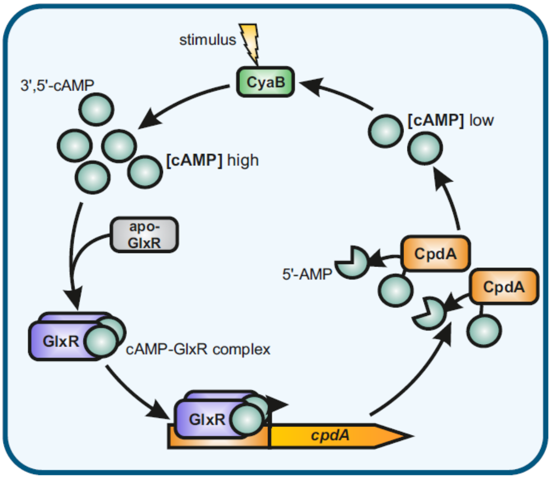

Figure 4: Prediction of a negative feedback loop formed via transcriptional activation of *cdpA* expression by the cAMP-GlxR complex (taken from Schulte et al., 2017). After activation of the adenylate cyclase (CyaB) by an unknown stimulus, the cAMP level increases. The increased cAMP concentration leads to more cAMP-GlxR complexes, which activate the expression of *cpdA* gene encoding a cAMP phosphodiesterase. Elevated CpdA activity thus lowers the intracellular cAMP level and resets the system.

1.2.4 cAMP levels in *C. glutamicum*

The intracellular cAMP concentration in *C. glutamicum* has been measured by several different groups using different strains and cultivation conditions. The first measurement was reported in the study in which GlxR was described for the first time (Kim et al., 2004). The cAMP concentration was reported to be high in the early exponential phase and low when the cells reached the stationary phase in a medium with glucose as carbon source. This finding indicated that the cAMP concentration was high when the glucose concentration was high, in contrast to the situation in *E. coli*, where the cAMP concentration is low in the presence of glucose. Several later studies showed that the intracellular cAMP level of *C. glutamicum* is higher during growth on glucose than during growth on acetate (Table 1). Additional studies determined the intracellular cAMP level in cells grown with citrate or a glucose-acetate mixture, showing that the cAMP levels on these substrates were higher than those on glucose alone (Bussmann, 2009; Cha et al., 2010; Polen et al., 2007; Schulte et al., 2017). The results of these cAMP measurements were presented in different units, which hinder a direct comparison. Therefore, in Table 1 the cAMP concentrations given in different studies were converted into cytoplasmic concentrations. The range of the reported cAMP concentrations in *C. glutamicum* was very broad and varied from ~1 µM to 7.6 mM. Except for one study (Kim et al. 2004), the cAMP concentration was typically found to be in the low µM range. As expected, the cAMP concentration was lower in mutants lacking a functional AC and higher in the mutant lacking CpdA (e.g. WT 30 ± 12 pmol/mg protein, Δ*cyaB* 18 ± 2 pmol/mg protein and Δc*pdA* 50 ± 12 pmol/mg protein, respectively) (Bussmann, 2009; Schulte et al., 2017).

The intracellular cAMP concentration of *C. glutamicum* is controlled by the rates of synthesis and degradation, as shown by the lower cAMP level of the Δ*cyaB* mutants (Bussmann, 2009; Cha et al., 2010) and the higher cAMP levels in the Δ*cpdA* mutant (Schulte et al., 2017). Transporters catalysing cAMP export or import have not been identified. To better understand how the levels of intracellular cAMP in *C. glutamicum* are controlled, one has to study the regulation and the activity of the AC and the PDE.

1.3 Aims of this doctoral thesis

In the course of studies on cAMP-dependent regulation in *C. glutamicum*, only one gene for the cAMP synthesis was identified (*cyaB*, cg0375) (Bussmann, 2009; Cha et al., 2010). Δ*cyaB* mutants showed comparable growth to the wild type with glucose, but impaired growth with acetate. The reason for the negative effect of acetate on growth of the Δ*cyaB* mutant is unknown and one aim of this thesis was to find an explanation for this phenotype. This part involved a detailed characterization of the *C. glutamicum* strain lacking CyaB, which should help to elaborate a theory why a *C. glutamicum* strain with a low or even absent intracellular cAMP level shows a higher sensitivity towards the weak acid acetate compared to the wild type strain. The second part of this thesis aimed at an *in vivo* analysis of GlxR-DNA binding in the wild type compared to the Δ*cyaB* mutant under different carbon source conditions. By this approach, the effects of low intracellular cAMP levels in the Δ*cyaB* mutant should be elucidated, shedding light on the relevance of cAMP for DNA-binding by GlxR *in vivo*. Despite the fact that numerous previous studies investigated the regulatory hub of GlxR, many open questions remain with respect to physiological role of GlxR and the impact of cAMP. Studies with strains that harbour a high or low cAMP level should provide new insights into this topic.

Table 1: Intracellular cAMP levels of different *C. glutamicum* strains measured in different studies. The values in µM were calculated from the pmol/mg protein values. All cAMP concentrations were measured with the competitive ELISA immunoassay (Biotrak™ cAMP enzyme immunoassay (EIA) system, Cytiva, USA formerly part of GE Healthcare).

Study	**Strain**	**Conditions**	**cAMP level**	
			pmol/mg protein	**µM[a]**
Kim et al., 2004	*C. glutamicum* AS019 (spontaneous mutation of *C. glutamicum* ATCC13059)	MCGC + glucose 1%	22000 (exp[b])	**7639**
			11000 (stat[b])	**3819**
		MCGC + acetate 2%	5 000 (exp)	**1736**
			5 000 (stat)	**1736**
Polen et al., 2007	*C. glutamicum* ATCC13032	CGXII + 50 mM glucose	10	**4**
		CGXII + 50 mM citrate	24	**8**
Bussmann 2009 (Doc. thesis)	*C. glutamicum* ATCC13032	CGXII + 200 mM glucose	30 ± 12 (exp)	**10 ± 4**
		CGXII + glucose-acetate (100 mM each)	88 ± 22 (exp)	**31 ± 8**
	C. glutamicum Δ*cyaB*	CGXII + 200 mM glucose	18 ± 2 (exp)	**6 ± 1**
		CGXII + glucose-acetate (100 mM each)	9 ± 5 (exp)	**3 ± 2**
Cha et al., 2010	*C. glutamicum* ATCC13032	MM + glucose 1%	448 ± 9 (exp)	**156 ± 3**
		LB + acetate 1%	108 ± 3 (exp)	**38 ± 1**
	C. glutamicum CgYA (partly deleted *cyaB* gene)	MM + glucose 1%	44 - 63	**15 - 21**
		LB + acetate 1%	44 - 63	**15 - 21**
Schulte et al., 2017	*C. glutamicum* ATCC13032	CGXII + glucose (200 mM)	27 ± 5	**9 ± 2**
	C. glutamicum Δ*cpdA*	CGXII + glucose (200 mM)	50 ± 12	**17 ± 4**
Study	**Strain**	**Conditions**	**pmol/OD$_{610}$**	**µM[c]**
Toyoda et al., 2011	*C. glutamicum* R	nutrient rich A medium glucose 1%	~ 4 - 9 (exp)	**~1.4 - 3.1**
			~16 (stat)	**~5.6**
		nutrient rich A medium acetate 1%	~ 4 (exp)	**~ 1.4**
			~ 3 (stat)	**~ 1.0**
	C. glutamicum KT23 (strain R with deletion of *cyaB* gene)	nutrient rich A medium glucose 1%	< 0.2	< **0.1**
		nutrient rich A medium acetate 1%	< 0.2	< **0.1**

a: Intracellular cAMP concentrations have been calculated from the pmol/mg protein values under the assumption that protein represents 50% of the cell dry weight (CDW) and assuming a cell volume of 1.44 µl/mg CDW (da Luz et al., 2017).

b: exp: concentration measured for cells in the exponential growth phase; stat: concentration measured for cells in the stationary phase.

c: Intracellular concentrations have been calculated under the assumption that OD$_{600}$ of 1 represents 0.25 mg CDW/ml (Kabus et al., 2007).

2 Results

The main topic of this thesis was the investigation of the molecular basis of the acetate sensitivity of an adenylate cyclase-lacking mutant of *C. glutamicum* and the impact of a lowered or even absent cAMP level on *in vivo*-DNA-binding of the global transcriptional regulator GlxR. The results of the first part have been published in the peer-review journal Frontiers in Microbiology. The results of the second part have been summarized in a manuscript to be submitted soon.

In the publication 'Molecular basis of growth inhibition by acetate of an adenylate cyclase-deficient mutant of *Corynebacterium glutamicum*' the main reason for the observed growth defect of the *cyaB* deletion strain in the presence of acetate is described. The inhibitory effect of acetate was shown to be concentration-dependent and stronger when cultivated in medium with lower external pH values. These results indicate that the negative effect of acetate on the Δ*cyaB* mutant is related to the uncoupler-like behaviour of acetate. In the protonated form the weak acid diffuses through the lipid bilayer of *C. glutamicum* into the cell, where it dissociates with release of a proton. While to a certain amount this is not problematic for the wild-type strain, the *cyaB* deletion strain was shown to be more sensitive towards such uncoupler-like behaviour. Studies with CCCP confirmed that the *cyaB* mutant was more sensitive towards uncouplers compared to the wild-type strain. As a possible explanation, the reduced expression of the cytochrome bc_1-aa_3 supercomplex and the F_1F_O-ATP synthase in the Δ*cyaB* mutant was proposed. The genes encoding these main players of energy metabolism in *C. glutamicum* were previously shown to be activated by GlxR. The low or absent cAMP level of the Δ*cyaB* mutant causes a reduction of active GlxR and thus of the expression of genes that are activated by the cAMP-GlxR protein. Additionally, it was shown that upon deletion of *cyaB*, no intracellular cAMP was detected via LC-MS/MS. Even in the double deletion mutant *C. glutamicum* Δ*cyaB*Δ*cpdA* (no functional adenylate cyclase and no phosphodiesterase catalysing cAMP degradation), no cAMP could be detected via LC-MS/MS. These data suggest that detection of cAMP via ELISA in extracts of *C. glutamicum* Δ*cyaB* is probably an artefact and that there is presumably no second active adenylate cyclase present in this organism. Finally, a suppressor mutant of the *cyaB* deletion strain was isolated, which had lost the acetate sensitivity and was shown to carry a single amino acid exchange in GlxR. The described results point out that cAMP and

GlxR play an important role in the energy metabolism of *C. glutamicum*, which may be useful also for strain engineering of this industrial workhorse.

The manuscript ‘Comparison of *in vivo* GlxR binding in *Corynebacterium glutamicum* ATCC 13032 and the adenylate cyclase deletion mutant Δ*cyaB* using ChAP-Seq‘ describes the investigation of a genome-wide target profiling of GlxR in the *C. glutamicum* wild-type strain and in the adenylate cyclase-deficient mutant (Δ*cyaB*). The method of choice for this protein-DNA interaction analysis was the so called ChAP-Seq method (chromatin affinity purification combined with DNA sequencing). The results of four data sets (WT$_{\text{GlxR-TS}}$ (glc), Δ*cyaB*$_{\text{GlxR-TS}}$ (glc), WT$_{\text{GlxR-TS}}$ (glc-ac), Δ*cyaB*$_{\text{GlxR-TS}}$ (glc-ac) identified 243 GlxR peaks when a cut-off of the enrichment factor (EF) ≥3 was used. 102 of these peaks represented novel GlxR binding sites not reported in previous studies. Many GlxR binding regions were found to be located intragenically or in a relatively large distance (>700 bp) upstream of the next transcriptional start site (TSS). Furthermore, as many GlxR binding sites were found upstream of non-coding proteins (such as asRNA, sRNA or tRNA), GlxR appears to play a more important role in the regulation of non-protein coding genetic elements than previously anticipated. The presence of acetate in the medium reduced GlxR binding, particularly in the Δ*cyaB* mutant. The comparison of the GlxR-DNA interaction of the wild type and the Δ*cyaB* mutant showed that for most DNA regions GlxR can apparently bind to DNA even without the presence of the effector cAMP, explaining why the phenotype of Δ*cyaB* is very moderate compared to the drastic growth defect of reported Δ*glxR* mutants. The observation that DNA-binding of GlxR *in vivo,* apparently occurs also in the absence of cAMP, raises the question if other, yet unknown factors, are involved in regulating *in vivo* GlxR-DNA binding.

2.1 Molecular basis of growth inhibition by acetate of an adenylate cyclase-deficient mutant of *Corynebacterium glutamicum*

Natalie Wolf[1], Michael Bussmann[1], Abigail Koch-Koerfges[1], Nino Katcharava[1], Julia Schulte[1], Tino Polen[1], Johannes Hartl[2], Julia A. Vorholt[2], Meike Baumgart[1] and Michael Bott[1]*

[1]IBG-1: Biotechnology, Institute of Bio- and Geosciences, Forschungszentrum Jülich, Jülich, Germany

[2]Institute of Microbiology, ETH Zürich, Zürich, Switzerland

*Corresponding author

Published in Frontiers in Microbiology, 11 February 2020 (doi: 10.3389/fmicb.2020.00087)

Author's contributions:

NW constructed mutants and plasmids and performed all experimental work except the one specified below for other authors. MBu constructed the Δ*cyaB* mutant and the plasmid pK19*mobsacB*-Δ*cyaB* and performed the growth experiment showed in Fig. 2. AKK performed the analysis of glucose and organic acids. NK and JS performed the growth experiments with the protonophore CCCP and the determination of the membrane potential. TP supervised genome resequencing and analysed the resulting data. JH and JAV performed LC-MS/MS measurements for cAMP determination. MBa coached the experimental work and supported the design of the study. All authors contributed to the interpretation of the data. NW wrote the first draft of the manuscript and prepared the figures and tables. MBo designed the study, supervised the experimental work, and wrote the final version of the manuscript.

Overall contribution **NW: 65%**

AKK: Abigail Koch-Koerfges, JAV: Julia Anne Vorholt-Zambelli, JH: Johannes Hartl, JS: Julia Schulte, MBa: Meike Baumgart, MBo: Michael Bott, MBu: Michael Bussmann, NK: Nino Katcharava, NW: Natalie Wolf, TP: Tino Polen

frontiers
in Microbiology

ORIGINAL RESEARCH
published: 11 February 2020
doi: 10.3389/fmicb.2020.00087

Molecular Basis of Growth Inhibition by Acetate of an Adenylate Cyclase-Deficient Mutant of *Corynebacterium glutamicum*

Natalie Wolf[1], Michael Bussmann[1], Abigail Koch-Koerfges[1], Nino Katcharava[1], Julia Schulte[1], Tino Polen[1], Johannes Hartl[2], Julia A. Vorholt[2], Meike Baumgart[1] and Michael Bott[1]*

[1] IBG-1: Biotechnology, Institute of Bio- and Geosciences, Forschungszentrum Jülich, Jülich, Germany, [2] Institute of Microbiology, ETH Zürich, Zurich, Switzerland

Edited by:
Haike Antelmann,
Freie Universität Berlin, Germany

Reviewed by:
Gerd M. Seibold,
Technical University of Denmark,
Denmark
Fabian M. Commichau,
Brandenburg University of Technology
Cottbus–Senftenberg, Germany
Reinhard Kraemer,
Universität zu Köln, Germany

***Correspondence:**
Michael Bott
m.bott@fz-juelich.de

Specialty section:
This article was submitted to
Microbial Physiology and Metabolism,
a section of the journal
Frontiers in Microbiology

Received: 13 November 2019
Accepted: 15 January 2020
Published: 11 February 2020

Citation:
Wolf N, Bussmann M,
Koch-Koerfges A, Katcharava N,
Schulte J, Polen T, Hartl J, Vorholt JA,
Baumgart M and Bott M (2020)
Molecular Basis of Growth Inhibition
by Acetate of an Adenylate
Cyclase-Deficient Mutant
of Corynebacterium glutamicum.
Front. Microbiol. 11:87.
doi: 10.3389/fmicb.2020.00087

In *Corynebacterium glutamicum*, cyclic adenosine monophosphate (cAMP) serves as an effector of the global transcriptional regulator GlxR. Synthesis of cAMP is catalyzed by the membrane-bound adenylate cyclase CyaB. In this study, we investigated the consequences of decreased intracellular cAMP levels in a Δ*cyaB* mutant. While no growth defect of the Δ*cyaB* strain was observed on glucose, fructose, sucrose, or gluconate alone, the addition of acetate to these growth media resulted in a severe growth inhibition, which could be reversed by plasmid-based *cyaB* expression or by supplementation of the medium with cAMP. The effect was concentration- and pH-dependent, suggesting a link to the uncoupling activity of acetate. In agreement, the Δ*cyaB* mutant had an increased sensitivity to the protonophore carbonyl cyanide *m*-chlorophenyl hydrazone (CCCP). The increased uncoupler sensitivity correlated with a lowered membrane potential of acetate-grown Δ*cyaB* cells compared to wild-type cells. A reduced membrane potential affects major cellular processes, such as ATP synthesis by F_1F_O-ATP synthase and numerous transport processes. The impaired membrane potential of the Δ*cyaB* mutant could be due to a decreased expression of the cytochrome bc_1-aa_3 supercomplex, which is the major contributor of proton-motive force in *C. glutamicum*. Expression of the supercomplex genes was previously reported to be activated by GlxR-cAMP. A suppressor mutant of the Δ*cyaB* strain with improved growth on acetate was isolated, which carried a single mutation in the genome leading to an Ala131Thr exchange in GlxR. Introduction of this point mutation into the original Δ*cyaB* mutant restored the growth defect on acetate. This supported the importance of GlxR for the phenotype of the Δ*cyaB* mutant and, more generally, of the cAMP-GlxR system for the control of energy metabolism in *C. glutamicum*.

Keywords: ***Corynebacterium glutamicum*, cAMP, adenylate cyclase, acetate, uncouplers, membrane potential, GlxR, cytochrome bc_1-aa_3 supercomplex**

INTRODUCTION

The Gram-positive soil bacterium *Corynebacterium glutamicum* was identified as a natural glutamate producer in the 1950s (Kinoshita et al., 1957). Since then, various strains of this bacterium are widely used for the production of amino acids, in particular L–glutamate and L–lysine (Eggeling and Bott, 2015). For several years now, *C. glutamicum* has also been employed in commercial protein production (Freudl, 2017). In addition, strains for the synthesis of numerous other industrially relevant compounds have been developed (Schneider and Wendisch, 2011; Becker and Wittmann, 2012; Wieschalka et al., 2013). The success in rational strain development by metabolic engineering is based on detailed studies of the metabolic and regulatory network of *C. glutamicum* (Eggeling and Bott, 2005; Burkovski, 2008; Yukawa and Inui, 2013). Furthermore, efficient novel technologies for strain development involving high-throughput screening approaches with single-cell metabolite biosensors based on transcriptional regulators have been established for *C. glutamicum* (Binder et al., 2012; Mustafi et al., 2012; Schendzielorz et al., 2014; Eggeling et al., 2015).

The transcriptional regulator GlxR, a homolog of the cAMP-receptor protein Crp of *Escherichia coli*, is a global regulator of *C. glutamicum* and activates or represses more than 100 genes. Transcriptional regulation by GlxR influences various cellular functions such as central carbon metabolism, respiration, ATP synthesis, or transport processes (Toyoda et al., 2011; Jungwirth et al., 2013). *In vitro,* purified GlxR binds to DNA when complexed with 3′,5′-cyclic adenosine monophosphate (cAMP) (Kim et al., 2004; Kohl et al., 2008; Bussmann et al., 2009). Crystal structures of apo- and cAMP-bound GlxR were solved and revealed conformational changes of the homodimer upon cAMP binding (Townsend et al., 2014). GlxR showed negative allosteric behavior, as binding of the first cAMP molecule ($K_{D1} = 17\ \mu M$) reduced the binding affinity of the second cAMP molecule ($K_{D2} = 130\ \mu M$) to the structurally identical site in the second monomer (Townsend et al., 2014). The affinity of purified GlxR to a double-stranded oligonucleotide containing a central GlxR consensus binding site increased about 100-fold upon cAMP binding from 8.3 μM to 87 nM (Townsend et al., 2014).

The intracellular cAMP level is determined by the rates of synthesis from ATP via adenylate cyclases (Shenoy et al., 2004), degradation to adenosine monophosphate (AMP) via phosphodiesterases (Richter, 2002), and possibly cAMP export and import processes. In *C. glutamicum*, a single adenylate cyclase was identified, which is encoded by the *cyaB* gene (cg0375) (Kalinowski et al., 2003). CyaB contains an N-terminal membrane-integral domain with six predicted transmembrane helices, which is linked via a HAMP domain to a class IIId catalytic domain (CHD). The HAMP domain might function as transmitter domain, as it was found to have a strong positive stimulatory effect on the adenylate cyclase activity of Rv3645 of *Mycobacterium tuberculosis*, which has the same domain composition as CyaB of *C. glutamicum* (Linder et al., 2004). A *C. glutamicum* mutant lacking about 200 bp of the coding region of the catalytic domain of CyaB (strain CgYA) showed strongly reduced cAMP levels both in glucose minimal medium and LB-acetate medium (Cha et al., 2010). Wild-type cAMP levels could be restored by plasmid-encoded *cyaB*, but not by supplementation of cAMP to the medium. Interestingly, this CgYA mutant had a strong growth defect in acetate and glucose-acetate minimal medium, but not in glucose or ethanol minimal medium (Cha et al., 2010). Since the activities of the glyoxylate cycle enzymes isocitrate lyase and malate synthase were even higher in the mutant than in the wild type (WT) during growth on LB-acetate, the authors speculated that the acetate uptake carrier might play a role in the growth defect of the CgYA mutant (Cha et al., 2010). Degradation of cAMP in *C. glutamicum* is catalyzed by the recently identified phosphodiesterase CpdA (Cg2761) (Schulte et al., 2017b). This enzyme belongs to the class II phosphodiesterases and deletion of the *cpdA* gene led to an increase of the intracellular cAMP concentration (Schulte et al., 2017b). The Δ*cpdA* mutant exhibited slower growth and a prolonged lag-phase on all tested carbon sources, including glucose, gluconate, citrate, acetate and ethanol (Schulte et al., 2017b). The growth defects could partially be complemented by overexpression of genes that are normally repressed by the cAMP-GlxR complex, such as *ptsI-ptsG* or *citH,* and that are involved in uptake or metabolism of the respective carbon source. This suggested that mainly the higher fraction of cAMP-bound GlxR caused by the increased cAMP level is responsible for the growth defects of the Δ*cpdA* mutant.

The major aim of our current study was to elucidate the molecular basis of the growth inhibition by acetate of a *C. glutamicum* mutant lacking the *cyaB* gene in order to understand the consequences of a reduced cAMP level. Our results suggest that the inhibitory effect of acetate is caused by its property to act as an uncoupler and that a Δ*cyaB* mutant has a reduced capability of generating membrane potential and possibly ATP by oxidative phosphorylation, which might be due to a reduced transcriptional activation of the genes encoding respiratory chain components and the *atp* operon. Support for the assumption that the growth defect of the Δ*cyaB* strain on acetate is due to a reduced activity of GlxR was obtained by the isolation of a suppressor mutant that had lost the growth defect on acetate. This mutant contained a single amino acid exchange in GlxR. In summary, we show that the cAMP level in combination with the global regulator GlxR plays an important role in the bioenergetics of *C. glutamicum*.

MATERIALS AND METHODS

Strains, Plasmids and Culture Conditions

All strains and plasmids used in this study are listed in **Table 1**. *C. glutamicum* strains were cultivated either in brain heart infusion (BHI) medium (Bacto^{TM} BHI, BD, Heidelberg, Germany) or in CGXII minimal medium (adjusted to pH 7.0 with KOH) supplemented with 3,4-dihydroxybenzoate (30 mg l^{-1}) as iron chelator and different carbon sources (Frunzke et al., 2008) as specified in the results section. For growth experiments, 5 ml BHI medium was inoculated with a single colony and incubated at 30°C and 130 rpm for 8 h. About 400 μl of this first preculture were used for the inoculation of the second

TABLE 1 | Bacterial strains and plasmids used in this study.

Strain or plasmid	Relevant characteristics	Source or references
Strains		
Escherichia coli DH5α	F$^-$ *thi-1 endA1 hsdR17*r-m +) *supE44*Δ*lacU169*Φ80*lacZ*Δ*M15*) *recA1 gyrA96 relA1*	Invitrogen
Escherichia coli BL21(DE3)	F$^-$ *ompT gal dcm lon hsdSB* (rB$^-$ mB$^-$) λ[DE3 (*lacI lacUV5-T7* gene 1 *ind1 sam7 nin5*)]	Studier and Moffatt, 1986
Corynebacterium glutamicum ATCC 13032	ATCC 13032, biotin-auxotrophic wild-type strain (WT)	Kinoshita et al., 1957
C. glutamicum Δ*cyaB*	ATCC 13032 with an in frame deletion of the adenylate cyclase gene *cyaB* (cg0375)	This study
C. glutamicum Δ*cpdA*	ATCC 13032 with an in frame deletion of the phosphodiesterase gene *cpdA* (cg2761)	Schulte et al., 2017b
C. glutamicum Δ*cyaB*Δ*cpdA*	ATCC 13032 with an in frame deletion of the gene *cyaB* and the phosphodiesterase gene *cpdA* (Δ*cyaB*Δ*cpdA*)	This study
*C. glutamicum*Δ*qcr*	ATCC 13032 with an in frame deletion of the *qcrCAB* genes (cg2405, cg2404, cg2403) encoding the three subunits of the cytochrome bc_1 complex	Niebisch and Bott, 2001
*C. glutamicum*Δ*cyaB*_sup1	*C. glutamicum* Δ*cyaB* suppressor mutant carrying a single genomic mutation (C to T) at position 307072 in BA000036.3 leading to the amino acid exchange Ala131Thr in GlxR (cg0350)	This study
*C. glutamicum*Δ*cyaB*_sup2	*C. glutamicum* Δ*cyaB* suppressor mutant carrying two genomic mutations in BA000036.3, one at position 877553 (A to G) located in the intergenic region of *serC* (cg0948) and *gltA* (cg0949) and one at position 1548741 (G to C) located in the intergenic region of *gpt* (cg1659) and cg1660	This study
*C. glutamicum*Δ*cyaB*_sup3	*C. glutamicum* Δ*cyaB* suppressor mutant carrying two genomic mutations in BA000036.3, one at position 307072 (C to T) leading to the amino acid exchange Ala131Thr in GlxR and one at position 2564086 (G to T) leading to a silent mutation of the Gly106 codon of ribose 5-phosphate isomerase (cg2658)	This study
*C. glutamicum::glxR*_A131T	*C. glutamicum* WT in which an Ala131Thr exchange in the *glxR* coding sequence was introduced by double homologous recombination	This study
*C. glutamicum*Δ*cyaB::glxR*_A131T	*C. glutamicum* Δ*cyaB* mutant in which an Ala131Thr exchange in the *glxR* coding sequence was introduced by double homologous recombination	This study
Plasmids		
pAN6	Kan^R; P$_{tac}$, *lacI*^{q} pBL1 oriV$_{Cg}$ pUC18 oriV$_{Ec}$, *C. glutamicum/E. coli* shuttle vector, derivative of pEKEx2	Frunzke et al., 2008
pAN6-*cyaB*	Kan^R; pAN6 derivative carrying the *cyaB* gene (cg0375) including 300 bp upstream of the start codon and a 3′-terminal StrepTag-II-encoding sequence under the control of an IPTG-inducible *tac* promoter	This study
pAN6-*glxR*-Twinstrep	Kan^R; pAN6 derivative carrying the *glxR* gene (cg0350) including a 3′-terminal Twinstrep-tag encoding sequence before the stop codon (WSHPQFEKGGGSGGGSGGSAWSHPQFEK)	This study
pAN6-*glxR*-A131T-Twinstrep	Kan^R; pAN6-*glxR*-Twinstrep derivative with a Ala131T exchange	This study
pK19*mobsacB*	Kan^R; oriT oriV$_{Ec}$ *sacB lacZ*α; vector for allelic exchange in *C. glutamicum*	Schäfer et al., 1994
pK19*mobsacB*-Δ*cyaB*	Kan^R; pK19*mobsacB* derivative containing an overlap extension PCR product covering the up- and downstream regions of *cyaB*	This study
pK19*mobsacB*-Δ*cpdA*	Kan^R; pK19*mobsacB* derivative containing an overlap extension PCR product covering the up- and downstream regions of *cpdA*	Schulte et al., 2017b
pK19*mobsacB*-*glxR*_mut	Kan^R; pK19*mobsacB* derivative containing a 800-bp PCR product covering the 3′-terminal 684 bp of *glxR* including the mutation leading to the Ala131Thr exchange and 116 bp of the downstream region	This study

preculture, which was cultivated for about 16 h at 30°C and 120 rpm in a 100 ml baffled shake flask containing 20 ml CGXII medium with 2% (w/v) glucose. For the main culture, 800 µl CGXII medium in FlowerPlates (m2p-labs, Baesweiler, Germany) was inoculated to an optical density at 600 nm (OD$_{600}$) of 1 and cultivated in a BioLector microcultivation system (m2p-labs, Baesweiler, Germany) at 1200 rpm, 30°C and 80% humidity. Growth was followed by measuring the backscatter at 620 nm, which reflects the cell density (Kensy et al., 2009). For cultivations in 500 ml shake flasks, 50 ml CGXII medium was inoculated with the second preculture to an OD$_{600}$ of 1. The cultivations in shake flasks were performed at 30°C and 120 rpm and growth was followed by measuring OD$_{600}$. *E. coli* DH5α was used as host for all cloning purposes and was cultivated at 37°C in LB medium (Sambrook and Russell, 2001). When required, media were supplemented with kanamycin (25 µg ml^{-1} for *C. glutamicum* and 50 µg ml^{-1} for *E. coli*).

Construction of Plasmids and Deletion Mutants

Plasmids were constructed by standard cloning procedures (Sambrook and Russell, 2001) using the oligonucleotides listed in **Supplementary Table S1**. Deletion mutants of *C. glutamicum* were constructed by double homologous recombination as described previously (Niebisch and Bott, 2001). In brief, *C. glutamicum* ATCC 13032 was transformed with the deletion plasmid carrying the up- and downstream regions of the target gene to be deleted. After selection for the first (kanamycin resistance) and second (kanamycin sensitivity, sucrose tolerance) recombination events, Kan^S-Suc^R clones were analyzed by colony

PCR and the PCR product of clones carrying the desired deletion was further verified by sequencing.

For construction of a Δ*cyaB* deletion mutant, it had to be considered that the length of the coding region of *cyaB* varies in different annotations, resulting in proteins of either 347 amino acids (MRPVAA...; Cgl0311 of strain ATCC 13032) (Ikeda and Nakagawa, 2003), 547 amino acids (MDTVLE...; Cg0375 of strain ATCC 13032) (Kalinowski et al., 2003), or 501 amino acids (MKWLWG...; cgR_0397 of strain R) (Yukawa et al., 2007). RNAseq analysis of strain ATCC 13032 identified a single transcriptional start site presumably leading to a leaderless *cyaB* mRNA encoding a protein of 508 amino acids (MSRLLR...) (Pfeifer-Sancar et al., 2013). We therefore assumed the latter size to be the correct one, although additional transcriptional start sites and CyaB variants of other length cannot be excluded. For construction of the Δ*cyaB* mutant, we deleted the entire coding region except for the 5′-terminal 37 codons and the 3′-terminal 12 codons including the stop codon. After the second homologous recombination event, nine kanamycin-sensitive and sucrose-resistant clones were analyzed by colony PCR. Four clones harbored the *cyaB* deletion whereas five clones contained the wild-type fragment. Thus, the Δ*cyaB* deletion mutant was obtained without any difficulties.

Isolation of Δ*cyaB* Suppressor Mutants With Improved Growth on Acetate

The acetate-sensitive Δ*cyaB* strain was cultivated in CGXII medium with 150 mM potassium acetate as sole carbon source. The culture was prepared as described above. To obtain acetate-tolerant suppressor clones, cultivations were performed for at least 90 h in a BioLector. Cultures that started to grow and reached comparable backscatter values as the WT were streaked out on BHI agar plates and single colonies were inoculated again in CGXII medium with 150 mM potassium acetate. Cultures that grew better than the Δ*cyaB* parental strain were streaked out again on BHI agar plates. The genomic DNA of such clones was isolated and used for whole genome sequencing.

Genomic DNA Sequencing

DNA of the samples was purified with the DNeasy Blood and Tissue kit (Qiagen, Hilden, Germany) starting with the "pretreatment of Gram-positive bacteria," as described in the manufacturer's instructions. The obtained DNA was dried and resuspended in max. 100 μl ddH$_2$O. For library preparation, the NEBNext Ultra II DNA Library Prep kit for Illumina (New England Biolabs GmbH, Frankfurt am Main, Germany) was used with 2 μg genomic DNA of each sample following the manufacturer's instructions. The resulting indexed libraries were quantified using the KAPA Library Quantification kit (VWR International GmbH, Darmstadt, Germany) and normalized for pooling. Sequencing was performed on a MiSeq instrument (Illumina, San Diego, CA, United States) using paired-end sequencing with a read-length of 2 × 150 bp. Data analysis and base calling were accomplished with the CLC Genomics workbench (Qiagen, Hilden, Germany). Reads of the parental Δ*cyaB* strain and the suppressor strains were mapped to the genome sequence BA000036.3 of *C. glutamicum* ATCC 13032 (Ikeda and Nakagawa, 2003).

Determination of mRNA Levels by Reverse Transcription Quantitative PCR (RT-qPCR)

For quantifying the mRNA levels of *ctaD*, *ctaC*, and *qcrC* in *C. glutamicum* WT and the Δ*cyaB* mutant, RT-qPCR was performed. Cells were grown in CGXII medium containing a glucose-acetate mixture (100 mM each) and harvested at an OD$_{600}$ of 6. Cells were disrupted by the addition of QIAzol Lysis Reagent (Qiagen, Hilden, Germany) followed by bead beating with a Precellys24 device (Peqlab Biotechnologie, Erlangen, Germany). RNA was purified and concentrated with an RNeasy Mini kit (Qiagen, Hilden, Germany) including a DNase I treatment. Reverse transcription of total RNA samples to cDNA was performed using Superscript^{TM} III reverse transcriptase and random primers (Invitrogen, Carlsbad, CA, United States) following the manufacturer's instructions. For the quantitative PCR, KAPA SYBR® FAST qPCR Master Mix (2×) (Roche, Basel, Switzerland) was used following the manufacturer's protocol. Primer pairs used for the reactions are listed in **Supplementary Table S1**. As reference gene, *hpt* (cg2985) was used with the oligonucleotides listed in **Supplementary Table S1**. Fluorescence measurements and analysis of the results were conducted using a qTower 2.2 and the software qPCR-soft 3.1 (Analytic Jena, Jena, Germany). RNA was isolated from three independent cultures of each strain (biological triplicates) and for each sample technical duplicates were performed.

Global Gene Expression Analysis Using DNA Microarrays

Preparation of RNA and synthesis of fluorescently labeled cDNA were carried out as described (Möker et al., 2004). Custom-made DNA microarrays for *C. glutamicum* ATCC 13032 printed with 70mer oligonucleotides were obtained from Operon (Cologne, Germany) and are based on the genome sequence entry NC_006958 (Kalinowski et al., 2003). Hybridization and stringent washing of the microarrays were performed according to the instructions of the supplier. Processed and normalized data as well as experimental details (Brazma et al., 2001) were stored in the in-house microarray database for further analysis (Polen and Wendisch, 2004). Using the DNA microarray technology, the genome-wide mRNA concentrations of *C. glutamicum* wild type were compared with those of the mutant strain *C. glutamicum*Δ*cyaB*. The strains were cultivated in CGXII medium with a glucose-acetate mixture (100 mM each). RNA used for the synthesis of labeled cDNA was prepared from cells in the exponential growth phase. Three independent DNA microarray experiments were performed, each starting from independent cultures.

Determination of cAMP

Cell extracts were prepared as described previously (Schulte et al., 2017b) and the cAMP concentration was measured without dilution with the direct cAMP ELISA kit (Enzo Life Sciences

GmbH, Lörrach, Germany) following the manufacturer's instructions. Amounts of cAMP were related to the protein content of the supernatant of the cell extract. The product specification of the used cAMP ELISA kit (Direct cAMP ELISA kit; Enzo, Lausen, Switzerland) reports the following cross-reactivities with nucleotides other than cAMP, which is set as 100%: AMP, 0.33%; ATP, 0.12%; cyclic GMP, GMP, GTP, cyclic UMP, CTP, all <0.001%. For determining the cross-reactivities, the nucleotides were dissolved in assay buffer to a concentration of 2000 pmol/ml, which is 10-fold higher than the highest concentration used for cAMP in the non-acetylated variant of the assay. The apparent concentrations determined for the non-cAMP nucleotides, e.g., 6.6 pmol/ml for AMP, was divided by the real AMP concentration in the assay (2000 pmol/ml) and multiplied with 100 to give the cross-reactivity in%.

Additionally, intracellular cAMP was measured by LC-MS/MS. *C. glutamicum* cells were grown to the exponential phase (OD_{600} of ∼5). For the sampling, cells from a culture volume corresponding to 4 ml of OD_{600} of 1 were harvested. Sampling, quenching, metabolite extraction and measurements were performed as previously described (Müller et al., 2015; Hartl et al., 2017). Briefly, metabolite separation was achieved by reverse-phase-ion-pairing (tributylamin) liquid chromatography using a nLC-ultra (Eksigent) system. The LC was hyphenated to a QExactive Plus Orbitrap (Thermo Fisher) mass spectrometer with an electrospray ionization probe. The MS was operating in negative mode; the resolution was set to 70,000 (at m/z 200). cAMP was measured using parent reaction monitoring (PRM) with m/z 328.045 as the precursor ion and quantified with the corresponding m/z 134.0465 fragment. Fragmentation was achieved by higher energy collisional dissociations (HCDs) with a normalized collision energy (NCE) of 30.0. cAMP was identified by exact mass (m/z tolerance of 0.003 Da) as well as matching retention time and fragmentation pattern with an analytical 3′,5′-cAMP standard. cAMP was quantified by peak integration using the trapezoid rule; absolute quantification was performed by external calibration. The calibration curve of reference solutions with known cAMP concentrations was fitted by linear regression. The intracellular cAMP concentrations in *Corynebacterium* were estimated assuming a correlation factor of 250 mg cell dry weight (CDW) l^{-1} at OD_{600} of 1 (Kabus et al., 2007) and a corresponding intracellular volume of 1.44 μl per mg CDW (da Luz et al., 2016). The limit of detection (LOD) was estimated to be 14 amol l^{-1} by calculating 3.3 standard deviations of the y-intercepts divided by the slope obtained from linear regression (ICH, 2005) of reference cAMP solutions; the LOD was confirmed by visual inspection. Assuming similar dilution factors as for measured *Corynebacterium* extracts, this corresponds to an LOD of ∼0.1 μmol l^{-1} from cell extracts.

Measurement of Membrane Potential via Flow Cytometry

The membrane potential of *C. glutamicum* cells was determined by flow cytometry using the fluorescent dye 3,3′-diethyloxacarbocyanine iodide [DiOC2(3)] (Novo et al., 1999, 2000). The assay was performed according to a previously established protocol for *C. glutamicum* (Neumeyer et al., 2013). In brief, the strains were cultivated in baffled shake flasks with 50 ml CGXII medium containing either 100 mM glucose, or 100 mM acetate, or 200 mM acetate (precultures as described for the BioLector cultivation). Measurement of the membrane potential was performed when cells had reached the mid-exponential growth phase (OD_{600} of ∼5). The culture was diluted with FACSFlow^{TM} buffer to an OD_{600} of 0.05 and cells were stained for 30 min with 30 μM DiOC2(3) (3 mM stock solution in dimethyl sulphoxide, Sigma-Aldrich, Germany) and analyzed using a FACS Aria II and BD Diva software (BD Biosciences, Heidelberg, Germany). Green fluorescence was measured at an excitation wavelength of 488 nm and an emission wavelength of 497 nm, red fluorescence at an excitation wavelength of 488 nm and an emission wavelength of 610 nm. For each sample, 100,000 cells were measured at 2000 cells s^{-1}. The red/green fluorescence ratio was analyzed using FlowJo V.10 software and plotted as a histogram with GraphPad Prism8.

Quantitative Determinations of Carbon Sources

Glucose, gluconate and acetate concentrations in culture supernatants were determined as described (Koch-Koerfges et al., 2012) by ion-exchange chromatography using an Agilent 1100 HPLC system (Agilent Technologies, Waldbronn, Germany) equipped with a cation exchange column (Organic Acid Resin 300 × 8 mm, CS Chromatographie Service, Langerwehe, Germany). Isocratic elution within 40 min with 100 mM H_2SO_4 and a flow rate of 0.4 ml/min at 40°C was used. Organic acids were detected using a diode array detector at 215 nm and glucose was analyzed by a refraction index (RI) detector in the same run. The quantification of organic acids and glucose was based on a calibration curve with external standards.

TMPD Enzyme Assay

N,*N*,*N*′,*N*′-tetramethyl-*p*-phenylenediamine (TMPD) oxidase activity was measured spectrophotometrically at 562 nm in a 96-well plate with an Infinite M1000 PRO microplate reader (Tecan, Männedorf, Switzerland). TMPD was added to 100 mM Tris–HCl buffer pH 7.5 containing isolated membrane proteins to a final concentration of 200 μM. For the calculation of the TMPD oxidation rate, an extinction coefficient of 10.5 mM^{-1} cm^{-1} was used (Sakamoto et al., 2001). The autoxidation rate of TMPD was recorded using samples containing only buffer and 200 μM TMPD and subtracted from the rates of the membranes. The cells for these measurements were cultivated at 30°C and 90 rpm in 5 l baffled shake flasks with 500 ml CGXII medium and glucose plus acetate (100 mM each) as carbon source. The cultures were harvested in the exponential growth phase at the OD_{600} of 10. The preparation of cell membranes was performed as described (Niebisch and Bott, 2003).

Electrophoretic Mobility Shift Assays (EMSAs) With Purified GlxR

EMSAs were performed to compare *in vitro* binding of the wild-type GlxR protein ($GlxR_{WT}$) and the variant $GlxR_{A131T}$ to selected DNA target sites. The gene *glxR* was amplified from genomic DNA of *C. glutamicum* WT with the oligonucleotides GlxR-twin1 and GlxR-twin2. A DNA fragment with a Twin-Strep tag-encoding sequence was amplified with the oligonucleotides GlxR-twin3 and GlxR-twin4 using a suitable plasmid with the corresponding sequence as template. Gibson assembly was performed with pAN6 cut with *Nde*I and *Nhe*I, the *glxR* fragment and the Twinstrep-tag fragment resulting in the plasmid pAN6-*glxR*-Twinstrep. The oligonucleotides GlxR-A131T_fw and GlxR-A131T_rv were used to introduce the mutation leading to the amino acid exchange A131T in GlxR using the QuickChange Site-Directed Mutagenesis Kit (Agilent, Waldbronn, Germany). The resulting plasmid was named pAN6-*glxR*-A131T-Twinstrep. Overproduction of $GlxR_{WT}$ or $GlxR_{A131T}$ was performed by cultivation of *E. coli* BL21(DE3) transformed with pAN6-*glxR*-Twinstrep or pAN6-*glxR*-A131T-Twinstrep in ZYM-5052 auto-induction medium (Studier, 2005). After harvesting and disrupting the cells, proteins were purified using Strep-Tactin XT affinity chromatography according to the protocol of the supplier (IBA Life Sciences, Göttingen, Germany). Subsequently, the proteins were further purified by size exclusion chromatography using a Superdex 200 increase column using a buffer composed of 100 mM Tris–HCl pH 7.5, 5% (v/v) glycerol, 100 mM KCl, 20 mM $MgCl_2$, and 1 mM EDTA.

EMSAs were performed as described previously (Bussmann et al., 2009) using the following DNA fragments: (i) a 140 bp DNA fragment upstream of *ctaD* extending from −127 to −261 upstream of the *ctaD* start codon; (ii) a 132 bp DNA fragment upstream of *ctaCF* extending from −102 to −234 upstream of the *ctaC* start codon; and (iii) a 136 bp DNA fragment covering an intragenic region of the gene cg3153. The first two DNA fragments contain previously described GlxR binding sites (Kohl et al., 2008; Toyoda et al., 2011). The respective DNA fragments were generated by PCR and purified with the DNA Clean & Concentrator Kit (Zymo Research, Freiburg im Breisgau, Germany).

RESULTS AND DISCUSSION

cAMP Levels in *C. glutamicum* WT and Mutants Lacking *cyaB* or *cpdA*

In order to confirm previous studies with the *C. glutamicum* mutant strain CgYA lacking approximately 200 bp coding region of the catalytic domain of the adenylate cyclase CyaB (Cha et al., 2010), we constructed another Δ*cyaB* mutant lacking almost the entire coding region (see section "Materials and Methods"). The cAMP level of this mutant was compared with that of the WT and the Δ*cpdA* mutant lacking the cAMP phosphodiesterase (Schulte et al., 2017b) using an enzyme-linked immunosorbent assay (ELISA). The strains were grown in CGXII glucose medium to an OD_{600} of about 5 (exponential growth phase). As shown in **Table 2**, the cAMP level of the Δ*cyaB* mutant (∼20 pmol (mg protein)$^{-1}$) amounts to only 20% of the cAMP level of the WT (∼100 pmol (mg protein) $^{-1}$), whereas that of the Δ*cpdA* mutant was higher (∼144 pmol (mg protein) $^{-1}$). These results confirmed that the lack of the adenylate cyclase CyaB causes a strong decrease of the cAMP level, which is in agreement with previous results (Cha et al., 2010; Toyoda et al., 2011; Schulte et al., 2017b). It should be noted that the absolute values obtained in the ELISA measurements published in these studies differ significantly.

Bioinformatic analysis revealed only a single adenylate cyclase-encoding gene (*cyaB*) in the genome of *C. glutamicum*. Therefore, deletion of *cyaB* should result in the complete lack of the cAMP. However, both in our Δ*cyaB* mutant as well as in previously analyzed *cyaB* mutants of strain ATCC 13032 (Cha et al., 2010) and strain R (Toyoda et al., 2011), a residual cAMP level was measured by ELISA assays, raising the question for the source of this residual cAMP. The kit used in this study (Enzo Life Sciences GmbH, Lörrach, Germany) shows low cross-reactivity to AMP and ATP, which might contribute to the residual signal in the Δ*cyaB* mutant. Alternatively or additionally, *C. glutamicum* might possess another enzyme with adenylate cyclase activity besides CyaB, which contributes to the residual cAMP level in the Δ*cyaB* mutants and which is not detectable in bioinformatic searches using members of the known classes of adenylate cyclases (Shenoy et al., 2004). If a yet unknown novel enzyme with adenylate cyclase activity exists in *C. glutamicum*, a deletion of the *cpdA* gene in the Δ*cyaB* background might lead to an increase of cAMP. Therefore, we constructed a Δ*cyaB*Δ*cpdA* double mutant and determined the cAMP level by the ELISA kit. Although a small increase was detected for the double mutant, the difference to the Δ*cyaB* mutant was not significant (**Table 2**). In growth experiments with glucose or acetate minimal medium, the Δ*cyaB*Δ*cpdA* mutant behaved like the Δ*cyaB* mutant (**Supplementary Figure S1**), arguing against the existence of an alternative adenylate cyclase besides CyaB.

TABLE 2 | cAMP levels in various *C. glutamicum* strains cultivated in CGXII medium with 100 mM glucose.

***C. glutamicum* strain**	**Intracellular cAMP concentration**[1]	
	pmol mg^{-1} protein (determined by ELISA)	**μM (determined by LC-MS/MS)**
WT	99.9 ± 31.8	0.9 ± 0.4
Δ*cyaB*	20.5 ± 4	n.d.[2]
Δ*cpdA*	144.1 ± 7.9	3.4 ± 1.5
Δ*cyaB*Δ*cpdA*	30 ± 6.8	n.d.

[1] *Each value represents the mean value with the standard deviation of three biological replicates.* [2] *n.d., not detectable.*

As the ELISA-based assay might be influenced by cross-reacting metabolites, LC-MS/MS was applied as an alternative method to quantify cAMP levels. With this method, we determined an absolute concentration of cAMP of ~1 μM in wild-type cells, whereas a ~3.5-fold higher concentration was determined in the Δ*cpdA* mutant. cAMP was not detected in the Δ*cyaB* mutant and in the Δ*cyaB*Δ*cpdA* double mutant. These results support the possibility that the residual cAMP levels determined by the ELISA assay in the latter two mutants might be caused by cross-reactivities and suggest that CyaB is the only adenylate cyclase present in *C. glutamicum*.

Sensitivity of the Δ*cyaB* Mutant to Acetate

Growth of the Δ*cyaB* mutant and the WT with different carbon sources was compared using the BioLector cultivation system. In CGXII minimal medium containing 100 mM of either glucose, gluconate, fructose, or sucrose as carbon source, the Δ*cyaB* mutant grew like the WT, whereas a clear growth defect was observed for the mutant when 100 mM acetate served as carbon source (**Figure 1**). In media containing mixtures of gluconate and acetate, glucose and acetate, fructose and acetate, or sucrose and acetate (100 mM of each carbon source), the Δ*cyaB* mutant showed a strong growth defect, whereas the WT was unaffected and grew to higher cell densities (measured as higher backscatter values) (**Figure 1**). The data obtained with the Δ*cyaB* mutant for glucose, acetate, and the glucose-acetate mixture are in agreement with those described previously for the CgYA mutant, whereas the results for fructose-acetate and sucrose-acetate disagree, as growth of the CgYA mutant on these mixtures was reported not to be impaired (Cha et al., 2010). Our results indicate that acetate inhibits growth of the Δ*cyaB* mutant irrespective of the presence of an additional carbon source.

With respect to the inhibitory effect of acetate, ethanol is a particularly interesting carbon source, as its catabolism in *C. glutamicum* involves acetate as an intermediate. Ethanol degradation proceeds via the initial oxidation to acetaldehyde by

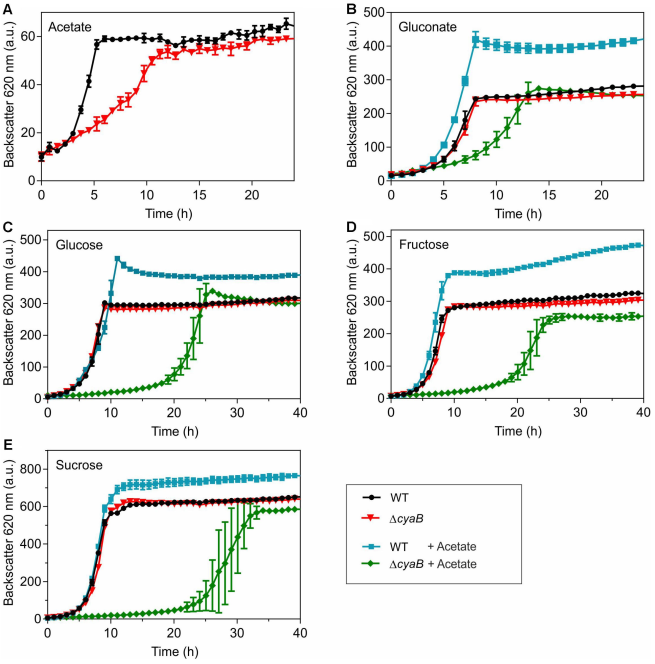

FIGURE 1 | Growth of *C. glutamicum* WT and the Δ*cyaB* mutant in CGXII medium with **(A)** 100 mM acetate, **(B)** 100 mM gluconate or gluconate-acetate mixture (100 mM each), **(C)** 100 mM glucose or glucose-acetate mixture (100 mM each), **(D)** 100 mM fructose or fructose-acetate mixture (100 mM each), and **(E)** 100 mM sucrose or sucrose-acetate mixture (100 mM each). Mean values and standard deviations of three biological replicates are shown.

alcohol dehydrogenase followed by a second oxidation to acetate by acetaldehyde dehydrogenase (Arndt and Eikmanns, 2007; Arndt et al., 2008). Acetate is then converted via acetyl phosphate to acetyl-CoA by acetate kinase and phosphotransacetylase and acetyl-CoA is oxidized in the TCA cycle with the glyoxylate cycle serving as an anaplerotic reaction (Wendisch et al., 2000; Gerstmeir et al., 2003; Bott, 2007). As shown in **Supplementary Figure S2**, the Δ*cyaB* mutant grew like the WT in CGXII medium containing 150 mM ethanol as carbon source. This result is in agreement with data reported previously for the CgYA mutant (Cha et al., 2010) and shows that acetate degradation is functional in the Δ*cyaB* mutant.

Growth of the WT and the Δ*cyaB* mutant was also compared in shake flasks in order to be able to follow the consumption of the carbon sources during cultivation (**Figure 2**). The growth defect of the Δ*cyaB* mutant during growth on a glucose-acetate mixture (100 mM each) was confirmed and resulted in a retarded consumption of both carbon sources compared to the WT. In CGXII medium containing a gluconate-acetate mixture, the Δ*cyaB* mutant also showed a growth defect and retarded consumption of gluconate and acetate compared to the WT. In contrast to glucose, fructose, and sucrose, gluconate is not taken up via the PEP-dependent phosphotransferase system (PTS), but via the secondary transporter GntP (Frunzke et al., 2008). The fact that acetate was completely consumed confirms that acetate catabolism is functional in the Δ*cyaB* mutant.

Abolishment of the Growth Defect of the Δ*cyaB* Mutant in the Presence of Acetate

The Δ*cyaB* mutant and the WT were transformed with the *cyaB* expression plasmid pAN6-*cyaB* or the parent vector pAN6. As shown in **Figure 3**, the growth defect of the Δ*cyaB* mutant in glucose-acetate medium was abolished by plasmid-based

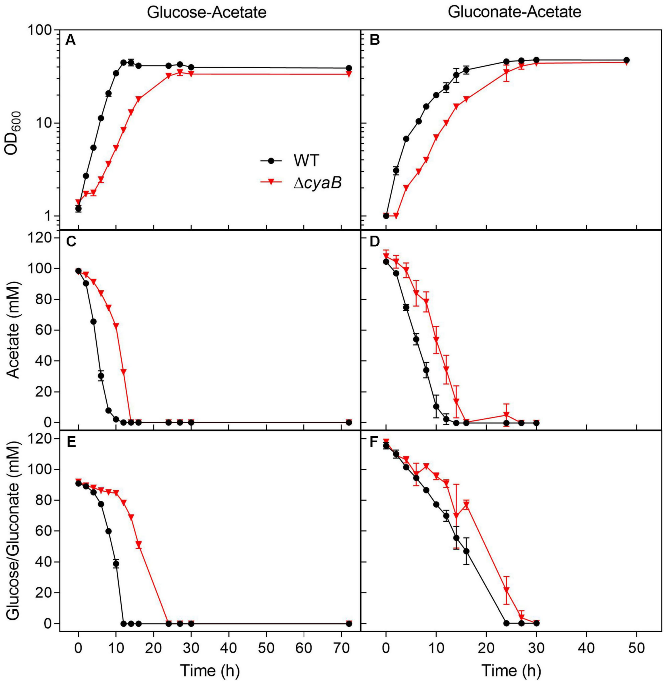

FIGURE 2 | Growth and substrate consumption of *C. glutamicum* WT and its Δ*cyaB* mutant in CGXII minimal medium containing either **(A)** glucose and acetate (100 mM each) or **(B)** gluconate and acetate (100 mM each). Panels **(C,D)** show the acetate consumption by the cultures displayed in panels **(A,B)**. Panel **(E)** shows the glucose consumption of the cultures displayed in panel **(A)**. Panel **(F)** shows the gluconate consumption of the cultures displayed in panel **(B)**. The strains were cultivated at 30°C and 120 rpm in 500 ml baffled shake flasks containing 50 ml CGXII minimal medium with the depicted carbon source. Mean values and standard deviations of three biological replicates are shown.

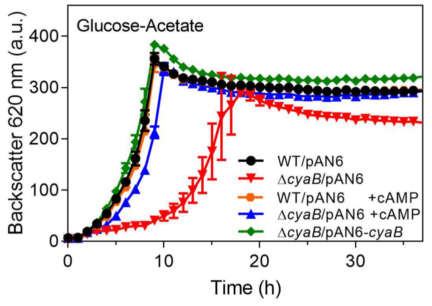

FIGURE 3 | Complementation of the Δ*cyaB* mutant with plasmid-encoded *cyaB* (pAN6-*cyaB*) or the addition of 10 mM extracellular cAMP (+ cAMP). The cultures contained 0.25 mM IPTG, 25 μg ml^{-1} kanamycin and, where indicated, 10 mM cAMP. Mean values and standard deviations of three biological replicates are shown.

expression of *cyaB*, but not by the presence of the vector alone. This result confirmed that the *cyaB* deletion rather than a hypothetical secondary mutation that might have occurred during mutant construction was responsible for the acetate sensitivity. In a previous study, we showed that cAMP addition to the medium influences GlxR-based gene expression, indicating that it can enter the cell (Schulte et al., 2017a). We therefore tested the influence of cAMP addition on growth of the Δ*cyaB* mutant and could show that 10 mM cAMP abrogated the growth defect in the presence of acetate, confirming that it is due to a lowered cAMP level (**Figure 3**). In the case of the CgYA mutant, addition of cAMP to the medium could not reverse the growth inhibition (Cha et al., 2010). The reason for this discrepancy is unknown. Uptake of 3′,5′-cAMP was previously reported for *E. coli* and marine bacteria, but no distinct transporter could be identified (Saier et al., 1975; Goldenbaum and Hall, 1979; Ammerman and Azam, 1982).

Concentration and pH Dependency of Growth Inhibition of the Δ*cyaB* Mutant by Acetate

As described above, the inhibitory effect of acetate on growth of the Δ*cyaB* mutant was independent of the presence of additional carbon sources. The difference when comparing growth on ethanol and growth on acetate is that during ethanol degradation acetate is only a metabolic intermediate that does not accumulate to high concentrations but is directly catabolized. In contrast, when acetate is used as carbon source, it is present in a high concentration outside of the cell. It was speculated that inhibition of acetate uptake by the secondary monocarboxylate transporter MctC (Cg0953) might play a role for the growth defect (Cha et al., 2010). However, under the conditions used in our studies (100 mM acetate, pH 7), uptake of acetate by passive diffusion is completely sufficient, as shown by the fact that growth of a *mctC* deletion mutant on acetate at pH 7 was unaffected (Jolkver et al., 2009).

Based on the above considerations, we assumed that the inhibitory effect of acetate on growth of the Δ*cyaB* mutant is due to its property to act as an uncoupler (Axe and Bailey, 1995; Pinhal et al., 2019). We tested whether the inhibitory effect of acetate is concentration- and pH-dependent. Weak acids such as acetate become more effective as proton translocator when the pH gets closer to their pK_a (4.76 in the case of acetic acid). In a first set of experiments, the WT and the Δ*cyaB* mutant were grown in CGXII medium containing 100 mM, 150 mM, or 200 mM acetate. In the case of the WT, increased acetate concentrations led to increased cell densities, but did not affect the growth rate strongly. In contrast, growth inhibition of the Δ*cyaB* mutant clearly correlated with increasing acetate concentrations (**Figure 4A**). The dose-dependent negative impact of acetate on growth of the Δ*cyaB* mutant was also observed in cultivations in CGXII medium with 100 mM glucose and either 50 mM or 100 mM acetate (**Supplementary Figure S3**). Furthermore, the inhibitory effect of acetate was observed independent of whether sodium acetate or potassium acetate were used for preparation of the media, showing that this effect is not caused by the cation (data not shown). For testing the pH dependency of growth inhibition by acetate, the MOPS buffer of the standard CGXII medium was substituted by a mixture of 20 g l^{-1} MOPS (pK_a 7.20) and 20 g l^{-1} MES (pK_a 6.15) and pH values of 6.0, 6.5, and 7.0 were adjusted by addition of KOH or HCl. Besides media with 100 mM acetate, also media with 100 mM glucose were used at the indicated pH values. As shown in **Figure 4B**, growth of the WT and the Δ*cyaB* mutant in glucose medium was comparable and hardly affected by the initial pH value. In contrast, growth of the mutant in acetate medium was strongly affected by the pH, showing almost no growth at pH 6.5 and pH 6.0 (**Figure 4C**). In summary, the inhibitory effect of acetate on growth of the Δ*cyaB* mutant was both concentration- and pH-dependent, supporting our assumption that it is due to the uncoupling properties of acetate.

Uncoupler Sensitivity and Membrane Potential of WT and the Δ*cyaB* Mutant

The results described above suggested that the Δ*cyaB* mutant is more sensitive to uncouplers than the WT. To further confirm this assumption, the influence of the protonophore carbonyl cyanide *m*-chlorophenyl hydrazone (CCCP) (Heytler and Prichard, 1962) on growth in CGXII medium with glucose was tested (**Figures 5A,B**). The Δ*cyaB* mutant was more sensitive to CCCP than the WT. In the presence of 5 μM CCCP, the mutant was stronger inhibited than the WT. In the presence of 10 μM CCCP, the mutant was not able to grow any more, while the WT showed residual growth. At 15 μM CCCP, neither strain was able to grow.

The increased sensitivity to acetate and CCCP of the Δ*cyaB* mutant compared to the WT might be due to a reduced capability of the mutant to build up pmf, which is composed of the membrane potential Δψ and the pH gradient ΔpH (Nicholls and Ferguson, 2002). At pH 7, the

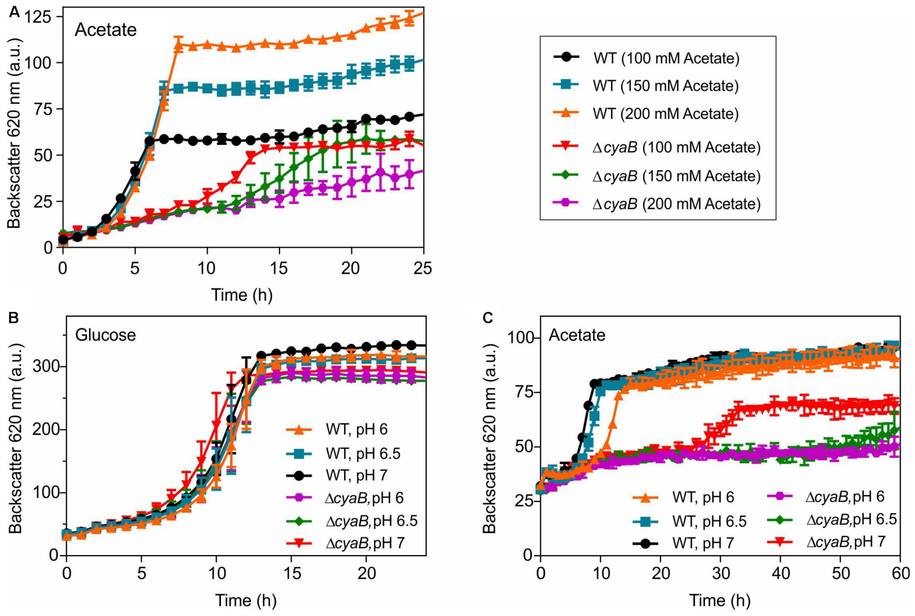

FIGURE 4 | Growth of *C. glutamicum* WT and the Δ*cyaB* mutant in CGXII medium with increasing sodium acetate concentrations **(A)**. pH dependency of growth of *C. glutamicum* WT and the Δ*cyaB* mutant in modified CGXII medium containing 20 g l^{-1} MOPS and 20 g l^{-1} MES buffer (pH adjusted with either KOH or HCl) with either 100 mM glucose **(B)** or 100 mM acetate **(C)** as carbon source. Mean values and standard deviations of three biological replicates are shown.

pmf of *C. glutamicum* WT is about 200 mV and formed almost exclusively by the membrane potential of 180 mV (Follmann et al., 2009; Koch-Koerfges et al., 2012). We compared $\Delta\psi$ of the WT and the Δ*cyaB* mutant using the dye 3,3′-diethyloxacarbocyanine iodide [$DiOC_2(3)$], which exhibits green fluorescence in all stained bacteria and shifts toward red emission due to self-association of dye molecules in dependency of $\Delta\psi$. Higher $\Delta\psi$ correlates with increased red fluorescence and the ratio of red/green fluorescence gives a relative measure of the membrane potential (Novo et al., 1999, 2000). This method does not give absolute values for the membrane potential but is useful for relative comparison of the membrane potential of different strains.

Using a previously established protocol (Neumeyer et al., 2013) we first confirmed that treatment of wild-type cells grown in CGXII glucose medium with 50 μM CCCP led to the expected decrease of the red/green fluorescence ratio indicating a collapsed or strongly reduced $\Delta\psi$ (**Figure 5C**, panel I). When cells of the WT and the Δ*cyaB* mutant cultivated in glucose medium to the exponential growth phase were analyzed, no significant differences of the red/green ratio was observed, indicating that both strains had a comparably high $\Delta\psi$ (**Figure 5C**, panel II). The histograms differed, however, when the strains were cultivated in CGXII medium with 100 mM acetate as carbon source. In this case, the mean fluorescence ratio of wild-type cells was almost unaltered, whereas that of the Δ*cyaB* mutant was strongly decreased (**Figure 5C**, panel III). This shift of the red/green ratio indicates that the membrane potential of the Δ*cyaB* mutant is reduced compared to the membrane potential of the WT. For wild-type cells cultivated with 200 mM acetate, the mean fluorescence ratio was reduced compared to cells grown with glucose or 100 mM acetate, in line with the concentration-dependent uncoupling effect of acetate, but the ratio of the Δ*cyaB* mutant was much stronger affected (**Figure 5C**, panel IV). These results indicate that acetate affects $\Delta\psi$ of the Δ*cyaB* mutant much more strongly than $\Delta\psi$ of the WT.

Role of the Cytochrome bc_1-aa_3 Supercomplex for Acetate Sensitivity

The results described above suggest that the cAMP deficiency of the Δ*cyaB* mutant causes a reduced ability to maintain a high membrane potential in the presence of the uncoupler

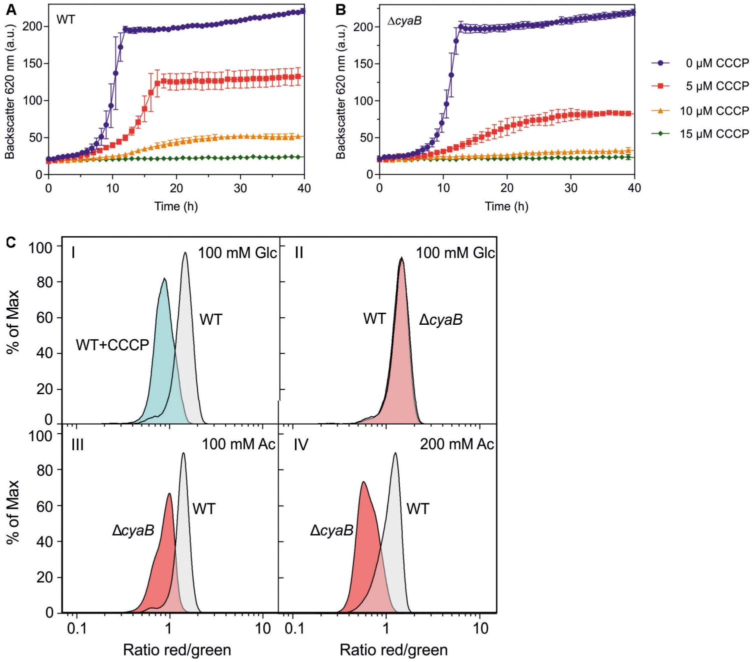

FIGURE 5 | Growth of *C. glutamicum* WT **(A)** and the Δ*cyaB* mutant **(B)** in CGXII medium with 2% (w/v) glucose in the presence of different CCCP concentrations. Mean values and standard deviations of three biological replicates are shown. **(C)** Relative comparison of the membrane potential (ΔΨ) of *C. glutamicum* cells by flow cytometry of [DiOC2(3)]-stained cells. Overlays of the histograms obtained with WT cells and Δ*cyaB* mutant cells are shown. The percentage of analyzed cells (% of Max) is plotted versus the logarithm of the red/green fluorescence ratio. This ratio serves as an indicator of ΔΨ, with a high value corresponding to a high ΔΨ. Panel I shows a control experiment with glucose-grown WT cells that were treated for 15 min without or with 50 µM CCCP to collapse ΔΨ. Panels II, III, and IV show comparisons of WT and Δ*cyaB* cells cultivated in CGXII medium with either 100 mM glucose (II), 100 mM acetate (III), or 200 mM acetate (IV). Representative histograms of three biological and three technical replicates each are shown. The histograms were generated with the software FlowJo V.10 and processed in GraphPad Prism8.

acetate. In *C. glutamicum* cultivated under oxic conditions, pmf is generated by the cytochrome bc_1-aa_3 supercomplex (6 $H^+/2\ e^-$) and by cytochrome *bd* oxidase (2 $H^+/2\ e^-$) (Bott and Niebisch, 2003; Niebisch and Bott, 2003; Kabashima et al., 2009). We previously showed that Δψ is reduced in a Δ*qcr* mutant lacking a functional supercomplex, whereas it is comparable to the WT in a Δ*cydAB* mutant lacking cytochrome *bd* oxidase (Koch-Koerfges et al., 2013). Therefore, a link between the cAMP level and the activity of the respiratory supercomplex might exist.

The transcriptional regulator GlxR is the only protein currently known in *C. glutamicum* whose activity is controlled by the cAMP level. In the presence of cAMP, purified GlxR was shown to bind to double-stranded 40-mer oligonucleotides covering predicted GlxR-binding sites in the promoter regions of the *ctaCF* operon, the *ctaE-qcrCAB* operon, and the *ctaD* gene, which encode the subunits of the cytochrome bc_1-aa_3 supercomplex (Kohl et al., 2008). In glucose-grown cells of strain R, chromatin affinity chromatography followed by DNA chip analysis of the enriched DNA fragments (ChIP-chip) confirmed that Strep-tagged GlxR binds *in vivo* to these proposed binding sites (Toyoda et al., 2011). Mutation of the GlxR-binding sites in the *ctaC* and *ctaD* promoter regions of genomically integrated single-copy transcriptional fusions reduced expression of the reporter gene *lacZ* in yeast extract-containing medium with either glucose or acetate by about 15 – 40% (Toyoda et al., 2011). These results indicated that GlxR acts as a transcriptional activator of the genes encoding the cytochrome bc_1-aa_3 supercomplex. The reduced cAMP level in the Δ*cyaB* mutant might thus cause a reduced expression of the genes for the bc_1-aa_3 supercomplex leading to a reduced capacity to build up membrane potential and to counteract the uncoupling activity of acetate. A transcriptome comparison of the Δ*cyaB* mutant with the WT revealed reduced expression of all genes encoding the supercomplex (**Supplementary Table S2**). Additionally, we also performed qRT-PCR of *ctaC*, *ctaD*, and *qcrC* and the resulting data also showed decreased expression of these genes in the Δ*cyaB* mutant (**Supplementary Table S2**).

To test for differences of cytochrome aa_3 oxidase activity in the Δ*cyaB* mutant and the WT, the TMPD oxidase activity of membrane fractions of the two strains grown in CGXII medium with glucose-acetate was determined. TMPD is supposed to donate electrons to cytochrome c_1. The TMPD oxidase activity of the Δ*cyaB* mutant was 35% reduced (280 ± 11 nmol TMPD oxidized min^{-1} (mg membrane protein) $^{-1}$) compared to the WT (433 ± 22 nmol TMPD oxidized min^{-1} (mg membrane protein) $^{-1}$), supporting the assumption that a reduced activity of the bc_1-aa_3 supercomplex contributes to the uncoupler sensitivity of the mutant during growth on acetate.

To further support the relevance of the cytochrome bc_1-aa_3 supercomplex for the acetate sensitivity of the Δ*cyaB* mutant, growth of the WT and the Δ*qcr* mutant was compared in CGXII medium with glucose, glucose plus acetate, or acetate (**Figure 6**). Already in glucose medium the Δ*qcr* mutant showed a growth defect, as known from previous studies (Niebisch and Bott, 2001). In medium with glucose and acetate, the growth defect of the Δ*qcr* mutant became more severe, whereas in minimal medium with acetate as sole carbon source the Δ*qcr* mutant showed no growth. These results support the assumption that the cytochrome bc_1-aa_3 branch of the respiratory chain is crucial for growth on acetate.

Growth on acetate does not allow net ATP synthesis by substrate level phosphorylation and is strictly dependent on oxidative phosphorylation by F_1F_O-ATP synthase (Koch-Koerfges et al., 2012). Interestingly, also the expression of the *atpBEFHAGDC* operon (cg1362-cg1369) encoding the eight subunits of F_1F_O-ATP synthase was shown to be activated by GlxR (Toyoda et al., 2011) and therefore might be lowered in the Δ*cyaB* mutant. The transcriptome comparison supported this assumption with about two-fold lowered mRNA levels of the *atp* genes in the Δ*cyaB* mutant. Consequently, the growth defect of the mutant on acetate is most likely additionally caused by a reduced ATP synthesis via oxidative phosphorylation, caused by reduced synthesis of the bc_1-aa_3 supercomplex and F_1F_O-ATP synthase.

Isolation of Suppressor Mutants of the Δ*cyaB* Strain With Improved Growth on Acetate

To get further insights into the molecular basis of the acetate sensitivity of the Δ*cyaB* mutant, we isolated Δ*cyaB* suppressor mutants that show improved growth on acetate. As shown in **Supplementary Figure S4A**, three independent cultures started to grow after about 80 h of incubation in acetate minimal medium. After plating on BHI agar plates, single colonies were picked from each of the three cultures and tested again for growth on acetate. As shown in **Supplementary Figure S4B**, two of the suppressor mutants, named Δ*cyaB*_sup1 and Δ*cyaB*_sup3, grew almost like the WT, whereas the third one, Δ*cyaB*_sup2, showed slower growth than the other two mutants. Genomic DNA of the three suppressor mutants was isolated and sequenced with average coverages of 82, 81, and 106 for Δ*cyaB* _sup1, Δ*cyaB* _sup2, and Δ*cyaB* _sup3, respectively. For strain Δ*cyaB*_sup1, a single point mutation was identified compared to the parent Δ*cyaB* mutant at position 307072 (numbering according to BA000036.3), which is located in the *glxR* gene and leads to an Ala131Thr exchange. The frequency of the mutation in the Δ*cyaB*_sup1 mutant was 100%. Interestingly, the same mutation was also identified in strain Δ*cyaB*_sup3, which additionally carried a second point mutation at position 2564086 (frequency 97.0%) leading to a silent mutation in codon 106 (Gly) of the ribose 5-phosphate isomerase gene *rpi* (cg2658). The suppressor mutant Δ*cyaB*_sup2 did not carry a mutation in *glxR*, but two point mutations in intergenic regions, one between promoters P1 and P2 of *gltA* (cg0949; citrate synthase) (van Ooyen et al., 2011) at position 877553 (A to G, frequency 100%) and the other one 39 bp upstream of the start codon of cg1660, encoding a putative manganese efflux pump (position 1548741, G to C, frequency 100%). The position of the point mutation in the *gltA* promoter does not overlap with known regulator binding sites for RamA and GlxR (van Ooyen et al., 2011)

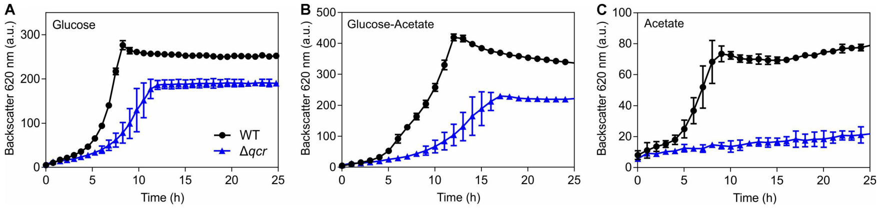

FIGURE 6 | Growth of the indicated *C. glutamicum* strains in CGXII medium with either 100 mM glucose **(A)**, 100 mM glucose plus 150 mM potassium acetate **(B)**, or 150 mM potassium acetate as carbon source **(C)**. Mean values and standard deviations of three biological replicates are shown.

and therefore the effect of this mutation cannot be predicted. Similarly, the effect of the second mutation upstream of cg1660 cannot be deduced as neither the promoter nor the regulation of this gene is known.

The finding that two of the three independently obtained suppressor mutants carried the same mutation (A131T) in GlxR supports the crucial role of this regulator for the acetate sensitivity of the Δ*cyaB* mutant. To confirm that this mutation can rescue the acetate sensitivity of the Δ*cyaB* strain, it was introduced by site-directed mutagenesis into the genome of the Δ*cyaB* mutant and for comparison into the WT. The resulting strains Δ*cyaB*::*glxR*_A131T and WT::*glxR*_A131T showed comparable growth in minimal medium with glucose compared to the parental strains Δ*cyaB* and the WT (**Supplementary Figure S4C**). Importantly, the Δ*cyaB*::*glxR*_A131T strain showed wild-type like growth in acetate minimal medium, confirming the phenotype of strain Δ*cyaB* _sup1 (**Supplementary Figure S4D**).

The alanine residue at position 131 of GlxR is highly conserved in homologs from other *Corynebacterium* species and *Mycobacterium tuberculosis* as well as in CRP of *E. coli* (**Supplementary Figure S4E**). Ala131 is located in the central α-helix of GlxR, which forms the dimer interface, and is positioned close to important cAMP-binding residues (Townsend et al., 2014) (**Supplementary Figures S4E,G**). Overlays of the crystal structures of apo- and holo-GlxR and of models with the Ala131T exchange are shown in **Supplementary Figures S4F,G**. The mutation apparently does not lead to large structural changes, making it difficult to predict the functional consequences of the amino acid exchange. Due to the vicinity of residue 131 to the cAMP-binding site, the A131T exchange might have altered the influence of cAMP on DNA-binding. We therefore tested whether purified GlxR-A131T still requires cAMP for binding to DNA targets in electrophoretic mobility shift assays. As shown in **Supplementary Figure S5**, binding of GlxR-A131T to DNA fragments covering the GlxR-binding sites in front of *ctaD* and *ctaC* was still dependent on cAMP. However, the *in vivo* situation is probably different. ChIP-Chip experiments with a *cyaB*-deletion strain of *C. glutamicum* R clearly showed GlxR-binding to target sites despite the lack of CyaB, although with decreased affinity (Toyoda et al., 2011).

The most intensively studied homolog of GlxR is CRP of *E. coli*. Many studies were performed in which *E. coli*Δ*cya* strains were used to select for mutants that regained the ability to grow on carbon sources such as lactose, maltose, or xylose requiring activation of gene expression by CRP. These studies have recently been summarized (Frendorf et al., 2019) and led the authors to conclude that adaptive mutations occur predominantly in the cAMP binding site, the D-α-helix, and in the RNA polymerase activating domains AR1 and AR2, which likely affect ligand binding, ligand-induced allosteric transitions, or the productive interaction with the core RNA polymerase, respectively. In these studies, no mutation was found in CRP residue A121, which corresponds to A131 of GlxR. However, it has to be considered that although the 3-dimensional fold of GlxR and CRP is very similar, the structural changes observed for GlxR upon cAMP binding are quite distinct from those observed for CRP (Townsend et al., 2014). It was concluded that the mechanisms of allosteric binding and activation of DNA-binding differ considerably in the CRP/FNR family without dramatic structural changes and that the same 3-dimensional fold is finetuned using small structural changes coupled with changes in dynamic behavior to achieve the optimal combination of allostery and DNA recognition (Townsend et al., 2014). This situation makes a prediction of the effects of the A131T mutation in GlxR based on studies of *E. coli* CRP virtually impossible.

CONCLUSION

The aim of this study was to elucidate the consequences of a reduced cAMP level in *C. glutamicum* caused by the lack of the adenylate cyclase CyaB and in particular the inhibitory effect of acetate on growth of the Δ*cyaB* mutant. Our results strongly suggest that this effect is mainly caused by the uncoupling activity of acetate, as it is concentration- and pH-dependent and occurs also in the presence of an additional carbon source such as glucose, fructose, sucrose, or gluconate. Evidence was obtained that the Δ*cyaB* mutant has a lower Δψ on acetate than the WT, suggesting a reduced capability to build up pmf. As the growth defect of the Δ*cyaB* mutant could be rescued by supplementation of the medium with cAMP, a link between the major second messenger cAMP and the ability to pmf generation was proposed. The major contributor to pmf in *C. glutamicum* is the cytochrome bc_1-aa_3 supercomplex and there is evidence from previous studies that expression of the genes encoding the supercomplex is activated by the cAMP-dependent transcriptional regulator GlxR. We observed reduced expression of the supercomplex genes and a reduced TMPD oxidase activity in the Δ*cyaB* mutant, supporting the idea that a decreased supercomplex activity contributes to the acetate sensitivity of the Δ*cyaB* mutant. Also the F_1F_O-ATP synthase genes are known to be transcriptionally activated by GlxR and showed reduced expression in the Δ*cyaB* mutant, additionally contributing to the energetic deficiencies of the strain. We could rescue the growth defect of the Δ*cyaB* mutant on acetate by a single point mutation (A131T) in GlxR, confirming the key role of GlxR for the phenotype of the Δ*cyaB* mutant. Additional studies are required to elucidate the functional consequences of this amino acid exchange *in vivo*. In summary, our results disclosed that cAMP in concert with GlxR plays a key role in the control of energy metabolism in *C. glutamicum*.

DATA AVAILABILITY STATEMENT

This manuscript contains previously unpublished data. The DNA microarray data are available in the GEO database with accession number GSE140408. The genome sequencing data (bam files) are available in the ENA database via accession number PRJEB36438.

AUTHOR CONTRIBUTIONS

NW and MBu constructed mutants and plasmids and performed all experimental work except the one specified below for other authors. AK-K performed the analysis of glucose and organic acids. NK and JS performed the growth experiments with the protonophore CCCP and the determination of the membrane potential. TP supervised the genome resequencing and analyzed the resulting data. JH and JV performed the LC-MS/MS measurements for cAMP determination. MBa coached the experimental work and supported the design of the study. All authors contributed to the interpretation of the data. NW wrote the first draft of the manuscript and prepared the figures and tables. MBo designed the study, supervised the experimental work, and wrote the final version of the manuscript.

FUNDING

Financial support (grant 0315598A) by the Bundesministerium für Bildung und Forschung (BMBF) is gratefully acknowledged.

SUPPLEMENTARY MATERIAL

The Supplementary Material for this article can be found online at: https://www.frontiersin.org/articles/10.3389/fmicb.2020.00087/full#supplementary-material

REFERENCES

Ammerman, J. W., and Azam, F. (1982). Uptake of cyclic AMP by natural populations of marine bacteria. *Appl. Environ. Microbiol.* 43, 869–876. doi: 10.1128/aem.43.4.869-876.1982

Arndt, A., Auchter, M., Ishige, T., Wendisch, V. F., and Eikmanns, B. J. (2008). Ethanol catabolism in *Corynebacterium glutamicum*. *J. Mol. Microbiol. Biotechnol.* 15, 222–233. doi: 10.1159/000107370

Arndt, A., and Eikmanns, B. J. (2007). The alcohol dehydrogenase gene *adhA* in *Corynebacterium glutamicum* is subject to carbon catabolite repression. *J. Bacteriol.* 189, 7408–7416. doi: 10.1128/JB.00791-07

Axe, D. D., and Bailey, J. E. (1995). Transport of lactate and acetate through the energized cytoplasmic membrane of *Escherichia coli*. *Biotechnol. Bioeng.* 47, 8–19. doi: 10.1002/bit.260470103

Becker, J., and Wittmann, C. (2012). Bio-based production of chemicals, materials and fuels -*Corynebacterium glutamicum* as versatile cell factory. *Curr. Opin. Biotechnol.* 23, 631–640. doi: 10.1016/j.copbio.2011.11.012

Binder, S., Schendzielorz, G., Stäbler, N., Krumbach, K., Hoffmann, K., Bott, M., et al. (2012). A high-throughput approach to identify genomic variants of bacterial metabolite producers at the single-cell level. *Genome Biol.* 13:R40. doi: 10.1186/Gb-2012-13-5-R40

Bott, M. (2007). Offering surprises: TCA cycle regulation in *Corynebacterium glutamicum*. *Trends Microbiol.* 15, 417–425. doi: 10.1016/j.tim.2007.08.004

Bott, M., and Niebisch, A. (2003). The respiratory chain of *Corynebacterium glutamicum*. *J. Biotechnol.* 104, 129–153. doi: 10.1016/s0168-1656(03)00144-5

Brazma, A., Hingamp, P., Quackenbush, J., Sherlock, G., Spellman, P., Stoeckert, C., et al. (2001). Minimum information about a microarray experiment (MIAME)-toward standards for microarray data. *Nat. Genet.* 29, 365–371. doi: 10.1038/ng1201-365

Burkovski, A. (ed.) (2008). *Corynebacteria: Genomics and Molecular Biology*. Norfolk: Caister Academic Press.

Bussmann, M., Emer, D., Hasenbein, S., Degraf, S., Eikmanns, B. J., and Bott, M. (2009). Transcriptional control of the succinate dehydrogenase operon *sdhCAB* of *Corynebacterium glutamicum* by the cAMP-dependent regulator GlxR and the LuxR-type regulator RamA. *J. Biotechnol.* 143, 173–182. doi: 10.1016/j.jbiotec.2009.06.025

Cha, P. H., Park, S. Y., Moon, M. W., Subhadra, B., Oh, T. K., Kim, E., et al. (2010). Characterization of an adenylate cyclase gene (*cyaB*) deletion mutant of *Corynebacterium glutamicum* ATCC 13032. *Appl. Microbiol. Biotechnol.* 85, 1061–1068. doi: 10.1007/s00253-009-2066-9

da Luz, J. A., Hans, E., Frank, D., and Zeng, A.-P. (2016). Analysis of intracellular metabolites of *Corynebacterium glutamicum* at high cell density with automated sampling and filtration and assessment of engineered enzymes for effective L-lysine production. *Eng. Life Sci.* 17, 512–522. doi: 10.1002/elsc.201600163

Eggeling, L., and Bott, M. (eds) (2005). *Handbook of Corynebacterium glutamicum*. Boca Raton, FL: CRC Press.

Eggeling, L., and Bott, M. (2015). A giant market and a powerful metabolism: L-lysine provided by *Corynebacterium glutamicum*. *Appl. Microbiol. Biotechnol.* 99, 3387–3394. doi: 10.1007/s00253-015-6508-2

Eggeling, L., Bott, M., and Marienhagen, J. (2015). Novel screening methods-biosensors. *Curr. Opin. Biotechnol.* 35, 30–36. doi: 10.1016/j.copbio.2014.12.021

Follmann, M., Ochrombel, I., Krämer, R., Trötschel, C., Poetsch, A., Rückert, C., et al. (2009). Functional genomics of pH homeostasis in *Corynebacterium glutamicum* revealed novel links between pH response, oxidative stress, iron homeostasis and methionine synthesis. *BMC Genomics* 10:621. doi: 10.1186/1471-2164-10-621

Frendorf, P. O., Lauritsen, I., Sekowska, A., Danchin, A., and Norholm, M. H. H. (2019). Mutations in the global transcription factor CRP/CAP: insights from experimental evolution and deep sequencing. *Comput. Struct. Biotechnol. J.* 17, 730–736. doi: 10.1016/j.csbj.2019.05.009

Freudl, R. (2017). Beyond amino acids: use of the *Corynebacterium glutamicum* cell factory for the secretion of heterologous proteins. *J. Biotechnol.* 258, 101–109. doi: 10.1016/j.jbiotec.2017.02.023

Frunzke, J., Engels, V., Hasenbein, S., Gätgens, C., and Bott, M. (2008). Co-ordinated regulation of gluconate catabolism and glucose uptake in *Corynebacterium glutamicum* by two functionally equivalent transcriptional regulators, GntR1 and GntR2. *Mol. Microbiol.* 67, 305–322. doi: 10.1111/j.1365-2958.2007.06020.x

Gerstmeir, R., Wendisch, V. F., Schnicke, S., Ruan, H., Farwick, M., Reinscheid, D., et al. (2003). Acetate metabolism and its regulation in *Corynebacterium glutamicum*. *J. Biotechnol.* 104, 99–122. doi: 10.1016/s0168-1656(03)00167-6

Goldenbaum, P. E., and Hall, G. A. (1979). Transport of cyclic adenosine 3′,5′-monophosphate across *Escherichia coli* vesicle membranes. *J. Bacteriol.* 140, 459–467. doi: 10.1128/jb.140.2.459-467.1979

Hartl, J., Kiefer, P., Meyer, F., and Vorholt, J. A. (2017). Longevity of major coenzymes allows minimal *de novo* synthesis in microorganisms. *Nat. Microbiol.* 2:17073. doi: 10.1038/nmicrobiol.2017.73

Heytler, P. G., and Prichard, W. W. (1962). A new class of uncoupling agents - carbonyl cyanide phenylhydrazones. *Biochem. Biophys. Res. Commun.* 7, 272–275. doi: 10.1016/0006-291x(62)90189-4

ICH, (2005). "Harmonised Tripartite Guideline, validation of analytical procedures: text and methodology Q2 (R1)"," in *International Conference on Harmonisation of Technical Requirements for Registration of Pharmaceuticals for Human Use*, (Geneva).

Ikeda, M., and Nakagawa, S. (2003). The *Corynebacterium glutamicum* genome: features and impacts on biotechnological processes. *Appl. Microbiol. Biotechnol.* 62, 99–109. doi: 10.1007/s00253-003-1328-1

Jolkver, E., Emer, D., Ballan, S., Krämer, R., Eikmanns, B. J., and Marin, K. (2009). Identification and characterization of a bacterial transport system for the uptake of pyruvate, propionate, and acetate in *Corynebacterium glutamicum*. *J. Bacteriol.* 191, 940–948. doi: 10.1128/JB.01155-08

Jungwirth, B., Sala, C., Kohl, T. A., Uplekar, S., Baumbach, J., Cole, S. T., et al. (2013). High-resolution detection of DNA binding sites of the global transcriptional regulator GlxR in *Corynebacterium glutamicum*. *Microbiology* 159, 12–22. doi: 10.1099/mic.0.062059-0

Kabashima, Y., Kishikawa, J., Kurokawa, T., and Sakamoto, J. (2009). Correlation between proton translocation and growth: genetic analysis of the respiratory chain of *Corynebacterium glutamicum*. *J. Biochem.* 146, 845–855. doi: 10.1093/jb/mvp140

Kabus, A., Niebisch, A., and Bott, M. (2007). Role of cytochrome *bd* oxidase from *Corynebacterium glutamicum* in growth and lysine production. *Appl. Environ. Microbiol.* 73, 861–868. doi: 10.1128/aem.01818-06

Kalinowski, J., Bathe, B., Bartels, D., Bischoff, N., Bott, M., Burkovski, A., et al. (2003). The complete *Corynebacterium glutamicum* ATCC 13032 genome sequence and its impact on the production of L-aspartate-derived amino acids and vitamins. *J. Biotechnol.* 104, 5–25. doi: 10.1016/s0168-1656(03)00154-8

Kensy, F., Zang, E., Faulhammer, C., Tan, R. K., and Büchs, J. (2009). Validation of a high-throughput fermentation system based on online monitoring of biomass and fluorescence in continuously shaken microtiter plates. *Microb. Cell Fact.* 8:31. doi: 10.1186/1475-2859-8-31

Kim, H. J., Kim, T. H., Kim, Y., and Lee, H. S. (2004). Identification and characterization of *glxR*, a gene involved in regulation of glyoxylate bypass in *Corynebacterium glutamicum*. *J. Bacteriol.* 186, 3453–3460. doi: 10.1128/jb.186.11.3453-3460.2004

Kinoshita, S., Udaka, S., and Shimono, M. (1957). Studies on amino acid fermentation. Part I. Production of L-glutamic acid by various microorganisms. *J. Gen. Appl. Microbiol.* 3, 193–205.

Koch-Koerfges, A., Kabus, A., Ochrombel, I., Marin, K., and Bott, M. (2012). Physiology and global gene expression of a *Corynebacterium glutamicum* ΔF_1F_O-ATP synthase mutant devoid of oxidative phosphorylation. *Biochim. Biophys. Acta* 1817, 370–380. doi: 10.1016/j.bbabio.2011.10.006

Koch-Koerfges, A., Pfelzer, N., Platzen, L., Oldiges, M., and Bott, M. (2013). Conversion of *Corynebacterium glutamicum* from an aerobic respiring to an aerobic fermenting bacterium by inactivation of the respiratory chain. *Biochim. Biophys. Acta* 1827, 699–708. doi: 10.1016/j.bbabio.2013.02.004

Kohl, T. A., Baumbach, J., Jungwirth, B., Pühler, A., and Tauch, A. (2008). The GlxR regulon of the amino acid producer *Corynebacterium glutamicum: In silico* and *in vitro* detection of DNA binding sites of a global transcription regulator. *J. Biotechnol.* 135, 340–350. doi: 10.1016/j.jbiotec.2008.05.011

Linder, J. U., Hammer, A., and Schultz, J. E. (2004). The effect of HAMP domains on class IIIb adenylyl cyclases from *Mycobacterium tuberculosis*. *Eur. J. Biochem.* 271, 2446–2451. doi: 10.1111/j.1432-1033.2004.04172.x

Möker, N., Brocker, M., Schaffer, S., Krämer, R., Morbach, S., and Bott, M. (2004). Deletion of the genes encoding the MtrA-MtrB two-component system of *Corynebacterium glutamicum* has a strong influence on cell morphology, antibiotics susceptibility and expression of genes involved in osmoprotection. *Mol. Microbiol.* 54, 420–438. doi: 10.1111/j.1365-2958.2004.04249.x

Müller, J. E., Meyer, F., Litsanov, B., Kiefer, P., and Vorholt, J. A. (2015). Core pathways operating during methylotrophy of *Bacillus methanolicus* MGA3 and induction of a bacillithiol-dependent detoxification pathway upon formaldehyde stress. *Mol. Microbiol.* 98, 1089–1100. doi: 10.1111/mmi.13200

Mustafi, N., Grünberger, A., Kohlheyer, D., Bott, M., and Frunzke, J. (2012). The development and application of a single-cell biosensor for the detection of L-methionine and branched-chain amino acids. *Metab. Eng.* 14, 449–457. doi: 10.1016/j.ymben.2012.02.002

Neumeyer, A., Hübschmann, T., Müller, S., and Frunzke, J. (2013). Monitoring of population dynamics of *Corynebacterium glutamicum* by multiparameter flow cytometry. *Microb. Biotechnol.* 6, 157–167. doi: 10.1111/1751-7915.12018

Nicholls, D. G., and Ferguson, S. J. (2002). *Bioenergetics 3*. London: Academic Press.

Niebisch, A., and Bott, M. (2001). Molecular analysis of the cytochrome bc_1-aa_3 branch of the *Corynebacterium glutamicum* respiratory chain containing an unusual diheme cytochrome c_1. *Arch. Microbiol.* 175, 282–294. doi: 10.1007/s002030100262

Niebisch, A., and Bott, M. (2003). Purification of a cytochrome bc_1-aa_3 supercomplex with quinol oxidase activity from *Corynebacterium glutamicum* - Identification of a fourth subunit of cytochrome aa_3 oxidase and mutational analysis of diheme cytochrome c_1. *J. Biol. Chem.* 278, 4339–4346. doi: 10.1074/jbc.m210499200

Novo, D., Perlmutter, N. G., Hunt, R. H., and Shapiro, H. M. (1999). Accurate flow cytometric membrane potential measurement in bacteria using diethyloxacarbocyanine and a ratiometric technique. *Cytometry* 35, 55–63. doi: 10.1002/(sici)1097-0320(19990101)35:1<55::aid-cyto8>3.0.co;2-2

Novo, D. J., Perlmutter, N. G., Hunt, R. H., and Shapiro, H. M. (2000). Multiparameter flow cytometric analysis of antibiotic effects on membrane potential, membrane permeability, and bacterial counts of *Staphylococcus aureus* and *Micrococcus luteus*. *Antimicrob. Agents Chemother.* 44, 827–834. doi: 10.1128/aac.44.4.827-834.2000

Pfeifer-Sancar, K., Mentz, A., Rückert, C., and Kalinowski, J. (2013). Comprehensive analysis of the *Corynebacterium glutamicum* transcriptome using an improved RNAseq technique. *BMC Genomics* 14:888. doi: 10.1186/1471-2164-14-888

Pinhal, S., Ropers, D., Geiselmann, J., and de Jong, H. (2019). Acetate metabolism and the inhibition of bacterial growth by acetate. *J. Bacteriol* 201:e00147-19. doi: 10.1128/JB.00147-19

Polen, T., and Wendisch, V. F. (2004). Genomewide expression analysis in amino acid-producing bacteria using DNA microarrays. *Appl. Biochem. Biotechnol.* 118, 215–232. doi: 10.1385/abab:118:1-3:215

Richter, W. (2002). 3′,5′-Cyclic nucleotide phosphodiesterases class III: members, structure, and catalytic mechanism. *Proteins* 46, 278–286. doi: 10.1002/prot.10049

Saier, M. H. Jr., Feucht, B. U., and McCaman, M. T. (1975). Regulation of intracellular adenosine cyclic 3′,5′-monophosphate levels in *Escherichia coli* and *Salmonella typhimurium*. Evidence for energy-dependent excretion of the cyclic nucleotide. *J. Biol. Chem.* 250, 7593–7601.

Sakamoto, J., Shibata, T., Mine, T., Miyahara, R., Torigoe, T., Noguchi, S., et al. (2001). Cytochrome *c* oxidase contains an extra charged amino acid cluster in a new type of respiratory chain in the amino-acid-producing Gram-positive bacterium *Corynebacterium glutamicum*. *Microbiology* 147, 2865–2871. doi: 10.1099/00221287-147-10-2865

Sambrook, J., and Russell, D. (2001). *Molecular Cloning. A Laboratory Manual*. Cold Spring Harbor, NY: Cold Spring Harbor Laboratory Press.

Schäfer, A., Tauch, A., Jäger, W., Kalinowski, J., Thierbach, G., and Pühler, A. (1994). Small mobilizable multipurpose cloning vectors derived from the *Escherichia coli* plasmids pK18 and pK19 - Selection of defined deletions in the chromosome of *Corynebacterium glutamicum*. *Gene* 145, 69–73. doi: 10.1016/0378-1119(94)90324-7

Schendzielorz, G., Dippong, M., Grünberger, A., Kohlheyer, D., Yoshida, A., Binder, S., et al. (2014). Taking control over control: use of product sensing in single cells to remove flux control at key enzymes in biosynthesis pathways. *ACS Synth. Biol.* 3, 21–29. doi: 10.1021/sb400059y

Schneider, J., and Wendisch, V. F. (2011). Biotechnological production of polyamines by bacteria: recent achievements and future perspectives. *Appl. Microbiol. Biotechnol.* 91, 17–30. doi: 10.1007/s00253-011-3252-0

Schulte, J., Baumgart, M., and Bott, M. (2017a). Development of a single-cell GlxR-based cAMP biosensor for *Corynebacterium glutamicum*. *J. Biotechnol.* 258, 33–40. doi: 10.1016/j.jbiotec.2017.07.004

Schulte, J., Baumgart, M., and Bott, M. (2017b). Identification of the cAMP phosphodiesterase CpdA as novel key player in cAMP-dependent regulation in *Corynebacterium glutamicum*. *Mol. Microbiol.* 103, 534–552. doi: 10.1111/mmi.13574

Shenoy, A. R., Sivakumar, K., Krupa, A., Srinivasan, N., and Visweswariah, S. S. (2004). A survey of nucleotide cyclases in Actinobacteria: unique domain organization and expansion of the class III cyclase family in *Mycobacterium tuberculosis*. *Comp. Funct. Genomics* 5, 17–38. doi: 10.1002/cfg.349

Studier, F. W. (2005). Protein production by auto-induction in high density shaking cultures. *Protein Expr. Purif.* 41, 207–234. doi: 10.1016/j.pep.2005.01.016

Studier, F. W., and Moffatt, B. A. (1986). Use of bacteriophage T7 RNA polymerase to direct selective high-level expression of cloned genes. *J. Mol. Biol.* 189, 113–130. doi: 10.1016/0022-2836(86)90385-2

Townsend, P. D., Jungwirth, B., Pojer, F., Bussmann, M., Money, V. A., Cole, S. T., et al. (2014). The crystal structures of apo and cAMP-bound GlxR from *Corynebacterium glutamicum* reveal structural and dynamic changes upon cAMP binding in CRP/FNR family transcription factors. *PLoS One* 9:e113265. doi: 10.1371/journal.pone.0113265

Toyoda, K., Teramoto, H., Inui, M., and Yukawa, H. (2011). Genome-wide identification of *in vivo* binding sites of GlxR, a cyclic AMP receptor protein-type regulator in *Corynebacterium glutamicum*. *J. Bacteriol.* 193, 4123–4133. doi: 10.1128/JB.00384-11

van Ooyen, J., Emer, D., Bussmann, M., Bott, M., Eikmanns, B. J., and Eggeling, L. (2011). Citrate synthase in *Corynebacterium glutamicum* is encoded by two *gltA* transcripts which are controlled by RamA, RamB, and GlxR. *J. Biotechnol.* 154, 140–148. doi: 10.1016/j.jbiotec.2010.07.004

Wendisch, V. F., De Graaf, A. A., Sahm, H., and Eikmanns, B. J. (2000). Quantitative determination of metabolic fluxes during coutilization of two carbon sources: comparative analyses with *Corynebacterium* glutamicum during growth on acetate and/or glucose. *J. Bacteriol.* 182, 3088–3096. doi: 10.1128/jb.182.11.3088-3096.2000

Wieschalka, S., Blombach, B., Bott, M., and Eikmanns, B. J. (2013). Bio-based production of organic acids with *Corynebacterium glutamicum*. *Microb. Biotechnol.* 6, 87–102. doi: 10.1111/1751-7915.12013

Yukawa, H., and Inui, M. (eds) (2013). *Corynebacterium glutamicum: Biology and Biotechnology*. Heidelberg: Springer.

Yukawa, H., Omumasaba, C. A., Nonaka, H., Kos, P., Okai, N., Suzuki, N., et al. (2007). Comparative analysis of the *Corynebacterium glutamicum* group and complete genome sequence of strain R. *Microbiology* 153, 1042–1058. doi: 10.1099/mic.0.2006/003657-0

Conflict of Interest: The authors declare that the research was conducted in the absence of any commercial or financial relationships that could be construed as a potential conflict of interest.

2.2 Supplementary materials ‘Molecular basis of growth inhibition by acetate of an adenylate cyclase-deficient mutant of *Corynebacterium glutamicum*’

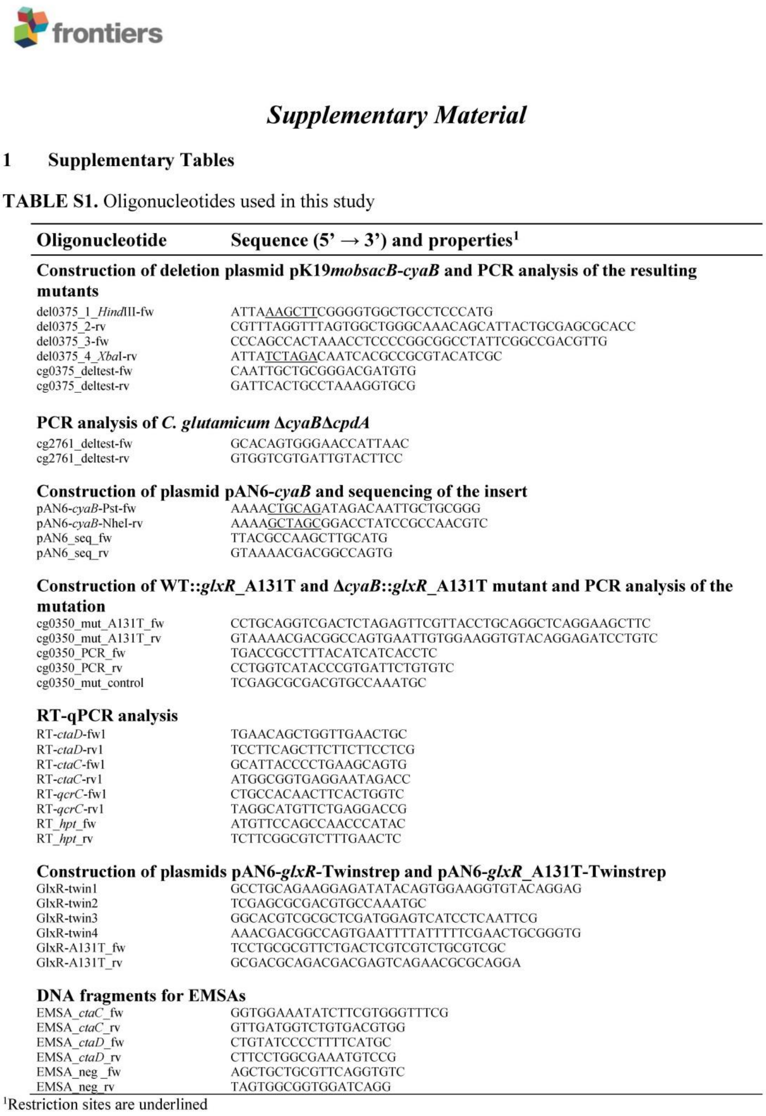

frontiers

Supplementary Material

1 Supplementary Tables

TABLE S1. Oligonucleotides used in this study

Oligonucleotide	Sequence (5’ → 3’) and properties[1]
Construction of deletion plasmid pK19*mobsacB-cyaB* and PCR analysis of the resulting mutants	
del0375_1_*Hind*III-fw	ATTAAAGCTTCGGGGTGGCTGCCTCCCATG
del0375_2-rv	CGTTTAGGTTTAGTGGCTGGGCAAACAGCATTACTGCGAGCGCACC
del0375_3-fw	CCCAGCCACTAAACCTCCCCGGCGGCCTATTCGGCCGACGTTG
del0375_4_*Xba*I-rv	ATTATCTAGACAATCACGCCGCGTACATCGC
cg0375_deltest-fw	CAATTGCTGCGGGACGATGTG
cg0375_deltest-rv	GATTCACTGCCTAAAGGTGCG
PCR analysis of *C. glutamicum* Δ*cyaB*Δ*cpdA*	
cg2761_deltest-fw	GCACAGTGGGAACCATTAAC
cg2761_deltest-rv	GTGGTCGTGATTGTACTTCC
Construction of plasmid pAN6-*cyaB* and sequencing of the insert	
pAN6-*cyaB*-Pst-fw	AAAACTGCAGATAGACAATTGCTGCGGG
pAN6-*cyaB*-NheI-rv	AAAAGCTAGCGGACCTATCCGCCAACGTC
pAN6_seq_fw	TTACGCCAAGCTTGCATG
pAN6_seq_rv	GTAAAACGACGGCCAGTG
Construction of WT::*glxR*_A131T and Δ*cyaB*::*glxR*_A131T mutant and PCR analysis of the mutation	
cg0350_mut_A131T_fw	CCTGCAGGTCGACTCTAGAGTTCGTTACCTGCAGGCTCAGGAAGCTTC
cg0350_mut_A131T_rv	GTAAAACGACGGCCAGTGAATTGTGGAAGGTGTACAGGAGATCCTGTC
cg0350_PCR_fw	TGACCGCCTTTACATCATCACCTC
cg0350_PCR_rv	CCTGGTCATACCCGTGATTCTGTGTC
cg0350_mut_control	TCGAGCGCGACGTGCCAAATGC
RT-qPCR analysis	
RT-*ctaD*-fw1	TGAACAGCTGGTTGAACTGC
RT-*ctaD*-rv1	TCCTTCAGCTTCTTCTTCCTCG
RT-*ctaC*-fw1	GCATTACCCCTGAAGCAGTG
RT-*ctaC*-rv1	ATGGCGGTGAGGAATAGACC
RT-*qcrC*-fw1	CTGCCACAACTTCACTGGTC
RT-*qcrC*-rv1	TAGGCATGTTCTGAGGACCG
RT_*hpt*_fw	ATGTTCCAGCCAACCCATAC
RT_*hpt*_rv	TCTTCGGCGTCTTTGAACTC
Construction of plasmids pAN6-*glxR*-Twinstrep and pAN6-*glxR*_A131T-Twinstrep	
GlxR-twin1	GCCTGCAGAAGGAGATATACAGTGGAAGGTGTACAGGAG
GlxR-twin2	TCGAGCGCGACGTGCCAAATGC
GlxR-twin3	GGCACGTCGCGCTCGATGGAGTCATCCTCAATTCG
GlxR-twin4	AAACGACGGCCAGTGAATTTTATTTTTCGAACTGCGGGTG
GlxR-A131T_fw	TCCTGCGCGTTCTGACTCGTCGTCTGCGTCGC
GlxR-A131T_rv	GCGACGCAGACGACGAGTCAGAACGCGCAGGA
DNA fragments for EMSAs	
EMSA_*ctaC*_fw	GGTGGAAATATCTTCGTGGGTTTCG
EMSA_*ctaC*_rv	GTTGATGGTCTGTGACGTGG
EMSA_*ctaD*_fw	CTGTATCCCCTTTTCATGC
EMSA_*ctaD*_rv	CTTCCTGGCGAAATGTCCG
EMSA_neg _fw	AGCTGCTGCGTTCAGGTGTC
EMSA_neg_rv	TAGTGGCGGTGGATCAGG

[1] Restriction sites are underlined

TABLE S2. mRNA ratios (Δ*cyaB*/WT) of the genes encoding F_1F_O-ATP synthase and the cytochrome bc_1-aa_3 supercomplex.[1]

Locus tag	Gene	Function	mRNA ratio Δ*cyaB*/WT	
			DNA microarrays[2]	qRT-PCR[3]
cg1362	*atpB*	ATP synthase subunit A	0.51	n.d.[4]
cg1363	*atpE*	ATP synthase subunit C	0.51[5]	n.d.
cg1364	*atpF*	ATP synthase subunit B	0.53	n.d.
cg1365	*atpH*	ATP synthase subunit δ	0.55	n.d.
cg1366	*atpA*	ATP synthase subunit α	0.41	n.d.
cg1367	*atpG*	ATP synthase subunit γ	0.40	n.d.
cg1368	*atpD*	ATP synthase subunit β	0.43	n.d.
cg1369	*atpC*	ATP synthase subunit ε	0.83	n.d.
cg2406	*ctaE*	cytochrome aa_3 oxidase subunit 3	0.67	n.d.
cg2409	*ctaC*	cytochrome aa_3 oxidase subunit 2	0.63	0.20
cg2408	*ctaF*	cytochrome aa_3 oxidase subunit 4	0.31	n.d.
cg2780	*ctaD*	cytochrome aa_3 oxidase subunit 1	0.69	0.32
cg2405	*qcrC*	cytochrome c_1	0.74	0.30
cg2404	*qcrA*	Rieske iron-sulfur protein	0.64	n.d.
cg2403	*qcrB*	cytochrome *b*	0.64	n.d.

[1] Cells of the Δ*cyaB* mutant and the WT were grown in CGXII medium with glucose plus acetate (100 mM each).

[2] mRNA ratios represent mean values of at least two DNA microarray analyses starting from independent cultures.

[3] qRT-PCR results represent mean values of three biological replicates and two technical replicates each

[4] n.d., not determined

[5] except for cg1363, the p-values for all other genes were ≤ 0.05

2 Supplementary Figures

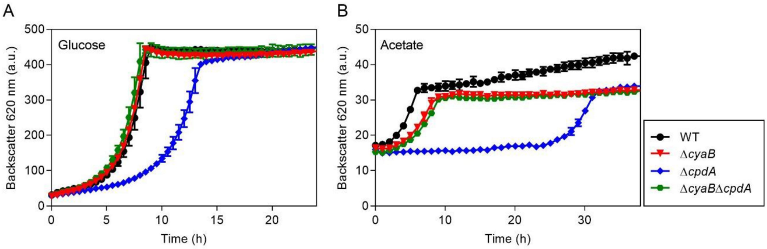

FIGURE S1. Growth of *C. glutamicum* WT and the mutant strains Δ*cyaB*, Δ*cpdA*, and Δ*cyaB*Δ*cpdA* in CGXII medium with 2% (w/v) glucose (**A**) or 100 mM sodium acetate (**B**). Mean values and standard deviations of three biological replicates are shown.

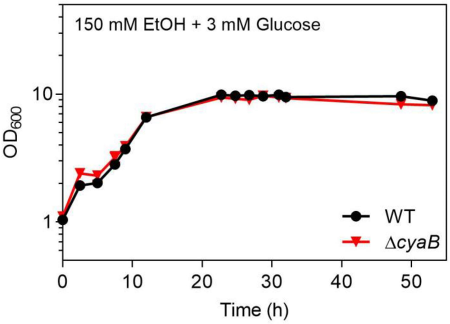

FIGURE S2. Growth of *C. glutamicum* WT and the Δ*cyaB* mutant in CGXII minimal medium with 150 mM ethanol and 3 mM glucose. Cultivation was performed in baffled shake flasks that were incubated at 30 °C and 120 rpm at 85% humidity. Mean values and standard deviations of three biological replicates are shown.

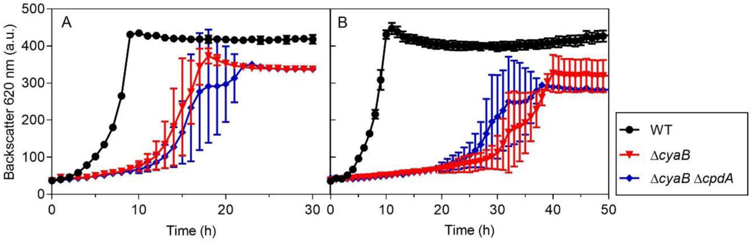

FIGURE S3. Growth of *C. glutamicum* WT and mutant strains Δ*cyaB* and Δ*cyaB*Δ*cpdA* in CGXII medium with 100 mM glucose and 50 mM potassium acetate (**A**) or with 100 mM glucose and 100 mM potassium acetate (**B**). Mean values and standard deviations of three biological replicates are shown.

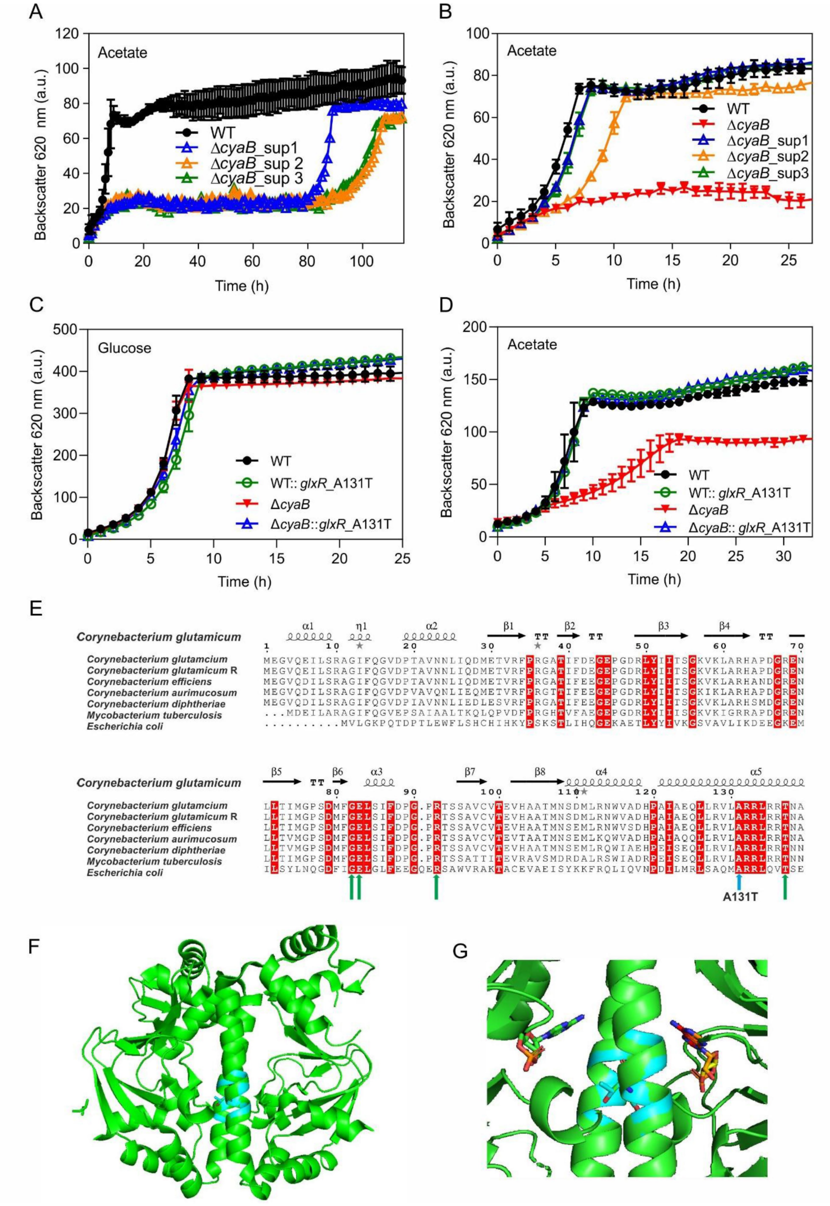
A
Acetate
Backscatter 620 nm (a.u.)
Time (h)
WT
ΔcyaB_sup1
ΔcyaB_sup 2
ΔcyaB_sup 3
0
20
40
60
80
100
120
B
Acetate
Backscatter 620 nm (a.u.)
Time (h)
WT
ΔcyaB
ΔcyaB_sup1
ΔcyaB_sup2
ΔcyaB_sup3
C
Glucose
Backscatter 620 nm (a.u.)
Time (h)
WT
WT:: glxR_A131T
ΔcyaB
ΔcyaB::glxR_A131T
D
Acetate
Backscatter 620 nm (a.u.)
Time (h)
WT
WT:: glxR_A131T
ΔcyaB
ΔcyaB:: glxR_A131T
E
Corynebacterium glutamicum
α1 η1 α2 β1 TT β2 TT β3 β4 TT
1 10 20 30 40 50 60 70
Corynebacterium glutamcium MEGVQEILSRAGIFQGVDPTAVNNLIQDMETVRFPRGATIFDEGEPGDRLYIITSGKVKLARHAPDGREN
Corynebacterium glutamicum R MEGVQEILSRAGIFQGVDPTAVNNLIQDMETVRFPRGATIFDEGEPGDRLYIITSGKVKLARHAPDGREN
Corynebacterium efficiens MEGVQDILSRAGIFQGVDPTAVNNLIQDMETVRFPRGATIFEEGEPGDRLYIITSGKVKLARHANDGREN
Corynebacterium aurimucosum MEGVQDILSRAGIFQGVDPVAVQNLIEQMETVRFPRGTTIFEEGEPGDRLYIITSGKIKLARHAPDGREN
Corynebacterium diphtheriae MEGVQDILSRAGIFQGVDPIAVNNLIEDLESVRFPRGATIFEEGEPGDRLYIITSGKVKLARHSMDGREN
Mycobacterium tuberculosis ...MDEILARAGIFQGVEPSAIAALTKQLQPVDFPRGHTVFAEGEPGDRLYIIISGKVKIGRRAPDGREN
Escherichia coli ..........MVLGKPQTDPTLEWFLSHCHIHKYPSKSTLIHQGEKAETLYYIVKGSVAVLIKDEEGKEM
Corynebacterium glutamicum
β5 TT β6 α3 β7 β8 α4 α5
80 90 100 110 120 130
Corynebacterium glutamcium LLTIMGPSDMFGELSIFDPG.PRTSSAVCVTEVHAATMNSDMLRNWVADHPAIAEQLLRVLARRLRRTNA
Corynebacterium glutamicum R LLTIMGPSDMFGELSIFDPG.PRTSSAVCVTEVHAATMNSDMLRNWVADHPAIAEQLLRVLARRLRRTNA
Corynebacterium efficiens LLTIMGPSDMFGELSIFDPG.PRTSSAVCVTEVHAATMNSEMLRNWVSDHPAIAEQLLRVLARRLRRTNA
Corynebacterium aurimucosum LLTVMGPSDMFGELSIFDPG.PRTSSAVCVTEVTAATMNSEMLKQWVADHPAIAQQLLRVLARRLRRTNA
Corynebacterium diphtheriae LLTVMGPSDMFGELSIFDPG.PRTSSAVCVTEVHAATMNSEMLRQWIAEHPEISEQLLRVLARRLRRTNN
Mycobacterium tuberculosis LLTIMGPSDMFGELSIFDPG.PRTSSATTITEVRAVSMDRDALRSWIADRPEISEQLLRVLARRLRRTNN
Escherichia coli ILSYLNQGDFIGELGLFEEGQERSAWVRAKTACEVAEISYKKFRQLIQVNPDILMRLSAQMARRLQVTSE
A131T
F
G

5

FIGURE S4. (A) Generation of suppressor mutants of *C. glutamicum* Δ*cyaB* with restored growth on acetate in a long-term cultivation in CGXII medium with 150 mM potassium acetate. **(B)** Growth of single colonies of the Δ*cyaB* suppressor mutant in CGXII medium with 150 mM acetate using *C. glutamicum* WT and the Δ*cyaB* mutant as controls. **(C, D)** Growth of indicated strains in CGXII medium with 100 mM glucose or 100 mM acetate. The *glxR*_A131T mutation identified in the Δ*cyaB* suppressor mutant was introduced by homologous recombination into the genomes of the WT and the Δ*cyaB* mutant. **(E)** Section of an amino acid sequence alignment of GlxR homologs from different bacterial strains. GlxR (Cg0350) of *C. glutamicum* WT and features derived from its crystal structure (PDB 4CYD) were used as reference. Red boxed amino acids are conserved in all selected sequences. Green arrows indicate residues important for cAMP binding in GlxR according to structural analysis (Townsend et al., 2014). The blue arrow shows the position of the A131T exchange in the Δ*cyaB*_sup1 mutant. The alignment was performed with Clustal W (https://www.genome.jp/tools-bin/clustalw) and processed with ESPript 3 (Robert and Gouet, 2014). The following sequences were used for the alignment: *C. glutamicum* strain R CgR0377; *Corynebacterium efficiens* YS-314 CE0287; C*orynebacterium aurimucosum* ATCC700975 Cauri0205; *Corynebacterium diphtheriae* NCTTC13129 CDIP0303; *Mycobacterium tuberculosis* H37Rv Rv3676; *Escherichia coli* MG1655 b3357. (**F**) Overlay of apo-GlxR$_{WT}$ (green) (PDB:4BYY) and model of apo-GlxR$_{A131T}$ (light blue). (**G**) Overlay of holo-GlxR$_{WT}$ (green) (PDB:4CYD) and a model of holo-GlxR$_{A131T}$ (light blue) showing an enlargement of the region close to A131T amino acid exchange including bound cAMP. The model of GlxR-A131T and the overlay were generated with PyMOL.

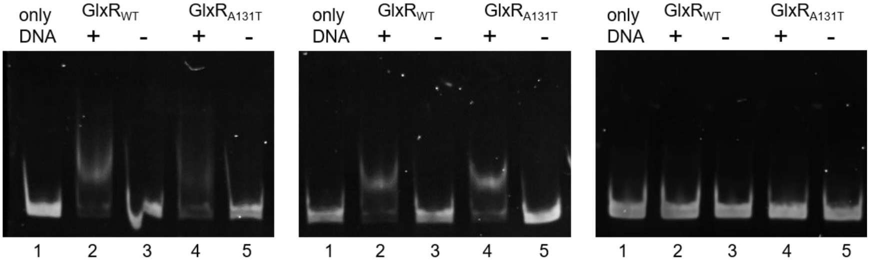

ctaC (cg2409)

ctaD (cg2780)

negative control

FIGURE S5. Electrophoretic mobility shift assays (EMSAs) with C-terminally Twin-Streptagged GlxR$_{WT}$ or GlxR$_{A131T}$ and DNA fragments covering the known GlxR-binding sites in the promoter regions of *ctaD* (-121 to -261 bp upstream of *ctaD* start codon) and *ctaCF* (-102 to -234 bp upstream of *ctaC* start codon) (Kohl et al., 2008; Toyoda et al., 2011) and an intragenic DNA fragment of cg3153 serving as negative control. 100 ng of the DNA fragments were incubated for 30 min at room temperature with 200 nM purified protein, either with (+) or without (-) 0.2 mM cAMP. After incubation, the reaction mixture was loaded on a 10% native polyacrylamide gel. Lane 1: control sample containing only DNA; lane 2: sample with GlxR$_{WT}$, the indicated DNA fragment, and cAMP; lane 3: sample with GlxR$_{WT}$ and the indicated DNA fragment, but without cAMP; lane 4: sample of GlxR$_{A131T}$ with the indicated DNA fragment and cAMP; lane 5: sample with GlxR$_{A131T}$ and the indicated DNA fragment, but without cAMP.

3 Supplementary References

Kohl, T.A., Baumbach, J., Jungwirth, B., Pühler, A., and Tauch, A. (2008). The GlxR regulon of the amino acid producer *Corynebacterium glutamicum*: *In silico* and *in vitro* detection of DNA binding sites of a global transcription regulator. *J. Biotechnol.* 135(4)**,** 340-350. doi: 10.1016/j.jbiotec.2008.05.011.

Robert, X., and Gouet, P. (2014). Deciphering key features in protein structures with the new ENDscript server. *Nucleic Acids Res.* 42**,** W320-324. doi: 10.1093/nar/gku316.

Townsend, P.D., Jungwirth, B., Pojer, F., Bussmann, M., Money, V.A., Cole, S.T., et al. (2014). The crystal structures of apo and cAMP-bound GlxR from *Corynebacterium glutamicum* reveal structural and dynamic changes upon cAMP binding in CRP/FNR family transcription factors. *PLoS One* 9(12)**,** e113265. doi: 10.1371/journal.pone.0113265.

Toyoda, K., Teramoto, H., Inui, M., and Yukawa, H. (2011). Genome-wide identification of *in vivo* binding sites of GlxR, a cyclic AMP receptor protein-type regulator in *Corynebacterium glutamicum*. *J. Bacteriol.* 193**,** 4123-4133. doi: 10.1128/JB.00384-11.

2.3 Comparison of *in vivo* GlxR binding in *Corynebacterium glutamicum* ATCC 13032 and the adenylate cyclase deletion mutant Δ*cyaB* using ChAP-Seq

Natalie Wolf[1], Lukas Lehmann[1], Andrei Filipchyk[1], Tino Polen[1], Michael Bussmann[1], Meike Baumgart[1] and Michael Bott[1]*

[1]IBG-1: Biotechnology, Institute of Bio- and Geosciences, Forschungszentrum Jülich, Jülich, Germany

*Corresponding author

To be submitted

Author's contributions:
NW constructed mutants, plasmids and performed all experimental work except the one specified below for other authors. LL constructed the strain *C. glutamicum*::*glxR*-TS, cultivated and generated one of the nine ChAP-Seq samples. MBu performed the microarray experiment. TP supervised the bioinformatics of the microarray analysis and the first evaluation of the ChAP-Seq results. AF normalized the data of the four ChAP-Seq sample conditions and performed comparisons of peak heights and generated the draft version of Fig. 1. NW wrote the first draft of the manuscript and prepared the figures and tables if not mentioned otherwise. MBa coached the experimental work and supported the design of this study. MBo designed the study, supervised the experimental work and was responsible for the final version of the manuscript.

Overall contribution **NW: 80%**

AF: Andrei Filipchyk, LL: Lukas Lehmann, MBa: Meike Baumgart, MBo: Michael Bott, MBu: Michael Bussmann, NW: Natalie Wolf, TP: Tino Polen

Comparison of *in vivo* GlxR binding in *Corynebacterium glutamicum* ATCC 13032 and the adenylate cyclase deletion mutant Δ*cyaB* using ChAP-Seq

Natalie Wolf[1], Lukas Lehmann[1], Andrei Filipchyk[1], Tino Polen[1], Michael Bussmann[1], Meike Baumgart[1], Michael Bott[1]*

[1]IBG-1: Biotechnology, Institute of Bio- and Geosciences, Forschungszentrum Jülich, Jülich, Germany

ABSTRACT

The Crp homolog GlxR is a cyclic adenosine monophosphate (cAMP)-binding global transcriptional regulator of *Corynebacterium glutamicum*, an important production host in industrial biotechnology. *C. glutamicum* contains only a single adenylate cyclase, encoded by *cyaB*. Strains lacking *cyaB* show a strongly reduced or even absent cAMP level. However, in contrast to Δ*glxR* mutants, which show severe growth defects, a Δ*cyaB* mutant grows like the wild type ATCC13032 (WT), except in the presence of acetate, which inhibits growth. To obtain a better understanding of the different growth phenotypes of Δ*glxR* and Δ*cyaB* mutants, we compared *in vivo* DNA-binding of GlxR in the WT and the Δ*cyaB* mutant during growth in minimal medium containing either only glucose or glucose plus acetate as carbon source. Analysis of the four data sets (WT$_{\text{GlxR-TS}}$ (glc), Δ*cyaB*$_{\text{GlxR-TS}}$ (glc), WT$_{\text{GlxR-TS}}$ (glc-ac) and Δ*cyaB*$_{\text{GlxR-TS}}$ (glc-ac)) comprising nine individual ChAP-Seq experiments identified 243 GlxR peaks with an enrichment factor (EF) of ≥3 in at least one data set. *De novo* motif search identified the consensus sequence TGTGN$_8$CACA in 242 of the GlxR peaks. 141 of these were also reported in previous studies, whereas 102 represent novel binding sites. Remarkably, the majority of the 243 GlxR binding sites were found to be enriched in all four data sets when using an EF ≥1.5 as cutoff. The average EF for the 243 GlxR peaks was 5.23 ± 2.68 for WT$_{\text{GlxR-TS}}$ (glc), 3.99 ± 2.53 for Δ*cyaB*$_{\text{GlxR-TS}}$ (glc), 4.81 ± 3.34 for WT$_{\text{GlxR-TS}}$ (glc-ac), and 2.87 ± 1.40 for Δ*cyaB*$_{\text{GlxR-TS}}$ (glc-ac). The results showed that the strongly diminished or completely absent cAMP level in the Δ*cyaB* mutant reduced GlxR binding, particularly in the presence of acetate, but did not prevent it. This suggests that GlxR binding *in vivo* is less dependent on cAMP than GlxR binding *in vitro* and that additional, yet unknown factors might be involved in the control of GlxR binding to DNA within the cell.

Keywords: *Corynebacterium glutamicum*, GlxR, cAMP, transcriptional regulator, adenylate cyclase, acetate, phosphodiesterase, ChAP-Seq

*Correspondence: Michael Bott (m.bott@fz-juelich.de)

INTRODUCTION

Regulation of gene expression at the level of transcription is one of the key steps in the control of metabolism in bacteria. Transcriptional regulators can be classified into global, master, and local regulators, depending on the number of target genes (Schröder & Tauch, 2010). One of the most intensively studied global regulators in bacteria is the cyclic adenosine monophosphate (cAMP) receptor protein (Crp) of *Escherichia coli* (Gosset et al., 2004; Zheng et al., 2004). Crp belongs to the Crp/Fnr-family of transcriptional regulators (Körner et al., 2003) and activates or represses its target genes in response to the internal cAMP concentration. Crp orthologs are widespread in bacteria and have been studied for example in *Mycobacterium*, *Pseudomonas*, and *Corynebacterium* species (Soberón-Chávez et al., 2017).

Corynebacterium glutamicum is a non-pathogenic soil bacterium, which was isolated due to its ability to secrete L-glutamate (Kinoshita et al., 1957). Today this species is widely used in industrial biotechnology for the production of amino acids, mainly L-glutamate and L-lysine (Eggeling & Bott, 2015). Additionally, *C. glutamicum* strains have been developed for the efficient production of organic acids, polyamines, and various other metabolites (Becker & Wittmann, 2012; Wendisch et al., 2018; Wieschalka et al., 2013; Wolf et al., 2021). Also proteins are meanwhile produced industrially with *C. glutamicum* (Freudl, 2017). Due to the importance of *C. glutamicum* in biotechnology and its close phylogenetic relationship to pathogenic bacteria, such as *Corynebacterium diphtheriae* and *Mycobacterium tuberculosis*, it has become a frequently used model organism (Burkovski, 2008; Eggeling & Bott, 2005; Yukawa & Inui, 2013).

C. glutamicum contains a Crp ortholog named GlxR, which has 27% amino acid sequence identity to Crp of *E. coli* and was shown to be a global regulator. More than 200 putative target genes of GlxR were identified, which are involved in central carbon metabolism and a variety of other cellular functions, such as transport processes, respiration, stress responses, or cell division (Jungwirth et al., 2013; Kohl et al., 2008; Letek et al., 2006; Nishimura et al., 2011; Toyoda et al., 2011). *In vitro* binding of purified GlxR to DNA target sites requires the presence of cAMP (Bussmann, 2009; Kim et al., 2004; Townsend et al., 2014). The crystal structures of apo-GlxR and holo-GlxR revealed structural changes upon cAMP binding that lead to the optimization of the orientation of the two DNA-binding helices (Townsend et al., 2014). The affinity of purified GlxR to a double-stranded oligonucleotide containing a GlxR-binding site increased about 100-fold upon cAMP binding (Townsend et al., 2014).

An important issue for understanding the physiological function of GlxR is therefore the control of the cAMP level within the cell. Two enzymes have been identified that are important in this context. One is the membrane-bound adenylate cyclase CyaB, which catalyses the synthesis of cAMP from ATP (Cha et al., 2010; Wolf et al., 2020). The deletion mutant *C. glutamicum* Δ*cyaB* lacks cAMP or at least has a strongly reduced cAMP level, depending on the method used for analysis (Wolf et al., 2020). Surprisingly, whereas Δ*glxR* mutants have severe growth defects (see below), the Δ*cyaB* mutant grew like the wild type in minimal medium with glucose, fructose, gluconate, or ethanol as carbon source (Cha et al., 2010; Wolf et al., 2020). Only in the presence of acetate (alone or in combination with another carbon source), a strong growth defect was observed (Cha et al., 2010; Wolf et al., 2020). This 'acetate effect' was partly explained by a higher uncoupler sensitivity of the Δ*cyaB* strain due to a lower transcriptional activation and activity of the cytochrome *bc*$_1$-*aa*$_3$ supercomplex in the Δ*cyaB* compared to the wild type (Wolf et al., 2020). The same study also described the isolation of a Δ*cyaB* strain that had regained wild type-like acetate tolerance. This suppressor mutant was shown to possess a single point mutation within the coding region of *glxR*, leading to the amino acid exchange Ala131Thr, which emphasizes the connection and importance of GlxR regulation in response to the intracellular cAMP level (Wolf et al., 2020). The second enzyme relevant for the intracellular cAMP level is the phosphodiesterase CpdA, which catalyses the hydrolysis of cAMP (Schulte et al., 2017). The deletion mutant *C. glutamicum* Δ*cpdA* has an increased intracellular cAMP level and shows growth defects in complex medium and in minimal medium with glucose, gluconate, citrate, acetate, or ethanol as carbon sources (Schulte et al., 2017). Many of these growth defects occurred due to stronger repression by GlxR of genes that code for transporters of the respective carbon sources (Schulte et al., 2017).

The search for target genes of transcriptional regulators often involves a transcriptome comparison of a deletion mutant lacking the regulator gene with the wild type. However, a deletion of *glxR* was extremely difficult to obtain and the mutants with only a partly deleted *glxR* showed severe growth defects (Moon et al., 2007; Park et al., 2010). Therefore, current knowledge of the direct target genes of GlxR is based on a variety of alternative approaches, such as (i) bioinformatic identification of GlxR binding sites within the genome combined with electrophoretic mobility shift assays (EMSAs), showing the cAMP-dependent binding of purified GlxR to these motifs (Kohl & Tauch, 2009), (ii) reporter gene assays at varying GlxR levels (Bussmann et al., 2009), (iii) impact of GlxR-binding site mutations on gene expression (Inui et al., 2004), (iv) transcriptome comparisons of strains with an increased (strain Δ*cpdA*) or reduced (strain Δ*cyaB*) cAMP level compared with the wild type (Schulte et al., 2017; Wolf et al., 2020) or (v) genome-wide identification of *in vivo* GlxR binding sites. In particular the latter approach is a highly valuable tool and two studies using it for GlxR were reported. In one study, chromatin immunoprecipitation with an anti-GlxR antibody and subsequent sequencing (ChIP-Seq) was performed with the type strain ATCC13032 grown on either glucose or acetate. Whereas 107 DNA fragments were enriched from glucose-grown cells, only two were also enriched from acetate-grown cells (Jungwirth et al., 2013). In a second study, ChIP-chip analysis was used to determine the GlxR binding sites in *C. glutamicum* strain R and led to the identification of 209 *in vivo* GlxR-binding sites (Toyoda et al., 2011). In the latter study, also a Δ*cyaB* mutant of strain R was analysed by ChIP-chip, which revealed that GlxR was still able to interact with its target sites, but with a markedly decreased binding affinity (Toyoda et al., 2011).

Besides ChIP-Seq and ChIP-chip, ChAP-Seq has been established as a variant of ChIP-Seq to detect *in vivo* binding sites of DNA-binding proteins. It involves affinity purification of a tagged DNA-binding protein covalently linked to its genomic target sites followed by sequencing of the enriched DNA fragments. In *C. glutamicum* ATCC13032, the ChAP-Seq method was already successfully applied to study, e.g., the role of the nucleoid-associated protein CgpS or to analyse the influence of intracellular heme concentrations on the binding of response regulator HrrA to target DNA (Keppel et al., 2020; Pfeifer et al., 2016). In the current study, we used ChAP-Seq to analyse *in vivo* GlxR-binding sites in the wild type and the Δ*cyaB* mutant of strain ATCC13032 after cultivation in minimal medium with either glucose or a glucose-acetate mixture as carbon sources. The aim was to explore the influence of a decreased or even absent cAMP level and of acetate on *in vivo* GlxR-binding and thus get a better understanding of the function of this global regulator. The results of this study led to the identification of about 100 hitherto unknown GlxR-binding sites and consequently a large expansion of the GlxR regulon. Furthermore, evidence was obtained that, as expected, cAMP promotes DNA-binding of GlxR, but apparently is not an essential prerequisite for binding.

METHODS

Bacterial strains, plasmids, oligonucleotides and cultivation conditions

All bacterial strains and plasmids used in this study are listed in Table 1. The oligonucleotides used in this study are listed in Table S1. *C. glutamicum* strains were cultivated in brain heart infusion (BHI) medium (Bacto™ BHI, BD, Heidelberg, Germany) or in CGXII minimal medium (adjusted to pH 7.0 with KOH) (Frunzke et al., 2008) containing either 100 mM glucose or a mixture of glucose and acetate (100 mM and 150 mM, respectively) as carbon source. For growth experiments, 5 ml BHI medium was inoculated with a single colony and incubated at 30 °C and 130 rpm for 8 h. The second preculture was inoculated with 400 µl of the first preculture and cultivated for about 16 h at 30 °C and 120 rpm in a 100 ml baffled shake flask containing 20 ml CGXII medium with 2% (w/v) glucose. For the main culture in a microcultivation system, 800 µl CGXII medium in FlowerPlates (m2p-labs, Baesweiler, Germany) was inoculated to an optical density at 600 nm (OD_{600}) of 1 and cultivated at 1200 rpm, 30 °C and 80% humidity in a BioLector microcultivation system (m2p-labs, Baesweiler, Germany). Growth was followed by measuring the backscatter at 620 nm, which reflects the cell density (Kensy et al., 2009). For cultivations in 5 L baffled-shake flasks, 500 ml CGXII medium was inoculated with the second preculture to an OD_{600} of 1. The cultivations in 5 L shake flasks were performed at 30 °C and 90 rpm and growth was followed by measuring OD_{600}. *E. coli* DH5α was used as host for all cloning purposes and was cultivated at 37 °C in lysogeny broth (LB) medium (Sambrook & Russell, 2001). *E. coli* BL21(DE3) was used for the production of proteins (Studier & Moffatt, 1986). For this purpose, the strain carrying an overexpression plasmid was cultivated in ZYM-5052 auto-induction medium (Studier, 2005) at 30 °C for 16 h. If required, media were supplemented with kanamycin (25 µg ml^{-1} for *C. glutamicum* and 50 µg ml^{-1} for *E. coli*).

Construction of *C. glutamicum* strains with chromosomally encoded GlxR with C-terminal Twin Strep-Tag

C. glutamicum WT and the Δ*cyaB* mutant carrying the coding sequence of a Twin Strep-tag at the 3' end of the chromosomal *glxR* gene were constructed by double homologous recombination with the pK19*mobsacB* system as described previously (Niebisch & Bott, 2001; Schäfer et al., 1994). Briefly, *C. glutamicum* WT was transformed with the deletion plasmid pK19*mobsacB-glxR-twinstrep* harbouring a 1143 bp PCR product comprising 540 bp representing the 3' end of *glxR* without the stop codon, followed by the sequence for the Twin Strep-tag (WSHPQFEKGGGSGGGSGGSAWSHPQFEK), a stop codon and 516 bp corresponding to the sequence downstream of *glxR*. After the second homologous recombination event, 25 kanamycin-sensitive and sucrose-resistant clones were analysed by colony PCR; 14 clones harboured the Twin Strep-tag-encoding sequence whereas eleven clones contained the wild-type fragment. The strain *C. glutamicum::glxR-TS* ('$WT_{GlxR-TS}$') with the chromosomally Twin Strep-tagged was obtained without any difficulties and served as parental strain for construction of *C. glutamicum::glxR-TS* Δ*cyaB* ('Δ$cyaB_{GlxR-TS}$') as described (Wolf et al., 2020).

Chromatin affinity purification and sequencing (ChAP-Seq)

The preparation of the samples for the ChAP-Seq runs were performed as described previously (Pfeifer et al., 2016) with the following adaptations: $WT_{GlxR-TS}$ and Δ$cyaB_{GlxR-TS}$ were cultivated in 500 ml CGXII medium with glucose or glucose-acetate

TABLE 1 | Bacterial strains and plasmids used in this study

Strain or plasmid	Relevant characteristics	Source or Reference
Strains		
E. coli DH5α	F^{-} φ80*lac*ZΔM15 Δ(*lac*ZYA-*arg*F)U169 *rec*A1 *end*A1 *hsd*R17(r_K^{-}, m_K^{+}) *pho*A *sup*E44 λ^{-}*thi*-1 *gyr*A96 *rel*A1	Invitrogen
E. coli BL21(DE3)	B F^{-} *ompT gal dcm lon* $hsdS_B(r_B^{-}m_B^{-})$ λ(DE3 [*lacI lacUV5-T7p07 ind1 sam7 nin5*]) $[malB^{+}]_{K\text{-}12}(\lambda^{S})$	(Studier & Moffatt, 1986)
C. glutamicum ATCC13032 (WT)	ATCC13032, biotin-auxotrophic wild-type strain (WT)	(Kinoshita et al., 1957)
C. glutamicum::*glxR*-TS ($WT_{GlxR\text{-}TS}$)	*C. glutamicum* ATCC13032 with a Twin Strep-tag encoding sequence at the 3' end of *glxR* (cg0350). The C-terminal tag has the following amino acid sequence: WSHPQFEKGGGSGGGSGGSAWSHPQFEK.	This study
C. glutamicum Δ*cyaB*	ATCC13032 with an in frame deletion of the adenylate cyclase gene *cyaB* (cg0375)	(Wolf et al., 2020)
C. glutamicum::*glxR*-TS Δ*cyaB* ($\Delta cyaB_{GlxR\text{-}TS}$)	$WT_{GlxR\text{-}TS}$ strain with a deletion of *cyaB* (cg0375)	This study
Plasmids		
pAN6	Kan^R; P_{tac}, $lacI^q$ pBL1 $oriV_{Cg}$ pUC18 $oriV_{Ec}$, *C. glutamicum/E. coli* shuttle vector, derivative of pEKEx2	(Frunzke et al., 2008)
pAN6-*glxR-twinstrep*	Kan^R; pAN6 derivative encoding C-terminal Twin Strep-tagged GlxR (Cg0350) under the control of P_{tac}	(Wolf et al., 2020)
pK19*mobsacB*	Kan^R; oriT $oriV_{Ec}$*sacBlacZα;* vector for allelic exchange in *C. glutamicum*	(Schäfer et al., 1994)
pK19*mobsacB*-Δ*cyaB*	Kan^R; pK19*mobsacB* derivative containing an overlap extension PCR product covering the up- and downstream regions of *cyaB* (cg0375)	(Wolf et al. 2020)
pK19*mobsacB*-*glxR*-*twinstrep*	KanR; pK19*mobsacB* derivative containing a 1143 bp PCR product covering the 3' terminal 540 bp of *glxR* (cg0350) without the stop codon but instead the coding sequence of the Twin Strep-tag (WSHPQFEKGGGSGGGSGGSAWSHPQFEK) and 516 bp of the *glxR* downstream region	This study

mixture, respectively. The cross-linking of GlxR carrying a C-terminal Twin Strep-tag (named $GlxR_{TS}$) to the bound DNA was performed in the exponential growth phase at an OD_{600} of 6. The $GlxR_{TS}$-DNA complexes were purified following the Strep-Tactin XT affinity chromatography purification protocol (IBA Life Sciences, Göttingen, Germany). The elution fractions of the $GlxR_{TS}$-DNA complexes were incubated overnight at 65 °C, followed by the digestion of $GlxR_{TS}$ with 400 µg ml^{-1} proteinase K (AppliChem GmbH, Darmstadt, Germany) for 3 h at 55 °C.

Subsequently, the DNA was purified as described previously (Pfeifer et al., 2016).

The purified DNA fragments of each sample were used for library preparation and indexing with the TrueSeq DNA PCR-free sample preparation kit (Illumina, San Diego, USA) or the NEBNext Ultra II DNA Library Prep kit for Illumina (New England Biolabs GmbH, Frankfurt am Main, Germany) following the manufacturer's instructions, yet omitting the DNA size selection steps. The resulting indexed libraries were quantified using the KAPA Library Quantification kit (Peqlab, Bonn, Germany) and normalized for pooling. Sequencing was performed on a MiSeq instrument (Illumina, San Diego, USA) using paired-end sequencing with a read-length of 2 × 150 bp. Data analysis and base calling were accomplished with the CLC Genomics workbench (Version 9, Qiagen, Hilden, Germany). The reads were mapped to the genome sequence BA000036.3 of *C. glutamicum* ATCC13032 (Ikeda & Nakagawa, 2003). Evaluation of genomic coverage, peak detection and normalization was essentially performed as described in Keppel et al., 2020. The enrichment factor (EF) was defined as ratio of the sequencing coverage at a certain position divided by the average background coverage of the whole genome. Genome regions with an EF ≥ 3 in at least one data set were considered as specifically enriched DNA regions and defined as peaks.

ChAP-Seq analysis and motif search

Genome regions with peaks found in at least two independent ChAP-Seq runs of the same strain and the same growth condition (data set) were defined as *in vivo* GlxR-DNA binding regions. For motif search, the DNA sequence of all defined *in vivo* GlxR-DNA binding regions was submitted to MEME-ChIP (Version 5.1.1) (Bailey & Elkan, 1994). The sequences used for MEME-ChIP were generated by taking the highest point of the ChAP-Seq peak and adding 250 bp on each side of the enriched DNA fragment (yielding sequences of 501 bp). Parameters of the tool were set to search for a palindromic motif with a 16 bp long sequence.

Electrophoretic mobility shift assays (EMSAs) with purified GlxR$_{TS}$

Protein production of GlxR$_{TS}$ and the subsequent purification was performed as described previously (Wolf et al., 2020). EMSAs with the purified GlxR$_{TS}$ were performed as described previously (Bussmann et al., 2009). The DNA fragments were chosen based on peak detection of the ChAP-Seq analysis and comprised a 100-120 bp fragment with the GlxR-binding site (predicted in our MEME-ChIP analysis) in the centre of the fragment. The respective DNA fragments were generated by PCR using the oligonucleotides listed in Table S1 and purified with the DNA Clean & Concentrator Kit (Zymo Research, Freiburg, Germany).

Transcriptome analysis using DNA microarrays

Preparation of RNA and synthesis of labelled cDNA was prepared from cells in the exponential growth phase. The microarrays were performed according to the description in Wolf et al., 2020. The genome-wide mRNA concentrations of *C. glutamicum* wild type were compared with those of the *C. glutamicum* Δ*cyaB* mutant. The strains were cultivated in CGXII medium with 100 mM glucose. Three independent DNA microarray experiments, each starting from independent cultures, were performed.

RESULTS

Experimental setup for the detection of *in vivo* GlxR$_{TS}$-DNA binding regions

In this study, we wanted to analyse the impact of a lowered cytoplasmic cAMP level and of acetate on the genome-wide GlxR-DNA binding patterns using ChAP-Seq. For this purpose, the ATCC13032 derivatives WT$_{GlxR\text{-}TS}$ and Δ*cyaB*$_{GlxR\text{-}TS}$ were constructed, which encode GlxR derivatives with a C-terminal Twin Strep-tag. The Δ*cyaB*$_{\mathrm{GlxR\text{-}TS}}$ mutant lacks the *cyaB* gene for adenylate cyclase and therefore has a low intracellular cAMP level or even no cAMP at all, depending on the method used for cAMP determination (Cha et al., 2010; Wolf et al., 2020). *C. glutamicum* ATCC13032 and WT$_{\mathrm{GlxR\text{-}TS}}$ showed the same growth behaviour in glucose minimal medium (Fig. S1), indicating that the replacement of native GlxR with a Twin Strep-tagged variant does not disturb the functionality of the protein. Furthermore, GlxR with a C-terminal Strep-tag has previously been used successfully for ChIP-chip analysis with the strain *C. glutamicum* R (Toyoda et al., 2011).

For the ChAP-Seq analysis, three biological replicates were performed for WT$_{\mathrm{GlxR\text{-}TS}}$ cultivated on glucose and two replicates each for WT$_{\mathrm{GlxR\text{-}TS}}$ cultivated on glucose and acetate, Δ*cyaB*$_{\mathrm{GlxR\text{-}TS}}$ cultivated on glucose, and Δ*cyaB*$_{\mathrm{GlxR\text{-}TS}}$ cultivated on glucose and acetate. The growth rates of the two strains were comparable during cultivation on glucose ($\mu = 0.36 - 0.38$), but differed during growth on glucose and acetate, where the Δ*cyaB*$_{\mathrm{GlxR\text{-}TS}}$ strain showed a reduced growth rate ($\mu = 0.36$ for WT$_{\mathrm{GlxR\text{-}TS}}$, $\mu = 0.16$ for Δ*cyaB*$_{\mathrm{GlxR\text{-}TS}}$). The sequencing data of all nine individual ChAP-Seq runs showed good quality and were used for further analysis. The number of reads, the mapping statistics, and the coverages are listed in Table S2. In ChAP-Seq analysis, a low amount of DNA fragments covering the entire genome is always isolated unspecifically, which enables the determination of the background coverage. This background coverage varies between different ChAP-Seq runs, depending, e.g., on the total number of reads. In order to enable a direct comparison of multiple ChAP-Seq runs, the data were normalized as described in (Keppel et al., 2020). This allowed the calculation of average enrichment factors (EF) for a certain genomic position based on the two or three replicate ChAP-Seq runs performed for each of the four conditions studied in this work. In this way four ChAP-data sets were obtained and used for further analysis: WT$_{\mathrm{GlxR\text{-}TS}}$ (glc), Δ*cyaB*$_{\mathrm{GlxR\text{-}TS}}$ (glc), WT$_{\mathrm{GlxR\text{-}TS}}$ (glc-ac), and Δ*cyaB*$_{\mathrm{GlxR\text{-}TS}}$ (glc-ac).

DNA regions bound by GlxR$_{\mathrm{TS}}$ and influence of acetate and adenylate cyclase

In our analysis we focused on those GlxR peaks, which were found to have an EF ≥3 in at least one ChAP-Seq data set. In the four data sets, in total 243 GlxR peaks with an EF ≥3 were identified (Table S3), with the highest number of 229 in WT$_{\mathrm{GlxR\text{-}TS}}$ (glc) (Table 2). The other 14 GlxR peaks with an EF ≥3 were present in Δ*cyaB*$_{\mathrm{GlxR\text{-}TS}}$ (glc) and/or WT$_{\mathrm{GlxR\text{-}TS}}$ (glc-ac). The distribution and the EFs of the GlxR peaks throughout the genome are shown for each of the four data sets in Fig. 1. Importantly, this figure and also the summarized data in Table S3 clearly show that for the vast majority of the GlxR peaks an enrichment was detected in all four data sets. When considering all peaks with an EF ≥1.5 as enriched, only two, nine, one, and 37 peaks of the total 243 GlxR peaks were non-enriched in one of the four data sets (Table 2). When looking at the mean EFs of the four data sets as a proxy for the overall effects, it is obvious that the presence of acetate reduced the mean EF in the WT by about 8% from 5.23 in the absence of acetate to 4.81 in its presence. In the Δ*cyaB* mutant, the presence of acetate reduced the mean EF by 28%, from 3.99 to 2.87, and thus had a stronger effect than in the WT. The absence of adenylate cyclase reduced the mean EF during growth on glucose by 24% from 5.23 in the WT to 3.99 in the *cyaB* mutant and during growth on glucose and acetate by even 40% from 4.81 in the WT to 2.87 in the Δ*cyaB* mutant. Thus, the absence of adenylate cyclase clearly reduced GlxR binding *in vivo*, but did not prevent it.

An interesting feature visible in Fig. 1B and D is a missing region of about 34 kb in the background coverage at about 2 Mb in strain Δ*cyaB*$_{\mathrm{GlxR\text{-}TS}}$.

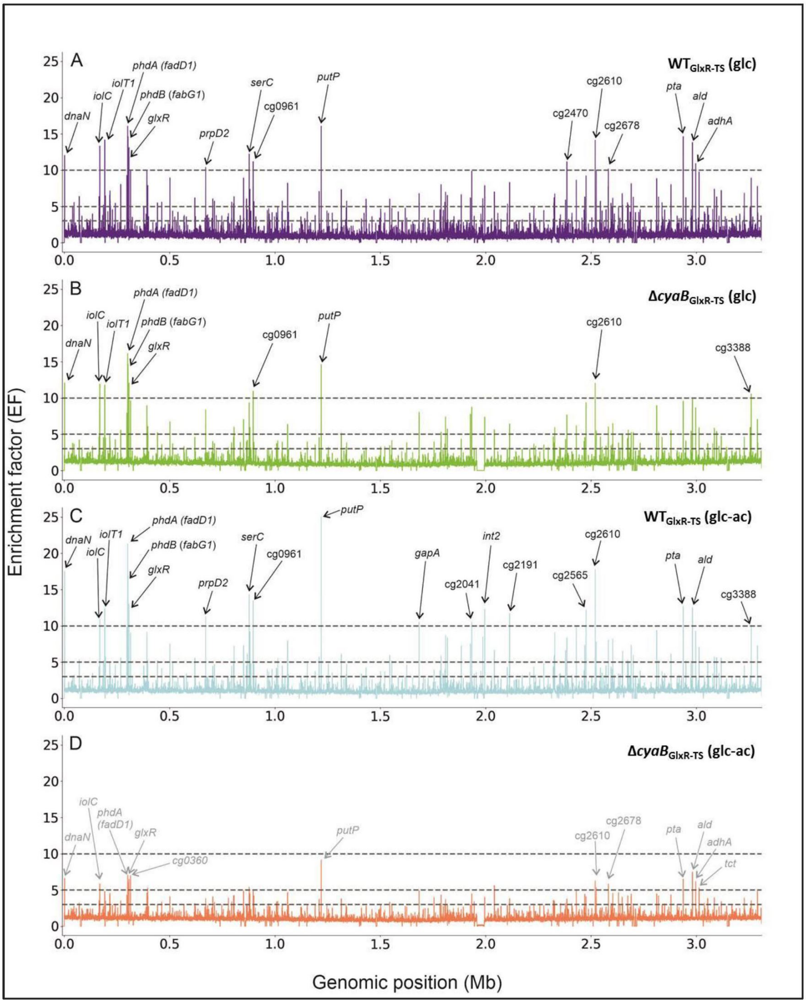

FIGURE 1 | Comparison of the four ChAP-Seq data sets (averaged values from two or three individual ChAP-Seq experiments) produced and analysed in this study. The strains and growth conditions are indicated for each of the four panels **A**, **B**, **C**, and **D**. The DNA sequencing data were normalized as described in (Keppel et al., 2020). The first dashed grey line indicates the EF threshold of 3 used in this work to consider a GlxR peak. When a GlxR-binding site was found to be located -700 bp to +60 bp relative to the TSS or TLS, the respective protein-coding gene was categorized as a neighbouring gene. For GlxR peaks with an EF ≥10 and some others, the neighbouring gene is labelled in black. In the case of the data set for Δ*cyaB*$_{\text{GlxR-TS}}$ (glc-ac), none of the GlxR peaks showed an EF ≥10 and in this case the genes next to the GlxR peaks with the highest EFs are labelled in grey.

The missing region corresponds to the CGP4 prophage region (Ikeda & Nakagawa, 2003). As strain Δ*cyaB*$_{\text{GlxR-TS}}$ was derived from WT$_{\text{GlxR-TS}}$, CGP4 must have been lost during the deletion of *cyaB*. We rechecked several Δ*cyaB* mutants with different strain backgrounds present in our strain collection, and out of seven tested clones, three had lost CGP4 (data not shown). The CGP3 and CGP4 prophage regions (CGP4 is located within the CGP3 region) share large homologous regions and therefore CGP4 can be excised by homologous recombination. We assume that the excision is favoured upon *cyaB* deletion. This phenomenon was not studied further, but could be interesting for future prophage studies.

DNA sequence motif search and location of GlxR binding sites

Using 501 bp DNA long sequences of the 243 identified GlxR peaks (250 bp on each side of the peak maximum), we performed a *de novo* motif search with MEME-ChIP (Bailey & Elkan, 1994). This resulted in the consensus motif TGTGWBNHDNVWCACA (Fig. 2) with highly conserved TGTG and CACA residues at position 1 to 4 and 13 to 16. These conserved bases correspond to the motif previously reported for GlxR (Jungwirth et al., 2013; Kohl et al., 2008; Toyoda et al., 2011). The bases 5 to 12 are hardly conserved in our consensus motif, suggesting that TGTG and CACA are the important residues for binding of GlxR, as also pointed out before (Toyoda et al., 2011). Within the 243 GlxR peaks, the *de novo* motif search found 242 fragments having a binding site with an e-value <0.03. This result provided strong support for the validity of our ChAP-Seq data. In the case of GlxR peak centred 66 bp upstream of the transcriptional start site (TSS) of *oxyR*, which is a leaderless transcript, no obvious GlxR motif was present and the basis for GlxR binding at this position is not known.

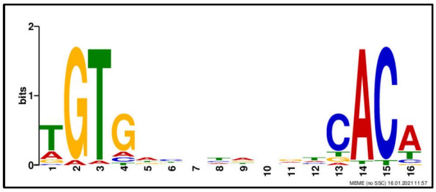

FIGURE 2 | GlxR consensus motif determined by MEME-ChIP analysis (Version 5.1.1) (Bailey & Elkan 1994) using the DNA sequences of the 243 defined GlxR peaks. For motif analysis, a 16 bp palindromic motif was searched in the region of the peak maximum.

Table S3 shows the distance of the detected GlxR binding motifs to the TSS, or, if this unknown, to the translational start site (TLS) of neighbouring genes. The position of the GlxR binding sites was sorted into five groups (Fig. 3): (i) GlxR binding sites (n = 79) located less than 500 bp upstream of a transcriptional start site (TSS), or if TSS is unknown, the translational start site (TLS) of a neighbouring gene or operon. (ii) GlxR binding sites (n = 69) located intergenic of two divergently transcribed genes with less than 500 bp upstream of a transcriptional start site (TSS), or if TSS is unknown, the translational start site (TLS) of a neighbouring gene or operon. (iii) GlxR binding sites (n = 10) located within intergenic regions of two convergently transcribed genes. (iv) GlxR binding sites (n = 40) located intragenically and less than 500 bp upstream of a transcriptional start site (TSS), or if TSS is unknown, the translational start site (TLS) of a neighbouring gene or operon. (v) GlxR binding sites (n = 45) located intragenically and more than 500 bp upstream of a transcriptional start site (TSS), or if TSS is unknown, the translational start site (TLS) of a neighbouring gene or operon. The GlxR binding sites of the latter three groups are summarized in Table S4. Whereas GlxR binding to the sites of groups (i), (ii) and (iv) is known or considered to influence the transcription of the downstream genes, this appears less likely for GlxR binding to the sites of groups (iii), and (v). Due to the lack of a genome-wide comparison of gene expression in a Δ*glxR* mutant and the WT, only selected

TABLE 2 | Overview on GlxR peaks identified in the four ChAP-Seq data sets.

ChAP-Seq data set	**WT$_{\text{GlxR-TS}}$ (glc)**	**Δ*cyaB*$_{\text{GlxR-TS}}$ (glc)**	**WT$_{\text{GlxR-TS}}$ (glc-ac)**	**Δ*cyaB*$_{\text{GlxR-TS}}$ (glc-ac)**
GlxR peaks with EF ≥3	229	135	163	90
No. of GlxR peaks with an EF ≥1.5 for the 243 total GlxR peaks	241	234	242	205
Mean EF and standard deviation for all 243 GlxR peaks with EF ≥3	5.23 ± 2.68	3.99 ± 2.53	4.81 ± 3.34	2.87 ± 1.40
Max. EF	16.12	16.10	25.00	9.09
No. of GlxR peaks with EF ≥10	17	12	12	0

GlxR target genes were experimentally analysed with respect to their activation or repression by GlxR (Bussmann et al., 2009; Nishimura et al., 2011; Park et al., 2010; Toyoda et al., 2011; van Ooyen et al., 2011).

New GlxR peaks and potential GlxR target genes in *C. glutamicum* ATCC13032

In the four ChAP-Seq data sets generated in this study, 243 GlxR peaks were identified based on the criterion that the peak had an EF ≥3 in at least one of the data sets. 141 of these GlxR binding sites had also been identified previously by ChIP-Seq or Chip-chip experiments (Jungwirth et al., 2013; Toyoda et al., 2011), or in EMSA studies (Kohl et al., 2008; Kohl & Tauch, 2009; Toyoda et al., 2011). 102 of the GlxR peaks detected in our study were not reported before and provide a large expansion of the GlxR regulon. In Table 3, all 102 new GlxR binding sites and their distance to the TSS or TLS of neighbouring genes are shown, whereas missing peaks that were reported in literature are listed in Table S5. As several of these GlxR binding sites were located within 200 bp upstream of a TSS or TLS, an influence of GlxR on the transcription of the corresponding gene appears likely. Genes that might be repressed by GlxR because its binding site is located downstream of the TSS or TLS are for example *guaA* (GMP synthase) or *siaE* (periplasmic binding protein of sialic acid ABC transporter).

In order to further confirm the ability of GlxR to bind to some of the newly identified binding sites in strain ATCC13032, DNA fragments covering the GlxR motif upstream of *hemL* (cg0518), *aspA* (cg1657), and the one in the intergenic region of region of *nanR* (cg2936) and *siaE* (cg2937) were amplified and used for EMSAs with purified GlxR. For all three fragments, a cAMP-dependent DNA shift was observed (Fig. S2).

Prediction of transcriptional activation or repression by GlxR in a cAMP-dependent manner

To evaluate whether a transcriptional regulator activates or represses a target gene, transcriptome comparisons of regulator deletion strains with the parental strain are frequently used. Due to the severe growth defects of the *glxR* deletion mutants, meaningful microarray experiments with such a strain were not possible (Moon et al., 2007; Park et al., 2010). Therefore, we performed a transcriptome comparison of the Δ*cyaB* mutant with the WT during growth in CGXII medium with glucose. The resulting mRNA ratios were then compared with those obtained in a previously established microarray data set (GEO accession number GSE81004) in which the Δ*cpdA* mutant lacking the cAMP

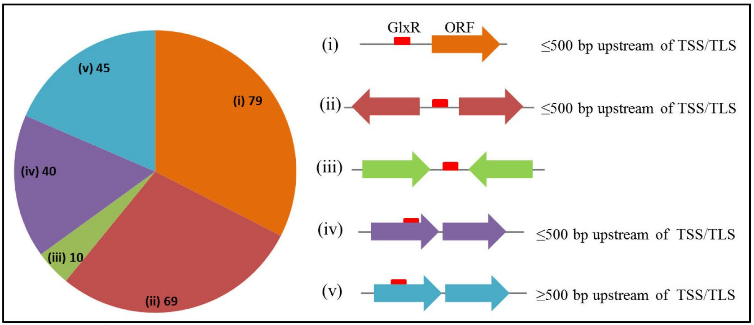

FIGURE 3 | Location of GlxR binding sites with respect to neighbouring TSS or TLS.

phosphodiesterase was compared with the WT (Schulte et al., 2017). Due to the opposing effects of the *cyaB* and *cpdA* on the cellular cAMP level (lowered and increased, respectively), a similar effect on the expression on GlxR target genes might be visible, at least in some cases (Table S6). mRNA ratios with a value ≤0.6 in the Δ*cpdA* mutant and a value ≥1.4 in the Δ*cyaB* mutant, are *here* predicted to be repressed by GlxR in a cAMP-dependent manner. This was found for example for the genes *cysR* (cg0156), *iolT1* (cg0223), *creJ* (cg0645), cg0961, *ptsG* (cg1537), *ptsI* (cg2117), *oppC* (cg2183), *oppD* (cg2184), *vanA* (cg2616), *ptsS* (cg2925), *pta* (cg3048), *cysZ* (cg3112), *tctC* (cg3127) and *gntP* (cg3216). Vice versa, if these mRNA ratios showed a value ≤0.6 in the Δ*cyaB* mutant and a value ≥1.4 in the Δ*cpdA* mutant, they were *here* predicted to be likely activated by GlxR in a cAMP-dependent manner. This was found for the genes cg2665 and cg2824.

GlxR binding sites upstream of sRNAs, asRNAs, tRNAs, and *rrn*-operons

Many small RNAs (sRNAs), antisense RNAs (asRNA), and intragenic transcripts have been detected in *C. glutamicum* ATCC13032 in the course of comprehensive RNA-Seq studies (Mentz et al., 2013; Pfeifer-Sancar et al., 2013). We identified more than 40 GlxR binding sites that were located closer to the TSSs of a sRNA, asRNA, or an intragenic transcript than to a TSS of a protein-coding gene (Table S7). For example GlxR binding sites were found that are closely located to the TSS of the asRNAs of cg1052, cg1609, cg1945 and cg3393, respectively (Fig. 4A-D); the sRNAs cgb_00545 (adjacent genes cg0054/ *crgA)* and cgb_27005 (adjacent genes *phoB*/*musI*) (Fig. 4E, F), or close to the TSS of an intragenic transcript within the gene cg0706 (Fig. 4G).

GlxR peaks were also found upstream or within the genes of tRNAs, i.e. tRNA^{Leu}, tRNA^{Arg}, tRNA^{Gly} and of tRNA^{Asp} and might influence their transcription (Table S7). In the initial process of peak detection, GlxR peaks containing GlxR binding motifs were found upstream of the 23S rRNA gene (TGTGTGATACCGAACG), within the 23S rRNA gene (TGTGCACTTACACTCA), and in four upstream regions of the 5S rRNA gene (TGTGCTGTGTCAGACA), belonging to the rrn operon of *rrnA*, *rrnB*, *rrnC* and *rrnF*). In the final version of the peak detection these regions and the peaks were excluded due to fact that the sequences of six *rrn* operons (*rrnA*, *rrnB*, *rrnC*, *rrnD*, *rrnE*, *rrnF*) each coding for 16S, 23S and 5S are very similar to each other and thus are not unique in the genome. Therefore it could not be shown in which of the six *rrn* regions the *in vivo* interaction of GlxR-DNA was detected.

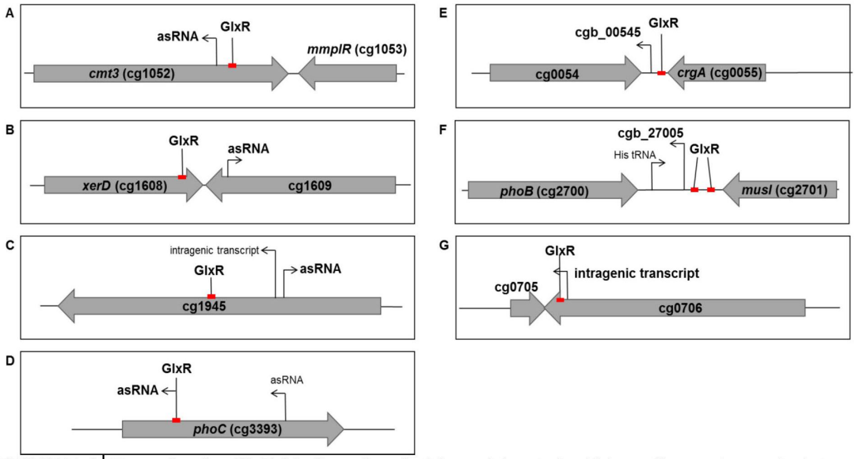

FIGURE 4 | Examples for GlxR binding sites (red boxes) located within coding region or in intergenic regions between convergently transcribed genes with a possible regulatory role for antisense transcripts (asRNA), small RNAs, or intragenic transcripts. GlxR binding site located: **(A)** -227 bp upstream of the TSS of an asRNA of *cmt3* (cg1052), **(B)** -114 bp upstream of the TSS of an asRNA of cg1609, **(C)** -618 bp upstream of an asRNA of cg1945. **(D)** on the TSS of an asRNA of *phoC* (cg3393), **(E)** GlxR binding site in the intergenic region of cg0054 and *crgA* (cg0055) located -121 bp upstream of the sRNA the TSS of cgb_00545, **(F)** in the intergenic region of *phoB* and *musI* located -190 bp and -432 bp upstream of the TSS of the sRNA cgb_27005 and **(G)** within the coding region of cg0706 located +34 bp downstream of an intragenic transcript. Information on sRNA, asRNA and intragenic transcripts was taken from Pfeifer-Sancar et al., 2013 and Mentz et al., 2013. The motifs of the GlxR binding sites are listed in Table S7.

DISCUSSION

In this study we analysed the influence of a missing adenylate cyclase CyaB on *in vivo* DNA binding of the global transcriptional regulator GlxR of *C. glutamicum* in order to better understand the different growth phenotypes of Δ*cyaB* and Δ*glxR* mutants. Whereas Δ*glxR* mutants show severe growth defects, Δ*cyaB* mutant grow like the WT except in the presence of acetate (Cha et al., 2010; Moon et al., 2007; Park et al., 2010; Toyoda et al., 2011; Wolf et al., 2020). Numerous *in vitro* studies have been performed with purified GlxR and target DNAs and binding of GlxR was found to be strictly dependent on the presence of cAMP (Bussmann et al., 2009; Jungwirth et al., 2013; Kohl & Tauch, 2009; Nishimura et al., 2011), except for two cases (cgR_1596, *mscL*), where weak binding was observed in the absence of cAMP (Toyoda et al., 2011). CyaB, which is composed of an N-terminal membrane-integral domain with six predicted transmembrane helices that is linked via a HAMP domain to a class IIId catalytic domain, is the only adenylate cyclase encoded in the genome of *C. glutamicum*. Our recent LC-MS/MS measurements indicated that a Δ*cyaB* mutant does not contain cAMP anymore (Wolf et al. 2020). Therefore, if cAMP is also essential for GlxR binding *in vivo*, the Δ*cyaB* mutant should show a similarly strong growth defect as a Δ*glxR* mutant, which is not the case. Our ChAP-Seq studies provide an explanation for this discrepancy, as they suggest that GlxR binds *in vivo* to its target sites also in the absence of cAMP.

The four ChAP-Seq data sets generated in this work comparing GlxR binding in the WT and the Δ*cyaB* mutant after growth on either glucose or glucose plus acetate identified 243 GlxR peaks, if an EF ≥3 in at least one data set was used as initial selection criterion. In the Δ*cyaB* mutant, 234 and 205 of these peaks had an EF ≥1.5 when cultivated on glucose or on glucose plus acetate, respectively (Table 2). Therefore, GlxR bound to these sites also the absence of cAMP, but with reduced affinity as shown by the lowered mean EFs in the Δ*cyaB* mutant, which was particularly evident in the presence of acetate (Table 2). This result agrees with ChIP-chip data obtained with *C. glutamicum* strain R (Toyoda et al., 2011) and suggests that *in vivo* cAMP is not essential for binding of GlxR to most of its target sites, in contrast to the *in vitro* situation. The difference between the growth phenotypes of Δ*cyaB* and Δ*glxR* mutants can thus be explained by the fact that GlxR can still exert its functions in the absence of cAMP.

If cAMP has a regulatory, but not an essential function for *in vivo* DNA-binding by GlxR, other, yet unknown factors might also be involved in the control of GlxR binding to DNA target sites within the cell. One possibility could be an interaction of GlxR with another protein, as has been shown, e.g., for CcpA and Hpr in *Bacillus subtilis* (Görke & Stülke, 2008). However, in the currently available literature there is no evidence so far for a protein interacting with GlxR. Another option for influencing the DNA-binding properties of GlxR *in vivo* can be posttranslational modifications. In a study globally analysing protein acetylation and protein succinylation in *C. glutamicum*, three succinylated lysine residues were detected in GlxR, i.e. Lys59, Lys155, and Lys212 (Mizuno et al., 2016). The influence of these modifications could be tested for example by replacing the positively charged lysine residues with a negatively charged glutamate residue. In the case of the 2-oxoglutarate dehydrogenase inhibitor protein OdhI (Niebisch et al., 2006), succinylation at Lys132 reduced the binding to OdhA and thus inhibition of 2-oxoglutarate dehydrogenase activity (Komine-Abe et al., 2017).

Besides succinylation, also pupylation was detected for the GlxR protein at Lys57 (Küberl et al., 2014). Pupylation is a post-translational modification mainly occurring in Actinobacteria resembling ubiquitination in eukaryotes and was first identified in *Mycobacterium tuberculosis* (Pearce et al., 2008). Selected lysine residues of target proteins are covalently linked by an isopeptide bond with the C-terminal glutamate residue of the small prokaryotic ubiquitin-like protein Pup and this modification typically serves in *Mycobacterium* as a tag for degradation via the proteasome PrcAB (Cerda-Maira & Darwin, 2009; Lin et al., 2006; Samanovic et al., 2013). However, *Corynebacterium* species do not contain a proteasome and the only currently known function of pupylation is in the release of iron from ferritin and Dps, as pupylation triggers unfolding of the tagged protein by the ATPase Arc (Küberl et al., 2016). Whether pupylation of GlxR influences its function has not been studied yet. Of the 243 GlxR peaks identified in this study, 242 contained the sequence motif TGTGN$_8$CACA, which agrees with the previously described motif (Jungwirth et al., 2013; Kohl et al., 2008; Toyoda et al., 2011) and supports the validity of our data. 141 of the GlxR peaks were also found in previous studies, whereas 102 were not reported before (Table 3). Therefore, our analysis further expands the already large GlxR regulon. The reason for the identification of new GlxR targets is probably due to differences in the experimental conditions, such as using a GlxR variant with a Twin Strep-tag. Nevertheless, not all GlxR binding sites reported previously were detected in our study, with at least 24 missing (Table S5).

TABLE 3 | Newly described GlxR peaks identified in the four ChAP-Seq data sets generated in this study with the corresponding GlxR binding sites that were found upstream, intergenic or in the indicated genes. The symbol '< >' denotes divergently and '> <' convergently oriented genes with a GlxR binding site in the intergenic region.

Locus tag (cg)	**Adjacent gene(s)**	**Annotation**	**GlxR binding motif sequence** [a]	**Distance to next TSS**[b]	**Distance to next TLS**[b]
cg0001	in *dnaA*	chromosomal replication initiation protein	`GGTTCAAATATGCACG`	-	+119
cg0054 > < cg0055	(cg0054) > < *crgA*	put. iron-chelator utilization protein > < put. cell division membrane protein	`TGACTGCCGCAGCACA`	-	+1188 > < +302
cg0061	*rodA (ftsW)*	put. FTSW/RODA/SPOVE-family cell cycle protein	`AGTATCAGCAGCCACA`	-	+48
cg0090	*citB*	two component response regulator	`AGTCTGATTTTGCACA`	-642; -807	-950
cg0156	*cysR*	transcriptional activator, ROK-family	`TGTTCCGCAGCAGACT`	-310	-310
cg0215	*cspA*	cold-shock protein A	`GGTGTAAAAGCAGACA`	-64	-245
cg0235	*emb (embC)*	arabinosyltransferase	`TGAGTAATTCCTCACC`	-73	-73
cg0261	in *moeA1*	molybdopterin cofactor synthesis protein A1, MoeA-family	`CGTGGCGAATCCCACT`	-	+132
cg0280	-	hypothetical protein	`TGTCTCATTTAACACA`	-632	-632
cg0427	*tnp17b*	transposase fragment	`AGTATACTTCCATACA`	+16	-281
cg0440	-	hypothetical protein	`TATGAGGATGCTCACA`	-	-331
cg0576	in *rpoB*	DNA-directed RNA polymerase β subunit	`TGAGTCAAACCAGACA`	+1518; +1520	+1308
cg0583	in *fusA*	elongation factor EF-2/G	`TGTAGGCGGTGCCACA`	+897; +990	+791
cg0645	*creJ (cytP)*	cytochrome P450	`CGTGATGGCTATCACT`	-	-74
cg0646 < > cg0647	*creR* < > *secY*	put. transcriptional regulator, IclR-family < > preprotein translocase subunit	`TATGATGCGTCTTACA`	-71; -115 < > -60; -140	-202 < > -176
cg0658	in *rptA*	terminal rhamnopyranosyl transferase	`TGTCGCCATGTTCACT`	-	+1393
cg0703	*guaA*	put. Gmp synthase	`TGTCTGAAGGCTCACA`	+7	+7
cg0706	in (cg0706)	put. membrane protein, conserved	`GGTCTCCAACATCACA`	+1070	+1070
cg0755 < > cg0756	*metY* < > *cstA*	O-acetylhomoserine sulfhydrylase < > carbon starvation protein A	`TATGACTAGCCCCACT`	-136 < > -30;-32;-42; -59	-175 < > -258

15

Locus tag (cg)	Adjacent gene(s)	Annotation	GlxR binding motif sequence [a]	Distance to next TSS[b]	Distance to next TLS[b]
cg0764	in (cg0764)	put. transcriptional regulator, GntR-family	TGTTCAACCAGCCACA	+126	+126
cg0773	-	put. exodeoxyribonuclease	GGTTCCTCATGCCACA	-667	-667
cg0788	in *pmmB*	phosphoglucomutase/phosphomannomutase	TGTCTGTCACCCCACA	+1423	+1386
cg0845	in (cg0845)	put. superfamily II DNA/RNA helicase, SNF2-family	AGTATGCAGGTTCACA	+1543	+1543
cg0866	-	purine/pyrimidine phosphoribosyl transferase	CGTGATATTTGTCACG	-	-311
cg0875	in (cg0875)	conserved hypothetical protein	TGTGTCTTCCACCACA	-	+935
cg0904	-	hypothetical protein	TGCTTGATCTCCCACA	-	-328
cg0926	-	put. iron-siderophore transporter	TGTTCTTTACAAGACA	-	-159
cg0933	-	put. DNA or RNA helicase of superfamily II	TGTGGATGAAGCCACA	-87	-115
cg0962	-	put. secreted protein	GGTCAATCAGATCACT	-337	-337
cg0973	*pgi*	glucose-6-phosphate isomerase	TGTCGTGTTTCCCACT	-59	-87
cg1052	in *cmt3*	corynomycolyl transferase	GGTGCCAAGGCTCACA	+1374;+1377	+1333
cg1075	in *prsA*	ribose-phosphate pyrophosphokinase	TGTTCCATGAGCCACT	+377	+225
cg1087	-	put. membrane protein	TGTGAAAGCTATCACA	-3	-29
cg1108	*porC*	put. secreted protein	AGTCACATAAATCACT	-	-90
cg1111	*eno*	enolase, phosphopyruvate hydratase	CGTGTCCGATCAGACA	-93	-163
cg1147	in *ssuI*	NADPH-dependent FMN reductase	TGTACCACCGCTCACA	+468	+468
cg1256	*dapD*	tetrahydrodipicolinate succinylase	AGTTTCAACTGTGACA	-275	-275
cg1432	*ilvD*	dihydroxy-acid dehydratase	CGTCTGAAACCTCACA	+24; -46	-165
cg1520	in (cg1520)	put. secreted protein CGP1 region	TGTACTGCTAATCACA	-	+299
cg1608 > < cg1609	*xerD* > < (cg1609)	tyrosine recombinase > < put. ATPase component of ABC transporter	TGAGCCCCGCGCCACA	-	+894 > < +1571
cg1697	*aspA*	aspartate ammonia-lyase aspartase	TGTACTGCCTCTCACA	+33	-8
cg1728 > < cg1730	(cg1728) > < (cg1730)	hypothetical protein, conserved > < put. secreted protease subunit	GGTGAGGTCTGCCACA	-	+727 > < +1486
cg1812	*pyrF*	orotidine 5-phosphate decarboxylase	TGTTCCGCTGATCACC	-	-119

16

Locus tag (cg)	**Adjacent gene(s)**	**Annotation**	**GlxR binding motif sequence [a]**	**Distance to next TSS[b]**	**Distance to next TLS[b]**
cg1895	in (cg1895)	put. secreted protein, CGP3 region	`TGTGGTCTTCAACACT`	-	+2116
cg1898	-	hypothetical protein CGP3 region	`TGTCGCCACTGCCACA`	-	-372
cg1909	-	hypothetical protein CGP3 region	`GGTAAGTATTCAGACA`	-	-160
cg1913	-	hypothetical protein CGP3 region	`TGTGCAGAATTTCACA`	-	+17
cg1924	-	hypothetical protein CGP3 region	`AGTAACACAGACCACA`	-	-534
cg1927	-	put. molecular chaperone CGP3 region	`TGTGCCTCGTAGCACA`	-	-362
cg1945	in (cg1945)	hypothetical protein, conserved CGP3 region	`TGTTCATCCCCTCACA`	+1175	+1175
cg1972	-	put. translation elongation factor, GTPase CGP3 region	`TGTGCATTTCTACACA`	-	-31
cg1995	in (cg1995)	hypothetical protein, CGP3 region	`TGTATCAGTTGCCACT`	-	+4218
cg1999	-	hypothetical protein, CGP3 region	`TGTCTACTCTGTTACA`	-	-511
cg2035	-	put. methyltransferase, CGP3 region	`TGTCTAATATGGTACT`	-256	-271
cg2064	-	put. DNA topoisomerase I omega-protein; CGP3 region	`CGTGAAATAGGACACA`	-	-619
cg2109	*oxyR*	hydrogen peroxide sensing regulator, Lys-family	`no motif`	-66	-66
cg2134	-	put. membrane protein	`GGTGGCTCCTGCCACA`	-60	-99
cg2157	*terC*	tellurium resistance membrane protein	`AGTAAACTTAGCCACA`	-210; -212	+13
cg2184	*oppD*	ATPase component of ABC-type transport system	`TGTTCCCAGTGCCACA`	-	-224
cg2324	-	hypothetical protein	`TATGTCTGACAACACT`	+10	+7
cg2404	*qcrA (qcrA1)*	cytochrome bc1 complex, Rieske iron-sulfur protein	`TGTCGCCTGCATCACC`	-	-650
cg2470 < > cg2471	(cg2470) < > (cg2471)	secreted ABC transporter substrate-binding protein < > put. protein	`TGAGACATTTCACATA`	+7 < > -202	-81 < > -205
cg2480	-	hypothetical protein	`TGTCGACACCGTCACA`	-484; -737	-737
cg2496 > < cg2497	(cg2496) > < (cg2497)	put. secreted protein > < hypothetical protein	`GGTCTCTTCGGTCACT`	+2090 > < -	+2090 > < +1213
cg2497	in (cg2497)	hypothetical protein	`AGTGAGATCCCCCACA`	-	+250
cg2521	*fadD15*	long-chain fatty acid CoA ligase	`TGTATCTAAATTCACA`	-292	-404

17

Locus tag (cg)	**Adjacent gene(s)**	**Annotation**	**GlxR binding motif sequence [a]**	**Distance to next TSS[b]**	**Distance to next TLS[b]**
cg2557 < > cg2558	(cg2557) < > (cg2558)	put. secondary Na+/bile acid symporter < > put. protein, related to aldose 1-epimerase	`TATGAAAGTTCGCACA`	- < > -73	-77 < > -73
cg2593 > < cg2594	(cg2593) > < *rpmA*	put. secreted or membrane protein > < 50S ribosomal protein L27	`TGACGCTTAAGTCACA`	+526 > < -	+447 > < +265
cg2642	in *benK1 (benK)*	benzoate transport protein, MFS transporter	`TGTTCCTCCTGCCACT`	-	+573
cg2651	-	put. protein-fragment	`TGTACAATAACACACT`	-229	-229
cg2678	-	put. ABC-type transport systems	`GGTGACATTATTCACA`	-312	-364
cg2692	-	put. thioesterase	`CGTCTCTTTGCTCACA`	+28	-50
cg2695	in (c2695)	put. ABC-type transport system, ATPase component	`TGTCCTTGCCGTCACA`	+666; +669	+630
cg2699 < > cg2700	*ctiP* < > *phoB*	copper transport and insertion protein < > alkaline phosphatase	`TGTGTGAAGCCCCACA`	-108 < > -551	-108 < > -542
cg2700 > < cg2701	*phoB* > < *musI*	alkaline phosphatase > < put. membrane protein	`TGTGTTGCAGGTCACA`	+1919 > < +1203	-1919 > < +1203
cg2700 > < cg2701	*phoB* > < *musI*	alkaline phosphatase > < put. membrane protein	`TGTGAGCCACGCCACT`	+2152 > < +961	+2161 > < +961
cg2741	-	hypothetical protein	`TGCATAGTTTGTCACT`	-160; -156	-286
cg2748	-	put. membrane protein, conserved	`GGTGCAGTTGGTCACC`	-56	-56
cg2785	-	put. membrane protein	`TGTCCGTAGACACACA`	-	-167
cg2797	-	hypothetical protein	`TGTTCAAAGCTTCACA`	-	-224
cg2811	in (cg2811)	put. ABC-type transport system	`CGTCTGGTTAGTCACA`	-	+1840
cg2843	in *pstB*	ABC-type phosphate transport system	`GGTCTGATCGGACACA`	-	+640
cg2898	in (cg2898)	put. 3-ketosteroid dehydrogenase	`TGTTGATTCCCACACC`	-	+379
cg2936 < > cg2937	*nanR* < > *siaE*	transcriptional regulator, GntR-family < > ABC-Transporter for sialic acid	`TGAGCATAGCGTCACA`	-230 < > +45	-255 < > -54
cg3030	-	put. hydrolase or acyltransferase α/β hydrolase superfamily	`AGTGCACCACGAGACA`	-	-359

Locus tag (cg)	Adjacent gene(s)	Annotation	GlxR binding motif sequence [a]	Distance to next TSS[b]	Distance to next TLS[b]
cg3041	-	put. ABC-type multidrug transport system	AGTCGCATTCAACACA	-	-196
cg3043	-	NTP pyrophosphohydrolase/oxidative damage repair enzyme	TGATGTATACAGCACA	-505	-505
cg3061	*cgtR6*	two component response regulator	TGTTGCATATGATACA	-179	-233
cg3091	-	hypothetical protein	AGTTTGTTGGCTTACA	-	-415
cg3092	in (cg3092)	put. 2-polyprenylphenol hydroxylase or related flavodoxin oxidoreductase	TGTTATTTATTGCACA	+750	+750
cg3112	*cysZ*	sulfate transporter	AGTTCCACACCATACT	-	-474
cg3174	in *mmpL1*	exporter of the MMPL-family	TGTTTGTTTTCCCACA	-	+909
cg3187	in *aftB*	arabinofuranosyltransferase	AGTCGCCCACAACACC	+595	+595
cg3203	in (cg3203)	hypothetical protein, conserved	TGCCTCATTTACCACT	+227	+223
cg3247	*hrrA (cgtR11)*	two component response regulator	TGAATGTTTCGCCACA	-352	-434
cg3255	*uspA3*	universal stress protein no 3	TGAGGCTTTTGACACT	-63; -65	-131
cg3313	*pbp1b (mcrB)*	membrane carboxypeptidase	TATTCTCTACAGCACA	+6; +202	-51
cg3332	in *qor3*	put. NADPH:quinone oxidoreductase	GGTACTCTGCGTTACT	+329	+329
cg3393	in *phoC*	put. secreted phosphoesterase	TGTACCACTCATCACA	-	+1341
cg3417	-	put. NTP pyrophosphohydrolase	GGTGAGCTTTCAGACA	-531	-970
cg3428	*gidB*	glucose-inhibited division protein B	TGTTCGGTGCGCCACT	-620; -623	-660
-	-	phage integrase	AATGAATCCACTCACC	-	-254

a: motif sequence was detected by using the program MEME-ChIP with the DNA fragment of the detected GlxR peaks as input sequences; the 16 bp sequence shows the most probable GlxR binding site within this sequences
b: distance counted from the centre of the GlxR binding site to the start of the TSS or TLS (counting includes the first base of TSS or TLS; information of TSS was taken from Pfeifer-Sancar et al. 2013; for some genes several TSS were identified

When checking these sites, we found that 14 of the corresponding DNA regions were enriched in our ChAP-Seq experiments not falling in our definition of a GlxR binding site due to EF <3 in a data set (e.g. *fumC*, *pabB*, *uspA2*, or *oxiC*). Ten of the 24 missing GlxR binding sites were not enriched in our data at all (e.g *aceA*, *aceB*, *glnA* or *ldhA*). Reasons therefore could be DNA regions that were not accessible for GlxR binding under the conditions used.

Table 3 lists newly identified GlxR binding sites and the distances to the neighbouring genes. A prediction of the influence of GlxR on the transcription of the neighbouring gene is possible for the repressed genes, where GlxR binding is assumed to interfere with binding of RNA polymerase (Browning and Busby 2004). This is likely for binding sites located between 0 and -40 bp upstream of a TSS or TLS and within about 50 bp downstream of a TSS or TLS. According to this assumption, *guaA* (cg0703), cg1087, *aspA* (cg1697), cg1913, cg1972, cg2470, *siaE* (cg2937) and *pbp1b* (cg3313) might represent novel target genes repressed by GlxR. For neighbouring genes with a GlxR binding site located >40 bp upstream of a TSS, an activator function of GlxR might be more likely, but needs to be tested experimentally. Examples for genes that might be activated by GlxR are *pgi* (cg0973, glucose 6-phosphate isomerase), *eno* (cg1111, enolase), or *ctiP* (cg2699, copper transport and insertion protein). The former two genes are involved in glycolysis and several other genes of this pathway were previously shown to be activated by GlxR, such as *pfkA*, *gapA*, or *aceE* (Toyoda et al., 2011). The *ctiP* gene is required for the transport and insertion of copper into the cytochrome aa_3 oxidase (Morosov et al., 2018), which in *C. glutamicum* forms a supercomplex with the cytochrome bc_1 complex (Moe et al., 2022; Niebisch & Bott, 2003). Expression of the genes *ctaD* and *ctaC* encoding subunit I and II of cytochrome aa_3 oxidase was shown to be activated by GlxR (Toyoda et al., 2011) and it seems reasonable that also the *ctiP* gene required for the maturation of cytochrome aa_3 oxidase is activated by GlxR. In this context, further approaches are required that allow a genome-wide analysis of the influence of GlxR on transcription of its target genes.

GlxR binding sites not clearly linked to the TSS of a protein-coding gene were further manually checked for nearby TSSs of non-protein coding RNAs. Indeed these GlxR binding sites were often found to be close to the TSS of sRNAs (adjacent to the genes cg0054/*crgA*, *metY*/*cstA*, *cgpS*/cg1967, *phoB*/*musI*, *cgtR6*/*purA*), asRNAs (e.g. of the gene *cmt3*, cg1609, cg1945, cg2362 or *phoC*) or tRNAs (tRNA$^{\text{Leu}}$, tRNA$^{\text{Arg}}$, tRNA$^{\text{Gly}}$ and tRNA$^{\text{Asp}}$), which suggests that GlxR might influence transcription of these RNAs (Table S7). Therefore, the regulatory influence of GlxR could be even broader than previously assumed (Kohl & Tauch, 2009). In prokaryotes, sRNAs can influence transcription, translation, RNA stability, or protein activity (Storz et al., 2011; Waters & Storz, 2009) and are involved in the regulation of metabolism, transcriptional regulation, transport mechanisms, stress responses, or virulence (Delihas & Forst, 2001; Georg & Hess, 2011; Vogel & Papenfort, 2006). A genome-wide analysis identified over 800 sRNA genes in *C. glutamicum*, which were classified into 316 UTRs of mRNAs, 543 cis-antisense RNAs, and 262 trans-encoded sRNAs (Mentz et al., 2013). Only few of them have been studied experimentally, such as the 6C RNA, which is highly conserved in Actinobacteria and was shown to highly abundant and stable in *C. glutamicum* (Pahlke et al., 2016). A GlxR binding site was identified upstream of the 6C RNA (Jungwirth et al., 2013), which was also found in our analysis. *In vivo* GlxR-DNA binding regions within the *rrn* operons and tRNA$^{\text{Glu}}$ of and tRNA$^{\text{Asp}}$ were mentioned in literature before, but were excluded from the analysis due to high variation in their read counts (Jungwirth et al., 2013). As our studies also showed *in vivo* GlxR binding upstream of some tRNAs (tRNA$^{\text{Leu}}$, tRNA$^{\text{Arg}}$, tRNA$^{\text{Gly}}$ and of tRNA$^{\text{Asp}}$) and within the *rrn* operons (*rrnA*, *rrnB*, *rrnC* and *rrnF*), this should be analysed in further studies.

Several GlxR binding sites were located intragenically far away from neighbouring genes or in intergenic regions of convergently transcribed genes. In these cases, a direct influence of GlxR on transcription appears unlikely. GlxR ortholog, for example Crp of *E. coli* and Crp of *M. tuberculosis*, also revealed a high number of intragenic binding sites in previous studies (Grainger et al., 2005; Knapp et al., 2015). It was suggested that this type of binding influences gene regulation by modifying the chromatin structure, similar to nucleoid associated proteins (NAPs), instead of direct interaction with RNA polymerase. This NAP-like function of Crp was supported by the observation that Crp is able to bend DNA in *in vitro* studies (Bai et al., 2005; Lin & Lee, 2003). On the other hand, one cannot exclude a regulation of transcription over a long distance, as shown for EspR in *M. tuberculosis* (Hunt et al., 2012). This transcriptional regulator activates the transcription of its target gene by binding to an enhancer-like sequence far upstream of the TSS of the target gene (~800 to 1000 bp), leading to looping of the DNA (Hunt et al., 2012; Rosenberg et al., 2011).

In conclusion, our study provides new potential target genes of GlxR in *C. glutamicum* and shows that *in vivo* DNA-binding by GlxR is enhanced by cAMP, but not strictly dependent on its presence. Therefore, additional factors might be involved in the control of GlxR activity, such as posttranslational modifications (succinylation, pupylation). Regarding a deeper physiological understanding of GlxR, identification of the stimulus sensed by CyaB would be a major breakthrough. If GlxR is considered as a global regulator coordinating catabolism and anabolism with growth and cell division, parameters such as the proton-motive force or the energy charge appear to be suitable for providing key information on the fitness status of the cell.

CONTRIBUTIONS

NW constructed mutants, plasmids and performed all experimental work except the one specified below for other authors, wrote the first draft of the manuscript and generated the figures and tables if not mentioned otherwise. LL constructed the strain *C. glutamicum*::*glxR-TS* (named $\mathrm{WT}_{\mathrm{GlxR\text{-}TS}}$), cultivated and generated one of the nine ChAP-Seq samples. MBu performed the microarray experiment with the WT and the Δ*cyaB* mutant on glucose. TP supervised the bioinformatics of the microarray analysis and the first evaluation of the ChAP-Seq results. AF normalized the data of the four ChAP-Seq sample conditions and performed comparisons of peak heights and generated the draft version of Fig. 1. MBa coached the experimental work and supported the design of this study. MBo designed the study, supervised the experimental work and was responsible for the final version of the manuscript.

REFERENCES

Bai, G., McCue, L. A., & McDonough, K. A. (2005). Characterization of *Mycobacterium tuberculosis* Rv3676 ($\mathrm{CRP_{Mt}}$), a cyclic AMP receptor protein-like DNA binding protein. *J Bacteriol*, *187*(22), 7795-7804.

Bailey, T. L., & Elkan, C. (1994). Fitting a mixture model by expectation maximization to discover motifs in biopolymers. *Proc Int Conf Intell Syst Mol Biol*, *2*, 28-36.

Becker, J., & Wittmann, C. (2012). Systems and synthetic metabolic engineering for amino acid production - the heartbeat of industrial strain development. *Curr Opin Biotechnol*, *23*(5), 718-726.

Burkovski, A. (2008). *Corynebacteria: Genomics and Molecular Biology* (1 ed.). Caister Academic Press.

Bussmann, M. (2009). cAMP dependent regulation of the TCA cycle by GlxR and oxidative stress response regulation by RosR in *Corynebacterium glutamicum*. urn:nbn:de:hbz:061-20101104-151101-4.

Bussmann, M., Emer, D., Hasenbein, S., Degraf, S., Eikmanns, B. J., & Bott, M. (2009). Transcriptional control of the succinate dehydrogenase operon *sdhCAB* of *Corynebacterium glutamicum* by the cAMP-dependent regulator GlxR and the LuxR-type regulator RamA. *J Biotechnol*, *143*(3), 173-182.

Cerda-Maira, F., & Darwin, K. H. (2009). The *Mycobacterium tuberculosis* proteasome: more than just a barrel-shaped protease. *Microbes Infect*, *11*(14-15), 1150-1155.

Cha, P. H., Park, S. Y., Moon, M. W., Subhadra, B., Oh, T. K., Kim, E., Kim, J. F., & Lee, J. K. (2010). Characterization of an adenylate cyclase gene (*cyaB*) deletion mutant of *Corynebacterium glutamicum* ATCC 13032. *Appl Microbiol Biotechnol*, *85*(4), 1061-1068.

Delihas, N., & Forst, S. (2001). MicF: an antisense RNA gene involved in response of *Escherichia coli* to global stress factors. *J Mol Biol*, *313*(1), 1-12.

Eggeling, L., & Bott, M. (2005). *Handbook of Corynebacterium glutamicum* (1 ed.). CRC Press.

Eggeling, L., & Bott, M. (2015). A giant market and a powerful metabolism: L-lysine provided by *Corynebacterium glutamicum*. *Appl Microbiol Biotechnol*, *99*(8), 3387-3394.

Freudl, R. (2017). Beyond amino acids: Use of the *Corynebacterium glutamicum* cell factory for the secretion of heterologous proteins. *J Biotechnol*, *258*, 101-109.

Frunzke, J., Engels, V., Hasenbein, S., Gätgens, C., & Bott, M. (2008). Co-ordinated regulation of gluconate catabolism and glucose uptake in *Corynebacterium glutamicum* by two functionally equivalent transcriptional regulators, GntR1 and GntR2. *Mol Microbiol*, *67*(2), 305-322.

Georg, J., & Hess, W. R. (2011). *cis*-antisense RNA, another level of gene regulation in bacteria. *Microbiol Mol Biol Rev*, *75*(2), 286-300.

Görke, B., & Stülke, J. (2008). Carbon catabolite repression in bacteria: many ways to make the most out of nutrients. *Nat Rev Microbiol*, *6*(8), 613-624.

Gosset, G., Zhang, Z., Nayyar, S., Cuevas, W. A., & Saier, M. H., Jr. (2004). Transcriptome analysis of Crp-dependent catabolite control of gene expression in *Escherichia coli*. *J Bacteriol*, *186*(11), 3516-3524.

Grainger, D. C., Hurd, D., Harrison, M., Holdstock, J., & Busby, S. J. W. (2005). Studies of the distribution of *Escherichia coli* cAMP-receptor protein and RNA polymerase along the *E. coli* chromosome. *Proc Natl Acad Sci U S A*, *102*(49), 17693-17698.

Hunt, D. M., Sweeney, N. P., Mori, L., Whalan, R. H., Comas, I., Norman, L., Cortes, T., Arnvig, K. B., Davis, E. O., Stapleton, M. R., Green, J., & Buxton, R. S. (2012). Long-range transcriptional control of an operon necessary for virulence-critical ESX-1 secretion in *Mycobacterium tuberculosis*. *J Bacteriol*, *194*(9), 2307-2320.

Ikeda, M., & Nakagawa, S. (2003). The *Corynebacterium glutamicum* genome: features and impacts on biotechnological processes. *Appl Microbiol Biotechnol*, *62*(2), 99-109.

Inui, M., Kawaguchi, H., Murakami, S., Vertès, A. A., & Yukawa, H. (2004). Metabolic engineering of *Corynebacterium glutamicum* for fuel ethanol production under oxygen-deprivation conditions. *J Mol Microbiol Biotechnol*, *8*(4), 243-254.

Jungwirth, B., Sala, C., Kohl, T. A., Uplekar, S., Baumbach, J., Cole, S. T., Puhler, A., & Tauch, A. (2013). High-resolution detection of DNA binding sites of the global transcriptional regulator GlxR in *Corynebacterium glutamicum*. *Microbiology*, *159*(Pt 1), 12-22.

Kensy, F., Zang, E., Faulhammer, C., Tan, R. K., & Büchs, J. (2009). Validation of a high-throughput fermentation system based on online monitoring of biomass and fluorescence in continuously shaken microtiter plates. *Microb. Cell Fact.*, *8*, 31.

Keppel, M., Hünnefeld, M., Filipchyk, A., Viets, U., Davoudi, C. F., Krüger, A., Mack, C., Pfeifer, E., Polen, T., Baumgart, M., Bott, M., & Frunzke, J. (2020). HrrSA orchestrates a systemic response to heme and determines prioritization of terminal cytochrome oxidase expression. *Nucleic Acids Res*, *48*(12), 6547-6562.

Kim, H. J., Kim, T. H., Kim, Y., & Lee, H. S. (2004). Identification and characterization of *glxR*, a gene involved in regulation of glyoxylate bypass in *Corynebacterium glutamicum*. *J Bacteriol*, *186*(11), 3453-3460.

Kinoshita, S., Udaka, S., & Shimono, M. (1957). Studies on amino acid fermentation. Part 1. Production of L-glutamic acid by various microorganisms. *J Gen Appl Microbiol*, *3*, 193-205.

Knapp, G. S., Lyubetskaya, A., Peterson, M. W., Gomes, A. L. C., Ma, Z., Galagan, J. E., & McDonough, K. A. (2015). Role of intragenic binding of cAMP responsive protein (CRP) in regulation of the succinate dehydrogenase genes Rv0249c-Rv0247c in TB complex mycobacteria. *Nucleic Acids Res*, *43*(11), 5377-5393

Kohl, T. A., Baumbach, J., Jungwirth, B., Puhler, A., & Tauch, A. (2008). The GlxR regulon of the amino acid producer *Corynebacterium glutamicum*: *in silico* and *in vitro* detection of DNA binding sites of a global transcription regulator. *J Biotechnol*, *135*(4), 340-350.

Kohl, T. A., & Tauch, A. (2009). The GlxR regulon of the amino acid producer *Corynebacterium glutamicum*: Detection of the corynebacterial core regulon and integration into the transcriptional regulatory network model. *J Biotechnol*, *143*(4), 239-246.

Komine-Abe, A., Nagano-Shoji, M., Kubo, S., Kawasaki, H., Yoshida, M., Nishiyama, M., & Kosono, S. (2017). Effect of lysine succinylation on the regulation of 2-oxoglutarate dehydrogenase inhibitor, OdhI, involved in glutamate production in *Corynebacterium glutamicum*. *Biosci Biotechnol Biochem*, *81*(11), 2130-2138.

Körner, H., Sofia, H. J., & Zumft, W. G. (2003). Phylogeny of the bacterial superfamily of Crp-Fnr transcription regulators: exploiting the metabolic spectrum by controlling alternative gene programs. *FEMS Microbiol Rev*, *27*(5), 559-592.

Küberl, A., Fränzel, B., Eggeling, L., Polen, T., Wolters, D. A., & Bott, M. (2014). Pupylated proteins in *Corynebacterium glutamicum* revealed by MudPIT analysis. *Proteomics*, *14*(12), 1531-1542.

Küberl, A., Polen, T., & Bott, M. (2016). The pupylation machinery is involved in iron homeostasis by targeting the iron storage protein ferritin. *Proc Natl Acad Sci U S A*, *113*(17), 4806-4811.

Letek, M., Valbuena, N., Ramos, A., Ordonez, E., Gil, J. A., & Mateos, L. M. (2006). Characterization and use of catabolite-repressed promoters from gluconate genes in *Corynebacterium glutamicum*. *J Bacteriol*, *188*(2), 409-423.

Lin, G., Hu, G., Tsu, C., Kunes, Y. Z., Li, H., Dick, L., Parsons, T., Li, P., Chen, Z., Zwickl, P., Weich, N., & Nathan, C. (2006). *Mycobacterium tuberculosis prcBA* genes encode a gated proteasome with broad oligopeptide specificity. *Mol Microbiol*, *59*(5), 1405-1416.

Lin, S. H., & Lee, J. C. (2003). Determinants of DNA bending in the DNA-cyclic AMP receptor protein complexes in *Escherichia coli*. *Biochemistry*, *42*(17), 4809-4818.

Mentz, A., Neshat, A., Pfeifer-Sancar, K., Puhler, A., Ruckert, C., & Kalinowski, J. (2013). Comprehensive discovery and characterization of small RNAs in *Corynebacterium glutamicum* ATCC 13032. *BMC Genomics*, *14*, 714.

Mizuno, Y., Nagano-Shoji, M., Kubo, S., Kawamura, Y., Yoshida, A., Kawasaki, H., Nishiyama, M., Yoshida, M., & Kosono, S. (2016). Altered acetylation and succinylation profiles in *Corynebacterium glutamicum* in response to conditions inducing glutamate overproduction. *Microbiologyopen*, *5*(1), 152-173.

Moe, A., Kovalova, T., Król, S., Yanofsky, D. J., Bott, M., Sjöstrand, D., Rubinstein, J. L., Högbom, M., & Brzezinski, P. (2022). The respiratory supercomplex from *C. glutamicum*. *Structure*, *30*(3); 338-349, e333.

Moon, M. W., Park, S. Y., Choi, S. K., & Lee, J. K. (2007). The phosphotransferase system of *Corynebacterium glutamicum*: features of sugar transport and carbon regulation. *J Mol Microbiol Biotechnol*, *12*(1-2), 43-50.

Morosov, X., Davoudi, C. F., Baumgart, M., Brocker, M., & Bott, M. (2018). The copper-deprivation stimulon of *Corynebacterium glutamicum* comprises proteins for biogenesis of the actinobacterial cytochrome bc_1-aa_3 supercomplex. *J Biol Chem*, *293*(40), 15628-15640.

Niebisch, A., & Bott, M. (2001). Molecular analysis of the cytochrome bc_1-aa_3 branch of the *Corynebacterium glutamicum* respiratory chain containing an unusual diheme cytochrome c_1. *Arch Microbiol*, *175*(4), 282-294.

Niebisch, A., & Bott, M. (2003). Purification of a cytochrome bc_1-aa_3 supercomplex with quinol oxidase activity from *Corynebacterium glutamicum*. Identification of a fourth subunity of cytochrome aa_3 oxidase and mutational analysis of diheme cytochrome c_1. *J Biol Chem*, *278*(6), 4339-4346.

Niebisch, A., Kabus, A., Schultz, C., Weil, B., & Bott, M. (2006). Corynebacterial protein kinase G controls 2-oxoglutarate dehydrogenase activity via the phosphorylation status of the OdhI protein. *J Biol Chem*, *281*(18), 12300-12307.

Nishimura, T., Teramoto, H., Toyoda, K., Inui, M., & Yukawa, H. (2011). Regulation of the nitrate reductase operon *narKGHJI* by the cAMP-dependent regulator GlxR in *Corynebacterium glutamicum*. *Microbiology*, *157*(Pt 1), 21-28.

Pahlke, J., Dostálová, H., Holátko, J., Degner, U., Bott, M., Pátek, M., & Polen, T. (2016). The small 6C RNA of *Corynebacterium glutamicum* is involved in the SOS response. *RNA Biol*, *13*(9), 848-860.

Park, S. Y., Moon, M. W., Subhadra, B., & Lee, J. K. (2010). Functional characterization of the *glxR* deletion mutant of *Corynebacterium glutamicum* ATCC 13032: involvement of GlxR in acetate metabolism and carbon catabolite repression. *FEMS Microbiol Lett*, *304*(2), 107-115.

Pearce, M. J., Mintseris, J., Ferreyra, J., Gygi, S. P., & Darwin, K. H. (2008). Ubiquitin-like protein involved in the proteasome pathway of *Mycobacterium tuberculosis*. *Science*, *322*(5904), 1104-1107.

Pfeifer-Sancar, K., Mentz, A., Ruckert, C., & Kalinowski, J. (2013). Comprehensive analysis of the *Corynebacterium glutamicum* transcriptome using an improved RNAseq technique. *BMC Genomics*, *14*, 888.

Pfeifer, E., Hünnefeld, M., Popa, O., Polen, T., Kohlheyer, D., Baumgart, M., & Frunzke, J. (2016). Silencing of cryptic prophages in *Corynebacterium glutamicum*. *Nucleic Acids Res.*, *44*(21), 10117-10131.

Rosenberg, O. S., Dovey, C., Tempesta, M., Robbins, R. A., Finer-Moore, J. S., Stroud, R. M., & Cox, J. S. (2011). EspR, a key regulator of *Mycobacterium tuberculosis* virulence, adopts a unique dimeric structure among helix-turn-helix proteins. *Proc Natl Acad Sci U S A*, *108*(33), 13450-13455.

Samanovic, M. I., Li, H., & Darwin, K. H. (2013). The pup-proteasome system of *Mycobacterium tuberculosis*. *Subcell Biochem*, *66*, 267-295.

Sambrook, J., & Russell, D. (2001). *Molecular Cloning. A Laboratory Manual* (3rd ed.). Cold Spring Harbor Laboratory Press.

Schäfer, A., Tauch, A., Jager, W., Kalinowski, J., Thierbach, G., & Puhler, A. (1994). Small mobilizable multi-purpose cloning vectors derived from the *Escherichia coli* plasmids pK18 and pK19: selection of defined deletions in the chromosome of *Corynebacterium glutamicum*. *Gene*, *145*(1), 69-73.

Schröder, J., & Tauch, A. (2010). Transcriptional regulation of gene expression in *Corynebacterium glutamicum*: the role of global, master and local regulators in the modular and hierarchical gene regulatory network. *FEMS Microbiol Rev*, *34*(5), 685-737.

Schulte, J., Baumgart, M., & Bott, M. (2017). Identification of the cAMP phosphodiesterase CpdA as novel key player in cAMP-dependent regulation in *Corynebacterium glutamicum*. *Mol Microbiol*, *103*(3), 534-552.

Soberón-Chávez, G., Alcaraz, L. D., Morales, E., Ponce-Soto, G. Y., & Servín-González, L. (2017). The transcriptional regulators of the CRP family regulate different essential bacterial functions and can be inherited vertically and horizontally. *Front Microbiol*, *8*(959).

Storz, G., Vogel, J., & Wassarman, K. M. (2011). Regulation by small RNAs in bacteria: expanding frontiers. *Mol Cell*, *43*(6), 880-891.

Studier, F. W. (2005). Protein production by auto-induction in high-density shaking cultures. *Protein Expr Pur*, *41*(1), 207-234.

Studier, F. W., & Moffatt, B. A. (1986). Use of bacteriophage T7 RNA polymerase to direct selective high-level expression of cloned genes. *J Mol Biol*, *189*(1), 113-130.

Townsend, P. D., Jungwirth, B., Pojer, F., Bussmann, M., Money, V. A., Cole, S. T., Puhler, A., Tauch, A., Bott, M., Cann, M. J., & Pohl, E. (2014). The crystal structures of apo and cAMP-bound GlxR from *Corynebacterium glutamicum* reveal structural and dynamic changes upon cAMP binding in CRP/FNR family transcription factors. *PLoS One*, *9*(12), e113265.

Toyoda, K., Teramoto, H., Inui, M., & Yukawa, H. (2011). Genome-wide identification of *in vivo* binding sites of GlxR, a cyclic AMP receptor protein-type regulator in *Corynebacterium glutamicum*. *J Bacteriol*, *193*(16), 4123-4133.

van Ooyen, J., Emer, D., Bussmann, M., Bott, M., Eikmanns, B. J., & Eggeling, L. (2011). Citrate synthase in *Corynebacterium glutamicum* is encoded by two *gltA* transcripts which are controlled by RamA, RamB, and GlxR. *J Biotechnol*, *154*(2-3), 140-148.

Vogel, J., & Papenfort, K. (2006). Small non-coding RNAs and the bacterial outer membrane. *Curr Opin Microbiol*, *9*(6), 605-611.

Waters, L. S., & Storz, G. (2009). Regulatory RNAs in bacteria. *Cell*, *136*(4), 615-628.

Wendisch, V. F., Mindt, M., & Perez-Garcia, F. (2018). Biotechnological production of mono- and diamines using bacteria: recent progress, applications, and perspectives. *Appl Microbiol Biotechnol*, *102*(8), 3583-3594.

Wieschalka, S., Blombach, B., Bott, M., & Eikmanns, B. J. (2013). Bio-based production of organic acids with *Corynebacterium glutamicum*. *Microb Biotechnol*, *6*(2), 87-102.

Wolf, N., Bussmann, M., Koch-Koerfges, A., Katcharava, N., Schulte, J., Polen, T., Hartl, J., Vorholt, J. A., Baumgart, M., & Bott, M. (2020). Molecular basis of growth inhibition by acetate of an adenylate cyclase-deficient mutant of *Corynebacterium glutamicum*. *Front Microbiol*, *11(11:87)*.

Wolf, S., Becker, J., Tsuge, Y., Kawaguchi, H., Kondo, A., Marienhagen, J., Bott, M., Wendisch, Volker F., & Wittmann, C. (2021). Advances in metabolic engineering of *Corynebacterium glutamicum* to produce high-value active ingredients for food, feed, human health, and well-being. *Essays Biochem*, *65*(2), 197-212.

Yukawa, H., & Inui, M. (2013). *Corynebacterium glutamicum: Biology and Biotechnology* (1 ed.). Springer-Verlag.

Zheng, D., Constantinidou, C., Hobman, J. L., & Minchin, S. D. (2004). Identification of the CRP regulon using *in vitro* and *in vivo* transcriptional profiling. *Nucleic Acids Res*, *32*(19), 5874-5893.

2.4 Supplementary materials ‘Comparison of *in vivo* GlxR binding in *Corynebacterium glutamicum* ATCC 13032 and the adenylate cyclase deletion mutant Δ*cyaB* using ChAP-Seq’

Supplementary materials ‘Comparison of *in vivo* GlxR binding in *Corynebacterium glutamicum* ATCC 13032 and the adenylate cyclase deletion mutant Δ*cyaB* using ChAP-Seq’

Natalie Wolf[1], Lukas Lehmann[1], Andrei Filipchyk[1], Tino Polen[1], Michael Bussmann[1], Meike Baumgart[1], Michael Bott[1]*

*** Correspondence:** Michael Bott (m.bott@fz-juelich.de)

TABLE S1 | Oligonucleotides used in this study

Oligonucleotide	**Sequence (5’ → 3’)**
Construction of plasmid pK19*mobsacB-glxR-twinstreptag* and PCR-analysis of the resulting mutants	
*glxR-twinstrep*_01-fw	TCACCAAAGCGCTAAAAAGCGCCTG
*glxR-twinstrep*_02-fw	GGCACGTCGCGCTCGATGGAGTCATCCTCAATTCG
*glxR-twinstrep*_03-rv	CTTTTTAGCGCTTTGGTGATTATTTTTCGAACTGCGGGTG
*glxR-twinstrep*_04-rv	TCGAGCGCGACGTGCCAAATGC
glxR-twinstrep-control-fw	TCAATTCGAGAAAGGTGGAG
glxR-twinstrep-control-rv	CTTCTCGACGCAAAAACCCATC
EMSA	
hemL(cg0518)_fw	TCACCATAACCGGGTTCGACG
hemL(cg0518)_rv	ACGCGCAGCCGAAACGGTAGC
aspA(cg1697)_fw	CATTCTTTGAGTCTGCTGAAG
aspA(cg1697)_rv	GTACGTAGGATAATCCACAGC
cg2936_cg2937_fw	GACACTACAGCAATTCAATG
cg2936_cg2937_rv	GGAGGAAATTGCGGCGAGT

TABLE S2 | Sequencing, mapping and coverage data from ChAP-Seq experiments

Sample	ChAP-Seq exp. No.	Total reads amount	Mapping		Coverage	
			Mapped uniquely	Mapped uniquely %	Median	Mean
Glucose						
$WT_{GlxR\text{-}TS}$	1	191 299	174.158	91.04%	11	12
	2	285 318	254 654	89.25%	14	16
	3	709 149	672 793	94.87%	50	54
$\Delta cyaB_{GlxR\text{-}TS}$	4	786 320	737 718	93.82%	63	65
	5	979 464	823 058	84.03%	72	77
Glucose-Acetate						
$WT_{GlxR\text{-}TS}$	6	1 035 286	971 112	93.80%	86	90
	7	1 572 052	1 441 562	91.70%	105	121
$\Delta cyaB_{GlxR\text{-}TS}$	8	691 265	614 185	88.85%	55	55
	9	1 812 475	1 702 348	93.92%	158	167

TABLE S3 | GlxR peaks and corresponding binding sites identified with ChAP-Seq.

TABLE S4 | GlxR peaks and corresponding binding sites from Table S3. (iii) lists binding sites found intergenic of two covalent transcribed genes (inter_conv); (iv) lists binding sites that are found located intragenic but less than 500 bp upstream of a gene start (intra_up); (v) lists binding sites that are located intragenic with more than 500 bp upstream from the next gene start (intragenic).

TABLE S5 | GlxR bindings sites and corresponding gene targets that are described in the literature but were not defined as GlxR peak in our ChAP-Seq analysis.

TABLE S6 | Microarray data of Δ*cpdA*/WT and Δ*cyaB*/WT of (putative) GlxR target genes

TABLE S7 | GlxR peaks and corresponding binding sites found upstream of non-protein coding elements, antisense transcripts or intragenic trasnscripts (less than 700 bp upstream of its TSS)

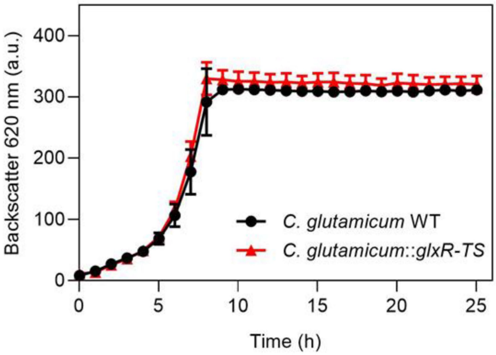

FIGURE S1│Growth of *C. glutamicum* ATCC13032 wild type (WT) and the mutant *C. glutamicum*::*glxR-TS* ($WT_{GlxR\text{-}TS}$) with a chromosomal Twin Strep-tag encoding sequence at the 3' end of *glxR*. The cells were cultivated in CGXII medium with 2% (w/v) glucose. The first preculture was inoculated in BHI medium and the second preculture in CGXII with 2% (w/v) glucose. Before inoculation of the main culture, cells were washed with saline [0.9% (w/v) NaCl]. The main culture was cultivated in 800 µl CGXII minimal medium, inoculated to an OD_{600} of 1, and cultivated with the respective amount of carbon sources in a BioLector. Mean values and standard deviation of three biological replicates each.

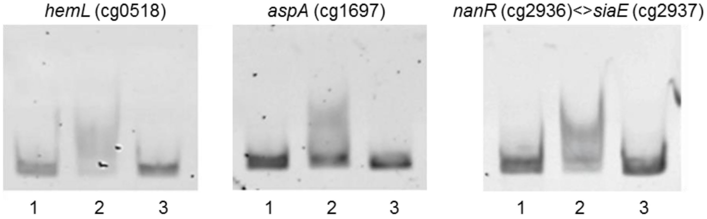

FIGURE S2│Electrophoretic mobility shift assays (EMSAs) with C-terminally Twin Strep-tagged GlxR ($GlxR_{TS}$) and DNA fragments covering new *in vivo* GlxR binding sites of *C. glutamicum* ATCC13032. DNA fragments are located upstream of depicted genes or in the intergenic region of two divergently transcribed genes (< >) of depicted genes. 100 ng of the 100 bp DNA fragments were incubated for 30 min with 200 nM purified protein at room temperature, either with or without 0.2 mM cAMP. After incubation, the reaction mixture was loaded onto a 10% native polyacrylamide gel. Lane 1: control sample containing only DNA; lane 2: sample with $GlxR_{TS}$, the indicated DNA fragment, and cAMP; lane 3: sample with $GlxR_{TS}$ and the indicated DNA fragment, but without cAMP.

TABLE S3 (Part 1/8) | **GlxR peaks and corresponding binding sites identified with ChAP-Seq.**

Locus tag (cg)	Locus tag (NCgl)	Start position[a]	End position[a]	GlxR binding site[b]	E-value	EF[c] $WT_{GlxR\text{-}TS}$ (glc)	EF[c] $\Delta cyaB_{GlxR\text{-}TS}$ (glc)	EF[c] $WT_{GlxR\text{-}TS}$ (glc-ac)	EF[c] $\Delta cyaB_{GlxR\text{-}TS}$ (glc-ac)	Neigboring gene(s)	Locus tag	Distance to next TSS[d]	Distance to next TLS[d]	Annotation	GlxR peak known or new[e]	operon[f]	further transcriptional regulator[f]	No.
cg0001	NCgl0001	0	208	GGTTCAAATATGCACG	1.57E-02	3.21	2.06	2.18	0.92	in *dnaA*	cg0001	-	+119	chromosomal replication initiation protein	NEW			240
cg0004	NCgl0002	1622	1949	AGTGAGCTTTGTCACA	2.48E-06	11.52	11.61	16.63	6.33	*dnaN*	cg0004	-392; -394	-523	DNA polymerase III subunit β	Toyoda et al. 2011	OP_cg0004-07		5
cg0054	NCgl0038	39981	40261	TGACTGCCGCAGCACA	3.10E-03	5.05	3.68	3.10	2.39	(cg0054) > < *crgA*	cg0054 > < cg0055	-	+1188 > < +302	put. iron-chelator utilization protein put. cell division membrane protein	NEW	OP_cg0052-54	cg0444 (ramB,R,pred), cg0051 (A,pred)	232
cg0061	NCgl0043	46430	46728	AGTATCAGCAGCCACA	5.46E-04	5.42	3.65	3.24	2.76	*rodA (ftsW)*	cg0061	-	+48	put. FTSW/RODA/SPOVE-family cell cycle protein	NEW	OP_cg0064-57		188
cg0088	NCgl0066	70195	70465	CGTGACACGCGCCACC	1.77E-04	4.77	3.23	3.21	3.17	*citH*	cg0088	-21[h], -22[h], -24[h]	-77	citrate transporter, CitMHS-family	Toyoda et al. 2011, Jungwirth et al 2013	-	cg2092 (sigA,A,exp), cg0090 (citB,A,exp)	140
cg0089	NCgl0067									*citA*	cg0089	-	-133	two component sensor kinase		OP_cg0089-90		140
cg0090	NCgl0068	71049	71315	AGTCTGATTTTGCACA	5.46E-04	6.30	4.19	5.33	2.89	*citB*	cg0090	-642; -807	-950	two component response regulator	NEW	OP_cg0089-90		187
cg0103	NCgl0074	83444	83782	TGTGGGGAGTGCCACA	1.33E-05	3.55	2.99	2.52	2.38	*crnT*	cg0103	-	-86	creatinine transporter	Toyoda et al. 2011	-	cg0986 (amtR,R,exp,cacatttctatcaatctataga aagtat)	28
cg0144	NCgl0109	123881	124241	TGTTAGATCCAGCACT	4.49E-04	3.24	1.49	1.64	2.40	*rbtT*	cg0144	-	-248	put. ribitol transporter, MFS-type	Toyoda et al. 2011	OP_cg0144-42	cg2092 (sigA,A,exp), cg0146 (atlR,R,exp,ctaacaacat)	181
cg0146	NCgl0110									*atlR (sucR, mtlR)*	cg0146	-33	-33	transcriptional regulator, DeoR-family		OP_cg0146-47	cg2092 (sigA,A,exp,ctaacaacat), cg0146 (atlR,exp)	181
cg0156	NCgl0120	134219	134522	TGTTCCGCAGCAGACT	1.58E-03	3.77	3.29	3.52	2.24	*cysR*	cg0156	-310	-310	transcriptional activator, ROK-family	NEW	-	cg2092 (sigA,A,exp), cg3253 (mcbR,R,pred,tagacagcgttgtcta)	222
cg0193	NCgl0151	165491	165776	TGTGGCACCAACCACA	2.96E-05	6.35	4.71	4.41	3.53	*pepO*	cg0193	-44	-44	endopeptidase O	pred. Kohl et al. 2008, Toyoda et al. 2011	-		50
cg0194	NCgl0152									-	cg0194	-60	-60	put. secreted protein		OP_cg0194-95		50
cg0196	NCgl0154	168843	169131	CGTGAGGGTCGCCACA	1.90E-04	13.18	11.85	10.90	5.74	*iolR*	cg0196	-263[i;] -264[i]	-400	repressor of myo-inositol utilization genes, GntR-family	Jungwirth et al. 2013	-	cg0196 (iolR,R,exp,tgtcctaaca)	141
cg0197	NCgl0155									*iolC*	cg0197	+15	-44	carbohydrate kinase, myo-inositol catabolism		OP_cg0197-05	cg0196 (iolR,R,exp,tgtcatgaca)	141
cg0210	NCgl0167	182606	182854	GGTATTGTGATCCACT	1.99E-03	3.73	2.58	2.74	1.37	-	cg0210	-	-85	put. transcriptional regulator, LacI-family	pred. Kohl et al. 2008	-	cg0196 (iolR,R,exp)	228
cg0211	NCgl0168									*oxiB*	cg0211	+25	-56	put. oxidoreductase dehydrogenase		OP_cg0211-12		228
cg0215	NCgl0171	186027	186335	GGTGTAAAAGCAGACA	7.27E-04	5.15	4.46	5.11	1.30	*cspA*	cg0215	-64	-245	cold-shock protein A	NEW	-		202
cg0223	NCgl0178	192087	192368	GGTGATGTGAATCACT	7.03E-05	13.69	11.65	12.17	4.72	*iolT1*	cg0223	+11[i]; +39[i]	-75	myo-Inositol transporter 1	pred. Kohl et al. 2008, Toyoda et al. 2011	-	cg0196 (iolR,R,exp,gtacataaca)	91
cg0228	NCgl0180	194929	195233	TGTGTTACACATCACA	1.19E-06	6.37	4.42	5.73	3.53	*hkm*	cg0228	-25	-58	put. sensor histidine kinase	Kohl & Tauch 2008, Jungwirth et al. 2013	-	cg0986(amtR,R, , cctgtttctatcaatcgttcgataataa)	4
cg0229	NCgl0181									*gltB*	cg0229	-104[g]	-145	glutamine 2-oxoglutarate aminotransferase		OP_cg0229-30	cg2092 (sigA,A,exp), cg0986 (amtR,R, exp, cgttttcctataggttgatcgaaagtaa), cg1585 (argR,R,pred)	4
cg0235	NCgl0184	206760	207155	TGAGTAATTCCTCACC	1.34E-03	4.20	2.72	2.65	2.05	*emb (embC)*	cg0235	-73	-73	arabinosyltransferase	NEW	OP_cg0236-35		219
cg0246	NCgl0195	215882	216192	TGTATGCCATGGCACA	7.03E-05	6.51	4.76	4.85	4.27	-	cg0246	+1	+1	put. glycosyl transferase	Toyoda et al. 2011	OP_cg0247-46		94
cg0247	NCgl0196	216785	217098	TGTGCCCGCCGCCACA	3.47E-05	7.05	3.83	4.27	4.42	-	cg0247	-272	-272	hypothetical protein	Jungwirth et al. 2013	OP_cg0247-46		55
cg0249	NCgl0198	218617	218889	CGTGAAATCGGACACA	1.33E-04	4.78	2.82	2.93	2.77	-	cg0249	+64	+64	put. polysaccharide/polyol phosphate export systems	Toyoda et al. 2011	OP_cg0249-48		125
cg0250	NCgl0199									-	cg0250	+41; -163	-177	put. aminotransferase class V		-		125
cg0261	NCgl0209	228447	228830	CGTGGCGAATCCCACT	4.06E-04	4.44	2.57	1.08	2.72	in *moeA1*	cg0261	-	+132	molybdopterin cofactor synthesis protein A1, MoeA-family	NEW			174
cg0261	NCgl0209	228936	229141	AGTATGGTGCGACACT	4.09E-04	3.33	1.51	1.54	0.00	*moeA1*	cg0261	-	-190	molybdopterin cofactor synthesis protein A1, MoeA-family	Toyoda et al. 2011	OP_cg0263-57		177
cg0280	NCgl0224	242137	242468	TGTCTCATTTAACACA	2.96E-05	3.81	4.24	4.49	2.96	-	cg0280	-632	-632	hypothetical protein	NEW	OP_cg0280-81		52
cg0303	NCgl0245	267974	268292	TGTATGCTTCACCACA	9.14E-05	7.65	5.44	5.57	3.49	*leuA*	cg0303	-	-248	2-isopropylmalate synthase	Toyoda et al. 2011	-	cg2092 (sigA,A,exp)	104
cg0336	NCgl0274	296794	297077	TGTCGAATGCATCACA	7.03E-05	9.33	7.89	9.82	4.30	*pbp1a*	cg0336	-579	-579	penicillin-binding protein 1A	Kohl & Tauch 2009, Jungwirth et al. 2013	-		92
cg0337	NCgl0275									*whcA (whiB4)*	cg0337	-40;+66	-89	put. regulatory protein (whiB related protein)		-	cg0878 (whiB1,A,pred)	92
cg0341	NCgl0279	301070	301362	CGTGATCTAAAGCACA	7.03E-05	16.03	16.10	21.24	7.00	*phdA (fadD1)*	cg0341	-	-22 (-16 alternative TLS)	acyl:CoA ligase transmembrane protein	predicted (Kohl et al. 2008), Toyoda et al. 2011	-	cg0343 (phdR,R,exp)	90
cg0343	NCgl0280	301997	302274	AGTGTCTGGGATCACA	4.02E-05	14.49	14.62	16.76	6.10	*phdR, regulator*	cg0343	-	-163	Repressor of phd operon, MarR-family	Kohl & Tauch 2008, Jungwirth et al. 2013	-		66
cg0344	NCgl0281									*phdB (fabG1)*	cg0344	-	-29	3-hydroxyacyl-CoA dehydrogenase		OP_cg0344-47	cg0343 (phdR,R,exp)	66
cg0350	NCgl0286	307411	307714	AGTGGTCTTTGCCACA	2.53E-05	13.19	12.05	12.95	6.44	*glxR*	cg0350	+3; +21; +200	-123	cAMP-dependent global transcriptional regulator, Crp-family	Jungwirth et al. 2008, Jungwirth et al. 2013, Subhadra et al. 2015	-	cg2092 (sigA,A,exp), cg2544 (A,exp,taaagtgtgacattt), cg0146 (pred,ctgccagcaa), cg0444	44
cg0360	NCgl0294	314402	314704	AGTGTCATTTGCCACA	8.01E-06	9.99	9.47	8.91	6.85	-	cg0360	-127	-127	put. phosphatase	Jungwirth et al 2013	-		13
cg0362	NCgl0295									-	cg0362	-	-318	put. septum site determining protein		OP_cg0362-69		13
cg0427	-	377613	377928	AGTATACTTCCATACA	1.71E-03	5.01	2.79	4.51	0.94	*tnp17b*	cg0427	+16	-281	transposase fragment	NEW	-		224
cg0440	-	387792	388032	TATGAGGATGCTCACA	1.51E-04	3.82	2.12	2.32	2.58	-	cg0440	-	-331	hypothetical protein	NEW	-		132
cg0444	NCgl0358	392318	392621	GGTGAGCTTCCTCACA	1.87E-05	9.89	8.82	9.02	4.55	*ramB, rgulator*	cg0444	-283	-283	transcriptional regulator, MerR-family	Jungwirth et al. 2008, Kohl & Tauch 2009, Han et al. 2008, Bussmann et al. 2009	-	cg2831 (ramA,A,exp), cg2092 (sigA,A,exp), cg0444 (ramB,R,exp,acaagtttgcaac)	33
cg0445	NCgl0359									*sdhC*	cg0445	-198; -200; -203	-215	succinate:menaquinone oxidoreductase, cytochrome b subunit		OP_cg0445-48,cg4001	(ramA,A,exp,tgggggtcatgggga), cg1120 (ripA,R,exp,atgagcgtcaaacgacaa), cg0444 (ramB,R,pred,gttgcaaacttgt),	33

TABLE S3 (Part 2/8) | **GlxR peaks and corresponding binding sites identified with ChAP-Seq.**

Locus tag (cg)	Locus tag (NCgl)	Start position[a]	End position[a]	GlxR binding site[b]	E-value	EF[c] WT$_{\mathrm{GlxR\text{-}TS}}$ (glc)	EF[c] Δ*cyaB* $_{\mathrm{GlxR\text{-}TS}}$ (glc)	EF[c] WT$_{\mathrm{GlxR\text{-}TS}}$ (glc-ac)	EF[c] Δ*cyaB* $_{\mathrm{GlxR\text{-}TS}}$ (glc-ac)	Neigboring gene(s)	Locus tag	Distance to next TSS[d]	Distance to next TLS[d]	Annotation	GlxR peak known or new[e]	operon[f]	further transcriptional regulator[f]	No.
cg0448	NCgl0362	396032	396338	GGTGACAGCTGCCACA	8.04E-05	7.87	6.06	5.22	5.23	-	cg0448	-61;+88	-100	put. membrane protein	Kohl & Tauch 2009, Han et al. 2008, Bussmann et al. 2009	OP_cg0445-48;cg4001	cg2831 (ramA,A,pred), cg2092 (sigA,A, exp), cg2103 (dtxR,A,exp), cg1120 (ripA,R,pred), cg0444 (ramB,R,pred)	96
cg0454	NCgl0368	400168	400515	AATGACTTAGGACACA	8.04E-05	3.54	2.60	2.26	2.63	*mfsR*	cg0454	-	-83	transcriptional regulator, TetR-family	predicted (Kohl et al. 2008)	OP_cg0454-56	cg0454 (mfsR,pred;ttacactaggtttac)	100
cg0500	NCgl0405	442349	442674	TGTACTATAGATCACA	2.18E-05	5.39	5.17	5.15	2.86	*qsuR, regulator*	cg0500	-	-70	transcriptional activator of qsuABCD genes, LysR-family	pred. Kohl et al. 2008, Toyoda et al. 2011	-	cg0500 (qsuR,A, pred)	40
cg0501	NCgl0406									*qsuA*	cg0501	-	-207	put. shikimate permease, MFS-type		-	cg0500 (qsuR,A,exp,tatgcaagagatggata)	40
cg0518	NCgl0422	462081	462410	TATGGAGTTGATCACA	2.39E-04	5.46	3.47	4.03	3.30	*hemL*	cg0518	-253	-253	glutamate-1-semialdehyde 2,1-aminomutase	Toyoda et al. 2011	OP_cg0516-24	cg3247 (hrrA,R,exp)	152
cg0565	NCgl0461	501405	501691	TGTATCTCACCTCACA	2.18E-05	8.83	6.69	7.54	3.98	*pwkR/gabR*	cg0565	-65	-124	put. transcriptional regulator	Jungwirth et al. 2013	-		39
cg0566	NCgl0462									*gabT*	cg0566	+19[k]	-18	4-aminobutyrate aminotransferase		OP_cg0566-67	cg0565 (gabR,R,exp)	39
cg0576	NCgl0471	514025	514322	TGAGTCAAACCAGACA	9.50E-04	4.17	3.56	4.86	2.50	in *rpoB*	cg0576	+1518; +1520	+1308	DNA-directed RNA polymerase β subunit	NEW			215
cg0583	NCgl0478	524435	524776	TGTAGGCGGTGCCACA	2.39E-04	3.45	2.17	2.32	1.94	in *fusA*	cg0583	+897; +990	+791	elongation factor EF-2/G	NEW			153
cg0607	NCgl0498	539307	539613	TGTATATCTAACCACA	4.06E-04	4.18	2.26	2.87	1.21	-	cg0607	-84; -63	-133	put. secreted protein	Toyoda et al. 2011	-	cg0696 (sigD,A,exp)	175
cg0608	NCgl0499									*rplN*	cg0608	-13; -10	-196	50S ribosomal protein L14		OP_cg0608-10		175
cg0645	NCgl0530	567989	568311	CGTGATGGCTATCACT	5.46E-04	3.58	3.22	2.82	2.93	*creJ (cytP)*	cg0645	-	-74 (-80 alternative TLS)	cytochrome P450	NEW	OP_cg0645-41	cg3352 (genR,A,pred,attccactgagtggaat), cg2115 (sugR,R,pred), cg0646 (creR,R,pred)	189
cg0646	NCgl0531	569106	569362	TATGATGCGTCTTACA	6.61E-04	3.79	2.44	2.82	2.20	*creR*	cg0646	-71; -115	-202	put. transcriptional regulator, IclR-family	NEW	-		200
cg0647	NCgl0532									*secY*	cg0647	-60; -140	-176	preprotein translocase subunit		OP_cg0647-49		200
cg0658	NCgl0543	579446	579759	TGTCGCCATGTTCACT	3.66E-04	2.62	1.61	3.27	1.09	*in rptA*	cg0658	-	+1393	terminal rhamnopyranosyl transferase	NEW	-		169
cg0703	NCgl0582	619819	620130	TGTCTGAAGGCTCACA	9.14E-05	6.23	4.58	5.57	3.08	*guaA*	cg0703	+7	+7	put. Gmp synthase	NEW	OP_cg0702-03		105
cg0706	NCgl0584	622394	622684	GGTCTCCAACATCACA	1.51E-04	3.60	2.59	2.75	2.64	in (cg0706)	cg0706	+1070	+1070	put. membrane protein, conserved	NEW			133
cg0755	NCgl0625	667808	668106	TATGACTAGCCCCACT	6.01E-04	3.32	2.32	2.69	1.54	*metY*	cg0755	-136	-175	O-acetylhomoserine sulfhydrylase	NEW	-	cg2092 (sigA,A,exp), cg3253 (mcbR,R,exp,tataccacacagtcta)	196
cg0756	NCgl0626									*cstA*	cg0756	-30;-32;-42; -59	-258	carbon starvation protein A		-		196
cg0759	-	670878	671219	TGTTGCACACCACACT	2.67E-04	10.30	8.11	11.09	3.70	*prpD2*	cg0759	-4[l]	-41	2-methycitrate dehydratase	Jungwirth et al. 2013	OP_cg0759-62	cg0800 (prpR,R,exp), cg2092 (sigA,A,exp), cg2831 (ramA,A,exp)	154
cg0764	NCgl0632	676645	676946	TGTTCAACCAGCCACA	7.27E-04	3.67	2.46	2.95	2.31	in (cg0764)	cg0764	+126	+126	put. transcriptional regulator, GntR-family	NEW			204
cg0766	NCgl0634	680094	680413	TGTGTTCTCCGCCACT	3.47E-05	3.75	2.43	3.01	2.89	*icd*	cg0766	-232	-263	isocitrate dehydrogenase	Toyoda et al. 2011	-	cg2092 (sigA,A,exp), cg2783 (gntR1 ,A,exp,cttggtgtgatcttt)	63
cg0773	NCgl0641	685592	685875	GGTTCCTCATGCCACA	5.46E-04	3.38	2.61	2.62	2.34	-	cg0773	-667	-667	put. exodeoxyribonuclease	NEW	OP_cg0773-74		190
cg0788	NCgl0656	700413	700712	TGTCTGTCACCCCACA	1.17E-04	3.32	2.44	2.56	2.50	in *pmmB*	cg0788	+1423	+1386	phosphoglucomutase/phosphomannomutase	NEW			121
cg0791	NCgl0659	705001	705298	GGTGATAGCAGTCACT	2.39E-04	5.97	3.92	4.47	4.01	*pyc*	cg0791	+14; +12; +10	-45	pyruvate carboxylase	Kohl & Tauch 2008	-	cg2092 (sigA,A,exp), cg0444 (ramB,exp,caaagtttgcaaa)	151
cg0796	NCgl0664	712467	712793	TGTGGCCTGTCACACA	3.65E-06	5.70	3.65	4.67	3.21	*prpD1*	cg0796	-32	-68	2-methylcitrate dehydratase	Kohl & Tauch 2009, Jungwirth et al. 2013	OP_cg0796-98		9
cg0803	NCgl0671	721377	721657	AGTAATTAAGGACACA	9.14E-05	3.65	2.81	2.75	1.03	*thtR*	cg0803	-37	-91	thiosulfate sulfurtransferase	pred. Kohl et al. 2008	-		110
cg0806	NCgl0672									-	cg0806	-61	-238	hypothetical protein		-		110
cg0835	NCgl0698	747845	748100	CATGGCAACGGTCACA	1.45E-03	3.57	2.34	2.49	2.95	*tusK (msiK2)*	cg0835	+7	+7	trehalose uptake system	Jungwirth et al. 2013	-		221
cg0836	NCgl0699									-	cg0836	-	-94			-		221
cg0845	NCgl0707	775275	775618	AGTATGCAGGTTCACA	4.96E-04	3.49	2.68	3.01	2.04	in (cg0845)	cg0845	+1543	+1543	put. superfamily II DNA/RNA helicase, SNF2-family	NEW			184
cg0847	NCgl0708	779163	779514	GGTGACGTTTCGCACA	2.96E-05	2.63	3.00	2.89	3.71	*lcpA*	cg0847	-	-656	put. transcriptional regulator, LytR	Toyoda et al. 2011	-		54
cg0866	NCgl0724	794231	794532	CGTGATATTTGTCACG	2.97E-04	3.38	2.26	2.46	2.48	-	cg0866	-	-311	purine/pyrimidine phosphoribosyl transferase	NEW	OP_cg0860-68		158
cg0867	NCgl0725	794859	795164	CGTGATGCATTGCACA	1.90E-04	5.45	3.68	4.31	3.33	*psrp-1*	cg0867	-162; -300; -303; -306	-384	put. ribosome-associated protein Y	Toyoda et al. 2011	OP_cg0860-68		144
cg0875	NCgl0732	803117	803421	TGTGTCTTCCACCACA	8.01E-06	5.29	4.62	4.80	4.17	in (cg0875)	cg0875	-	+935	conserved hypothetical protein	NEW			15
cg0878	NCgl0734	805907	806235	TGTGGGGTGGAACACA	8.01E-06	6.37	5.89	7.10	4.23	*whcE (whiB1)*	cg0878	-114	-316	transcriptional regulator	Kohl & Tauch 2008, Jungwirth et al. 2013	-	cg0876 (sigH,A,exp), cg0695 (whiB3,A,pred)	14
cg0879	NCgl0735									-	cg0879	-217	-217	put. membrane protein		-		14
cg0904	-	835617	835898	TGCTTGATCTCCCACA	6.81E-03	3.64	3.85	2.62	1.12	-	cg0904	-	-328	hypothetical protein	NEW	-		238
cg0923	NCgl0775	850933	851232	TGTCTAATTTGGCACT	3.29E-04	8.86	7.05	7.25	4.79	-	cg0923	-81	-117	put. membrane protein	pred. Kohl et al. 2008	-		162
cg0924	NCgl0776									-	cg0924	-156	-236	put. ABC-type put. iron-siderophore transporter	-	-	cg2103 (dtxR,R,exp,ttaggtaacctaacctcac)	162
cg0926	NCgl0777	852274	852564	TGTTCTTTACAAGACA	5.46E-04	3.31	2.35	3.23	2.55	-	cg0926	-	-159	put. put. iron-siderophore transporter	NEW	OP_cg0926-28	cg2103 (dtxR,R,exp,ttaggttaggctctaatat)	191
cg0933	NCgl0782	864962	865265	TGTGGATGAAGCCACA	3.47E-05	5.96	3.84	4.54	2.89	-	cg0933	-87	-115	put. DNA or RNA helicase of superfamily II	NEW	OP_cg0934-32		56
cg0936	NCgl0785	868599	868896	TGTAACATAAATCACA	2.48E-06	4.45	4.20	6.10	2.89	*rpf1*	cg0936	-122; -211; -402	-406	resuscitation promoting factor	Kohl & Tauch 2008	-		8
cg0938	NCgl0786									*cspB*	cg0938	-84	152	cold shock protein		-	cg2092 (sigA,A,exp)	8
cg0948	NCgl0794	877235	877540	TGTCGCGTGCATCACA	1.87E-05	12.02	9.06	13.92	5.36	*serC*	cg0948	-258	-318	phosphoserine aminotransferase	Han et al. 2008, Kohl & Tauch 2009, van Ooyen	-	cg0444 (ramB,R,pred,tttgcaaaact)	30
cg0949	NCgl0795									*gltA*	cg0949	-288	-409	citrate synthase		OP_cg0949-50	cg2831 (ramA,A,exp), cg0444 (ramB, ,exp), cg2092 (sigA,A,exp)	30

TABLE S3 (Part 3/8) | **GlxR peaks and corresponding binding sites identified with ChAP-Seq.**

Locus tag (cg)	Locus tag (NCgl)	Start position^{a}	End position^{a}	GlxR binding site^{b}	E-value	EF^{c} WT$_{GlxR-TS}$ (glc)	EF^{c} Δ*cyaB* $_{GlxR-TS}$ (glc)	EF^{c} WT$_{GlxR-TS}$ (glc-ac)	EF^{c} Δ*cyaB* $_{GlxR-TS}$ (glc-ac)	Neigboring gene(s)	Locus tag	Distance to next TSS^{d}	Distance to next TLS^{d}	Annotation	GlxR peak known or new^{e}	operon^{f}	further transcriptional regulator^{f}	No.
cg0951	NCgl0797	881238	881608	AGTTACCTAACTCACA	4.02E-05	7.19	5.96	8.90	4.51	*accD3*	cg0951	-220; -397	-397	acetyl-coenzyme A carboxylase carboxyl transferase	Kohl & Tauch 2008	-	cg0444 (ramB,R,pred,tttgcaaagattg)	68
cg0952	NCgl0798									*mctB*	cg0952	-17;+274	-170	put. integral membrane protein		OP_cg0952-53	cg0444 (ramB,R,exp,caatctttgcaaa), cg2831 (ramA, ,exp,aggggtatttcggggt)	68
cg0955	NCgl0801	885340	885633	CGTGAGCAACATCACA	4.02E-05	4.37	3.17	4.82	2.32	-	cg0955	-84	-128	put. secreted protein	Kohl & Tauch 2008	-	cg2103 (dtxR,R,exp,ttacgtgagcgtagccgaa)	71
cg0957	NCgl0802									*fas-IB*	cg0957	-92; -104	-157	fatty acid synthase, Fas-I-type		-	cg2737 (fasR,R,exp,ccgcaaaagatgacgttttcctc atgatt)	71
cg0961	NCgl0805	896520	896789	TGGGGTGTAGGTCACA	4.96E-04	11.13	11.00	13.44	4.94	-	cg0961	-	-26	put. homoserine O-acetyltransferase	Jungwirth et al. 2013	-		182
cg0962	NCgl0806	897324	897585	GGTCAATCAGATCACT	7.96E-04	2.74	2.83	3.10	0.98	-	cg0962	-337	-337	put. secreted protein	NEW	-		211
cg0967	NCgl0811	900194	900525	AGTGATATTGGGCACA	1.12E-05	5.59	3.88	4.67	4.15	*cysQ*	cg0967	-405	-405	3-phosphoadenosine 5-phosphosulfate PAPS 3-phosphatase	Toyoda et al. 2011	-		23
cg0967	NCgl0811	899976	900140	CATGGCTAAAAGCATT	1.92E-02	3.49	0.00	1.62	0.00	*cysQ*	cg0967	-42	-42	3-phosphoadenosine 5-phosphosulfate PAPS 3-phosphatase	Jungwirth et al. 2013	-		241
cg0968	NCgl0812									-	cg0968	+7	+7	put. ATP-dependent helicase		OP_cg0968-70		241
cg0973	NCgl0817	909291	909583	TGTCGTGTTTCCCACT	3.29E-04	3.50	3.00	2.77	0.88	*pgi*	cg0973	-59	-87	glucose-6-phosphate isomerase	NEW	-		163
cg1037	NCgl0872	963499	963773	CGTGAGGTAGCTCACA	1.87E-05	4.39	2.77	3.91	2.79	*rpf2*	cg1037	-132	-163	resuscitation promoting factor	Jungwirth et al. 2008, Jungwirth et al. 2013	OP_cg1037-41	cg0862 (mtrA,R,exp,gtcacaatacggtaacaaa), cg0444 (ramB,R,exp,tattgtgactaat), cg2831 (ramA,A,exp), cg2092(sigA,A,exp)	37
cg1043	NCgl0877	969818	970084	AGTGACCCCGCACACA	4.02E-05	4.59	2.92	3.59	3.03	-	cg1043	-	-30	put. thiol-disulfide isomerase and thioredoxins	pred. Kohl et al. 2008, Toyoda et al. 2011	-		69
cg1044	NCgl0878									-	cg1044	-60	-60	hypothetical protein		OP_cg1044-45		69
cg1048	NCgl0881	972932	973227	AGTGTGGCACATCACA	1.12E-05	3.92	1.90	2.49	2.69	-	cg1048	-59	-89	put. haloacid dehalogenase/epoxide hydrolase-family	pred. Kohl et al. 2008, Toyoda et al. 2011	-		25
cg1049	NCgl0882									-	cg1049	-16	-16	put. enoyl-CoA hydratase/isomerase		-		25
cg1052	NCgl0885	977403	977763	GGTGCCAAGGCTCACA	8.04E-05	3.13	2.22	2.22	2.65	in *cmt3*	cg1052	+1374;+1377	+1333	corynomycolyl transferase	NEW			101
cg1060	NCgl0892	986460	986754	TGTAAGACACGTCACT	3.47E-05	4.02	2.75	3.84	2.13	*prfC*	cg1060	-134	-134	put. peptide chain release factor 3 EF-G	Kohl & Tauch 2009	-		60
cg1061	NCgl0893									*urtA*	cg1061	-	-96	ABC-type urea uptake system		OP_cg1061-66	cg0986 (amtR,R,exp,caactacctataggctgacag aaactct)	60
cg1075	NCgl0905	998005	998314	TGTTCCATGAGCCACT	2.97E-04	3.45	0.77	2.39	0.00	in *prsA*	cg1075	+377	+225	ribose-phosphate pyrophosphokinase	NEW			157
cg1085	-	1006689	1007046	AGTGCTTCACATCACA	2.53E-05	4.05	3.14	4.07	3.06	-	cg1085	+1	-71	hypothetical protein	Jungwirth et al. 2013	-		47
cg1086	NCgl0913									-	cg1086	-126	-126	put. membrane protein		-		47
cg1087	-	1008041	1008335	TGTGAAAGCTATCACA	1.87E-05	3.41	3.71	4.01	3.42	-	cg1087	-3	-29	put. membrane protein	NEW	-		38
cg1090	NCgl0916	1013562	1013852	TGTGCTTTGGGTCACT	1.59E-05	4.93	4.08	5.42	3.32	*ggtB*	cg1090	+13	+13	γ-glutamyltranspeptidase precursor PR	pred. Kohl et al. 2008, Toyoda et al. 2011	-		29
cg1091	NCgl0917									-	cg1091	-133	-262	hypothetical protein		-	cg3420 (sigM,A,pred)	29
cg1108	NCgl0932	1033014	1033307	AGTCACATAAATCACT	7.03E-05	4.25	2.42	2.61	2.45	*porC*	cg1108	-	-90	put. secreted protein	NEW	-		95
cg1111	NCgl0935	1034624	1034903	CGTGTCCGATCAGACA	7.96E-04	5.77	3.84	4.47	3.05	*eno*	cg1111	-93	-163	enolase, phosphopyruvate hydratase	NEW	-	cg2092 (sigA,A,exp), cg2102 (sigB,A,pred), cg2115 (sugR,R,exp)	206
cg1142	NCgl0963	1059896	1060164	TGTGCTATAGGACACA	1.19E-06	8.22	6.29	7.93	4.60	-	cg1142	-	-114	put. Na+/proline, Na+/panthothenate symporter	Kohl & Tauch 2008, Jungwirth et al. 2013	OP_cg1142-39	cg1143 (pred)	3
cg1143	NCgl0965									-*(regulator)*	cg1143	-98	-98	put. transcriptional regulator, GntR-family		OP_cg1143-44		3
cg1147	NCgl0968	1064223	1064532	TGTACCACCGCTCACA	1.33E-04	4.13	2.91	3.30	2.93	in *ssuI*	cg1147	+468	+468	Conserved protein/domain typically associated with flavoprotein oxygenases, DIM6/NTAB family NADPH-dependent FMN reductase	NEW			127
cg1222	NCgl1029	1122823	1123148	TATGGCGCGGGTCACA	1.03E-04	3.40	2.49	2.80	2.60	*lplA*	cg1222	-116	-116	lipoate-protein ligase A	pred. Kohl et al. 2008, Toyoda et al. 2011	OP_cg1222-20		116
cg1224	NCgl1030									*phnB2*	cg1224	-28	-62	similarity to alkylphosphonate uptake operon protein PhnB *E. coli*		-		116
cg1244	NCgl1049	1141185	1141511	TATGCCGAAGGCCACA	1.51E-04	3.32	1.83	2.34	2.06	*arsC4*	cg1244	-128	-128	arsenate reductase, glutaredoxin-family	Toyoda et al. 2011	-		134
cg1256	NCgl1061	1153247	1153654	AGTTTCAACTGTGACA	1.04E-03	4.16	3.89	4.71	2.93	*dapD*	cg1256	-275	-275	tetrahydrodipicolinate succinylase	NEW	OP_cg1259-56	cg0986 (amtR,R,exp,ctatcggcctatca), cg2092 (sigA,A,exp)	216
cg1290	NCgl1094	1190886	1191208	TGGGTGGTGGGTCACA	7.96E-04	3.81	3.43	3.65	2.92	*metE*	cg1290	-252; -254	-494	homocysteine methyltransferase	Toyoda et al. 2011	-	cg2092 (sigA,A,exp), cg3253 (mcbR,R,pred,tcaagcagaaagtctt)	209
cg1291	NCgl1095									-	cg1291	-83	-83	put. membrane protein		-		209
cg1305	NCgl1108	1209605	1209877	GGTGGCGCGTGTCACT	1.03E-04	6.85	4.56	5.65	3.65	*pheP*	cg1305	-104	-149	L-phenylalanine transporter	Jungwirth et al. 2013	-		114
cg1307	NCgl1109									-	cg1307	-168;-170	-171	put. superfamily II DNA and RNA helicase		-		114
cg1314	NCgl1116	1219536	1219818	AGTGTTGTAGTTCACA	9.44E-06	16.13	14.57	25.00	9.09	*putP*	cg1314	-	-68	proline transport system	Kohl & Tauch 2009, Jungwirth et al. 2013	-	cg2114 (lexA,A,exp,tcgtaaccttgtgcga)	19
cg1316	NCgl1117									-	cg1316	-	-226	put. superfamily II DNA/RNA helicases, SNF2-family		OP_cg1316-17		19
cg1341	NCgl1139	1246346	1246644	CGTTCCCCACCTCACA	7.27E-04	4.35	2.21	3.15	3.04	*narI*	cg1341	-	-33	dissimilatory nitrate reductase, γ-subunit, cytochrome b	Toyoda et al. 2011	OP_cg1345-41	cg1340 (arnR,R,exp), cg1324 (rosR,A,exp), cg1120 (ripA,A,exp), cg2092 (sigA,A,exp)	203

TABLE S3 (Part 4/8)| **GlxR peaks and corresponding binding sites identified with ChAP-Seq.**

Locus tag (cg)	Locus tag (NCgl)	Start position[a]	End position[a]	GlxR binding site[b]	E-value	EF[c] WT$_{GlxR-TS}$ (glc)	EF[c] Δ*cyaB* $_{GlxR-TS}$ (glc)	EF[c] WT$_{GlxR-TS}$ (glc-ac)	EF[c] Δ*cyaB* $_{GlxR-TS}$ (glc-ac)	Neigboring gene(s)	Locus tag	Distance to next TSS[d]	Distance to next TLS[d]	Annotation	GlxR peak known or new[e]	operon[f]	further transcriptional regulator[f]	No.
cg1345	NCgl1143	1253789	1254094	GATAACAGCTCTGACC	2.11E-02	3.98	3.10	4.65	2.31	*narK*	cg1345	-18	-79	nitrate/nitrite antiporter	Kohl & Tauch 2008, Nishimura et al. 2011	OP_cg1345-41	cg1324 (rosR,A,exp,atgttgatataagcacaa), cg1120 (ripA,R,exp,taaagtgaattacgacac), cg2092 (sigA,A,exp), cg1340 (arnR,R,exp,taattaaata)	242
cg1346	NCgl1144									*mog*	cg1346	-146	-180	put. molybdopterin biosynthesis MOG protein		-		242
cg1362	NCgl1159	1271688	1272121	TGTTATGTGTGTCACA	1.12E-05	2.53	2.36	3.51	1.34	*atpB*	cg1362	-119; -121	-172	F1FO-ATP synthase, a-subunit of FO part	Toyoda et al. 2011	OP_cg1362-69	cg0876 (sigH,A,exp), cg2831 (ramA, ,pred)	26
cg1408	NCgl1201	1314746	1315043	TGTGCAGCACACCACA	2.53E-05	7.04	4.98	5.83	3.69	-	cg1408	-102	-102	put. membrane protein	Toyoda et al. 2011	-	cg2115 (sugR,R,pred), cg2114 (lexA,R,exp,tcggacacatttttgc)	45
cg1409	NCgl1202									*pfkA*	cg1409	-165; -167	-167	6-phosphofructokinase		-	cg2102 (sigB,pred), cg2092 (sigA,exp), cg2115 (sugR,R,exp), cg2831 (ramA,R,exp)	45
cg1432	NCgl1219	1335160	1335532	CGTCTGAAACCTCACA	4.96E-04	3.04	2.11	2.76	1.76	*ilvD*	cg1432	+24; -46	-165	dihydroxy-acid dehydratase	NEW	-	cg2092 (sigA,A,exp), cg0876 (sigH,A,exp)	186
cg1434	NCgl1221	1337674	1337947	TGTGTAGCATGACACA	4.44E-06	4.79	3.18	3.30	3.05	*yggB (mscCG)*	cg1434	-137	-137	small-conductance mechanosensitive channel, MscS-family	Kohl & Tauch 2009, Jungwirth et al. 2013	-		11
cg1435	NCgl1222									*ilvB*	cg1435	-	-302	acetolactate synthase I AHAS		OP_cg1435-37	cg2092 (sigA,A,exp)	11
cg1437	NCgl1224	1340406	1340698	TGTTTGACTAGTCACA	9.14E-05	5.67	3.81	4.72	2.58	*ilvC*	cg1437	-43	-139	ketol-acid reductoisomerase	Kohl & Tauch 2009, Jungwirth et al. 2013	OP_cg1435-37	cg2092 (sigA,A,exp), cg0876 (sigH,A,exp)	107
cg1520	NCgl1294	1410547	1410841	TGTACTGCTAATCACA	1.33E-04	3.29	2.09	3.35	2.50	in (cg1520)	cg1520	-	+299	put. secreted protein CGP1 region	NEW			129
cg1537	NCgl1305	1422809	1423121	AGTGTGATCCACCACA	6.09E-05	3.86	2.72	2.82	1.07	*ptsG*	cg1537	+31	-255	glucose-specific EIIABC component EIIGlc of PTS	Kohl & Tauch 2009, Subhadra & Lee 2013	-	cg2115 (sugR,R,exptcggacata,), cg2783 (gntR1,A,exp,aaaagtattaccttt), cg1935 (gntR2,A,exp,aaaagtattaccttt), cg2831 (ramA,R,exp), cg0444 (ramB, ,exp,caaattgtgcaat), cg2092 (sigA,A,exp)	85
cg1547	NCgl1312	1432353	1432667	TGTCTCCATCGCCACA	6.09E-05	6.00	3.16	4.22	2.79	*uriR*	cg1547	+127	+62	transcriptional regulator, LacI-family	Toyoda et al. 2011	OP_cg1547-43	cg2092 (sigA,A,exp), cg1410 (rbsR,R,exp,tgtaatcgtttgca), cg1547 (uriR,R,exp,tgtaatcgtttgca)	83
cg1548	NCgl1313									-	cg1548	-	-265	hypothetical protein		-		83
cg1577	NCgl1337	1460472	1460771	GGTGTCGCAGTTCACA	3.47E-05	3.66	1.01	2.55	2.28	-	cg1577	-347; -408	-469	put. secreted hydrolase	pred. Kohl et al. 2008	OP_cg1577-579		64
cg1608 > < cg1609	NCgl1364 > < NCgl1365	1496565	1496868	TGAGCCCCGCGCCACA	4.49E-04	3.34	2.04	2.20	2.35	*xerD* > < (cg1609)	cg1608 > < cg1609	-	+894 > < +1571	tyrosine recombinase > < put. ATPase component of antibiotics ABC transporter	NEW			180
cg1611 > < cg1612	NCgl1367 > < NCgl1368	1500579	1500875	TGTAGCTTAGGTCACT	2.35E-05	3.19	1.80	2.60	0.78	*scpA* > < *cg1612*	cg1611 > < cg1612	+1015 > < -728	+813 > < -728	put. segregation and condensation protein A > <	Toyoda et al. 2011			43
cg1612	NCgl1368	1501343	1501672	CGTGAGAACCATCACA	1.33E-04	4.49	3.23	3.70	1.86	-	cg1612	-40	-40	put. acetyltransferase	pred. Kohl et al. 2008, Toyoda et al. 2011	-	cg0862 (mtrA,A,exp,gtcacaaaatgatttcagt)	126
cg1613	NCgl1369									*sseA2*	cg1613	-200	-200	rhodanese-related sulfurtransferase		-		126
cg1633	NCgl1388	1521430	1521704	GGTGTGATTAGTCACA	2.18E-05	4.05	3.24	3.68	1.43	-	cg1633	-85; -97	-169	put. transcriptional regulator, MerR-family	predicted (Kohl et al. 2008)	-		41
cg1656	NCgl1409	1544586	1544879	TATGGCATATGTCACG	2.97E-04	5.99	3.32	5.76	3.32	*ndh*	cg1656	-28; -30; -121; -123	-220	NADH dehydrogenase type II, NDH-II	Kohl & Tauch 2008	-		156
cg1657	NCgl1410									*ufaA*	cg1657	-121	-203	put. cyclopropane fatty acid synthase		-		156
cg1665	NCgl1418	1554534	1554868	TGTATTAAAGATCACA	2.96E-05	4.72	4.10	5.14	3.04	-	cg1665	-54	-80	put. secreted protein	pred. Kohl et al. 2008, Toyoda et al. 2011	-	cg0862 (mtrA,A,exp,gtaacagatctgtttctat)	51
cg1697	NCgl1446	1585301	1585596	TGTACTGCCTCTCACA	1.90E-04	4.19	2.06	2.86	1.98	*aspA*	cg1697	+33	-8	aspartate ammonia-lyase aspartase	NEW	-		145
cg1728> < cg1730	NCgl1474> < NCgl1475	1617934	1618277	GGTGAGGTCTGCCACA	4.02E-05	4.57	2.39	2.99	2.68	-	cg1728 > < cg1730	-	+727 > < +1486	hypothetical protein, conserved > < put. secreted protease subunit, stomatin/prohibitin homolog	NEW			70
cg1735	NCgl1480	1625124	1625436	AGTGATAAACATCACA	3.65E-06	2.21	3.78	4.58	2.65	*envC*	cg1735	-133	-490	secreted cell wall-associated hydrolase	Kohl & Tauch 2009, Toyoda et al. 2011	-		10
cg1791	NCgl1526	1683784	1684164	TGTGAGTTGCATCACA	7.66E-07	5.09	7.95	10.15	4.88	*gapA (gap)*	cg1791	-245; -300	-429	glyceraldehyde-3-phosphate dehydrogenase glycolysis	Han et al. 2007, Kohl & Tauch 2008, Kohl & Tauch 2009, Toyoda et al. 2009	-	cg2092 (sigA,A,exp), cg2102 (sigB,- ,pred), cg2115 (sugR,R,exp), cg2831 (ramA,A,exp,acgggggt, gcccccgtctggggt, ccccattcgggggga)	2
cg1812	NCgl1546	1704186	1704609	TGTTCCGCTGATCACC	6.61E-04	3.14	1.91	2.84	2.36	*pyrF*	cg1812	-	-119	orotidine 5-phosphate decarboxylase	NEW	-	cg1585 (argR,R,pred)	201
cg1837	NCgl1569	1727026	1727309	TGTGCCTTGCAACACA	5.47E-06	3.24	2.29	2.72	2.34	-	cg1837	-	-54	put. holliday junction resolvase-like protein	pred. Kohl et al. 2008, Toyoda et al. 2011	OP_cg1838-35		12
cg1862	NCgl1591	1755387	1755684	TGTGCGATCTATCACA	8.01E-06	4.43	3.88	3.89	3.92	*apt*	cg1862	+91; +126	-90	adenine phosphoribosyltransferase	pred. Kohl et al. 2008, Toyoda et al. 2011	OP_cg1864-61		16
cg1895	NCgl1616	1783094	1783431	TGTGGTCTTCAACACT	3.47E-05	4.45	2.38	3.78	1.75	in (cg1895)	cg1895	-	+2116	put. secreted protein, CGP3 region	NEW			57
cg1898	NCgl1619	1788537	1788805	TGTCGCCACTGCCACA	1.33E-04	7.79	5.27	5.86	4.29	-	cg1898	-	-372	hypothetical protein CGP3 region	NEW	OP_cg1898-99		124
cg1909	-	1797026	1797319	GGTAAGTATTCAGACA	2.32E-03	3.59	2.83	3.41	1.05	-	cg1909	-	-160	hypothetical protein CGP3 region	NEW	-		230
cg1913	NCgl1631	1799335	1799591	TGTGCAGAATTTCACA	1.87E-05	4.40	2.11	3.16	2.71	-	cg1913	-	+17	hypothetical protein CGP3 region	NEW	-		36
cg1924	-	1806046	1806328	AGTAACACAGACCACA	9.14E-05	5.62	3.61	3.94	2.90	-	cg1924	-	-534	hypothetical protein CGP3 region	NEW	-		108
cg1927	NCgl1643	1807623	1807914	TGTGCCTCGTAGCACA	2.96E-05	3.52	1.07	2.68	2.95	-	cg1927	-	-362	put. molecular chaperone CGP3 region	NEW	OP_cg1926-27		53
cg1929	NCgl1645	1809376	1809668	AGTGGGAATTGGCACA	8.04E-05	6.84	7.36	8.71	3.70	*res*	cg1929	-	-210	resolvase,-family recombinase CGP3 region	pred. Kohl et al. 2008	-		97
cg1942	NCgl1656	1818200	1818503	TGTACAGTAAGTCACA	2.96E-05	6.44	5.59	8.26	2.89	-	cg1942	-40	-103	put. secreted protein CGP3 region	pred. Kohl et al. 2008	-	cg0862 (mtrA,A,exp,atatcattcctataacaat)	49

TABLE S3 (Part 5/8)│ GlxR peaks and corresponding binding sites identified with ChAP-Seq.

Locus tag (cg)	Locus tag (NCgl)	Start position[a]	End position[a]	GlxR binding site[b]	E-value	EF[c] WT$_{GlxR-TS}$ (glc)	EF[c] Δ*cyaB* $_{GlxR-TS}$ (glc)	EF[c] WT$_{GlxR-TS}$ (glc-ac)	EF[c] Δ*cyaB* $_{GlxR-TS}$ (glc-ac)	Neigboring gene(s)	Locus tag	Distance to next TSS[d]	Distance to next TLS[d]	Annotation	GlxR peak known or new[e]	operon[f]	further transcriptional regulator[f]	No.
cg1945	NCgl1658	1821008	1821281	TGTTCATCCCCTCACA	6.01E-04	3.21	2.28	2.50	2.19	in (cg1945)	cg1945	+1175	+1175	hypothetical protein, conserved CGP3 region	NEW			198
cg1966	NCgl1676	1847031	1847319	AGTGCGGTGCATCACT	9.14E-05	3.04	2.22	2.63	2.34	*cgpS*	cg1966	-379; -447; -517	-552	prophage silencing protein	pred. Kohl et al. 2008	-		113
cg1967	NCgl1677									-	cg1967	-	-78	hypothetical protein, CGP3 region		OP_cg1967-68		113
cg1972	-	1849874	1850148	TGTGCATTTCTACACA	5.29E-05	3.55	1.72	2.57	1.92	-	cg1972	-	-31	put. translation elongation factor, GTPase CGP3 region	NEW	-		82
cg1995	NCgl1702	1873481	1873791	TGTATCAGTTGCCACT	2.97E-04	3.10	2.01	2.35	1.87	in (cg1995)	cg1995	-	+4218	hypothetical protein, CGP3 region	NEW			160
cg1999	NCgl1706	1884323	1884613	TGTCTACTCTGTTACA	4.06E-04	6.38	4.23	7.17	2.31	-	cg1999	-	-511	hypothetical protein, CGP3 region	NEW	-		171
cg2035	NCgl1740	1927741	1928035	TGTCTAATATGGTACT	8.70E-04	6.09	7.74	7.49	2.98	-	cg2035	-256	-271	put. methyltransferase, CGP3 region	NEW	-		213
cg2041	NCgl1746	1933851	1934130	AGTATGCCGGATCACT	7.96E-04	9.80	8.69	10.42	4.51	-	cg2041	-689	-1155	hypothetical protein, CGP3 region	pred. Kohl et al. 2008	-		205
cg2058	-	1945696	1945994	GGTGATGGACGGCACA	4.62E-05	3.62	2.89	3.39	3.36	-	cg2058	-	-12	hypothetical protein, CGP3 region	pred. Kohl et al. 2008	-		75
cg2064	NCgl1769	1955246	1955557	CGTGAAATAGGACACA	3.47E-05	2.55	2.80	3.59	1.06	-	cg2064	-	-619	put. DNA topoisomerase I omega-protein; CGP3 region	NEW	-		65
cg2071	NCgl1816	1995412	1995693	AATGAATCCACTCACC	4.08E-03	7.58	7.35	12.25	3.97	*int2*	cg2071	-123	-275	put. phage integrase N-terminal fragment, CGP3 region	pred. Kohl et al. 2008	-		234
cg2109	NCgl1850	2029075	2029371	no motif	9.63E-01	3.11	1.90	2.97	0.97	*oxyR*	cg2109	-66	-66	hydrogen peroxide sensing regulator, Lys-family	NEW	-	cg2109 (oxyR,R,pred)	243
cg2117	NCgl1858	2041243	2041604	TGTGGCCTCAGTCACT	6.29E-05	6.86	3.25	6.50	5.45	*ptsI*	cg2117	-197; -132; -130	-225	EI enzyme, general component of PTS	Kohl & Tauch 2008, Jungwirth et al. 2013	-	cg2118 (fruR,R,exp), cg2092 (sigA,A,exp), cg2115 (sugR,R,exp)	22
cg2118	NCgl1859									*fruR*	cg2118	+108	-183	transcriptional regulator, DeoR-family		OP_cg2118-20	cg3224 (lldR,R,exp), cg2118 (fruR,R,exp), cg2092 (sigA,A,exp), cg2115 (sugR,R,exp)	22
cg2117	NCgl1858	2041674	2041942	TGTTTCGGTTGTCACA	7.23E-05	5.29	2.05	3.66	4.30	*ptsI*	cg2117	-412; -414; -479	-507	EI enzyme, general component of PTS	Kohl & Tauch 2008, Jungwirth et al. 2013	-	cg2118 (fruR,R,exp), cg2092 (sigA,A,exp), cg2115 (sugR,R,exp)	24
cg2118	NCgl1859									*fruR*	cg2118	+100	+390	transcriptional regulator, DeoR-family		OP_cg2118-20	cg3224 (lldR,R,exp), cg2118 (fruR,R,exp), cg2092 (sigA,A,exp), cg2115 (sugR,R,exp)	24
cg2118	NCgl1859	2040573	2040845	TGTGGGACTTGTCACT	5.53E-05	3.54	2.12	2.17	2.61	*fruR*	cg2118	-670	960	transcriptional regulator, DeoR-family	Kohl & Tauch 2008, Jungwirth et al. 2013	OP_cg2118-20	cg3224 (lldR,R,exp), cg2118 (fruR,R,exp,tcggaacca), cg2092 (sigA,A,exp), cg2115 (sugR,R,exp,tcggaacca)	42
cg2134	NCgl1873	2057714	2058023	GGTGGCTCCTGCCACA	1.51E-04	3.92	2.60	2.81	2.37	-	cg2134	-60	-99	put. membrane protein	NEW	-		131
cg2135	NCgl1874	2059481	2059848	TATGACGCAGACCACA	8.04E-05	3.00	2.11	2.42	2.42	*miaB*	cg2135	-325	-325	tRNA methylthiotransferase	Park et al. 2010, Kohl & Tauch 2009	-		102
cg2136	NCgl1875									*gluA*	cg2136	+7	+7	glutamate uptake system		OP_cg2136-39	cg0986 (amtR,R,exp,gcaatatctatcatgtgataggtaaatt)	102
cg2157	NCgl1892	2072640	2073015	AGTAAACTTAGCCACA	2.13E-04	3.19	2.09	2.65	2.63	*terC*	cg2157	-210; -212	+13	tellurium resistance membrane protein	NEW	-	cg2115 (sugR,R,pred)	149
cg2183	NCgl1917	2102610	2102934	TGTCTCCATTGTCACT	9.14E-05	3.92	3.04	4.19	2.90	*oppC*	cg2183	-	-85	ABC-type peptide transport system	Toyoda et al. 2011	OP_cg2181-84	cg0986 (amtR,R,exp)	109
cg2184	NCgl1918	2103502	2103846	TGTTCCCAGTGCCACA	1.69E-04	5.23	2.97	3.46	2.69	*oppD*	cg2184	-	-224	ATPase component of peptide ABC-type transport system	NEW	OP_cg2181-84	cg0986 (amtR,R,exp)	137
cg2191	NCgl1925	2113470	2113818	TGTCGCCTAAATCACA	1.12E-05	8.17	6.12	11.53	3.76	-	cg2191	-104	-104	hypothetical protein, conserved	pred. Kohl et al. 2008, Toyoda et al. 2011	-		21
cg2261	NCgl1983	2173513	2173795	TGTTAAGTGCATCACA	4.62E-05	3.12	2.92	3.08	2.11	*amtB*	cg2261	-	-201	low affinity ammonium uptake protein	Kohl & Tauch 2009	OP_cg2261-58	cg0986 (amtR,R,exp,aaattacctgttaaactatagaaaatat)	76
cg2293	NCgl2010	2209052	2209377	AGACATTGACTTCACC	8.14E-03	3.96	3.04	3.60	2.74	-	cg2293	-104	-130	put. indole-3-glycerol phosphate synthase	Toyoda et al. 2011	-		239
cg2314 > < cg2315	NCgl2030 > < NCgl2031	2228924	2229203	AGTCTGGTCTGCCACA	2.67E-04	4.91	3.63	4.34	2.81	(cg2314) > < (cg231	cg2314 > < cg2315	+1198 > < -	+1177 > < +745	put. transcriptional regulator, LacI-family > < put. ABC-typeironIII dicitrate transporter, ATPase subunit	Toyoda et al. 2011			155
cg2324	NCgl2038	2237135	2237409	TATGTCTGACAACACT	6.01E-04	3.21	3.29	3.20	2.03	-	cg2324	+10	+7	hypothetical protein	NEW	OP_cg2323-24		197
cg2361	NCgl2070	2276036	2276342	TGTTATCCTTGTCACA	3.47E-05	4.31	3.53	4.79	2.81	*divIVA*	cg2361	-126; -260; -280	-360	cell division initiation protein	Kohl & Tauch 2009	-		59
cg2380	NCgl2088	2296822	2297130	TATGCCAATAACGACA	1.99E-03	1.72	3.15	2.69	1.23	-	cg2380	-39; -47	-88	put. membrane protein	Toyoda et al. 2011	-	cg0876 (sigH,A,exp)	229
cg2402	NCgl2108	2320901	2321183	GGTGATTAATGTCACA	8.01E-06	3.26	4.65	4.36	3.45	*nlpC*	cg2402	-254; -295	-497	put. secreted cell wall peptidase	Kohl & Tauch 2008	-	cg0862 (mtrA, ,exp,ataaggttacgaaaccgca), cg0709 (cgtR7,R,exp)	18
cg2404	NCgl2110	2324785	2325080	TGTCGCCTGCATCACC	1.90E-04	5.97	3.56	5.46	3.50	*qcrA (qcrA1)*	cg2404	-	-650	cytochrome bc1 complex, Rieske iron-sulfur protein	NEW	OP_cg2406-03	cg3247 (hrrA,A,exp), cg0309 (sigC,A, exp.)	142
cg2404	NCgl2110	2324430	2324672	TGTCGCCTGCATCACC	1.90E-04	5.45	1.61	2.30	3.14	*qcrA (qcrA1)*	cg2404	-	-313	cytochrome bc1 complex, Rieske iron-sulfur protein	Toyoda et al. 2011	OP_cg2406-03	cg3247 (hrrA,A,exp), cg0309 (sigC,A, exp.)	143
cg2406	NCgl2112	2325943	2326265	TGAGAGACACGTCACA	5.29E-05	4.90	3.75	5.86	3.42	*ctaE*	cg2406	-274; -277	-277	cytochrome aa3 oxidase, subunit 3	Kohl & Tauch 2008	OP_cg2406-03	cg3247 (hrrA,A,exp), cg0444 (ramB,R,pred,aaaagtttgcgaa), cg0309 (sigC,A,exp)	79
cg2409	NCgl2115	2328003	2328318	TGTATGCCACGTCACA	1.87E-05	6.59	5.67	8.80	2.98	*ctaC*	cg2409	-30; -157; -161; -163	-216	cytochrome aa3 oxidase, subunit 2	Kohl & Tauch 2008, Toyoda et al 2011	OP_cg2409-08	cg0876 (sigH,A,exp)	34
cg2410	NCgl2116									*ltsA*	cg2410	-	-304	glutamine-dependent amidotransferase		-		34
cg2430	NCgl2134	2350440	2350746	AGTGATTTGAACCACA	2.53E-05	3.19	3.24	3.35	0.00	-	cg2430	+26	-47	hypothetical protein	pred. Kohl et al. 2008, Toyoda et al. 2011	-		48
cg2437	NCgl2139	2354949	2355229	AGTGTTGCTGATCACT	1.17E-04	3.70	2.93	3.41	3.13	*thrC*	cg2437	-101	-101	threonine synthase	pred. Kohl et al. 2008, Toyoda et al. 2011	-	cg2092 (sigA,A,exp)	120
cg2438	NCgl2140									-	cg2438	+2	-41	hypothetical protein		-		120
cg2460 > < cg2461	NCgl2160 > < NCgl2161	2376667	2377030	TATGATCTACACCACA	6.09E-05	2.91	2.23	3.09	2.32	-	cg2460 > < cg2461	+1194 > < -	+1194 > < +475	put. membrane protein > < transposase	Toyoda et al. 2011			88

TABLE S3 (Part 6/8)| GlxR peaks and corresponding binding sites identified with ChAP-Seq.

Locus tag (cg)	Locus tag (NCgl)	Start position[a]	End position[a]	GlxR binding site[b]	E-value	EF[c] WT$_{GlxR-TS}$ (glc)	EF[c] Δ*cyaB* $_{GlxR-TS}$ (glc)	EF[c] WT$_{GlxR-TS}$ (glc-ac)	EF[c] Δ*cyaB* $_{GlxR-TS}$ (glc-ac)	Neigboring gene(s)	Locus tag	Distance to next TSS[d]	Distance to next TLS[d]	Annotation	GlxR peak known or new[e]	operon[f]	further transcriptional regulator[f]	No.
cg2464	NCgl2165	2379477	2379771	TGAGAGAAACATCACA	9.14E-05	5.82	4.27	6.57	3.13	-	cg2464	-246	-330	hypothetical protein	Toyoda et al. 2011	-		106
cg2466	NCgl2167									*aceE*	cg2466	-220; -268	-338	pyruvate dehydrogenase, E1 subunit of PDHc		-	cg0444 (ramB,A,exp,aaaactttgcaaa), cg2092 (sigA,A,exp)	106
cg2470	NCgl2170	2385443	2385729	TGAGACATTTCACATA	1.34E-03	11.09	7.69	8.33	3.78	-	cg2470	+7	-81	secreted ABC transporter substrate-binding protein	NEW	OP_cg2470-67		217
cg2471	NCgl2172									-	cg2471	-202	-205	put. protein		-		217
cg2480	NCgl2180	2393676	2393986	TGTCGACACCGTCACA	1.69E-04	3.13	2.02	2.08	2.26	-	cg2480	-484; -737	-737	hypothetical protein	NEW	-		139
cg2496 > < cg2497	NCgl2195	2408847	2409185	GGTCTCTTCGGTCACT	5.46E-04	2.59	2.48	3.19	2.93	-	cg2496 > < cg2497	+2090 > < -	+2090 > < +1213	put. secreted protein	NEW	-		192
cg2497	NCgl2196	2409768	2410123	AGTGAGATCCCCCACA	3.47E-05	3.92	2.65	2.75	3.06	in (cg2497)	cg2497	-	+250	hypothetical protein	NEW			62
cg2521	NCgl2216	2430262	2430557	TGTATCTAAATTCACA	5.29E-05	8.57	6.11	9.85	4.93	*fadD15*	cg2521	-292	-404	long-chain fatty acid CoA ligase	NEW	OP_cg2521-20		77
cg2546	NCgl2236	2457005	2457297	AGTGGATTACGTCACA	8.01E-06	3.28	2.13	1.77	1.27	-	cg2546	-113	-134	put. secondary C4-dicarboxylate transporter	pred. Kohl et al. 2008, Toyoda et al. 2011	OP_cg2546-45		17
cg2557	NCgl2245	2466921	2467200	TATGAAAGTTCGCACA	7.96E-04	4.47	4.05	3.81	2.58	-	cg2557	-	-77	put. secondary Na+/bile acid symporter	NEW	-		207
cg2558	NCgl2246									-	cg2558	-73	-73	put. protein, related to aldose 1-epimerase		-		207
cg2564	NCgl2252	2476186	2476502	GGTGATTCTAGTCACT	1.17E-04	9.23	9.19	12.04	4.02	-	cg2564	-207	-265	hypothetical protein	pred. Kohl et al. 2008, Toyoda et al. 2011	-		118
cg2565	NCgl2253									-	cg2565	-83	-115	hypothetical protein		-		118
cg2593 > < cg2594	- > < NCgl2279	2503806	2504093	TGACGCTTAAGTCACA	3.66E-04	3.41	2.23	3.03	2.43	(cg2593) > < *rpmA*	cg2593 > < cg2594	+526 > < -	+447 > < +265	put. secreted or membrane protein > < 50S ribosomal protein L27	NEW			166
cg2610	NCgl2294	2519892	2520186	GGTGTGGTGAGTCACT	9.14E-05	13.90	11.80	17.52	6.24	-	cg2610	-	-91	put. ABC-type transport system	Jungwirth et al. 2013	-		103
cg2611	NCgl2295									*hscA*	cg2611	-147	-147	molecular chaperone, HSP70-family		-		103
cg2615	NCgl2299	2524846	2525135	TATGGCGTAGGTCATA	4.49E-04	9.75	5.23	7.54	5.30	*vanR*	cg2615	-125	-125	transcriptional regulator, PadR-family	Kohl & Tauch 2008, Jungwirth et al 2013	-		178
cg2616	NCgl2300									*vanA*	cg2616	-	-59	vanillate demethylase, oxygenase subunit		OP_cg2616-18	cg2615 (vanR,R,exp,taaactaactaagagttta), cg2092 (sigA,A,exp)	178
cg2636	NCgl2319	2544816	2545061	GATGATTCAGGCCACA	6.01E-04	5.66	4.61	4.21	2.52	*catA1 (catA)*	cg2636	-	-108	catechol 1,2-dioxygenase	Kohl & Tauch 2008	-	cg1120 (ripA,R,exp,tgaagcggtgtgtgacat), cg2641 (benR,A,pred)	195
cg2637	NCgl2320									*benA*	cg2637	-	-311	benzoate 1,2-dioxygenase α subunit		OP_cg2637-40	cg2641 (benR,A,pred)	195
cg2642	NCgl2325	2552384	2552680	GGTGATGTGATTCACA	3.47E-05	4.35	3.17	3.46	2.53	*benK1 (benK)*	cg2642	-	-56	benzoate transport protein	Toyoda et al. 2011	OP_cg2642-43	cg2641 (benR,A,pred)	58
cg2642	NCgl2325	2553033	2553285	TGTTCCTCCTGCCACT	5.50E-04	3.26	1.73	2.32	2.10	*in benK1 (benK)*	cg2642	-	+573	benzoate transport protein, MFS transporter, AAHS family	NEW			193
cg2651	NCgl2333	2560699	2560992	TGTACAATAACACACT	3.66E-04	2.89	2.25	3.06	1.05	-	cg2651	-229	-229	put. protein-fragment	NEW	-		168
cg2665	NCgl2342	2571134	2571446	TGTCACTTTCTTCACA	1.87E-05	4.43	3.28	4.41	2.62	-	cg2665	-	-15	hypothetical protein	pred. Kohl et al. 2008	-		35
cg2666	NCgl2343									-	cg2666	-187	-213	hypothetical protein		-		35
cg2678	NCgl2353	2582586	2582892	GGTGACATTATTCACA	1.87E-05	10.03	5.87	8.05	5.79	-	cg2678	-312	-364	put. ABC-type transport systems	NEW	OP_cg2678-74	cg2766 (R,pred), cg3253 (mcbR,R,pred,tataccgatcagtcta)	32
cg2692	NCgl2365	2594933	2595246	CGTCTCTTTGCTCACA	4.06E-04	5.26	3.39	4.34	3.12	-	cg2692	+28	-50	put. thioesterase	NEW	OP_cg2692-91		172
cg2695	NCgl2368	2596754	2597196	TGTCCTTGCCGTCACA	2.13E-04	3.040	2.17	2.08	2.21	in (c2695)	cg2695	+666; +669	+630	put. ABC-type transport system, ATPase component	NEW			150
cg2699	NCgl2370	2600743	2601017	TGTGTGAAGCCCCACA	9.65E-06	4.89	3.52	4.05	3.05	*ctiP*	cg2699	-108	-108	copper transport and insertion protein	NEW	-		20
cg2700	NCgl2371									*phoB*	cg2700	-551	-542	alkaline phosphatase		-		20
cg2700 > < cg2701	NCgl2371 > < NCgl2372	2603255	2603478	TGTGTTGCAGGTCACA	5.76E-07	6.02	3.81	3.36	0.00	*phoB* > < *musI*	cg2700 > < cg2701	+1919 > < +1203	-1919 > < +1203	alkaline phosphatase > < put. membrane protein	NEW			1
cg2700 > < cg2701	NCgl2371 > < NCgl2372	2603276	2603715	TGTGAGCCACGCCACT	2.48E-06	5.88	3.50	7.90	2.91	*phoB* > < *musI*	cg2700 > < cg2701	+2152 > < +961	+2161 > < +961	alkaline phosphatase > < put. membrane protein	NEW			7
cg2708	NCgl2377	2610517	2610832	AGTGAAGTGAGTCACT	3.47E-05	3.94	2.78	3.17	2.48	*musK (msiK1)*	cg2708	+27	-64	ABC-type maltose transport system	Jungwirth et al. 2013	OP_cg2708-07		61
cg2732	NCgl2399	2630319	2630629	GGTGTGTATGGTCACA	6.09E-05	4.77	3.82	3.35	4.65	*gntV (gntK)*	cg2732	-	-129	put. gluconokinase	Letek et al. 2006, Kohl & Tauch 2008	-	cg2092 (sigA,A,exp), cg2783 (gntR1,R,exp,tatgatagtaccaat), cg1935 (gntR2,R,exp,tatgatagtaccaat)	84
cg2739	NCgl2406	2636559	2636851	AGTGAAATCACACACA	6.09E-05	3.42	2.69	2.22	1.50	-	cg2739	-49	-149	put. permease of the major facilitator superfamily	pred. Kohl et al. 2008	OP_cg2739-38		87
cg2740	NCgl2407									-	cg2740	-	-132	put. membrane protein		-		87
cg2741	NCgl2408	2637721	2638035	TGCATAGTTTGTCACT	4.66E-03	2.90	2.77	3.29	2.85	-	cg2741	-160; -156	-286	hypothetical protein	NEW	-		236
cg2743	NCgl2409	2647825	2648109	GGTGAACAAGGCCACA	5.29E-05	6.53	5.09	4.83	3.98	*fas-IA*	cg2743	-155	-347	fatty acid synthase, Fas-I-type	Kohl & Tauch 2008	-	cg2737 (fasR,R,exp,ccgaaatagatgactaaaccct catgttt)	78
cg2748	NCgl2412	2650220	2650497	GGTGCAGTTGGTCACC	4.06E-04	5.08	4.58	6.33	2.92	-	cg2748	-56	-56	put. membrane protein, conserved	NEW	-		173
cg2780	NCgl2437	2672843	2673129	TGTGAACCCCTTCACA	2.53E-05	5.42	4.33	4.87	3.03	*ctaD*	cg2780	-114; -116; -118; -170;	-228	cytochrome aa3 oxidase	Kohl & Tauch 2008	-	cg3247 (hrrA,exp), cg3247 (cgtR11,A,exp)	46
cg2781	NCgl2438	2674372	2674631	CGTGATCTTAGTCACT	1.03E-04	3.80	4.47	5.25	2.41	*nrdF*	cg2781	-83; -122	-187	ribonucleotide-diphosphate reductase β subunit	Kohl & Tauch 2008	-		115
cg2782	NCgl2439									*ftn*	cg2782	-246; -279	-279	ferritin		-	cg2092 (sigA,A,exp), cg2109 (oxyR, ,exp,tttattgccctaa,), cg2103 (dtxR,R,exp,ttatgctgcgctaacctat)	115
cg2781	NCgl2438	2673427	2673772	AGTCTCCTTCGCGACA	6.01E-04	0.80	1.15	3.17	0.00	-	cg2781	-735; -774	-670	ribonucleotide-diphosphate reductase β subunit	Kohl & Tauch 2008			199
cg2785	NCgl2442	2677174	2677493	TGTCCGTAGACACACA	3.66E-04	5.03	5.50	4.90	1.47	-	cg2785	-	-167	put. membrane protein	NEW	-		165
cg2797	NCgl2451	2685869	2686208	TGTTCAAAGCTTCACA	4.96E-04	4.17	3.15	3.15	2.69	-	cg2797	-	-224	hypothetical protein	NEW	-	cg2103 (dtxR,R,exp)	183
cg2804	NCgl2457	2691030	2691325	TGTATGAAACCTCACT	1.33E-04	8.11	5.17	7.30	4.42	*tnp21a*	cg2804	-	-476	transposase	Toyoda et al. 2011	-		123

TABLE S3 (Part 7/8) | **GlxR peaks and corresponding binding sites identified with ChAP-Seq.**

Locus tag (cg)	Locus tag (NCgl)	Start position[a]	End position[a]	GlxR binding site[b]	E-value	EF[c] WT$_{\text{GlxR-TS}}$ (glc)	EF[c] Δ*cyaB* $_{\text{GlxR-TS}}$ (glc)	EF[c] WT$_{\text{GlxR-TS}}$ (glc-ac)	EF[c] Δ*cyaB* $_{\text{GlxR-TS}}$ (glc-ac)	Neigboring gene(s)	Locus tag	Distance to next TSS[d]	Distance to next TLS[d]	Annotation	GlxR peak known or new[e]	operon[f]	further transcriptional regulator[f]	No.
cg2810	NCgl2463	2699482	2699804	GGTTAATTTGGTCACA	2.97E-04	3.35	2.50	3.52	1.04	*cynT*	cg2810	-	-77	high affinity cysteine importer	pred. Kohl et al. 2008, Toyoda et al. 2011	-	cg0156 (cysR,R,pred), cg2092 (sigA,A,exp), cg0876 (sigH,A,exp)	159
cg2811	NCgl2464	2700486	2700775	CGTCTGGTTAGTCACA	3.66E-04	6.25	5.19	5.93	3.01	in (cg2811)	cg2811	-	+1840	put. ABC-type transport system, involved in lipoprotein release, ATPase component	NEW			164
cg2824	NCgl2468	2711131	2711482	TGTAATCCAGCACACA	4.02E-05	4.13	2.64	3.05	2.34	-	cg2824	-	-491	put. SAM-dependent methyltransferase	Jungwirth et al. 2013	-		73
cg2837	NCgl2477	2726483	2726779	TGTGAAGTCTAACACT	4.02E-05	4.19	2.68	2.70	2.41	*sucC*	cg2837	-	-94	succinyl-CoA synthetase subunit β	Kohl & Tauch 2009, Han et al. 2008	OP_cg2837-36	cg2831 (ramA,A,exp), cg0444 (ramB,R,pred,tttgcaaagttta), cg2092 (sigA,A,exp)	72
cg2837	NCgl2477	2727036	2727290	TGTGCAGCATTTCACT	4.02E-05	3.53	2.10	2.25	2.10	*sucC*	cg2837	-	-574	succinyl-CoA synthetase subunit β	Han et al. 2008, Kohl & Tauch 2009	OP_cg2837-36	cg2831 (ramA,A,exp), cg0444 (ramB,R,pred,tttgcaaagttta), cg2092 (sigA,A,exp)	74
cg2842	NCgl2482	2732520	2732779	GATGAATTCGCACACA	1.71E-03	2.93	3.02	2.22	0.79	*phoU*	cg2842	+35	+35	phosphate uptake regulator	Toyoda et al. 2011	-		226
cg2843	NCgl2483	2733426	2733695	GGTCTGATCGGACACA	4.49E-04	4.45	3.72	3.79	2.68	in *pstB*	cg2843	-	+640	ABC-type phosphate transport system, ATPase component	NEW			179
cg2898	NCgl2526	2785006	2785289	TGTTGATTCCCACACC	1.85E-03	3.18	2.00	2.13	2.10	in (cg2898)	cg2898	-	+379	put. 3-ketosteroid dehydrogenase	NEW			227
cg2925	NCgl2553	2811766	2812103	TGTACAATTCGCCACA	1.33E-04	8.58	8.69	9.23	4.36	*ptsS*	cg2925	-63	-124	sucrose-specific EIIABC component EIISuc of PTS	Toyoda et al. 2011	-	cg0444 (ramB,R,exp), cg2092 (sigA,A,exp), cg2115 (sugR,R,exp,tcggacaca), cg2783 (gntR1,A,exp), cg1935 (gntR2,A,exp)	122
cg2936	NCgl2561	2820373	2820686	TGAGCATAGCGTCACA	6.01E-04	6.13	5.16	5.08	4.05	*nanR*	cg2936	-230	-255	transcriptional regulator, GntR-family	NEW	OP_cg2936-35	cg2936 (nanR,R,exp)	194
cg2937	NCgl2562									*siaE*	cg2937	+45	-54	ABC-Transporter for sialic acid		OP_cg2937-38	cg2936 (nanR,R,exp)	194
cg2953	NCgl2578	2837393	2837726	TGTACCTTTAGTTACA	2.13E-04	5.39	4.55	3.72	1.69	*vdh*	cg2953	-18	-46	vanillin dehydrogenase	Kohl & Tauch 2008	-		147
cg2954	NCgl2579	2838418	2838709	TGTACTGACTGGCACT	7.96E-04	3.49	2.78	2.70	2.88	*bca (cynT)*	cg2954	-47	-47	carbonic anhydrase, carbonate dehydratase	Toyoda et al. 2011	-	cg2831 (ramA,R,exp)	210
cg2955	NCgl2580									*mutY*	cg2955	-18	-21	A/g-specific adenine glycosylase		-		210
cg2966	NCgl2588	2849547	2849937	TGTAGTTCAGATCACA	5.29E-05	4.64	2.72	3.39	3.10	-	cg2966	-	-74	put. phenol 2-monooxygenase	Kohl & Tauch 2008, Jungwirth et al. 2013	-	cg2965 (A,exp)	81
cg2999	NCgl2615	2879656	2879968	TGTGTGCTGCCTCACA	2.48E-06	7.87	5.48	6.00	4.26	-	cg2999	-77	-137	put. ferredoxin reductase	pred. Kohl et al. 2008, Toyoda et al. 2011	-		6
cg3000	NCgl2616									-	cg3000	-75	-119	put. rhodanese-related sulfurtransferase		-		6
cg3022	NCgl2632	2908679	2909092	AGTGAATCAAGACACT	9.14E-05	3.48	2.73	2.75	2.90	-	cg3022	-35	-254	put. acetyl-CoA acetyltransferase	pred. Kohl et al. 2008	-		112
cg3030	NCgl2639	2917792	2918090	AGTGCACCACGAGACA	3.66E-04	3.36	2.45	3.23	1.41	-	cg3030	-	-359	put. hydrolase or acyltransferase α/β hydrolase superfamily	NEW	OP_cg3031-30		167
cg3041	NCgl2650	2928359	2928637	AGTCGCATTCAACACA	1.51E-04	3.27	2.08	2.44	1.96	-	cg3041	-	-196	put. ABC-type multidrug transport system	NEW	OP_cg3043-40		135
cg3043	NCgl2652	2930106	2930403	TGATGTATACAGCACA	1.71E-03	3.24	2.36	2.83	1.30	-	cg3043	-505	-505	NTP pyrophosphohydrolase/oxidative damage repair enzyme	NEW	OP_cg3043-40		225
cg3048	NCgl2657	2937788	2938072	TGTGCCTCCTGGCACT	1.17E-04	14.56	9.45	12.69	6.47	*pta*	cg3048	-	-62	phosphotransacetylase	Jungwirth et al. 2013	OP_cg3048-47	cg2092 (sigA,A,exp), cg2831 (ramA, ,exp,accccattaatggggggt),	117
cg3049	NCgl2658									*fprA (fpr1)*	cg3049	-340	-452	put. ferredoxin/ferredoxin-NADP reductase		-		117
cg3061	NCgl2668	2949950	2950260	TGTTGCATATGATACA	1.51E-04	6.10	4.07	5.11	1.49	*cgtR6*	cg3061	-179	-233	two component response regulator	NEW	OP_cg3061-60		130
cg3091	NCgl2693	2974964	2975268	AGTTTGTTGGCTTACA	1.34E-03	4.50	5.40	5.08	1.40	-	cg3091	-	-415	hypothetical protein	NEW	OP_cg3090-91		218
cg3092	NCgl2694	2977156	2977490	TGTTATTTATTGCACA	9.14E-05	3.62	2.37	2.49	2.10	in (cg3092)	cg3092	+750	+750	put. 2-polyprenylphenol hydroxylase or related flavodoxin oxidoreductase	NEW			111
cg3096	NCgl2698	2981595	2981870	TGTGCGCGTTGTCACA	1.33E-05	13.71	9.54	12.32	7.26	*ald*	cg3096	+19	-75	aldehyde degyhdrogenase	Kohl & Tauch 2009, Jungwirth et al. 2013, Subhadra & Lee 2013	-	cg2831 (ramA,A,exp), cg0444 (ramB,R,exp,'ataacttttgaaa), cg2092 (sigA,A,exp)	27
cg3107	NCgl2709	2996691	2996976	TGTAATTTAAGGCACA	1.87E-05	10.89	8.47	9.26	6.12	*adhA*	cg3107	-	-83	Zn-dependent alcohol dehydrogenase	Kohl & Tauch 2008, Jungwirth et al. 2013, Subhadra & Lee 2013	-	cg2092 (sigA,exp), cg0876 (sigH,A,exp), cg0146 (atlR,R,exp,tcaacaaccg), cg0444 (ramB, ,exp,agcaatttgccaa), cg2831 (ramA,A,exp)	31
cg4002	-									-	cg4002	-	-288	hypothetical protein		-		31
cg3112	NCgl2713	2999688	3000019	AGTTCCACACCATACT	3.10E-03	3.17	2.71	2.83	2.34	*cysZ*	cg3112	-	-474	sulfate transporter	NEW	OP_cg3118-12	cg2103 (dtxR,R,exp), cg2092 (sigA,A,exp), cg0156 (cysR,A,pred), cg3253 (mcbR,R,pred)	233
cg3122	NCgl2722	3009012	3009296	CGTAATGTGGGTCACA	1.69E-04	3.20	2.09	2.45	2.01	*phnB1*	cg3122	+8	-41	put. protein	pred. Kohl et al. 2008, Toyoda et al. 2011	-		138
cg3124	NCgl2723									-	cg3124	-18	-40	hypothetical protein		-		138
cg3127	NCgl2726	3012797	3013206	GGAGTCCTAGCTCACA	4.06E-04	9.46	5.88	6.96	5.03	*tctC*	cg3127	-	-296	citrate uptake transporter	Kohl & Tauch 2009	OP_cg3127-25	cg2092 (sigA,A,exp), cg0090 (citB,A,exp)	170
cg3155	NCgl2751	3037647	3037931	TGCGCACTACATCACA	7.96E-04	4.18	2.81	3.14	3.04	*dcd*	cg3155	-405	-405	deoxycytidine triphosphate deaminase	pred. Kohl et al. 2008	-		208
cg3156	NCgl2752									*htaD*	cg3156	-	-357	secreted heme transport-associated protein		-	cg2103 (dtxR,R,exp,taaggcaagcctaaattag)	208
cg3157	NCgl2753	3041008	3041338	TGTGCGAATCGCCACT	8.04E-05	3.85	2.29	2.24	2.34	-	cg3157	-530	-530	put. secreted protein	Toyoda et al. 2011	-		99
cg3169	NCgl2765	3053790	3054071	TGAGACAACGGACACA	2.13E-04	4.57	3.73	4.80	3.80	*pck*	cg3169	-24; -55	-92	phosphoenolpyruvate carboxykinase GTP	Kohl & Tauch 2008, Han et al. 2008	-	cg0196 (iolR,R,exp,acacttaaca), cg0444 (ramB, ,pred,ttttcaaagtatt), cg2831 (ramA,A,pred,tggggtaacgtgggga), cg2092 (sigA,A,exp)	148

TABLE S3 (Part 8/8)| **GlxR peaks and corresponding binding sites identified with ChAP-Seq.**

Locus tag (cg)	Locus tag (NCgl)	Start position[a]	End position[a]	GlxR binding site[b]	E-value	EF[c] WT$_{GlxR\text{-}TS}$ (glc)	EF[c] Δ*cyaB* $_{GlxR\text{-}TS}$ (glc)	EF[c] WT$_{GlxR\text{-}TS}$ (glc-ac)	EF[c] Δ*cyaB* $_{GlxR\text{-}TS}$ (glc-ac)	Neigboring gene(s)	Locus tag	Distance to next TSS[d]	Distance to next TLS[d]	Annotation	GlxR peak known or new[e]	operon[f]	further transcriptional regulator[f]	No.
cg3170	NCgl2766	3054542	3054815	TGTGCGCTCGATCACT	5.29E-05	4.78	2.67	3.14	3.60	-	cg3170	-	-52	put. tellurite resistance protein or related permease	Jungwirth et al. 2013	-		80
cg3174	NCgl2769	3058079	3058349	TGTTTGTTTTCCCACA	1.90E-04	3.77	2.67	2.79	2.24	in *mmpL1*	cg3174	-	+909	exporter of the MMPL-family	NEW			146
cg3187	NCgl2780	3078011	3078313	AGTCGCCCACAACACC	8.70E-04	4.53	3.69	3.41	2.29	in *aftB*	cg3187	+595	+595	arabinofuranosyltransferase	NEW			214
cg3194	NCgl2786	3085035	3085340	AGTGTCGTGACTCACT	4.02E-05	7.31	5.84	5.68	3.90	-	cg3194	-222	-222	put. membrane-associated PA-phosphatase	Jungwirth et al. 2013	OP_cg3194-93		67
cg3195	NCgl2787									-	cg3195	-	-26	put. flavin-containing monooxygenase FMO		-	cg2910 (ipsA,A,exp,acaggatccatccagt)	67
cg3203	NCgl2795	3096357	3096690	TGCCTCATTTACCACT	5.31E-03	6.24	5.32	5.52	1.40	in (cg3203)	cg3203	+227	+223	hypothetical protein, conserved	NEW	-	cg3202 (farR,R,pred)	237
cg3215	NCgl2807	3107540	3107891	AGTAATCTGCATCACA	6.09E-05	1.18	1.42	3.27	0.00	*glpQ1*	cg3215	-82; -76	-112	put. glycerophosphoryl diester phosphodiesterase 1	Letek et al. 2006, Kohl & Tauch 2008	OP_cg3215-14		89
cg3216	NCgl2808									*gntP*	cg3216	-	-311	gluconate permease, gluconate:H+ symporter GntP-family		-	cg2092 (sigA,A,exp), cg2783 (gntR1,R,exp,tttgatcatactaat), cg1935 (gntR2,R,exp,tttgatcatactaat)	89
cg3226	NCgl2816	3118026	3118304	TGTAAGGCGTGTCACC	1.69E-04	7.13	4.76	5.58	3.34	-	cg3226	-17;-21	-90	L-lactate permease, operon with lldD, MFS-type	Kohl & Tauch 2008, Jungwirth et al. 2013	OP_cg3226-27	cg2831 (ramA,R,exp), cg2092 (sigA,A,exp), cg3224 (lldR,R,exp)	136
cg3247	NCgl2834	3136728	3137037	TGAATGTTTCGCCACA	1.34E-03	3.58	2.60	2.41	1.15	*hrrA (cgtR11)*	cg3247	-352	-434	two component response regulator	NEW	-	cg2103 (dtxR,R,exp,atgagtaaggctagactaa), cg2200 (chrA,R,exp,aaggctagactaaagtacgattcat)	220
cg3255	NCgl2842	3143307	3143606	TGAGGCTTTTGACACT	4.96E-04	3.16	3.17	2.63	2.73	*uspA3*	cg3255	-63; -65	-131	universal stress protein no. 3	NEW	-		185
cg3313	NCgl2884	3189069	3189309	TATTCTCTACAGCACA	1.58E-03	3.57	1.29	2.57	1.25	*pbp1b (mcrB)*	cg3313	+6; +202	-51	membrane carboxypeptidase	NEW	OP_cg3313-11		223
cg3332	NCgl2902	3205746	3206075	GGTACTCTGCGTTACT	2.50E-03	3.91	3.01	2.95	2.40	in *qor3*	cg3332	+329	+329	put. NADPH:quinone oxidoreductase	NEW			231
cg3351	NCgl2920	3226611	3226916	TATGTTCGAAGTCACA	1.33E-04	3.55	2.64	2.54	1.32	*nagI (genD)*	cg3351	-	-114	gentisate 1,2-dioxygenase	Kohl & Tauch 2008, Chao & Zhou 2014	OP_cg3351-49	cg3352 (genR, ,exp,attccacatagcggaat)	128
cg3352	NCgl2921	3227576	3227889	GGTGAGCCAAGTTACA	1.17E-04	6.76	4.59	4.48	3.87	*nagR (genR)*	cg3352	-	-43	transcriptional regulator, IclR-family	Kohl & Tauch 2008, Jungwirth et al. 2013, Chao & Zhou 2014	-	cg3352 (genR,R,exp,attctggtgcgtgtgat)	119
cg3353	NCgl2922									*nagT (genK)*	cg3353	-	-56	gentisate transporter, MFS-type		OP_cg3353-54	cg3352 (genR,A,exp,tttccagatagcggaat)	119
cg3382	NCgl2949	3255510	3255816	AGTGGACTTCCACACA	8.04E-05	4.69	5.90	3.16	2.46	-	cg3382	-335	'-335	put. dipeptide/tripeptide permease	Jungwirth et al. 2013	-		98
cg3387	NCgl2953	3260058	3260546	AGTAACCCACAACACA	7.03E-05	8.86	10.38	10.04	3.48	*iolT2*	cg3387	-52	-317	myo-Inositol transporter 2	Kohl & Tauch 2008, Jungwirth et al. 2013	OP_cg3387-85	cg3388 (A,pred)	93
cg3388	NCgl2954									*ihtR*	cg3388	-84	-108	put. transcriptional regulator, IclR-family		-		93
cg3393	NCgl2959	3267837	3268141	TGTACCACTCATCACA	6.09E-05	3.47	2.50	2.22	2.27	in *phoC*	cg3393	-	+1341	put. secreted phosphoesterase	NEW			86
cg3413	NCgl2977	3289998	3290261	TGATTGGTTCGTCACA	8.70E-04	7.68	7.03	7.26	4.81	*azlC*	cg3413	-	-132	branched-chain amino acid permease azaleucine resistance	Toyoda et al. 2011	OP_cg3415-12		212
cg3417	NCgl2980	3291726	3292103	GGTGAGCTTTCAGACA	2.97E-04	2.56	3.68	2.83	2.94	-	cg3417	-531	-970	put. NTP pyrophosphohydrolase	NEW	OP_cg3417-18		161
cg3428	NCgl2990	3306926	3307262	TGTTCGGTGCGCCACT	4.06E-04	3.63	2.65	2.46	2.48	*gidB*	cg3428	-620; -623	-660	glucose-inhibited division protein B	NEW	OP_cg3428-25		176
-	NCgl1806*[m]	1986698	1986947	AATGAATCCACTCACC	4.08E-03	5.94	0.00	8.52	0.00	-	NCgl1806	-	-254	phage integrase	NEW			235

a: Reference genome sequence BA000036.3 of *C. glutamicum* ATCC13032 (Ikeda & Nakagawa 2003)

b: motif was detected by using the program MEME-ChIP with the DNA fragment of the detected GlxR peaks as input sequences; the 16 bp sequence shows the most probable GlxR binding site within this sequences

c: enrichment factor (EF) of ChAP-Seq experiments of normalized peak heights

d: distance counted from the center of the GlxR binding site to the start of the TSS or TLS (counting includes the fist base of TSS or TLS); if not other mentioned information of TSS was taken from Pfeifer-Sancar et al. 2013; for some genes several TSS were identified

e: if GlxR peak is previously described, the respective literature is mentioned; if the site is only found in our ChAP-Seq results it is described as 'NEW'

f: Information taken from CoryneRegNet 7.0 (Parise et al. 2021)

g: Beckers et al. 2001, doi: 10.1099/00221287-147-11-2961

h: Brocker et al. 2009, doi: 10.1128/JB.00113-09

i: Klaffl et al. 2013, doi: 10.1128/jb.00265-13

k: Zhu et al. 2020, doi: 10.3389/fmicb.2020.544045

l: Plassmeier et al. 2012, DOI: 10.1016/j.jbiotec.2011.09.009

m: only found in genome of *C. glutamicum* ATCC13032 genome (Ikeda & Nakagawa 2003) as phage regione lacks in BX927147 *C. glutamicum* ATCC13032 genome (Kalinowski et al 2003)

n: No. refering from lowest to highest E-value

TABLE S4 (Part 1/3)

(iii) GlxR binding sites (n = 10) located within intergenic regions of two convergently transcribed genes

Gene loci (cg)	Gene name	Gene locus (NCgl)	EF in $WT_{GlxR-TS}$ (glc)[a]	Start position[b]	End position[b]	GlxR binding site[c]	E-value	GlxR peak known or new[f]	No.[a]
cg0054 > < cg0055	cg0054 > < *crgA*	NCgl0038 > < NCgl0039	5.05	39981	40261	TGACTGCCGCAGCACA	3.10E-03	NEW	232
cg1608 > < cg1609	*xerD* > < cg1609	NCgl1364 > < NCgl1365	3.34	1496565	1496868	TGAGCCCCGCGCCACA	4.49E-04	NEW	180
cg1611 > < cg1612	*scpA* > < cg1612	NCgl1367 > < NCgl1368	3.19	1500579	1500875	TGTAGCTTAGGTCACT	2.35E-05	Toyoda et al. 2011	43
cg1728 > < cg1730	cg1728 > < cg1730	NCgl1474 > < NCgl1475	4.57	1617934	1618277	GGTGAGGTCTGCCACA	4.02E-05	NEW	70
cg2314 > < cg2315	cg2314 > < cg2315	NCgl2030 > < NCgl2031	4.91	2228924	2229203	AGTCTGGTCTGCCACA	2.67E-04	Toyoda et al. 2011	155
cg2460 > < cg2461	cg2460 > < cg2461	NCgl2160 > < NCgl2161	2.91	2376667	2377030	TATGATCTACACCACA	6.09E-05	Toyoda et al. 2011	88
cg2496 > < cg2497	cg2496 > < cg2497	NCgl2195 > < NCgl2196	2.59	2408847	2409185	GGTCTCTTCGGTCACT	5.46E-04	NEW	192
cg2593 > < cg2594	cg2593 > < *rpmA*	- > < NCgl2279	3.41	2503806	2504093	TGACGCTTAAGTCACA	3.66E-04	NEW	166
cg2700 > < cg2701	*phoB* > < *mus*	NCgl2371 > < NCgl2372	6.02	2603255	2603478	TGTGTTGCAGGTCACA	5.76E-07	NEW	1
cg2700 > < cg2701	*phoB* > < *musI*	NCgl2371 > < NCgl2372	5.88	2603276	2603715	TGTGAGCCACGCCACT	2.48E-06	NEW	7

(iv) GlxR binding sites (n=40) located intragenically and less than 500 bp upstream of a transcriptional start site (TSS), or if TSS is unknown, the translational start site (TLS) of a neighbouring gene or operon

Gene locus (cg)	rel. GlxR motif location	Gene name	Gene locus (NCgl)	EF in $WT_{GlxR-TS}$ (glc)[a]	Start position[b]	End position[b]	GlxR binding site[c]	E-value[c]	GlxR peak known or new[e]	No.[f]
cg0002	in	-	-							
cg0004	upstream	*dnaN*	NCgl0002	11.52	1622	1949	AGTGAGCTTTGTCACA	2.48E-06	Toyoda et al. 2011	5
cg0261	upstream	*moeA1*	NCgl0209	3.33	228936	229141	CGTGGCGAATCCCACT	4.06E-04	Toyoda et al. 2011	177
cg0262	in	*modB*	NCgl0210							
cg0426	in	*tnp17a*	NCgl0348							
cg0427	upstream	*tnp17b*	-	5.01	377613	377928	AGTATACTTCCATACA	1.71E-03	NEW	224
cg0440	upstream	-	-	3.82	387792	388032	TATGAGGATGCTCACA	1.51E-04	NEW	132
cg0441	in	*lpd*	NCgl0355							
cg0447	in	*sdhB*	NCgl0361						Kohl & Tauch 2009,	
cg0448	upstream	-	NCgl0362	7.87	396032	396338	GGTGACAGCTGCCACA	8.04E-05	Han et al. 2008,	96
cg0517	in	*hemY*	NCgl0421							
cg0518	upstream	*hemL*	NCgl0422	5.46	462081	462410	TATGGAGTTGATCACA	2.39E-04	Toyoda et al. 2011	152
cg0766	upstream	*icd*	NCgl0634	3.75	680094	680413	TGTGTTCTCCGCCACT	3.47E-05	Toyoda et al. 2011	63
cg0767	in	-	NCgl0635							
cg0865	in	-	NCgl0723							
cg0866	upstream	-	NCgl0724	3.38	794231	794532	CGTGATATTTGTCACG	2.97E-04	NEW	158
cg0866	in	-	NCgl0724							
cg0867	upstream	*psrp-1*	NCgl0725	5.45	794859	795164	CGTGATGCATTGCACA	1.90E-04	Toyoda et al. 2011	144
cg0903	in	-	NCgl0759							
cg0904	upstream	-	-	3.64	835617	835898	TGCTTGATCTCCCACA	6.81E-03	NEW	238
cg0933	upstream	-	NCgl0782	5.96	864962	865265	TGTGGATGAAGCCACA	3.47E-05	NEW	56
cg0934	in	-	NCgl0783							
cg0962	upstream	-	NCgl0806	2.74	897324	897585	GGTCAATCAGATCACT	7.96E-04	NEW	211
cg0963	in	-	-							
cg0967	upstream	cysQ	NCgl0811	5.59	900194	900525	AGTGATATTGGGCACA	1.12E-05	Toyoda et al. 2011	23
cg0968	in	-	NCgl0812							
cg1244	upstream	*arsC4*	NCgl1049	3.32	1141185	1141511	TATGCCGAAGGCCACA	1.51E-04	Toyoda et al. 2011	134
cg1245	in	-	NCgl1050							
cg1256	upstream	*dapD*	NCgl1061	4.16	1153247	1153654	AGTTTCAACTGTGACA	1.04E-03	NEW	216
cg1257	in	*aroP*	NCgl1062							
cg1361	in	*atpI*	NCgl1158							
cg1362	upstream	*atpB*	NCgl1159	2.53	1271688	1272121	TGTTATGTGTGTCACA	1.12E-05	Toyoda et al 2011	26
cg1432	upstream	*ilvD*	NCgl1219	3.04	1335160	1335532	CGTCTGAAACCTCACA	4.96E-04	NEW	186
cg1433	in	-	NCgl1220							
cg1812	upstream	*pyrF*	NCgl1546	3.14	1704186	1704609	TGTTCCGCTGATCACC	6.61E-04	NEW	201
cg1813	in	*carB*	NCgl1547							
cg1862	upstream	*apt*	NCgl1591	4.43	1755387	1755684	TGTGCGATCTATCACA	8.01E-06	predicted Kohl et al. 2008, Toyoda et al. 2011	16
cg1864	in	-	NCgl1592							

TABLE S4 (Part 2/3)

(iv) GlxR binding sites (n=40) located intragenically and less than 500 bp upstream of a transcriptional start site (TSS), or if TSS is unknown, the translational start site (TLS) of a neighbouring gene or operon

Gene locus (cg)	rel. GlxR motif location	Gene name	Gene locus (NCgl)	EF in $WT_{GlxR\text{-}TS}$ (glc)[a]	Start position[b]	End position[b]	GlxR binding site[c]	E-value[c]	GlxR peak known or new[e]	No.[f]
cg1897	in	-	NCgl1618							
cg1898	upstream	-	NCgl1619	7.79	1788537	1788805	TGTCGCCACTGCCACA	1.33E-04	NEW	124
cg1926	in	-	NCgl1642							
cg1927	upstream	-	NCgl1643	3.52	1807623	1807914	TGTGCCTCGTAGCACA	2.96E-05	NEW	53
cg2034	in	-	NCgl1739							
cg2035	upstream	-	NCgl1740	6.09	1927741	1928035	TGTCTAATATGGTACT	8.70E-04	NEW	213
cg2134	upstream	-	NCgl1873	3.92	2057714	2058023	GGTGGCTCCTGCCACA	1.51E-04	NEW	131
cg2135	in	*miaB*	NCgl1874							
cg2182	in	*oppB*	NCgl1916							
cg2183	upstream	*oppC*	NCgl1917	3.92	2102610	2102934	TGTCTCCATTGTCACT	9.14E-05	Toyoda et al. 2011	109
cg2183	in	*oppC*	NCgl1917							
cg2184	upstream	*oppD*	NCgl1918	5.23	2103502	2103846	TGTTCCCAGTGCCACA	1.69E-04	NEW	137
cg2402	upstream	*nlpC*	NCgl2108	3.26	2320901	2321183	GGTGATTAATGTCACA	8.01E-06	Kohl & Tauch 2008	18
IGTR_cg2402_cg2403	in	-	-							
cg2404	upstream	*qcrA (qcrA1)*	NCgl2110	5.45	2324430	2324672	TGTCGCCTGCATCACC	1.90E-04	Toyoda et al. 2011	143
cg2405	in	*qcrC*	NCgl2111							
cg2406	upstream	*ctaE*	NCgl2112	4.90	2325943	2326265	TGAGAGACACGTCACA	5.29E-05	Kohl & Tauch 2008	79
cg2407	in	-	-							
cg2480	upstream	-	NCgl2180	3.13	2393676	2393986	TGTCGACACCGTCACA	1.69E-04	NEW	139
cg2482	in	-	NCgl2182							
cg2521	upstream	*fadD15*	NCgl2216	8.57	2430262	2430557	TGTATCTAAATTCACA	5.29E-05	NEW	77
cg2523	in	*malQ*	NCgl2217							
cg2546	upstream	-	NCgl2236	3.28	2457005	2457297	AGTGGATTACGTCACA	8.01E-06	pred. Kohl et al. 2008, Toyoda et al. 2011	17
IGTR_cg2546_cg2549	in	-	-							
cg2678	upstream	-	NCgl2353	10.03	2582586	2582892	GGTGACATTATTCACA	1.87E-05	NEW	32
cg2679	in	-	NCgl2354							
cg2743	upstream	*fas-IA*	NCgl2409	6.53	2647825	2648109	GGTGAACAAGGCCACA	5.29E-05	Kohl & Tauch 2008	78
cg2745	in	-	-							
cg2796	in	-	NCgl2450							
cg2797	upstream	-	NCgl2451	4.17	2685869	2686208	TGTTCAAAGCTTCACA	4.96E-04	NEW	183
cg2803	in	-	NCgl2456							
cg2804	upstream	*tnp21a*	NCgl2457	8.11	2691030	2691325	TGTATGAAACCTCACT	1.33E-04	Toyoda et al. 2011	123
cg3030	upstream	-	NCgl2639	3.36	2917792	2918090	AGTGCACCACGAGACA	3.66E-04	NEW	167
cg3031	in	-	NCgl2640							
cg3041	upstream	-	NCgl2650	3.27	2928359	2928637	AGTCGCATTCAACACA	1.51E-04	NEW	135
cg3042	in	-	NCgl2651							
cg3090	in	-	NCgl2692							
cg3091	upstream	-	NCgl2693	4.50	2974964	2975268	AGTTTGTTGGCTTACA	1.34E-03	NEW	218
cg3247	upstream	*hrrA (cgtR11)*	NCgl2834	3.58	3136728	3137037	TGAATGTTTCGCCACA	1.34E-03	NEW	220
cg3248	in	*hrrS*	NCgl2835							
cg3413	upstream	*azlC*	NCgl2977	7.68	3289998	3290261	TGATTGGTTCGTCACA	8.70E-04	Toyoda et al. 2011	212
cg3414	in	-	NCgl2978							

TABLE S4 (Part 3/3)

(v) GlxR binding sites (n=45) located intragenically and more than 500 bp upstream of a transcriptional start site (TSS), or if TSS is unknown, the translational start site (TLS) of a neighbouring gene or operon.

in gene locus (cg)	Gene name	Gene locus (NCgl)	EF in $WT_{GlxR-TS}$ (glc)[a]	Start position[b]	End position[b]	GlxR binding site[c]	E-value[c]	GlxR peak known or new[d]	No.[f]
cg0001	*dnaA*	NCgl0001	3.21	0	208	GGTTCAAATATGCACG	1.57E-02	NEW	240
cg0089	*citA*	NCgl0067	6.30	71049	71315	AGTCTGATTTTGCACA	5.46E-04	NEW	187
cg0261	*moeA1*	NCgl0209	4.44	228447	228830	CGTGGCGAATCCCACT	4.06E-04	NEW	174
cg0279	*tyrA*	NCgl0223	3.81	242137	242468	TGTCTCATTTAACACA	2.96E-05	NEW	52
cg0576	*rpoB*	NCgl0471	4.17	514025	514322	TGAGTCAAACCAGACA	9.50E-04	NEW	215
cg0583	*fusA*	NCgl0478	3.45	524435	524776	TGTAGGCGGTGCCACA	2.39E-04	NEW	153
cg0658	*rptA*	NCgl0543	2.62	579446	579759	TGTCGCCATGTTCACT	3.66E-04	NEW	169
cg0706	-	NCgl0584	3.60	622394	622684	GGTCTCCAACATCACA	1.51E-04	NEW	133
cg0764	-	NCgl0632	3.67	676645	676946	TGTTCAACCAGCCACA	7.27E-04	NEW	204
cg0772	-	NCgl0640	3.38	685592	685875	GGTTCCTCATGCCACA	5.46E-04	NEW	190
cg0788	*pmmB*	NCgl0656	3.32	700413	700712	TGTCTGTCACCCCACA	1.17E-04	NEW	121
cg0845	-	NCgl0707	3.49	775275	775618	AGTATGCAGGTTCACA	4.96E-04	NEW	184
cg0848	*wbbL*	NCgl0709	2.63	779163	779514	GGTGACGTTTCGCACA	2.96E-05	Toyoda et al. 2011	54
cg0875	-	NCgl0732	5.29	803117	803421	TGTGTCTTCCACCACA	8.01E-06	NEW	15
cg1052	*cmt3*	NCgl0885	3.13	977403	977763	GGTGCCAAGGCTCACA	8.04E-05	NEW	101
cg1075	*prsA*	NCgl0905	3.45	998005	998314	TGTTCCATGAGCCACT	2.97E-04	NEW	157
cg1147	*ssuI*	NCgl0968	4.13	1064223	1064532	TGTACCACCGCTCACA	1.33E-04	NEW	127
cg1520	-	NCgl1294	3.29	1410547	1410841	TGTACTGCTAATCACA	1.33E-04	NEW	129
cg1895	-	NCgl1616	4.45	1783094	1783431	TGTGGTCTTCAACACT	3.47E-05	NEW	57
cg1924	-	-	5.62	1806046	1806328	AGTAACACAGACCACA	9.14E-05	NEW	108
cg1945	-	NCgl1658	3.21	1821008	1821281	TGTTCATCCCCTCACA	6.01E-04	NEW	198
cg1995	-	NCgl1702	3.10	1873481	1873791	TGTATCAGTTGCCACT	2.97E-04	NEW	160
cg2000	-	NCgl1707	6.34	1884323	1884613	TGTCTACTCTGTTACA	4.06E-04	NEW	171
cg2042	-	NCgl1747	9.80	1933851	1934130	AGTATGCCGGATCACT	7.96E-04	pred. Kohl et al. 2008	205
cg2064	-	NCgl1769	2.55	1955246	1955557	CGTGAAATAGGACACA	3.47E-05	NEW	65
cg2117	*pstI*	NCgl1858	3.54	2040573	2040845	TGTGGGACTTGTCACT	5.53E-05	Kohl & Tauch 2008, Jungwirth et al. 2013	42
cg2405	-	NCgl2111	5.97	2324785	2325080	TGTCGCCTGCATCACC	1.90E-04	NEW	142
cg2497		NCgl2196	3.92	2409768	2410123	AGTGAGATCCCCCACA	3.47E-05	NEW	62
cg2642	-	NCgl2325	3.26	2553033	2553285	TGTTCCTCCTGCCACT	5.50E-04	NEW	193
cg2695	-	NCgl2368	3.04	2596754	2597196	TGTCCTTGCCGTCACA	2.13E-04	NEW	150
cg2781	*nrdF*	NCgl2438	0.80	2673427	2673772	AGTCTCCTTCGCGACA	6.01E-04	Kohl & Tauch 2008	199
cg2811	-	NCgl2464	6.25	2700486	2700775	CGTCTGGTTAGTCACA	3.66E-04	NEW	164
cg2837	*sucC*	NCgl2477	3.53	2727036	2727290	TGTGCAGCATTTCACT	4.02E-05	Tauch 2009	74
cg2843	*pstB*	NCgl2483	4.45	2733426	2733695	GGTCTGATCGGACACA	4.49E-04	NEW	179
cg2898	-	NCgl2526	3.18	2785006	2785289	TGTTGATTCCCACACC	1.85E-03	NEW	227
cg3044	*glnX*	NCgl2653	3.24	2930106	2930403	TGATGTATACAGCACA	1.71E-03	NEW	225
cg3092	-	NCgl2694	3.62	2977156	2977490	TGTTATTTATTGCACA	9.14E-05	NEW	111
cg3158	*nagA2*	NCgl2754	3.85	3041008	3041338	TGTGCGAATCGCCACT	8.04E-05	Toyoda et al. 2011	99
cg3174	*mmpL1*	NCgl2769	3.77	3058079	3058349	TGTTTGTTTTCCCACA	1.90E-04	NEW	146
cg3187	*aftB*	NCgl2780	4.53	3078011	3078313	AGTCGCCCACAACACC	8.70E-04	NEW	214
cg3203	-	NCgl2795	6.24	3096357	3096690	TGCCTCATTTACCACT	5.31E-03	NEW	237
cg3332	*qor3*	NCgl2902	3.91	3205746	3206075	GGTACTCTGCGTTACT	2.50E-03	NEW	231
cg3393	*phoC*	NCgl2959	3.47	3267837	3268141	TGTACCACTCATCACA	6.09E-05	NEW	86
cg3415	-	NCgl2979	2.56	3291726	3292103	GGTGAGCTTTCAGACA	2.97E-04	NEW	161
cg3429	-	NCgl2991	3.63	3306926	3307262	TGTTCGGTGCGCCACT	4.06E-04	NEW	176

a: average of enrichment factor (EF) of GlxR peak of $WT_{GlxR-TS}$ (glc) ChAP-Seq samples (n=3)

b: Reference genome sequence BA000036.3 of *C. glutamicum* ATCC13032 (Ikeda & Nakagawa 2003)

c: motif was detected by using the program MEME-ChIP with the DNA fragment of the detected GlxR peaks as input sequences; the 16 bp sequence shows the most probable GlxR binding site within this sequences

d: distance was counted from the center of the GlxR binding site to the first base of TLS or TSS; information of the TSS and TLS was taken from transcriptomes study (Pfeifer-Sancar et al. 2013)

e: if GlxR peak is previously described, the respective literature is mentioned; if the site is only found in our ChAP-Seq results it is described as 'NEW'

f: No. according to numbering in Table S3

TABLE S5 I Genes described in literature as GlxR gene targets due to detection of GlxR peak or/and GlxR binding site upstream of TSS but no GlxR peaks in our ChAP-Seq experiment with the previous cultivation condition with carbon source glucose or glucose-acetate mixture

Relative location of GlxR motif taken from literature	Gene locus (Cg)	Gene losuc (NCgl)	Gene name	Description	GlxR (act./rep.)	regulation (pred./exp.)	motif from the literature	other regulator	enriched DNA region (61 bp) in our 9 ChAP-Seq experiments but not counted as GlxR peak (due to EF value <3 of one data set)									
									enriched DNA region (61 bp)	EF $WT_{GlxR\text{-}TS}$ (glu)			EF $\Delta cyaB_{GlxR\text{-}TS}$ (glu)		EF $WT_{GlxR\text{-}TS}$ (glu-ac)		EF $\Delta cyaB_{GlxR\text{-}TS}$ (glu-ac)	
cg0812 < > cg0814	cg0812 cg0814	NCgl0678 NCgl0679	*dtsR1 (accD1)* *birA*	acetyl/propionyl-CoA carboxylase biotin-protein ligase	R R	pred. pred.	AGTGATGTAAATCACC GGTGATTTACATCACT	cg2737(*fasR* ,exp) -	TAAAAACTACCCGCACGCAGCACGAACCTGTTCA GTGATGTAAATCACCGCGGAAATATTG	0	0	0	0	0	1.57	1.58	0	1.71
cg1132	cg1132	NCgl0953	*coaA*	pantothenate kinase	R	pred.	AATAACCCCGATCACA	-	-									
cg1145< > cg1147	cg1145	NCgl0967	*fumC (fum)*	fumarase fumarate hydratase	R	exp.	TATTAACCTAGACAAT, CCTTATTTCTCACACT, TATTACCCACCTCACT, GTTGTC, GCGAAACACT	cg2092(*sigA* ,exp), cg2102(*sigB* ,pred), cg2831(*ramA* ,exp)	CCCTAGAGTGAGGTGGGTAATAGAAAGTGTGAG AAATAAGGCACAATCCACTCCTAAATGT	3.12	2.62	2.35	1.92	2.37	1.77	2.81	0	2.01
cg1226 < > cg1227	cg1226	NCgl1032	*pobB (pobA)*		R	pred.	TGTGACTTCAACCTCA, TGAGTCCCAAATCACT	cg2627(*pcaO* ,pred), cg2624(*pcaR* ,pred)	CGAACAGGTTGTCACGGAATGCACTTTCACTTAC ATTGAGTCCCAAATCACTGTGAGGTGC	2.69	3.73	2.57	1.89	2.41	1.91	2.96	2.11	3.00
cg1308 < > cg1309	cg1309	NCgl1111	*rolH (mhpA)*	2-polyprenyl-6-methoxyphenol hydroxylase	R	pred.	TGTTGTTCAGTTCACT	cg1308(*rolR* ,exp)	GATGTCTGCATCGTCGGTGGAGGTCCTACCGGA ACGCTCCTTGCAGTACTGCTCGGCCAAA	2.34	2.49	2.88	2.24	3.33	1.92	2.24	1.64	2.20
cg1568	cg1568	NCgl1329	*ugpA*	ABC-type sn-glycerol-3-phosphate transport system	R	pred.	GGACATTTAGGTCACA	cg2888(*phoR* ,exp), cg2092(*sigA* ,exp)	-									
cg1595	cg1595	NCgl1353	*uspA2*	universal stress protein no. 2, nucleotide-binding protein			TGTGAGCTGAAACTCA	-	CGGACAATAGTAAGATGTGAGCTGAAACTCAGT TTCCATCCTTATTCAACCTGGAAGGTAG	2.60	3.11	2.19	0	0	0	2.50	1.65	2.08
cg1753	cg1753	NCgl1493	-	putative ATPase component of ABC transporters	R	pred.	TGTGATTGTCACCAAT	-	-									
cg1765 < > cg1766	cg1766	NCgl1505	*mptB*	mannosyltransferase	A	pred.	TGAGATTTAGCTCACA	-	TTTGAGATTTAGCTCACACTATCCCCCTTCGGGTC ACCACCAGACTCTGATGCGAGGTAAA	2.77	2.90	2.82	2.18	2.78	2.22	3.38	0	2.00
cg1790	cg1790	NCgl1525	*pgk*	phosphoglycerate kinase	R	pred.	ATTGATTAAAGACACA	cg2092(*sigA* ,exp), cg2102(*sigB* ,pred)	CACCCCGGGCTATTTTGTGTCTTTAATCAATACA ATTGAATACCGGTGCCAGCGCCACACA	0	0	2.84	1.55	2.17	1.74	2.97	1.58	2.14
cg1840	cg1840	NCgl1572	-	hypothetical protein, conserved	R	pred.	GGTGAGTTAGATAACA	-	GGGGGTGATGTTATCTAACTCACCCCCATTTTCT ATGGTGCTCTGTACCATAGAATGAGGA	2.51	2.83	2.43	0	1.69	1.51	1.89	1.41	1.82
cg1956	cg1956	NCgl1667	*recJ*	single-stranded-DNA-specific exonuclease CGP3 region	R	pred.	TATGACCGTTACCTCA	-	-									
cg2280	cg2280	NCgl1999	*gdh*	glutamate dehydrogenase, NADP-specific	R	pred.	AGTGAGTTAAGTCTCA	cg1585(*argR* ,pred), cg2092(*sigA* ,exp), cg3202(*farR* ,exp), cg0986(*amtR* ,exp)	TTACCAGCCTAAATGCCCGCAGTGAGTTAAGTCT CAAAGCAAGAAGTTGCTCTTTAGGGCA	0	2.14	0	0	1.67	1.53	1.63	1.64	2.36
cg2429	cg2429	NCgl2133	*glnA*	glutamine synthetase I	R	pred.	TGTGAACAAAGCTACA	cg2092(*sigA* ,exp), cg0986(*amtR* ,exp)	-									
cg2559	cg2559	NCgl2247	*aceB*	malate synthase	R	exp.	GGTGACGGTGATCACT, TGTGACCTAGATAAAA	cg2092(*sigA* ,exp), cg2831(*ramA* ,exp), cg0371(*cspA2* ,exp), cg0444(*ramB* ,exp)	-									
cg2560	cg2560	NCgl2248	*aceA*	isocitrate lyase	R	exp.	TGTGAACCACGCCACC	cg2831(*ramA* ,exp), cg0444(*ramB* ,exp), cg2092(*sigA* ,exp)	-									
cg2631	cg2631	NCgl2315	*pcaH*	protocatechuate dioxygenase β subunit	R	pred.	TGAGATCTATATCACT	cg2624(*pcaR* ,pred), cg2627(*pcaO* ,exp)	AATCATCCCTACTTTGAGATCTATATCACTAGAC GCAGAAAGGTCTCGCATGGACATCCCA	3.12	3.11	2.47	1.71	2.51	2.05	2.69	0	2.71
cg2831	cg2831	NCgl2472	*ramA*	transcriptional regulator, acetate metabolism, LuxR-family	A	exp.	AGTGTTCTATGACACT	cg2831(*ramA* ,exp), cg2092(*sigA* ,exp), cg2115(*sugR* ,exp), cg0764(pred)	-									
cg2840 < > cg2841	cg2840	NCgl2480	*actA (ctfA)*	Acetyl-CoA:CoA transferase	A	pred.	AGTGGGGTACATCATA	cg0444(*ramB* ,pred)	TTCGACCAATCTTTTCAGATAGGTCACTTCAACC GGAAGCATATGATGTACCCCACTTTGA	3.64	0	3.22	1.71	2.21	1.72	0	2.03	2.44
cg2846	cg2846	NCgl2486	*pstS*	ABC-type phosphate transport system	A	exp.	TGTGATTAGAGTCTCC	cg2092(*sigA* ,exp), cg2888(*phoR* ,exp)	ATCGGTGATTTTCGTTCCGCAGGGGTCGAAAATT GCCGATTTTTGTGATTAGAGTCTCCAA	0	0	0	1.69	1.73	0	0	0	0
cg2965	cg2965	NCgl2587	-	putative transcriptional regulator, AraC-type	R	pred.	TGTGATCTAAGACTCT	-	GACTTATGTGATCTAAGACTCTATTGTGGTACGC ACCATGACTGCTCAACCAGCCCACGAG	3.03	2.97	2.33	1.90	2.03	2.10	2.24	0	2.15
cg3219 < > cg3220	cg3219 cg3220	NCgl2810 NCgl2811	*ldhA (ldh)* -	NAD-dependent L-lactate dehydrogenase putative membrane protein	A R	exp. pred.	TGTGATTTTTTCAACA TGTTGAAAAAATCACA	cg3224(*lldR* ,exp), cg2831(*ramA* ,exp), cg2115(*sugR* ,exp), cg2092(*sigA* ,exp) -	-									
cg3250	cg3250	NCgl2837	-	putative membrane protein	R	pred.	no motif	-	-									
cg3389	cg3389	NCgl2955	*oxiC*	myo-Inositol dehydrogenase	R	exp.	AGTGATGCGTGTCATG	-	GTAACCCCTCTGAGCATTGTGGTTTAAGCAATTC ATTGACGTACAAAGTGATGCGTGTCAT	2.25	2.00	2.05	2.11	1.95	1.67	1.75	0	1.58

EF: enrichment factor of ChAP-Seq experiments of normalized peak heights

TABLE S6 (Part 1/2) I Microarray data of Δ*cpdA* /WT and Δ*cyaB* /WT of (putative) GlxR target genes

Locus tag (cg)	Gene name	Annotation	Distance to next TSS[a]	Distance to next TLS[a]	mRNA ratio Δ*cpdA* /WT[b]	p-value [c]	mRNA ratio Δ*cyaB* /WT glc[d]	p-value[c]	pred. due to data of microarray[e]	pred. in literature[f]
cg0061	*rodA (ftsW)*	putative FTSW/RODA/SPOVE-family cell cycle protein	-	+48	0.63	0.07	1.04	0.01	-	-
cg0088	*citH*	citrate transporter, CitMHS-family	-21[h], -22[h], -24[h]	-77	0.41	0.00	0.12	n.d.	-	exp. R
cg0103	*crnT*	creatinine transporter	-	-86	0.88	0.04	0.12	n.d.	-	-
cg0156	*cysR*	transcriptional activator, ROK-family	-310	-310	0.52	0.04	1.47	0.03	**R**	-
cg0196	*iolR*	repressor of myo-inositol utilization genes, GntR-family	-263[i]; -264[i]	-400	1.60	0.05	0.50	0.18	-	-
cg0197	*iolC*	carbohydrate kinase, myo-inositol catabolism	+15	-44	0.87	0.30	1.24	0.02	-	-
cg0210	-	putative transcriptional regulator, LacI-family	-	-85	1.11	0.13	1.23	0.03	-	-
cg0211	*oxiB*	putative oxidoreductase dehydrogenase	+25	-56	1.09	0.10	1.40	0.02	-	-
cg0223	*iolT1*	myo-Inositol transporter 1	+11[i]; +39[i]	-75	0.34	0.01	3.22	0.01	**R**	-
cg0228	*hkm*	putative sensor histidine kinase	-25	-58	1.00	0.21	1.17	0.02	-	-
cg0249	-	putative polysaccharide/polyol phosphate export systems	+64	+64	1.25	0.01	1.00	0.13	-	-
cg0250	-	putative aminotransferase class V	+41; -163	-177	0.88	0.43	1.34	0.02	-	-
cg0261	*moeA1*	molybdopterin cofactor synthesis protein A1, MoeA-family	-	-190	0.73	0.28	1.71	0.04	-	-
cg0303	*leuA*	2-isopropylmalate synthase	-	-248	0.99	0.07	1.51	0.01	-	-
cg0336	*pbp1a*	penicillin-binding protein 1A	-579	-579	1.06	0.14	1.29	0.02	-	-
cg0337	*whcA (whiB4)*	putative regulatory protein (whiB related protein)	-40;+66	-89	1.43	0.03	0.85	0.48	-	-
cg0341	*phdA (fadD1)*	acyl:CoA ligase transmembrane protein	-	-22	0.00	0.00	1.93	n.d.	-	-
cg0343	*phdR*	Repressor of phd operon, MarR-family	-	-163	0.83	0.12	1.51	0.03	-	-
cg0344	*phdB (fabG1)*	3-hydroxyacyl-CoA dehydrogenase	-	-29	0.48	0.01	1.40	n.d.	-	-
cg0360	-	putative phosphatase	-127	-127	0.76	0.12	1.28	0.00	-	-
cg0444	*ramB*	transcriptional regulator, MerR-family	-283	-283	3.99	0.00	0.82	0.40	-	exp. R
cg0445	*sdhC*	succinate:menaquinone oxidoreductase, cytochrome b subunit	-198; -200; -203	-215	0.71	0.22	1.27	0.00	-	exp. R
cg0448	-	putative membrane protein	-61;+88	-100	0.67	0.06	1.62	0.00	-	-
cg0500	*qsuR*	transcriptional activator of qsuABCD genes, LysR-family	-	-70	1.33	0.03	1.60	0.09	-	-
cg0501	*qsuA*	putative shikimate permease, MFS-type	-	-207	1.07	0.03	0.08	0.04	-	-
cg0518	*hemL*	glutamate-1-semialdehyde 2,1-aminomutase	-253	-253	1.10	0.08	1.22	0.02	-	-
cg0565	*pwkR/gabR*	putative transcriptional regulator	-65	-124	0.69	0.05	1.32	0.02	-	-
cg0607	-	putative secreted protein	-84; -63	-133	0.79	0.31	1.45	0.00	-	-
cg0645	*creJ (cytP)*	cytochrome P450	-	-74	0.41	0.05	2.99	0.00	**R**	-
cg0646	*creR*	putative transcriptional regulator, IclR-family	-71; -115	-202	0.88	0.22	0.10	0.00	-	-
cg0703	*guaA*	putative Gmp synthase	+7	+7	0.84	0.37	1.06	0.04	-	-
cg0755	*metY*	O-acetylhomoserine sulfhydrylase	-136	-175	1.30	0.02	1.39	0.00	-	-
cg0756	*cstA*	carbon starvation protein A	-30;-32;-42; -59	-258	3.24	0.00	0.71	0.17	-	-
cg0759	*prpD2*	2-methycitrate dehydratase	-4[l]	-41	0.49	0.03	2.79	0.00	**R**	exp. R
cg0791	*pyc*	pyruvate carboxylase	+14; +12; +10	-45	0.31	0.02	1.06	0.01	-	pred. R
cg0796	*prpD1*	2-methylcitrate dehydratase	-32	-68	2.34	0.00	0.97	0.06	-	pred. R
cg0803	*thtR*	thiosulfate sulfurtransferase	-37	-91	0.69	0.07	1.12	0.00	-	-
cg0806	-	hypothetical protein	-61	-238	1.28	0.01	0.96	0.26	-	-
cg0835	*tusK (msiK2)*	trehalose uptake system	+7	+7	0.76	0.04	0.13	0.00	-	-
cg0836	-		-	-94	0.95	0.42	0.02	0.00	-	-
cg0866	-	purine/pyrimidine phosphoribosyl transferase	-	-311	0.74	0.02	n.d.	n.d.	-	-
cg0867	*psrp-1*	putative ribosome-associated protein Y	-162; -300; -303; -306	-384	0.34	0.03	0.85	0.49	-	-
cg0878	*whcE (whiB1)*	transcriptional regulator	-114	-316	1.03	0.15	0.97	0.02	-	pred. A
cg0924	-	putative ABC-type putative iron-siderophore transporter	-156	-236	1.14	0.04	0.95	0.02	-	-
cg0926	-	putative putative iron-siderophore transporter	-	-159	0.78	0.23	1.10	0.05	-	-
cg0933	-	putative DNA or RNA helicase of superfamily II	-87	-115	1.12	0.15	1.14	0.01	-	-
cg0936	*rpf1*	resuscitation promoting factor	-122; -211; -402	-406	1.13	0.24	0.96	0.03	-	pred. A
cg0948	*serC*	phosphoserine aminotransferase	-258	-318	1.92	0.00	1.08	0.03	-	pred. A
cg0949	*gltA*	citrate synthase	-288	-409	1.41	0.01	0.99	0.16	-	pred. A
cg0952	*mctB*	putative integral membrane protein	-17;+274	-170	1.51	0.05	1.48	0.01	-	pred. R
cg0955	-	putative secreted protein	-84	-128	1.78	0.00	1.16	0.04	-	-
cg0961	-	putative homoserine O-acetyltransferase	-	-26	0.31	0.00	1.85	0.00	**R**	pred. R
cg0967	*cysQ*	3-phosphoadenosine 5-phosphosulfate PAPS 3-phosphatase	-405	-405	0.50	0.00	0.94	0.05	-	-
cg0967	*cysQ*	3-phosphoadenosine 5-phosphosulfate PAPS 3-phosphatase	-42	-42	0.50	0.00	0.94	0.05	-	-
cg0973	*pgi*	glucose-6-phosphate isomerase	-59	-87	0.40	0.01	1.29	0.04	-	-
cg1037	*rpf2*	resuscitation promoting factor	-132	-163	1.17	0.02	1.07	0.01	-	exp. A
cg1043	-	putative thiol-disulfide isomerase and thioredoxins	-	-30	0.94	0.03	1.36	0.04	-	-
cg1048	-	putative haloacid dehalogenase/epoxide hydrolase-family	-59	-89	0.88	0.41	1.22	0.03	-	-
cg1086	-	putative membrane protein	-126	-126	1.05	0.09	1.28	0.00	-	-
cg1087	-	putative membrane protein	-3	-29	1.63	0.00	1.01	0.07	-	-
cg1090	*ggtB*	γ-glutamyltranspeptidase precursor PR	+13	+13	0.64	0.02	1.25	0.00	-	-
cg1091	-	hypothetical protein	-133	-262	4.75	0.00	1.30	0.02	-	-
cg1108	*porC*	putative secreted protein	-	-90	2.24	0.02	1.19	0.02	-	-
cg1111	*eno*	enolase, phosphopyruvate hydratase	-93	-163	0.62	0.09	1.14	0.02	-	-
cg1142	-	putative Na+/proline, Na+/panthothenate symporter	-	-114	0.46	0.03	1.12	0.02	-	pred. R
cg1143	*-(regulator)*	putative transcriptional regulator, GntR-family	-98	-98	1.41	0.01	1.71	0.03	-	pred. R
cg1224	*phnB2*	similarity to alkylphosphonate uptake operon protein PhnB *E. coli*	-28	-62	1.91	0.00	0.97	0.12	-	-
cg1244	*arsC4*	arsenate reductase, glutaredoxin-family	-128	-128	1.21	0.00	1.24	0.01	-	-
cg1256	*dapD*	tetrahydrodipicolinate succinylase	-275	-275	1.28	0.04	0.97	0.11	-	-
cg1290	*metE*	homocysteine methyltransferase	-252; -254	-494	0.78	0.31	1.32	0.00	-	-
cg1291	-	putative membrane protein	-83	-83	0.41	0.00	0.20	n.d.	-	-
cg1314	*putP*	proline transport system	-	-68	1.54	0.02	1.34	0.00	-	-
cg1345	*narK*	nitrate/nitrite antiporter	-18	-79	0.84	0.39	1.11	0.04	-	exp. A
cg1346	*mog*	putative molybdopterin biosynthesis MOG protein	-146	-180	0.51	0.01	1.35	0.03	-	exp. A
cg1362	*atpB*	F1FO-ATP synthase, a-subunit of FO part	-119; -121	-172	1.40	0.10	0.79	0.01	-	exp. A
cg1409	*pfkA*	6-phosphofructokinase	-165; -167	-167	0.35	0.02	1.27	0.12	-	exp. A
cg1432	*ilvD*	dihydroxy-acid dehydratase	+24; -46	-165	1.06	0.00	1.06	0.04	-	-
cg1434	*yggB (mscCG)*	small-conductance mechanosensitive channel, MscS-family	-137	-137	1.47	0.02	1.37	0.00	-	-
cg1435	*ilvB*	acetolactate synthase I AHAS	-	-302	1.53	0.02	0.95	0.32	-	-
cg1437	*ilvC*	ketol-acid reductoisomerase	-43	-139	0.90	0.50	1.47	0.00	-	pred. R
cg1537	*ptsG*	glucose-specific EIIABC component EIIGlc of PTS	+31	-255	0.25	0.01	1.64	0.00	**R**	pred. R
cg1547	*uriR*	transcriptional regulator, LacI-family	+127	+62	1.99	0.00	1.55	0.02	-	-
cg1577	-	putative secreted hydrolase	-347; -408	-469	1.44	0.03	1.35	0.01	-	-
cg1612	-	putative acetyltransferase	-40	-40	0.26	0.00	3.16	0.00	**R**	-
cg1613	*sseA2*	rhodanese-related sulfurtransferase	-200	-200	0.57	0.05	1.35	0.00	-	-
cg1633	-	putative transcriptional regulator, MerR-family	-85; -97	-169	1.00	0.05	1.01	0.03	-	-
cg1656	*ndh*	NADH dehydrogenase type II, NDH-II	-28; -30; -121; -123	-220	0.93	0.44	1.30	0.00	-	pred. A
cg1665	-	putative secreted protein	-54	-80	2.18	0.01	0.29	0.08	-	-
cg1697	*aspA*	aspartate ammonia-lyase aspartase	+33	-8	2.19	0.01	1.03	0.01	-	-

TABLE S6 (Part 2/2) I Microarray data of Δ*cpdA* /WT and Δ*cyaB* /WT of (putative) GlxR target genes

Locus tag (cg)	Gene name	Annotation	Distance to next TSS^{a}	Distance to next TLS^{a}	mRNA ratio Δ*cpdA* /WT^{b}	p-value ^{c}	mRNA ratio Δ*cyaB* /WT glc^{d}	p-value^{c}	pred. due to data of microarray^{e}	pred. in literature^{f}
cg1791	*gapA (gap)*	glyceraldehyde-3-phosphate dehydrogenase glycolysis	-245; -300	-429	0.37	0.00	1.13	0.01	-	exp. R
cg1812	*pyrF*	orotidine 5-phosphate decarboxylase	-	-119	0.53	0.02	1.02	0.02	-	-
cg1837	-	putative holliday junction resolvase-like protein	-	-54	1.44	0.01	0.86	0.49	-	-
cg1862	*apt*	adenine phosphoribosyltransferase	+91; +126	-90	1.49	0.04	0.93	0.17	-	-
cg1929	*res*	resolvase,-family recombinase CGP3 region	-	-210	0.84	0.36	1.81	0.02	-	-
cg1942	-	putative secreted protein CGP3 region	-40	-103	1.10	0.03	0.91	0.25	-	-
cg1967	-	hypothetical protein, CGP3 region	-	-78	0.56	0.12	2.52	0.04	-	-
cg2035	-	putative methyltransferase, CGP3 region	-256	-271	1.42	0.03	n.d.	n.d.	-	-
cg2071	*int2*	putative phage integrase N-terminal fragment, CGP3 region	-123	-275	1.41	0.05	1.20	0.02	-	-
cg2109	*oxyR*	hydrogen peroxide sensing regulator, Lys-family	-66	-66	0.82	0.05	1.08	0.05	-	-
cg2117	*pstI*	EI enzyme, general component of PTS	-197; -132; -130	-225	0.23	0.00	1.66	0.00	**R**	pred.R
cg2118	*fruR*	transcriptional regulator, DeoR-family	+108	-183	1.01	0.17	1.42	0.01	-	pred. R
cg2134	-	putative membrane protein	-60	-99	0.44	0.01	1.16	0.01	-	-
cg2135	*miaB*	tRNA methylthiotransferase	-325	-325	1.15	0.14	1.11	0.02	-	-
cg2136	*gluA*	glutamate uptake system	+7	+7	0.81	0.25	1.08	0.01	-	-
cg2157	*terC*	tellurium resistance membrane protein	-210; -212	+13	1.52	0.08	1.18	0.04	-	-
cg2183	*oppC*	ABC-type peptide transport system	-	-85	0.02	0.00	1.48	0.00	**R**	-
cg2184	*oppD*	ATPase component of peptide ABC-type transport system	-	-224	0.00	0.00	1.55	0.01	**R**	-
cg2191	-	hypothetical protein, conserved	-104	-104	1.56	0.00	0.80	0.25	-	-
cg2261	*amtB*	low affinity ammonium uptake protein	-	-201	0.69	0.02	0.73	0.02	-	pred. R
cg2293	-	putative indole-3-glycerol phosphate synthase	-104	-130	1.37	0.01	0.86	0.47	-	-
cg2361	*divIVA*	cell division initiation protein	-126; -260; -280	-360	1.41	0.02	0.74	0.27	-	pred. A
cg2402	*nlpC*	putative secreted cell wall peptidase	-254; -295	-497	1.04	0.26	1.36	0.02	-	-
cg2409	*ctaC*	cytochrome aa3 oxidase, subunit 2	-30; -157; -161; -163	-216	1.39	0.00	1.10	0.10	-	exp. A
cg2410	*ltsA*	glutamine-dependent amidotransferase	-	-304	1.04	0.15	1.34	0.02	-	exp. A
cg2430	-	hypothetical protein	+26	-47	0.65	0.12	3.81	0.02	-	-
cg2437	*thrC*	threonine synthase	-101	-101	0.89	0.47	1.30	0.02	-	-
cg2438	-	hypothetical protein	+2	-41	2.33	0.02	1.24	0.00	-	-
cg2464	-	hypothetical protein	-246	-330	0.92	0.36	1.23	0.01	-	-
cg2471	-	putative protein	-202	-205	0.62	0.01	0.97	0.02	-	-
cg2521	*fadD15*	long-chain fatty acid CoA ligase	-292	-404	0.86	0.41	1.19	0.02	-	-
cg2546	-	putative secondary C4-dicarboxylate transporter	-113	-134	0.35	0.00	0.18	0.15	-	-
cg2557	-	putative secondary Na+/bile acid symporter	-	-77	2.23	0.00	0.95	0.12	-	-
cg2564	-	hypothetical protein	-207	-265	3.22	0.01	1.20	0.05	-	-
cg2565	-	hypothetical protein	-83	-115	0.84	0.31	1.18	0.02	-	-
cg2610	-	putative ABC-type transport system	-	-91	0.07	0.00	2.70	0.00	**R**	exp.R
cg2615	*vanR*	transcriptional regulator, PadR-family	-125	-125	0.72	0.05	n.d.	n.d.	-	-
cg2616	*vanA*	vanillate demethylase, oxygenase subunit	-	-59	0.54	0.03	4.25	0.01	**R**	-
cg2636	*catA1 (catA)*	catechol 1,2-dioxygenase	-	-108	0.59	0.00	1.23	0.05	-	pred. R
cg2651	-	putative protein-fragment	-229	-229	3.51	0.01	0.86	0.03	-	-
cg2665	-	hypothetical protein	-	-15	1.71	0.00	0.26	0.04	**A**	-
cg2666	-	hypothetical protein	-187	-213	1.97	0.01	0.43	0.16	-	-
cg2692	-	putative thioesterase	+28	-50	1.14	0.04	0.96	0.00	-	-
cg2700	*phoB*	alkaline phosphatase	-551	-542	0.00	0.00	n.d.	n.d.	-	-
cg2708	*musK (msiK1)*	ABC-type maltose transport system	+27	-64	0.54	0.01	0.96	0.17	-	pred. R
cg2732	*gntV (gntK)*	putative gluconokinase	-	-129	0.14	0.01	n.d.	n.d.	-	-
cg2748	-	putative membrane protein, conserved	-56	-56	0.77	0.28	1.23	0.05	-	-
cg2781	*nrdF*	ribonucleotide-diphosphate reductase β subunit	-83; -122	-187	1.40	0.01	0.92	0.21	-	pred. R
cg2785	-	putative membrane protein	-	-167	0.00	0.00	n.d.	n.d	-	-
cg2797	-	hypothetical protein	-	-224	1.22	0.01	n.d.	n.d.	-	-
cg2824	-	putative SAM-dependent methyltransferase	-	-491	1.42	0.04	0.35	0.05	**A**	exp. A
cg2837	*sucC*	succinyl-CoA synthetase subunit β	-	-94	0.54	0.03	1.02	0.21	-	-
cg2925	*ptsS*	sucrose-specific EIIABC component EIISuc of PTS	-63	-124	0.27	0.01	2.23	0.00	**R**	-
cg2936	*nanR*	transcriptional regulator, GntR-family	-230	-255	0.96	0.20	1.71	0.00	-	-
cg2937	*siaE*	ABC-Transporter for sialic acid	+45	-54	1.31	0.08	1.24	0.01	-	-
cg2953	*vdh*	vanillin dehydrogenase	-18	-46	0.50	0.04	1.09	0.07	-	pred. R
cg2954	*bca (cynT)*	carbonic anhydrase, carbonate dehydratase	-47	-47	1.37	0.00	0.95	0.19	-	-
cg2966	-	putative phenol 2-monooxygenase	-	-74	0.55	0.00	4.26	0.00	**R**	pred. R
cg2999	-	putative ferredoxin reductase	-77	-137	0.58	0.08	0.16	0.04	-	-
cg3000	-	putative rhodanese-related sulfurtransferase	-75	-119	1.57	0.05	1.03	0.14	-	-
cg3022	-	putative acetyl-CoA acetyltransferase	-35	-254	2.19	0.02	0.90	0.23	-	-
cg3041	-	putative ABC-type multidrug transport system	-	-196	1.01	0.17	0.93	0.00	-	-
cg3048	*pta*	phosphotransacetylase	-	-62	0.19	0.00	1.43	0.01	**R**	pred. R
cg3061	*cgtR6*	two component response regulator	-179	-233	1.25	0.05	1.08	0.02	-	-
cg3096	*ald*	aldehyde degyhdrogenase	+19	-75	0.15	0.00	3.07	0.00	**R**	exp. R
cg3107	*adhA*	Zn-dependent alcohol dehydrogenase	-	-83	0.27	0.00	1.84	0.00	**R**	-
cg3112	*cysZ*	sulfate transporter	-	-474	0.29	0.01	1.91	0.02	**R**	-
cg3122	*phnB1*	putative protein	+8	-41	1.81	0.03	0.08	0.06	-	-
cg3124	-	hypothetical protein	-18	-40	1.30	0.17	1.00	0.01	-	-
cg3127	*tctC*	citrate uptake transporter	-	-296	0.60	0.00	1.58	0.04	**R**	-
cg3169	*pck*	phosphoenolpyruvate carboxykinase GTP	-24; -55	-92	0.78	0.19	0.54	0.01	-	exp. R
cg3195	-	putative flavin-containing monooxygenase FMO	-	-26	0.07	0.00	3.29	0.00	**R**	-
cg3216	*gntP*	gluconate permease, gluconate:H+ symporter GntP-family	-	-311	0.52	0.01	2.37	0.00	**R**	-
cg3226	-	L-lactate permease, operon with lldD, MFS-type	-17;-21	-90	0.02	0.01	2.10	0.01	**R**	pred. R
cg3247	*hrrA (cgtR11)*	two component response regulator	-352	-434	1.10	0.03	0.96	0.11	-	-
cg3255	*uspA3*	universal stress protein no. 3	-63; -65	-131	0.38	0.03	1.00	0.10	-	-
cg3313	*pbp1b (mcrB)*	membrane carboxypeptidase	+6; +202	-51	0.74	0.01	0.98	0.00	-	-
cg3352	*nagR (genR)*	transcriptional regulator, IclR-family	-	-43	1.13	0.05	0.82	0.46	-	exp. R
cg3353	*nagT (genK)*	gentisate transporter, MFS-type	-	-56	0.00	0.00	0.05	n.d.	-	exp. R
cg3387	*iolT2*	myo-Inositol transporter 2	-52	-317	1.83	0.04	1.14	0.04	-	-
cg3388	*ihtR*	putative transcriptional regulator, IclR-family	-84	-108	1.27	0.05	1.38	0.00	-	-
cg3413	*azlC*	branched-chain amino acid permease azaleucine resistance	-	-132	0.73	0.29	1.23	0.05	-	-

a: distance of GlxR motif sequence to corresponding TSS or TLS

b: ratios of mRNA of Δ*cpdA* /WT are taken from Schulte et al. 2017 (GEO database GSE81004); Δ*cpdA* and WT were cultivated in CGXII minimal medium with 100 mM glucose as carbon source

c: n.d. means that *p* -value was not calculated due to only one sample (n=1) instead of standard three samples (n=3); red *p* -value is highlighed due to p-value >0.05 which makes the result not reliable

d: ratios of mRNA of Δ*cyaB* and WT cultivated in CGXII minimal medium with 100 mM glucose as carbon source

e: regulation deduced due to opposite values in the microarray results analysis with the strains Δ*cpdA* (Schulte et al., 2017) and Δ*cyaB*

f: regulation of the gene by GlxR was predicted (pred.) or experimentally verified (exp.) according to CoryneRegNet7.0 (Parise, 2020)

TABLE S7 (Part 1/2) I GlxR peaks and corresponding binding sites found less than 700 bp upstream of the TSS of antisense transcripts, non-protein coding elements or intragenic trasnscripts; information of TSS of asRNA, non-protein coding genes and intragenic transcriptswas taken from Mentz et al. 2013 and Pfeifer-Sancar et al. 2013

antisense transcript (asRNA)	GlxR motif rel. located to asRNA	Distance to respective TSS	neighbouring genes (< 700 bp of a gene start)	EF in WT$_{GlxR-TS}$ (glc)[a]	Start position[b]	End position[b]	GlxR binding site[c]	E-value	GlxR peak known or new[d]	No.[e]
antisense transcript of cg0236	downstream	+62	*emb (embC)* cg0235	4.20	206760	207155	TGAGTAATTCCTCACC	1.34E-03	NEW	219
antisense transcript to *cmt3* (cg1052)	upstream	-227		3.13	977403	977763	GGTGCCAAGGCTCACA	8.04E-05	NEW	101
antisense transcript to cg1609	upstream	-114		3.34	1496565	1496868	TGAGCCCCGCGCCACA	4.49E-04	NEW	180
antisense transcripts 3x of cg1908	upstream	-108;-179; -225	- cg1909	3.59	1797026	1797319	GGTAAGTATTCAGACA	2.32E-03	NEW	230
antisense transcript cg1945	upstream	-618		3.21	1821008	1821281	TGTTCATCCCCTCACA	6.01E-04	NEW	198
antisense transcript of cg2042	upstream	-383	- cg2041	9.80	1933851	1934130	AGTATGCCGGATCACT	7.96E-04	predicted (Kohl et al. 2008)	205
antisense transcript of cg2362 cgb_23615	on TSS of asRNA upstream cgb_23615	+3 -126	*divIVA* cg2361	4.31	2276036	2276342	TGTTATCCTTGTCACA	3.47E-05	Kohl & Tauch 2009	59
antisense transcript of cg3031	upstream	-66	- cg3030	3.36	2917792	2918090	AGTGCACCACGAGACA	3.66E-04	NEW	167
antisense transcript to *phoC* (cg3393)	on TSS of asRNA	+1		3.47	3267837	3268141	TGTACCACTCATCACA	6.09E-05	NEW	86

trans-encoded sRNA (cgb_xxxxx)	motif rel. located to sRNA	Distance to respective TSS	neighbouring genes (< 700 bp of a gene start)	EF in WT$_{GlxR-TS}$ (glc)[a]	Start position[b]	End position[b]	GlxR binding site[c]	E-value	GlxR peak known or new[d]	No.[e]
cgb_00025	upstream	-382	*dnaN* cg0004	11.52	1622	1949	AGTGAGCTTTGTCACA	2.48E-06	Toyoda et al. 2011	5
cgb_00545	upstream	-121		5.05	39981	40261	TGACTGCCGCAGCACA	3.10E-03	NEW	232
cgb_03505	on TSS	+3	*glxR* cg0350	13.19	307411	307714	AGTGGTCTTTGCCACA	2.53E-05	Jungwirth et al. 2008, Jungwirth et al. 2013, Subhadra et al. 2015	44
cgb_03605	in 6C RNA	-89	- cg0360 - cg0362	9.99	314402	314704	AGTGTCATTTGCCACA	8.01E-06	Jungwirth et al. 2013	13
cgb_06465	upstream	-60	*creR* cg0646 *secY* cg0647	3.79	569106	569362	TATGATGCGTCTTACA	6.61E-04	NEW	200
cgb_07555	upstream	-32	*metY* cg0755 *cstA* cg0756	3.32	667808	668106	TATGACTAGCCCCACT	6.01E-04	NEW	196
cgb_08033	upstream	-61	*thtR* cg0803 - cg0806	3.65	721377	721657	AGTAATTAAGGACACA	9.14E-05	pred. Kohl et al. 2008	110
cgb_08785	upstream	-114	*whcE (whiB1)* cg0878 - cg0879	6.37	805907	806235	TGTGGGGTGGAACACA	8.01E-06	Kohl & Tauch 2008, Jungwirth et a.l 2013	14
cgb_09366	upstream	-190	*rpf1* cg0936 *cspB* cg0938	4.45	868599	868896	TGTAACATAAATCACA	2.48E-06	Kohl & Tauch 2008	8
cgb_09513	uptream in cgb_09516	-220	*accD3* cg0951 *mctB* cg0952	7.19	881238	881608	AGTTACCTAACTCACA	4.02E-05	Kohl & Tauch 2008	68
cgb_15755	upstream	-347	- cg1577	3.66	1460472	1460771	GGTGTCGCAGTTCACA	3.47E-05	pred. Kohl et al. 2008	64
cgb_16115	upstream	-12	- cg1612 *sseA2* cg1613	3.19	1500579	1500875	AGTGACCTAAGCTACA	1.33E-04	Toyoda et al. 2011	43
cgb_16565	upstream	-30	*ndh* cg1656 *ufaA* cg1657	5.99	1544586	1544879	TATGGCATATGTCACG	2.97E-04	Kohl & Tauch 2008	156
cgb_19666	upstream	-34	*cgpS* cg1966 - cg1967	3.04	1847031	1847319	AGTGCGGTGCATCACT	9.14E-05	pred. Kohl et al. 2008	113
cgb_20643	upstream	-377	cg2064	2.55	1955246	1955557	CGTGAAATAGGACACA	3.47E-05	NEW	65
cgb_20715 antisense transcripts	upstream	-47 -47	*int2* cg2071	7.58	1995412	1995693	AATGAATCCACTCACC	4.08E-03	pred. Kohl et al. 2008	234
cgb_27005	upstream	-190		6.02	2603255	2603478	TGTGTTGCAGGTCACA	5.76E-07	NEW	1
cgb_27005	upstream	-432		5.88	2603276	2603715	TGTGAGCCACGCCACT	2.48E-06	NEW	7
cgb_27413	upstream	-556	- cg2741	2.90	2637721	2638035	TGCATAGTTTGTCACT	4.66E-03	NEW	236
cgb_27803	upstream	-116	*ctaD* cg2780	5.42	2672843	2673129	TGTGAACCCCTTCACA	2.53E-05	Kohl & Tauch 2008	46
cgb_30215	upstream	-35	- cg3022	3.48	2908679	2909092	AGTGAATCAAGACACT	9.14E-05	pred. Kohl et al. 2008	112
cgb_30615	on TSS	-8	*cgtR6* cg3061	6.10	2949950	2950260	TGTTGCATATGATACA	1.51E-04	NEW	130

TABLE S7 (Part 2/2) I GlxR peaks and corresponding binding sites found less than 700 bp upstream of the TSS of antisense transcripts, non-protein coding elements or intragenic trasnscripts; information of TSS of asRNA, non-protein coding genes and intragenic transcriptswas taken from Mentz et al. 2013 and Pfeifer-Sancar et al. 2013

intragenic transcript	motif rel. located to intragenic transcript	Distance to respective TSS	neighbouring genes (< 700 bp of a gene start)	EF in $WT_{GlxR\text{-}TS}$ (glc)[a]	Start position[b]	End position[b]	GlxR binding site[c]	E-value	GlxR peak known or new[d]	No.[e]
intragenic transcript within cg0706	downstream	+34		3.60	622394	622684	GGTCTCCAACATCACA	1.51E-04	NEW	133
intragenic transcript within cg1044	upstream	-164	- cg1043 - cg1044	4.59	969818	970084	AGTGACCCCGCACACA	4.02E-05	Toyoda et al. 2011	69
intragenic transcript within cg1111	upstream	-189	*eno* cg1111	5.77	1034624	1034903	CGTGTCCGATCAGACA	7.96E-04	NEW	206
intragenic transcript within cg3313	upstream	-134	*pbp1b (mcrB)* cg3313	3.57	3189069	3189309	TATTCTCTACAGCACA	1.58E-03	NEW	223

tRNA	motif rel. located tRNA	Distance to respective TSS	neighbouring genes (< 700 bp of a gene start)	EF in $WT_{GlxR\text{-}TS}$ (glc)[a]	Start position[b]	End position[b]	GlxR binding site[c]	E-value	GlxR peak known or new[d]	No.[e]
Arg tRNA (cgtRNA_3549)	upstream	-179	- cg0962	2.74	897324	897585	GGTCAATCAGATCACT	7.96E-04	NEW	211
Arg tRNA (cgtRNA_3575)	upstream	-102	- cg2699 *phoB* cg2700	4.89	2600743	2601017	TGTGTGAAGCCCCACA	9.65E-06	NEW	20
Asp tRNA (cgtRNA_3583)	upstream	-12	*sucC* cg2837	3.53	2727036	2727290	TGTGCAGCATTTCACT	4.02E-05	Han et al. 2008, Kohl & Tauch 2009	74
Gly tRNA (cgtRNA_3574)	upstream	-208	- cg2651	2.89	2560699	2560992	TGTACAATAACACACT	3.66E-04	NEW	168
Leu tRNA (cgtRNA_3579)	upstream	-58	- cg2748	5.08	2650220	2650497	GGTGCAGTTGGTCACC	4.06E-04	NEW	173

new annotated genes	motif rel. located tRNA	Distance to respective TSS	neighbouring genes (< 700 bp of a gene start)	EF in $WT_{GlxR\text{-}TS}$ (glc)[a]	Start position[b]	End position[b]	GlxR binding site[c]	E-value	GlxR peak known or new[d]	No.[e]
cg4015	on TSS	+6	*leuA* cg0303	7.65	267974	268292	TGTATGCTTCACCACA	9.14E-05	Toyoda et al. 2011	104
cg4016	upstream	-11	*yggB (mscCG)* cg1434	4.79	1337674	1337947	TGTGTAGCATGACACA	4.44E-06	Kohl & Tauch 2009, Jungwirth et al. 2013	11

a: enrichment factor (EF) of GlxR peak of WTGlxR-TS (glc) ChAP-Seq samples (n=3)

b: nucleotide position refers to genome sequence of BX927147 of *C. glutamicum* ATCC13032 (Kalinowski et al. 2003)

c: motif was detected by using the program MEME-ChIP with the DNA fragment of the detected GlxR peaks as input sequences; the 16 bp sequence shows the most probable GlxR binding site within this sequences

d: if GlxR peak is previously described, the respective literature is mentioned; if the site is only found in our ChAP-Seq results it is described as 'NEW'

e: No. according to Table S3

3 Discussion

In order to survive in a changing environment, organisms have to sense the changing conditions and react in an appropriate way. On the molecular level, complex signalling networks exist for this purpose. Signal transduction at the cellular level often involves small molecules that act as second messengers to transduce external stimuli to one or more effectors in the cell. Such second messengers are for example cyclic nucleotides, (p)ppGpp, or Ca^{2+} (Cashel, 1975; Endo, 2006; Valentini & Filloux, 2016). The cyclic nucleotide cAMP is a ubiquitous molecule and plays a central role in numerous signalling processes throughout all kingdoms of life (Gancedo, 2013). In mammalian cells, for example, cAMP activates protein kinases leading to the phosphorylation of several different proteins involved in diverse cellular mechanisms, such as ion transport or transcriptional regulation (Kopperud et al., 2003). In plants, cAMP was found to be involved in sensing and responding to biotic and abiotic environmental stresses (Gehring, 2010; Jha et al., 2016; Maathuis & Sanders, 2001). In prokaryotes, cAMP was first found to play an important role in carbon catabolite repression (Botsford & Harman, 1992) and later also in virulence and pathogenesis of human pathogenic bacteria and in biofilm formation (Liu et al., 2020; McDonough & Rodriguez, 2011). The cAMP receptor protein (CRP), first described in *E. coli*, is a transcriptional regulator that is able to activate or repress the transcription of various gene targets. CRP homologs are found in various other bacterial genera, such as *Mycobacterium*, *Pseudomonas, Vibrio* or *Corynebacterium* and the plasticity of this system emphasizes the adaptation to the individual needs of the respective organism (Arce-Rodríguez et al., 2012; Skorupski & Taylor, 1997; Stapleton et al., 2010).

The aim of this thesis was to better understand the cAMP signalling network in *Corynebacterium glutamicum,* a model organism for Actinobacteria and in industrial biotechnology. Therefore, the thesis is focused on two aspects: the characterization of an adenylate cyclase-deficient *C. glutamicum* strain, and the investigation of the consequences of a low intracellular cAMP level for the transcriptional activity of the global regulator GlxR.

3.1 The role of CyaB activity in *C. glutamicum*

Four years after the detection of intracellular cAMP in *C. glutamicum*, two groups reported the identification of a membrane-bound adenylate cyclase, named CyaB, an enzyme that catalyses the synthesis of cAMP (Bussmann, 2009; Cha et al., 2010; Kim et al., 2004). Strains with a partly or entirely deleted *cyaB* gene showed a significant drop in the concentration of intracellular cAMP (Cha et al., 2010; Toyoda et al., 2011; Wolf et al., 2020). Moreover, the Δ*cyaB* mutants had a strong growth defect in minimal medium with acetate or glucose plus acetate as carbon source, but not with glucose or ethanol (Bussmann, 2009; Cha et al., 2010; Wolf et al., 2020). As the growth defect in the presence of acetate could be reverted by the addition of cAMP to the medium, the effect was shown to be specific for the deletion of *cyaB* (Bussmann, 2009; Wolf et al., 2020). The reason for the growth defect remained unknown and the theory that it was due to inhibition of acetate uptake by the transporter MctC (Cg0953) could be disproved by the fact that acetate uptake in a *mctC* deletion mutant by passive diffusion across the membrane was sufficient to maintain wild type-like growth (Jolkver et al., 2009). The uptake of acetate was also shown to be transporter-independent in other microorganisms, such as *E. coli* and *Saccharomyces cerevisiae* (Lindahl et al., 2017; Orr et al., 2018).

The 'acetate effect' of the Δ*cyaB* mutant was then hypothesized to be due to a higher sensitivity towards acetate compared to the wild-type strain (Wolf et al., 2020). At higher concentrations, acetate is known to have uncoupler-like behaviour causing a net import of protons, which affects the proton-motive force (PMF) (Axe & Bailey, 1995). A strong incidence for the assmuption that the growth-defect of the Δ*cyaB* mutant was caused by the uncoupling function of acetate was the finding that the acetate sensitivity was concentration- and pH-dependent. The molecular basis for the higher uncoupler sensitivity of the Δ*cyaB* mutant was explained by reduced expression of the genes encoding the cytochrome bc_1-aa_3 supercomplex and the F_1F_O-ATP synthase, as shown in transcriptome array results and RT-qPCR (Wolf et al., 2020). Strong support for this explanation comes from the fact that mutants lacking a functional cytochrome bc_1-aa_3 supercomplex are unable to grow with acetate as sole carbon source (Wolf et al. 2020). Figure 5 illustrates the features described above.

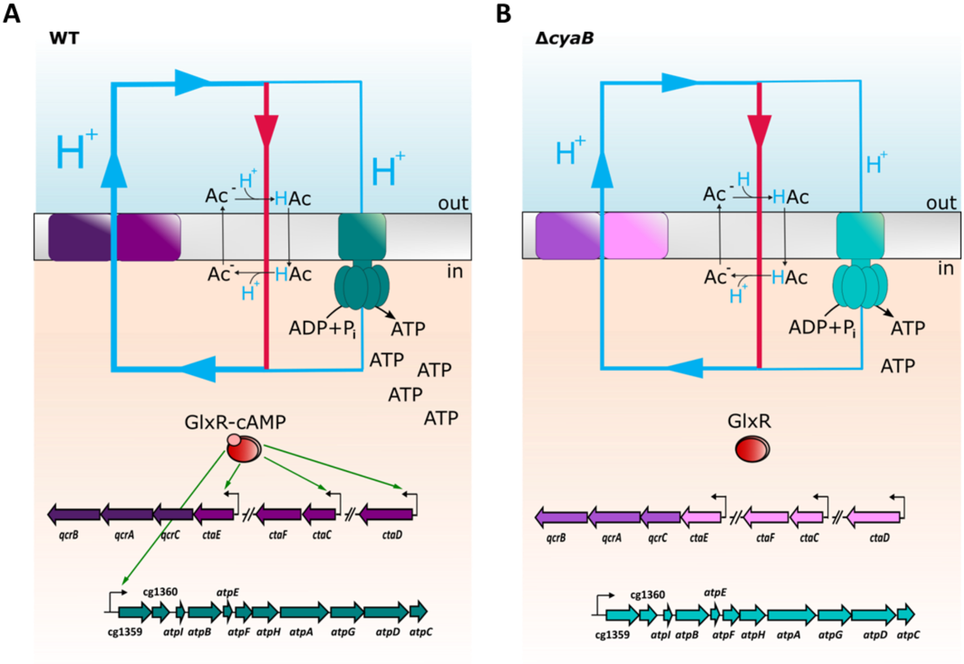

Figure 5: **Model of the proton circuit in the presence of acetate in the *C. glutamicum* WT** (**A**) **and the Δ*cyaB* mutant** (**B**). In this model acetate acts as an uncoupler (red arrow) and disturbs the proton circuit (blue lines) of the respiratory chain (purple) and the ATP synthase (green). In the wild-type strain (WT), the cAMP-GlxR complex (red) activates the transcription of the genes encoding the cytochrome bc_1-aa_3 supercomplex and the F_1F_O-ATP synthase. In the presence of acetate, the capability of generating pmf is disturbed, but not strong enough to cause a growth defect. In the Δ*cyaB* mutant, the reduced or even absent cAMP level causes a lowered expression of the genes for the cytochrome bc_1-aa_3 supercomplex, leading to a reduced capacity to build up pmf and to counteract the uncoupling activity of acetate. Additionally, the growth defect of the Δ*cyaB* mutant on acetate is caused by the reduced ATP synthesis via oxidative phosphorylation due to reduced synthesis of the F_1F_O-ATP synthase.

A Δ*cyaB* strain transformed with fluorescence reporters carrying native promoters of genes of the cytochrome bc_1-aa_3 supercomplex (*ctaC*, *ctaE*, or *ctaD*) in front of a gene encoding a fluorescent protein (mVenus) revealed lower fluorescence and thus lower promoter activity compared to the wild type when cultivated in minimal medium with acetate (Figure 6). The reduction of promoter activity can be explained by a reduced activation of transcription by GlxR due the absence of cAMP in the Δ*cyaB* mutant.

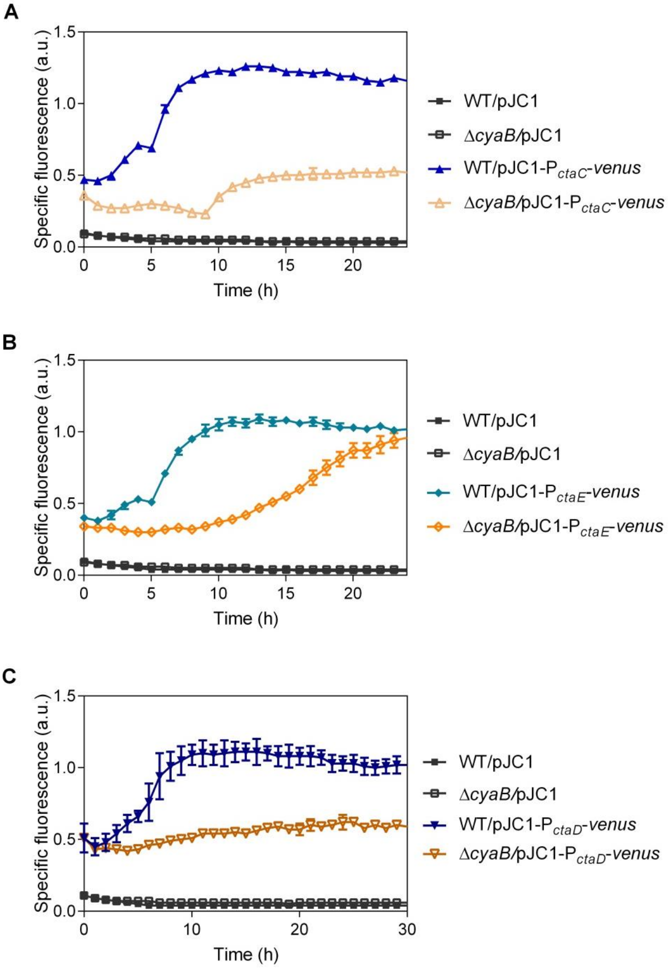

Figure 6: Specific fluorescence of *C. glutamicum* wild type (WT) and the Δ*cyaB* mutant carrying fluorescence reporters with the native promoter of *ctaC* (A), *ctaE* (B), or *ctaD* (C). The first preculture was inoculated in BHI medium and the second preculture was grown in CGXII medium with 2% glucose. The cells were washed with saline (0.9% (w/v) NaCl) and used to inoculate the main cultures in 800 µl CGXII minimal medium with 100 mM potassium acetate as sole carbon sources to an OD_{600} of 1. Cultivation was performed in the BioLector at 30 °C and 1200 rpm. Growth was monitored as scattered light at 620 nm and fluorescence was monitored with an eYFP filter (ex. 508 nm/em. 532 nm). The results of three biological replicates with standard deviations are shown.

In the strain SC^+, the native promoters of *ctaC*, *ctaE*, and *ctaD* have been replaced by the constitutive *tuf* promoter (Platzen, 2013) and therefore their transcription is independent of the cAMP-GlxR complex. However, the inhibitory effect of acetate was also observed in the SC^+ Δ*cyaB* strain (Figure 7). A possible explanation for this result was obtained by the ChAP-Seq results of this work, in which *ctiP* (cg2699) was identified as an additional GlxR target gene. CtiP is a large transmembrane protein that was recently shown to be involved in copper transport and insertion into cytochrome *aa*$_3$ oxidase (Morosov et al., 2018). The GlxR binding site is located 108 bp upstream of the TSS of *ctiP* and therefore transcription of *ctiP* is probably activated by GlxR. Insufficient expression of *ctiP* in the SC$^+$ Δ*cyaB* strain could be responsible for the still observed inhibition by acetate, if only insufficient amounts of functional cytochrome *bc*$_1$-*aa*$_3$ supercomplex can be formed. In addition, a lower expression of the ATP synthase could also contribute to the inhibition of the SC$^+$ Δ*cyaB* strain by acetate, in particular when acetate serves as sole carbon source, which does not allow net ATP synthesis via substrate level phosphorylation.

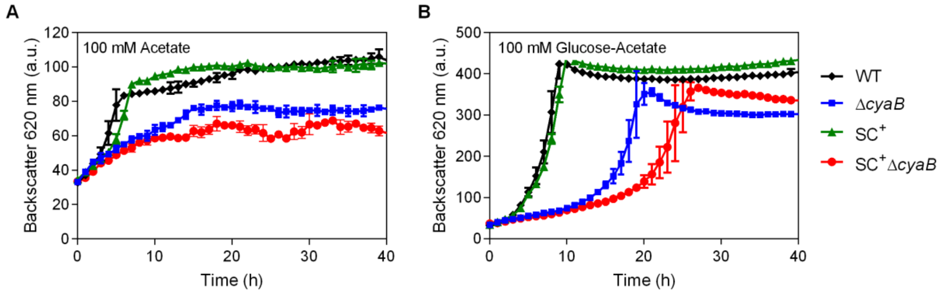

Figure 7: Growth of *C. glutamicum* wild type (WT), the Δ*cyaB* mutant, strain SC$^+$, and the SC$^+$Δ*cyaB* strain. Cells were cultivated in CGXII medium with 100 mM potassium acetate (**A**) or a glucose-acetate mixture, each 100 mM (**B**). The results of three biological replicates with standard deviations are shown. The first preculture was inoculated in BHI medium and the second preculture was grown in CGXII medium with 2% glucose. The cells were washed with saline (0.9% (w/v) NaCl) and used to inoculate the main cultures in 800 µl CGXII minimal medium with the indicated carbon sources to an OD$_{600}$ of 1. Cultivation was performed in a BioLector at 30 °C and 1200 rpm and growth was monitored as scattered light at 620 nm.

3.1.1 Further effects contributing to the ‘acetate effect’ of the Δ*cyaB* mutant

The uncoupler-like behaviour of acetate in combination with the lower transcription and activity of the respiratory chain and ATP synthase in the *cyaB* deletion strain is believed to be the main reason for the inhibition of growth. However, further effects can contribute to the effect of the acetate sensitivity of the *cyaB* mutant. It can be excluded that the change of the extracellular pH during cultivation with acetate is responsible for the inhibited growth, as the initial pH of 7 was the same as the pH at the end of experiments (data not shown). Furthermore, growth experiments in minimal medium with glucose as sole carbon source and with different initial pH values (pH 6-7) showed that the growth of the *cyaB* deletion strain was comparable, suggesting that the absence of CyaB did not lead to problems in the pH homeostasis *per se* (Wolf et al., 2020). Only the combination of pH 6 and the presence of acetate in the medium increased the growth inhibition of the Δ*cyaB* mutant compared to the growth at pH 7 (Wolf et al., 2020). This could be explained due to the fact that weak acids such as acetic acid act as a proton translocator more effectively if the pH of the medium is closer to its pK_a (acetic acid pK_a 4.76). So the acetate effect was described as pH-dependent. Growth of the *cyaB* deletion strain was tested with other salts such as citrate and L-lactate. Only slightly impaired growth of the *cyaB* deletion strain was observed when cultivated with citrate (100 mM) or L-lactate (100 mM) as carbon source (Figure 8). The growth differences of WT and the *cyaB* deletion strain with citrate and lactate as carbon sources is a further phenotypical characterisation of the *cyaB* deletion strain. However, the growth differences are more likely due to reduced GlxR activity in the Δ*cyaB* mutant and are not a pH-effect.

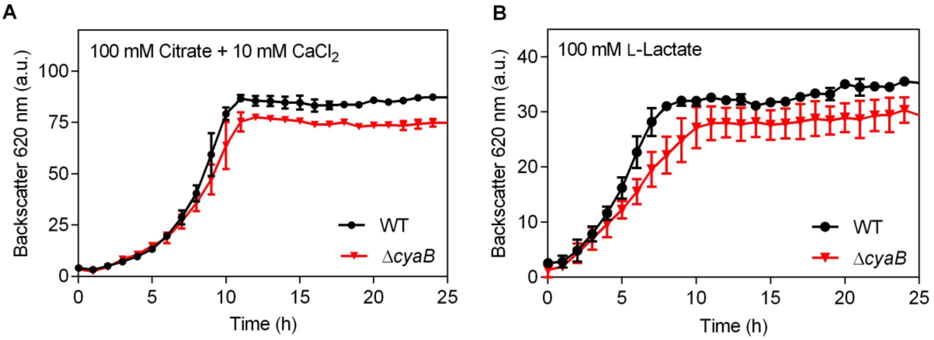

Figure 8: Growth of *C. glutamicum* WT and the Δ*cyaB* mutant in CGXII minimal medium with 100 mM citrate (A) or 100 mM L-lactate (B). The first preculture was inoculated in BHI medium and the second preculture was performed in CGXII medium with 2% (w/v) glucose. The cells were washed with saline (0.9% (w/v) NaCl) and used to inoculate the main cultures in 800 µl CGXII minimal medium with the indicated carbon sources to an OD_{600} of 1. Growth was monitored as scattered light at 620 nm in a BioLector at 30 °C and 1200 rpm. Mean values and standard deviations of three biological replicates are shown.

As GlxR is a global regulator, one cannot exclude further transcriptional changes of genes to be involved in the higher sensitivity towards acetate and the strong sensitivity towards the protonophore CCCP. Due to the absence of cAMP in the Δ*cyaB* mutant, genes that would normally be activated by the cAMP-GlxR complex often showed a lower transcription compared to the genes in the wild-type strain (Wolf et al., 2020). As already mentioned, a lower transcription of the newly identified GlxR target gene *ctiP*, a gene coding for a transmembrane protein involved in copper transport and insertion into cytochrome *aa*$_3$

oxidase (Morosov et al., 2018) probably contributes to the enhanced sensitivity of the Δ*cyaB* mutant towards uncouplers.

Moreover, changes in cell envelope of *C. glutamicum* Δ*cyaB* compared to the wild-type strain could also favour the higher uncoupler-sensitivity. Recent studies on the role of cAMP in *Mycobacterium* revealed that decreased intracellular cAMP level led to a perturbation of the peptidoglycan biosynthesis that probably resulted to increased cell envelope permeability (Thomson et al., 2022). The higher cell envelope permeability was supposed to be the reason for a higher susceptibility towards antimicrobials targeting the cell wall synthesis (e.g. ethambutol or vancomycin).

In the yeast *S. cerevisiae* it was shown that changes in the membrane lipid profile increased the acetic-acid tolerance (Guo et al., 2018; Zheng et al., 2013). For example, the acetic acid-tolerant *S. cerevisiae* YJS329ELO1 (carrying a plasmid, overexpressing a fatty acid desaturase) showed 17.6% higher levels of oleic acids (C18:1n-9) and an improved tolerance to acetic acid compared to the parental strain YJS329 (Guo et al., 2018; Zheng et al., 2013). The increased amount of unsaturated fatty acids in the plasma membrane probably led to a reduction of the diffusion rate of acetic acid, which is in yeast critical because the weak acid was shown to enter the cell mainly in a transporter-independent way by passive diffusion through the membrane lipid bilayer (Lindahl et al., 2017).

Previous studies showed that the *C. glutamicum* wild-type strain is moderately alkali-tolerant and is able to maintain a quite stable intracellular pH around pH 7.5 when cultivated at external pH values between 6.0 and 9.0 (Barriuso-Iglesias et al., 2008; Follmann et al., 2009). To sustain a physiological intracellular pH value, *C. glutamicum* has different cellular mechanisms to resist external acidic or alkaline pH stress. Sigma factors were shown to play a crucial role under pH stress conditions in *C. glutamicum* (Barriuso-Iglesias et al., 2013; Jakob et al., 2007). For example *sigB* (cg2102), which is related to the general stress response, was upregulated under acidic stress conditions and therefore this sigma factor probably contributes to the maintenance of pH homeostasis (Jakob et al., 2007). Experiments with bacteria such as *B. subtilis* and *Listeria monocytogenes* showed that the absence of a functional *sigB* gene led to higher sensitivity towards acidic pH (Hecker & Völker, 2001; Wiedmann et al., 1998). In *C. glutamicum*, the sigma factor H (SigH, Cg0876) is important in the response to heat shock and oxidative stress (Kim et al., 2005) and later experiments suggested that SigH was involved in the transcriptional control of the F_1F_0-

ATPase operon at alkaline pH of 9 (Barriuso-Iglesias et al., 2013). Not only stress responses, but several cellular processes are involved in sustaining intracellular pH homeostasis. For example, a connection between pH responses, oxidative stress, iron homeostasis, and methionine synthesis was suggested (Follmann et al., 2009). Furthermore, a link between sulphur assimilation and the repression of oxidative stress in the maintenance of pH homeostasis was reported (Xu et al., 2019). It was stated that the repression of genes involved in sulphur metabolism by the transcriptional regulator McbR lead to a reduction of L-cysteine accumulation, which turned out to be advantageous under acidic acid stress conditions (Xu et al., 2019). If the bacterium is not able to react properly to changing pH conditions, a change of the cytoplasmic pH by one unit can lead to changes not only in the PMF, but also in the activity and stability of enzymes, in transcription or translation, in solubility of trace elements, or in the structure of nucleic acids (Follmann et al., 2009; Krulwich et al., 2011; Olson, 1993). The ability to maintain a physiological internal pH could be impaired in the *cyaB* deletion strain, which could contribute to the acetate effect.

These effects could add to the effect that the Δ*cyaB* mutant has already an impaired energy metabolism due to lower expression of the respiratory chain genes and the genes coding for the F_1F_0 ATP synthase as shown in Toyoda et al., 2011 and in Wolf et al., 2020. In order to prove whether the pH homeostasis is less efficient in Δ*cyaB* mutant one could compare the intracellular pH (pH_i) of the wild-type strain and the Δ*cyaB* mutant when cultivated with acetate as carbon source. Such measurements were already successfully performed by staining the cells with pH-sensitive fluorochromes and comparison of the cell fluorescence by a flow cytometer (Leyval et al., 1997). Nowadays, pH_i can be monitored online within different *C. glutamicum* strains when they carry a plasmid encoding a pH sensitive variant of GFP, called pHlourin (Kirsch, 2014; Miesenböck et al., 1998). A difference in the pH_i between the *C. glutamicum* wild type and the *cyaB* deletion strain cannot be excluded. However, despite many possible reasons for an impaired pH homeostasis (e.g. malfunction of transporters or regulatory proteins), these should contribute only to a lesser extent to the acetate sensitivity in the Δ*cyaB* mutant. Still, a functional respiratory chain is obviously the most important factor that contributes to the pH regulation in acidic environments in *C. glutamicum*. All secondary active transporters, such as Mrp1, require the proton motive force (pmf) established by the cytochrome *bc*$_1$-*aa*$_3$ supercomplex to be active. In the *C. glutamicum* DOOR strain that is absent of terminal oxidases (Koch-Koerfges et al., 2013), it was shown that the pH homeostasis was disturbed compared to the wild type strain, especially when the external pH drops below pH 7 (ΔpH 0.51 and 1.09 at pH 6, respectively). Experiments with *E. coli* showed that the direct involvement of terminal oxidases and oxidative phosphorylation plays a crucial role in the pH homeostasis. Acid stress led to an upregulation of the proton-pumping components of the respiratory chain in *E. coli* (Cotter et al., 1990; Maurer et al., 2005; Slonczewski et al., 2009; Sun et al., 2012). These experiments underline that the cytochrome *bc*$_1$-*aa*$_3$ supercomplex is the most important factor for the adaptation of *C. glutamicum* to acidic conditions, because it ensures that protons are pumped out of the cell.

3.1.2 CyaB as the main adenylate cyclase in *C. glutamicum*

Because a residual intracellular cAMP concentration was still detected in AC-deficient mutants of *C. glutamicum* (Bussmann, 2009; Cha et al., 2010; Toyoda et al., 2011), the existence of a second AC was expected. However, bioinformatic analyses using a protein-protein basic local alignment search tool (BLASTP) did not reveal hits for another AC besides CyaB (Cg0375) in *C. glutamicum*. A domain-enhanced lookup time accelerated blast (DELTA-BLAST) (Boratyn et al., 2012) with the amino acid sequence of the representative AC of class IV (AC2 or CyaB$_{Aer}$ of *Aeromonas hydrophila*) (Sismeiro et al., 1998) and a proteome database of *C. glutamicum* ATCC13032 as a reference, resulted in one hit (Table 2).

Table 2: Results of DELTA-BLAST (Boratyn et al., 2012). DELTA-BLAST of the amino acid sequence of AC2 (also described as CyaB$_{Aer,}$; UniProt No. O69199/CYAB_AERHY) of *Aeromonas hydrophila* as query sequence and a database comprising non-redundant protein sequences of *C. glutamicum* ATCC13032 as the search set.

Protein Name	Percent Identity	Query Cover	Max Score	Total Score	E-value
Cgl2231*[1]	16.86%	74%	74.3	74.3	9e-17

*[1]: The gene encoding for Cgl2231 (Accession: BAB99624.1) has the same coding sequence as cg2450 in the genome of *C. glutamicum* ATCC13032 (BX927147) sequenced by Kalinowski et al., 2003.

The 191 aa long AC2 of *A. hydrophila* showed sequence similarities within the first 240 aa of the protein Cg2450 of *C. glutamicum*. Cg2450 is an uncharacterized protein that is predicted to be putative pyridoxine biosynthesis enzyme (CoryneRegNet 6.0) (Pauling et al., 2012). It contains a CYTH domain and a CHAD domain (PF01928/IPR023577 and PF05235/IPR007899, respectively). The CHAD protein domain stands for ‘conserved histidine α-helical domain’ and is found in all kingdoms of life and putatively involved in binding of inorganic polyphosphates (Lorenzo-Orts et al., 2019). The CYTH domain is a catalytic domain that is named after the first known members, the AC CyaB of *A. hydrophila* and thiamine triphosphatase of mammalian cells (Bettendorff & Wins, 2013). Both enzymes have in common that they need triphosphorylated substrates and require at least one divalent metal cation for the catalytic reaction (Bettendorff & Wins, 2013). The AC2 (CyaB_{Aer}) of *A. hydrophila* was first described in 1998 and was until 2006 the only bacterial AC member of the class IV AC (Smith et al., 2006). A cAMP-synthesizing activity was only shown under *in vitro* conditions, revealing extraordinary biochemical characteristics, with an optimal activity at 65 °C and a pH of 9.5 (Sismeiro et al., 1998). Under physiological conditions the gene coding for the AC2 was not expressed in *A. hydrophila* and so far no cultivation conditions were found that led to transcription of the AC2 gene (Sismeiro et al., 1998). The presence of a CYTH domain in the protein Cg2450 of *C. glutamicum* suggests that this could be a second AC. Previous studies in our lab by Julia Schulte showed that it was easily possible to obtain a cg2450 deletion mutant and also a double mutant lacking both *cyaB* and the cg2450 gene. The double deletion mutant Δcg2450Δ*cyaB* had comparable growth curves with the Δ*cyaB* mutant when cultivated in medium containing acetate as carbon source (data not shown). Also, the Δcg2450 strain showed no growth defect in minimal medium that contained acetate, which argues against the assumption that cg2450 encodes a second functional AC in *C. glutamicum* (data not shown). Whether Cg2450 catalyses cAMP synthesis *in vitro,* was not tested yet.

3.2 Intracellular cAMP concentration of *C. glutamicum* compared to other bacteria

Intracellular cAMP levels are controlled by the rate of synthesis by adenylate cyclases, the rate of degradation by phosphodiesterases, and possibly by export of cAMP. Because of the various ways of regulation, intracellular cAMP levels are highly variable in different bacterial species. Whereas *M. tuberculosis* and *M. smegmatis* are considered to be species with a high intracellular cAMP concentration, harbouring up to 4 mM cAMP (Dass et al., 2008; Padh & Venkitasubramanian, 1976), *E. coli* is considered as a bacterium with a moderate cAMP level of about 35-40 µM (Bennett et al., 2009; Notley-McRobb et al., 1997) and *Pseudomonas putida* has a cAMP concentration around 0.07-0.12 µM (measured by cAMP radioimmunoassay), whereas no cAMP could be detected applying HPLC methods (Arce-Rodríguez et al., 2012; Arce-Rodríguez et al., 2021; Phillips & Mulfinger, 1981). When comparing the intracellular cAMP levels of the mentioned bacteria with those reported for *C. glutamicum,* one would consider *C. glutamicum* as a species with a low cAMP level. Table 3 gives an overview of the intracellular cAMP concentrations and the binding affinities of CRP-like proteins to cAMP. In all earlier mentioned bacteria, cAMP is a part of a signalling pathway that involves binding of a CRP-like protein which harbours a cAMP-binding domain. And similar to the different intracellular cAMP concentrations, the cAMP-binding affinities for the respective CRP-like proteins are different (Arce-Rodríguez et al., 2012; Ren et al., 1990; Stapleton et al., 2010; Townsend et al., 2014).

Table 3: Comparison of cAMP concentrations and the properties of CRP-like proteins and cAMP phosphodiesterases in *P. putida, C. glutamicum*, *E. coli*, and *M. tuberculosis*.

Species	***P. putida***	***C. glutamicum***	***E. coli***	***M. tuberculosis***
Cytoplasmic cAMP concentration	**Low** (0.07 µM-0.12 µM or below detection limit) (Arce-Rodríguez et al., 2021; Milanesio et al., 2011; Phillips & Mulfinger, 1981)	**Low** (~ 1 µM) (Wolf et al., 2020)	**Moderate** (35 µM-40 µM) (Bennett et al., 2009; Notley-McRobb et al., 1997)	**High** (up to 4 mM) (Bai et al., 2009; Padh & Venkitasubramanian, 1976)
CRP-like protein: K_d for cAMP	**CRP (PP0424):** 23 nM–45 nM (Arce-Rodríguez et al., 2012; Arce-Rodríguez et al., 2021)	**GlxR (Cg0350)**: K_{d1}: 17 µM, K_{d2}: 130 µM (Townsend et al., 2014)	**CRP (ECK3345)**: 19 µM–39 µM (Ren et al., 1990; Takahashi et al., 1980)	**Crp (Rv3676)**: 170 µM (Stapleton et al., 2010) **Cmr (Rv1675c)**: n.d. (Gazdik et al., 2009; McCue et al., 2000)
Phosphodiesterase (PDE): K_m for cAMP	**PDE (PP4917)**: n.d.	**CpdA (Cg2761)** K_m: 2.5 mM (Schulte et al., 2017)	**CpdA (ECK3032)**: 500 µM (Imamura et al., 1996)	**CpdA (Rv0805)**: 200 µM (Shenoy et al., 2005) **Rv1339**: n.d. (Thomson et al., 2022)

The highest binding affinity of a CRP-like protein to cAMP shows the CRP protein of *P. putida*. This correlates with the fact that this organism has a very low intracellular cAMP concentration. When comparing the cAMP-binding affinities of the CRP-like proteins of *M. tuberculosis*, *E. coli* and *P. putida* it seems as if there is a link between binding affinities and the intracellular cAMP concentration. *C. glutamicum* would be considered to be an organism with a low intracellular cAMP level, but the cAMP-binding affinity of GlxR seems rather low compared to the intracellular cAMP concentration. *In vivo* GlxR binding studies performed in this work showed that GlxR binding to DNA can occur independent of cAMP and that in most cases the presence of cAMP only enhanced the affinity to DNA binding regions. On the other hand a high intracellular cAMP level seems to be detrimental for *C. glutamicum* as seen in the mutant lacking the phosphodiesterase CpdA (Schulte et al., 2017). The presence and activity of the CpdA plays a key role in the regulation of the intracellular cAMP level. This is surprising considering that the *in vitro* assays with purified CpdA showed a relatively high K_m for cAMP (2.5 mM), far above the measured cytoplasmic concentrations (~1 µM).

It is noticeable that not only the cAMP levels between different species can vary, but also the level within the same strain can be drastically different (Table 1). Literature references provide data of different intracellular cAMP levels of the same strain, for example due to different cultivation conditions (Bai et al., 2009; Kim et al., 2004). The variation of the cAMP concentration in cells of a particular species can be due to differences in the analytical methods used to determine the cAMP concentrations. However, many other factors can also have an influence on the intracellular cAMP level, such as stress conditions or carbon sources.

3.3 The role of cAMP for the *in vivo* activity of GlxR

In 2004 the protein GlxR (Cg0350) was identified as a CRP-like transcriptional regulator with cAMP- and DNA-binding properties (Kim et al., 2004; Townsend et al., 2014). As an approach to determine the role of intracellular cAMP for the *in vivo* activity of GlxR, transcriptome and ChAP-Seq studies with the wild type and an adenylate cyclase deletion strain were performed. Previous studies assumed that GlxR only binds DNA when cAMP is present, as shown by *in vitro* tests, such as electrophoretic mobility shift assays (EMSAs) (Bussmann et al., 2009; Jungwirth et al., 2013; Kohl et al., 2008). First studies of the *in vivo* GlxR binding activity also in the genome background of a *cyaB* deletion mutant of strain R showed that GlxR did still bind to DNA (Toyoda et al., 2011). It was assumed that the reason for that result was residual cAMP that was still measured in the *cyaB* mutant. However, in the ChAP-Seq assays that were performed during this work, it was shown that *in vivo* GlxR binds in a Δ*cyaB* mutant in which cAMP was under the detection limit of an LC-MS/MS method (Wolf et al., 2020). This suggests that GlxR can bind to many DNA regions also in the absence of its physiological effector cAMP. In the Δ*cyaB* mutant the binding of GlxR to DNA was reduced particularly in the presence of acetate. Thus GlxR binding *in vivo* is probably less dependent on cAMP than GlxR binding *in vitro* and additional, yet unknown factors might be involved in the control of GlxR binding to DNA within the cell.

3.3.1 Further CRP-like proteins in *C. glutamicum*

As already mentioned in the introduction of this work, *C. glutamicum* encodes two additional proteins sharing protein domains with GlxR (Figure 2C). The protein Cg1327 is composed of the same protein domains as GlxR, whereas the protein Cg3291 lacks the cNMP-binding domain but carries the HTH_CRP domain that is found in CRP-like proteins (Figure 2C). Therefore, these proteins, especially Cg1327 might have functions related to GlxR. To find out more about the role of Cg1327 in *C. glutamicum*, the corresponding gene cg1327 was successfully deleted and first growth experiments of the Δcg1327 mutant in comparison with the WT were performed in minimal medium containing glucose, gluconate, acetate, citrate, or ethanol as carbon sources (Figure 9A-E).

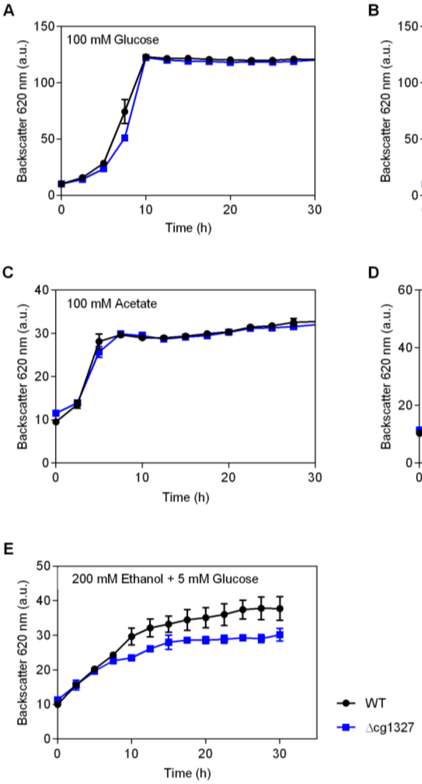

Figure 9: Growth behaviour of *C. glutamicum* wild type (WT) and a Δcg1327 mutant on different carbon sources. The strains were cultivated in CGXII minimal medium containing 100 mM glucose (**A**), 100 mM gluconate (**B**), 100 mM acetate (**C**), 50 mM citrate supplemented with 5 mM $CaCl_2$ (**D**) or 200 mM ethanol supplemented with 5 mM glucose (**E**). The first preculture was inoculated in BHI medium and the second preculture was grown in CGXII medium with 2% glucose. The cells were washed with saline (0.9% (w/v) NaCl) and used to inoculate the main cultures in 800 µl CGXII minimal medium with the indicated carbon sources to an OD_{600} of 1. Growth was monitored as scattered light at 620 nm in a BioLector at 30 °C and 1200 rpm. Mean values and standard deviations of three biological replicates are shown.

No differences in growth behaviour were observed on the tested carbon sources except during cultivation with ethanol (Figure 9E), where the initial growth kinetics was comparable, but the Δcg1327 mutant did not reach the same final backscatter as the WT control. This suggests that Cg1327 is functional in *C. glutamicum* and directly or indirectly involved in ethanol metabolism. Further experiments, such as analysis of DNA-protein interactions (e.g. by fluorescence anisotropy), cAMP-binding studies with purified Cg1327 as well as ChAP-Seq and microarray experiments should be performed to characterize the biochemical properties, target genes, and physiological functions of Cg1327.

Species phylogenetically related to *Corynebacterium*, such as *M. smegmatis*, have two active CRP-like proteins (Msmeg_0539 and Msmeg_6189; 78.48% identity and 99% query cover using BLASTP), which were shown recognize the same consensus sequence, but possess distinct regulons with a small set of overlapping genes, such as the succinate dehydrogenase operon *sdh1* (Aung et al., 2015). EMSAs with the two purified Crp proteins showed that Msmeg_0539 bound to the promoter DNA of the succinate dehydrogenase operon in a cAMP-independent way. BLASTP alignment results of GlxR with Msmeg_0539 and Msmeg_6189 showed 70.59% and 80.36% identity with 97% and 98% query cover, respectively. On the other hand, the results for BLASTP alignment of Cg1327 with Msmeg_0539 and Msmeg_6189 had a low identity (23.65% and 25.87%, respectively) and a lower query cover (both 80%).

3.3.2 cAMP-GlxR system important for energy metabolism in *C. glutamicum*

In this work, for the first time suppressor mutants of *C. glutamicum* Δ*cyaB* were isolated that no longer showed the growth inhibition by acetate. The suppressor mutants were obtained by an at least 80 h cultivation of a Δ*cyaB* mutant in minimal medium with an initial acetate concentration of 150 mM as only carbon source (Wolf et al., 2020). One suppressor mutant showed clear evidence for the correlation of acetate sensitivity and GlxR regulation: Δ*cyaB*_sup1 had only one point mutation in *glxR*, which indicated that the acetate sensitivity of the parental Δ*cyaB* strain is due to a malfunction of GlxR-dependent regulation at low intracellular cAMP levels in the presence of acetate. This suppressor mutant expressed the transcriptional regulator GlxR with an amino acid exchange Ala131Thr. Amino acid residue 131 is located within the central alpha helix 5, which is involved in cAMP-binding (Townsend et al. 2014). When this amino acid exchange was introduced into the original Δ*cyaB* mutant, it abolished the acetate sensitivity of this strain, confirming that this single amino acid exchange was responsible for phenotype of the suppressor mutant. First experiments with the GlxR$_{\text{Ala131Thr}}$ variant revealed that *in vitro* DNA-binding was still dependent on cAMP (Wolf et al., 2020). Further experiments are needed to elucidate why the cell benefits from this mutation when the intracellular cAMP level is low.

3.3.3 Closer look at suppressor mutants *C. glutamicum* Δ*cyaB* _sup2 and Δ*cyaB* _sup3

The suppressor strain Δ*cyaB*_sup3 showed the same Ala131Thr mutation in the coding region of *glxR* as strain Δ*cyaB*_sup1, but carried also an additional silent mutation in the *rpi* gene (cg2658) encoding ribose 5-phosphate isomerase. The mutation is a change from C to A (318 bp) in the open reading frame of *rpi*, leading to a change of the base triplet GGC to GGA coding for the amino acid glycine at amino acid position 106. Tables of the codon usage frequency show that the triplet GGA is less favoured than the triplet GGC (15.2% and 34.1%, respectively) (https://www.kazusa.or.jp/codon/) in *C. glutamicum*. It remains unclear if the *rpi* mutation in the suppressor strain Δ*cyaB*_sup3 has additional benefits beside the *glxR*-Ala131Thr mutation.

Another suppressor mutant, strain Δ*cyaB*_sup2, did not show any mutation in the *glxR* coding region, but instead in two intergenic regions. One point mutation was located in the intergenic region of *serC* (cg0948) and *gltA* (cg0949) and second one in the intergenic region of *gpt* (cg1659) and cg1660. The transcription of *gltA* is known to be repressed by GlxR (van Ooyen et al., 2011). However, the mutation in the intergenic region of *serC* and *gltA* is not located within the GlxR binding motif (Figure 10).

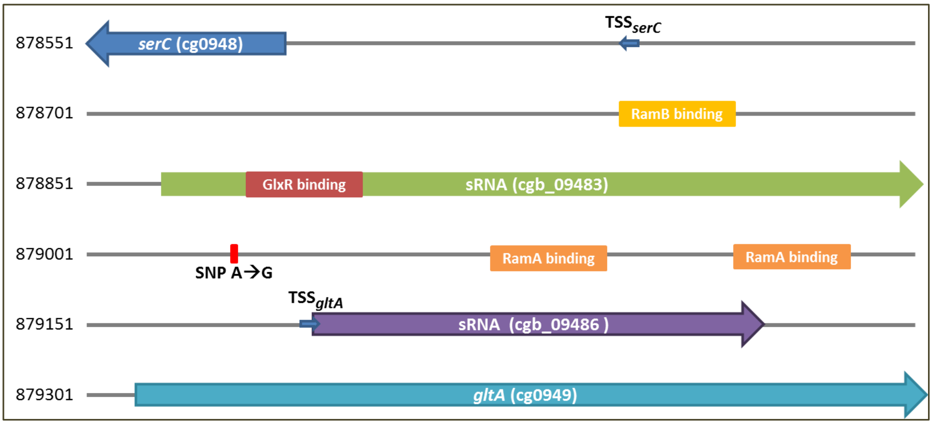

Figure 10: Schematic overview of the genomic region with the single nucleotide polymorphism (SNP) in the *C. glutamicum* Δ*cyaB*_sup2 suppressor mutant. The mutation is located in the intergenic region of *serC* and *gltA*. The mutation is located upstream of an sRNA (cgb_09486). Binding sites of the transcriptional regulators RamB, GlxR, and RamA are highlighted. Information on sRNAs and transcriptional start sites (TSS) were taken from Mentz et al., 2013 and Pfeifer-Sancar et al., 2013.

However, when having a closer look at the location of the mutation in the intergenic region of *serC* and *gltA*, one can see that the mutation is between the sRNA cgb_09483 and closely located upstream of another sRNA, cgb_09486. So far, the biological functions of these two sRNAs are not known, but the mutation could influence the transcription of an sRNA. In general, sRNAs are often located within intergenic regions and can regulate transcription or translation of their target genes or can alter a protein activity upon binding (Georg & Hess, 2011; Storz et al., 2011).

The second mutation in the Δ*cyaB*_sup2 suppressor strain was located in the intergenic region of *gpt* and cg1660 and could lead to an altered gene transcription. The genes *gpt* and cg1660 were not described as GlxR targets so far and other transcriptional regulators involved in the expression of these genes are not known yet. Transcriptome data showed that in the Δ*cyaB* mutant, the expression of *gpt* was lower compared to the wild type (mRNA ratio Δ*cyaB*/WT 0.56, p-value 0.045), whereas expression of cg1660 was significantly higher in the Δ*cyaB* mutant compared to the wild type (mRNA ratio 3.16, p-value 0.0068) when cultivated in minimal media with a glucose-acetate mixture (Bussmann, 2009; Wolf et al., 2020). This shows that the lack of the adenylate cyclase has an influence on the transcription of *gpt* and cg1660. It would be interesting to know if the suppressor mutant Δ*cyaB*_sup2 has a wild type-like transcription of *gpt* and cg1660, which would suggest that Gpt and/or

Cg1660 play a role in the tolerance to high acetate concentrations. Gpt is annotated as a purine phosphoribosyltransferase (PRT) (Kalinowski et al., 2003). In general, purine PRTs are described to catalyse the reversible transfer of a phosphoribosyl group from phosphoribosylpyrophosphate (PRPP) to a purine base (adenine, guanine, hypoxanthine, or xanthine) (Craig III & Eakin, 2000). Bioinformatic analysis of Cg1660 suggests that it might function as a manganese (Mn^{2+}) efflux pump belonging to the MntP family (PF02659/IPR003810) (Waters et al., 2011). In some bacteria Mn^{2+} is important for the protection against oxidative stress (Anjem et al., 2009). It is possible that already one of the mutations found in the suppressor strain Δ*cyaB*_sup2 is sufficient to rescue the acetate effect. To clarify this point, the mutations have to be introduced separately and together in the Δ*cyaB* mutant and tested. Furthermore, the effects of these mutations on the expression of the neighbouring genes need to be analysed.

The suppressor strain Δ*cyaB*_sup2 shows that there is an alternative way beside the described *glxR* mutation to overcome the 'acetate sensitivity' and thus the lack of cAMP in the *C. glutamicum* Δ*cyaB* strain. It would be interesting to test if the mutations in *C. glutamicum* lead to an improved acetate tolerance. This ability could be interesting for biotechnological applications in which strains in fermentation processes are confronted with high acetate concentrations.

3.4 Universal stress protein as putative cAMP binding protein

Recently, a universal stress protein (Usp) of *M. tuberculosis* and *M. smegmatis* was described to be a cAMP-binding protein (Rv1636 and MSMEG_3811, respectively) (Banerjee et al., 2015). These proteins do not have a classical cyclic nucleotide-binding domain, but the binding of Usp to cAMP in *M. smegmatis* was confirmed by cAMP affinity chromatography and verified by isothermal titration calorimetry (ITC) (Banerjee et al., 2015). Proteins that belong to the Usp protein family were described to be involved in stress responses because their synthesis was induced upon different stress conditions, such as starvation for glucose or phosphate, the entry into the stationary phase in rich medium, exposure to heat, or in the presence of uncouplers (Nystrom & Neidhardt, 1992). The biological function of cAMP-binding to Usp in mycobacteria was described to be an additional regulation of the intracellular 'free' cAMP level and therefore a regulation of the downstream effects of cAMP. In another publication, it was shown that Rv1636 of *M. tuberculosis* is in the top twenty of the most abundant proteins of the organism, which supports the hypothesis that this protein acts as a cAMP reservoir (Schubert et al., 2013).

To find out if *C. glutamicum* harbours orthologues of Rv1636 and MSMEG_3811, a BLASTP search (States and Gish 1994) was performed and revealed that the *C. glutamicum* genome harbours five proteins that belong to the Usp family (Figure 11).

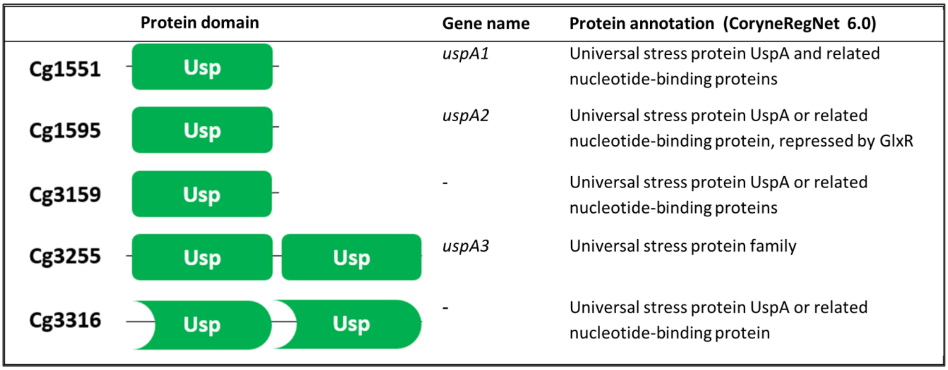

	Protein domain	Gene name	Protein annotation (CoryneRegNet 6.0)
Cg1551	Usp	*uspA1*	Universal stress protein UspA and related nucleotide-binding proteins
Cg1595	Usp	*uspA2*	Universal stress protein UspA or related nucleotide-binding protein, repressed by GlxR
Cg3159	Usp	-	Universal stress protein UspA or related nucleotide-binding proteins
Cg3255	Usp Usp	*uspA3*	Universal stress protein family
Cg3316	Usp Usp	-	Universal stress protein UspA or related nucleotide-binding protein

Figure 11: **Proteins of *C. glutamicum* that are carrying at least one Usp (universal stress protein) domain** (Pfam: PF00582 (El-Gebali et al., 2018); InterPro IPR014729 (Mulder & Apweiler, 2008)).

Cg1551 (UspA1) showed the highest sequence identity (44-50%) to MSMEG_3811 of *M. smegmatis* and Rv1636 of *M. tuberculosis* (Table 4).

Table 4: Results of BLASTP alignment (Altschul et al., 1990) of two sequences using Usp (MSMEG_3811) of *M. smegmatis* as reference protein and depicted protein sequence (Cg1551, Cg1595, Cg3195, Cg3255 or Cg3316) as subject sequence.

Protein name	Percent identity	Query cover	Max score	Total score	E-value
Cg1551/ UspA1	51.75%	97%	105	105	3e-34
Cg1595/ UspA2	28.40%	97%	35	35	8e-08
Cg3159/-	24.31%	95%	30.8	30.8	2e-06
Cg3255/ UspA3	27.81%	97%	36.2	70.8	9e-08
Cg3316/-	29.73%	30%	41.2	41.2	0.013

Therefore, Cg1551 of *C. glutamicum* was further analysed in this work. A crystal structure of MSMEG_3811 with bound cAMP (PDB: 5ahw) revealed the amino acid residues that are most important for binding of cAMP, namely Gly10, Ala40, and Gly114 (Banerjee et al., 2015). These residues are conserved in Cg1551 (Figure 12), as well as the ATP-binding motif ($GX_2GX_9G(S/T)$) that is found in some Usp family proteins (Mbah, 2014; Sousa & McKay, 2001). If Rv1636 and MSMEG_3811 serve as cAMP reservoirs in mycobacteria, this could also be true for *C. glutamicum*. Similar to the situation in mycobacteria, cg1551 is highly expressed (top 50 proteins) on the transcriptional level (personal communication Jörn Kalinowski, Bielefeld, Germany) and the protein was found to be highly abundant on 2D gels (Schaffer et al., 2001).

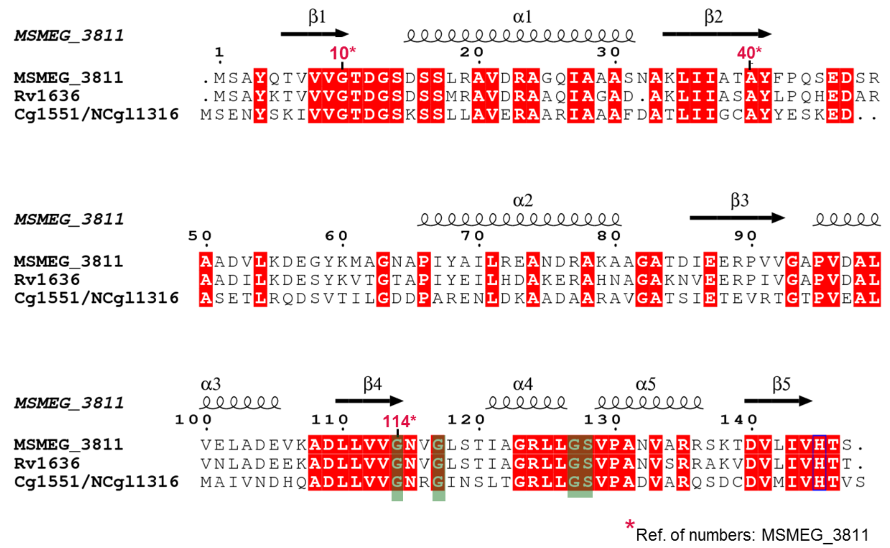

Figure 12: **ClustalW alignment of MSMEG_3811, Rv1636 and Cg1551 (UspA1).** The amino acid sequence of MSMEG_3811 was used as the query. Identical amino acids of the three proteins are highlighted in red. Red numbers marked with an asterisk designate amino acids (Gly10, Ala40, and Gly114) important for cAMP binding according to Banerjee et al., 2015. Green highlighted are the conserved amino acids of the motif $GX_2GX_9G(S/T)$, an ATP-binding domain found in USPs (Mbah, 2014; Sousa & McKay, 2001). The alignment was performed with ClustalW (Thompson et al., 1994) and further processed with Espript (Robert & Gouet, 2014).

ITC experiments with purified Cg1551 could be used to determine if the protein binds cAMP. In mycobacteria, the affinity of Usp for cAMP (K_d ~3 µM) was more than 50 times higher compared to the affinity of CRP for cAMP (K_d ~170 µM), which is also a hint for the possible role of UspA as a cAMP reservoir (Banerjee et al., 2015; Stapleton et al., 2010). Previous analysis of *uspA* mutants of *E. coli* showed a growth rate similar to the parental strain, but the growth was delayed, no matter in which medium the mutant was grown (Nystrom & Neidhardt, 1993). In this work, a *C. glutamicum* Δcg1551 deletion mutant was generated to find out if the lack of this gene has likewise an influence on the cell vitality. The cultivations indeed revealed that the Δcg1551 mutant has a prolonged lag phase (around 3 h in BHI and 5 h in minimal media) compared to the wild type (Figure 13). Moreover, the Δcg1551 mutant had a lower final backscatter when cultivated in CGXII minimal medium with glucose.

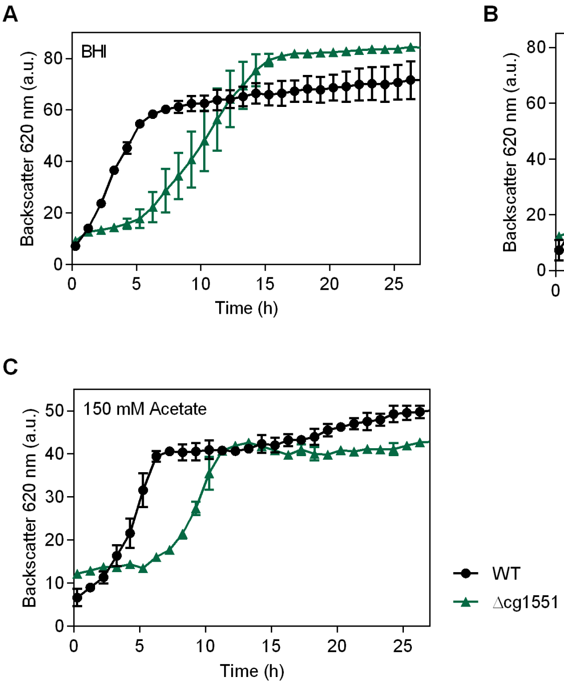

Figure 13: Growth behaviour of *C. glutamicum* wild type (WT) and a Δcg1551 mutant on different carbon sources. The first preculture was inoculated in BHI medium and the second preculture was performed in BHI (**A**) in CGXII medium with 50 mM glucose (**B**) or with 150 mM acetate (**C**) as carbon source. The cells were washed with saline (0.9% (w/v) NaCl) and used to inoculate the main cultures in 800 µl CGXII minimal medium to an OD_{600} of 1. Growth was monitored as scattered light at 620 nm in a BioLector at 30°C and 1200 rpm. Mean values and standard deviation of three biological replicates are shown.

A hypothesis for explaining the prolonged lag phase is that the absence of Cg1551 could lead to an elevated cAMP level, which would cause increased DNA-binding of GlxR. As reported previously, a *C. glutamicum* Δ*cpdA* strain with a 2-fold higher intracellular cAMP level compared to the wild type had growth defects on all tested carbon sources (Schulte et al., 2017). Further experiments are required to test this idea and the function of Cg1551 in cAMP homeostasis in *C. glutamicum*.

4 Literature

Agarwal, N., Lamichhane, G., Gupta, R., Nolan, S., & Bishai, W. R. (2009). Cyclic AMP intoxication of macrophages by a *Mycobacterium tuberculosis* adenylate cyclase. *Nature*, *460*(7251), 98-102.

Altschul, S. F., Gish, W., Miller, W., Myers, E. W., & Lipman, D. J. (1990). Basic local alignment search tool. *J Mol Biol*, *215*(3), 403-410.

Anjem, A., Varghese, S., & Imlay, J. A. (2009). Manganese import is a key element of the OxyR response to hydrogen peroxide in *Escherichia coli*. *Mol Microbiol*, *72*(4), 844-858.

Aravind, L., & Ponting, C. P. (1999). The cytoplasmic helical linker domain of receptor histidine kinase and methyl-accepting proteins is common to many prokaryotic signalling proteins. *FEMS Microbiol Lett*, *176*(1), 111-116.

Arce-Rodríguez, A., Durante-Rodríguez, G., Platero, R., Krell, T., Calles, B., & de Lorenzo, V. (2012). The Crp regulator of *Pseudomonas putida*: evidence of an unusually high affinity for its physiological effector, cAMP. *Environ Microbiol*, *14*(3), 702-713.

Arce-Rodríguez, A., Nikel, P. I., Calles, B., Chavarría, M., Platero, R., Krell, T., & de Lorenzo, V. (2021). Low CyaA expression and anti-cooperative binding of cAMP to CRP frames the scope of the cognate regulon of *Pseudomonas putida*. *Environ Microbiol*, *23*(3), 1732-1749.

Arumugham, V. B., Ulivieri, C., Onnis, A., Finetti, F., Tonello, F., Ladant, D., & Baldari, C. T. (2018). Compartmentalized cyclic AMP production by the *Bordetella pertussis* and *Bacillus anthracis* adenylate cyclase toxins differentially affects the immune synapse in T lymphocytes. *Front Immunol*, *9*, 919.

Attey, A., Belyaeva, T., Savery, N., Hoggett, J., Fujita, N., Ishihama, A., & Busby, S. (1994). Interactions between the cyclic AMP receptor protein and the alpha subunit of RNA polymerase at the *Escherichia coli* galactose operon P1 promoter. *Nucleic Acids Res*, *22*(21), 4375-4380.

Aung, H. L., Berney, M., & Cook, G. M. (2014). Hypoxia-activated cytochrome *bd* expression in *Mycobacterium smegmatis* is cyclic AMP receptor protein dependent. *J Bacteriol*, *196*(17), 3091-3097.

Aung, H. L., Dixon, L. L., Smith, L. J., Sweeney, N. P., Robson, J. R., Berney, M., Buxton, R. S., Green, J., & Cook, G. M. (2015). Novel regulatory roles of cAMP receptor proteins in fast-growing environmental mycobacteria. *Microbiology*, *161*(Pt 3), 648-661.

Axe, D. D., & Bailey, J. E. (1995). Transport of lactate and acetate through the energized cytoplasmic membrane of *Escherichia coli*. *Biotechnol Bioeng*, *47*(1), 8-19.

Bai, G., Schaak, D. D., & McDonough, K. A. (2009). cAMP levels within *Mycobacterium tuberculosis* and *Mycobacterium bovis* BCG increase upon infection of macrophages. *FEMS Immun Med Microbiol*, *55*(1), 68-73.

Bai, G., Schaak, D. D., Smith, E. A., & McDonough, K. A. (2011). Dysregulation of serine biosynthesis contributes to the growth defect of a *Mycobacterium tuberculosis crp* mutant. *Mol Microbiol*, *82*(1), 180-198.

Banerjee, A., Adolph, R. S., Gopalakrishnapai, J., Kleinboelting, S., Emmerich, C., Steegborn, C., & Visweswariah, S. S. (2015). A universal stress protein (USP) in mycobacteria binds cAMP. *J Biol Chem*, *290*(20), 12731-12743.

Barriuso-Iglesias, M., Barreiro, C., Sola-Landa, A., & Martín, J. F. (2013). Transcriptional control of the F_0F_1-ATP synthase operon of *Corynebacterium glutamicum*: SigmaH factor binds to its promoter and regulates its expression at different pH values. *Microb Biotechnol*, *6*(2), 178-188.

Barriuso-Iglesias, M., Schluesener, D., Barreiro, C., Poetsch, A., & Martín, J. F. (2008). Response of the cytoplasmic and membrane proteome of *Corynebacterium glutamicum* ATCC 13032 to pH changes. *BMC Microbiol*, *8*, 225.

Bârzu, O., & Danchin, A. (1994). Adenylyl cyclases: a heterogeneous class of ATP-utilizing enzymes. *Prog Nucleic Acid Res Mol Biol*, *49*, 241-283.

Bassler, J., Schultz, J. E., & Lupas, A. N. (2018). Adenylate cyclases: Receivers, transducers, and generators of signals. *Cell Signal*, *46*, 135-144.

Becker, J., & Wittmann, C. (2012). Systems and synthetic metabolic engineering for amino acid production - the heartbeat of industrial strain development. *Curr Opin Biotechnol*, *23*(5), 718-726.

Bennett, B. D., Kimball, E. H., Gao, M., Osterhout, R., Van Dien, S. J., & Rabinowitz, J. D. (2009). Absolute metabolite concentrations and implied enzyme active site occupancy in *Escherichia coli*. *Nat Chem Biol*, *5*(8), 593-599.

Benoff, B., Yang, H., Lawson, C. L., Parkinson, G., Liu, J., Blatter, E., Ebright, Y. W., Berman, H. M., & Ebright, R. H. (2002). Structural basis of transcription activation: the CAP-alpha CTD-DNA complex. *Science*, *297*(5586), 1562-1566.

Berthet, J., Rall, T. W., & Sutherland, E. W. (1957). The relationship of epinephrine and glucagon to liver phosphorylase. IV. Effect of epinephrine and glucagon on the reactivation of phosphorylase in liver homogenates. *J Biol Chem*, *224*(1), 463-475.

Bettenbrock, K., Sauter, T., Jahreis, K., Kremling, A., Lengeler, J. W., & Gilles, E. D. (2007). Correlation between growth rates, EIIA^{Crr} phosphorylation, and intracellular cyclic AMP levels in *Escherichia coli* K-12. *J Bacteriol*, *189*(19), 6891-6900.

Bettendorff, L., & Wins, P. (2013). Thiamine triphosphatase and the CYTH superfamily of proteins. *FEBS J*, *280*(24), 6443-6455.

Binder, S., Schendzielorz, G., Stabler, N., Krumbach, K., Hoffmann, K., Bott, M., & Eggeling, L. (2012). A high-throughput approach to identify genomic variants of bacterial metabolite producers at the single-cell level. *Genome Biol*, *13*(5), R40.

Blanco, E., Fortunato, S., Viggiano, L., & de Pinto, M. C. (2020). Cyclic AMP: A polyhedral signalling molecule in plants. *Int J Mol Sci*, *21*(14).

Blombach, B., Riester, T., Wieschalka, S., Ziert, C., Youn, J., Wendisch, V. F., & Eikmanns, B. J. (2011). *Corynebacterium glutamicum* tailored for efficient isobutanol production. *Appl Environ Microbiol*, *77*(10), 3300-3310.

Boratyn, G. M., Schäffer, A. A., Agarwala, R., Altschul, S. F., Lipman, D. J., & Madden, T. L. (2012). Domain enhanced lookup time accelerated BLAST. *Biol Direct*, *7*(1), 12.

Botsford, J. L., & Harman, J. G. (1992). Cyclic AMP in prokaryotes. *Microbiol Rev*, *56*(1), 100-122.

Busby, S., & Ebright, R. H. (1997). Transcription activation at class II CAP-dependent promoters. *Mol Microbiol*, *23*(5), 853-859.

Busby, S., & Ebright, R. H. (1999). Transcription activation by catabolite activator protein (CAP). *J Mol Biol*, *293*(2), 199-213.

Bussmann, M. (2009). cAMP dependent regulation of the TCA cycle by GlxR and oxidative stress response regulation by RosR in *Corynebacterium glutamicum*. urn:nbn:de:hbz:061-20101104-151101-4.

Bussmann, M., Emer, D., Hasenbein, S., Degraf, S., Eikmanns, B. J., & Bott, M. (2009). Transcriptional control of the succinate dehydrogenase operon *sdhCAB* of *Corynebacterium glutamicum* by the cAMP-dependent regulator GlxR and the LuxR-type regulator RamA. *J Biotechnol*, *143*(3), 173-182.

Callahan, S. M., Cornell, N. W., & Dunlap, P. V. (1995). Purification and properties of periplasmic 3':5'-cyclic nucleotide phosphodiesterase. A novel zinc-containing enzyme from the marine symbiotic bacterium *Vibrio fischeri*. *J Biol Chem*, *270*(29), 17627-17632.

Cashel, M. (1975). Regulation of bacterial ppGpp and pppGpp. *Ann Rev Microbiol*, *29*(1), 301-318.

Cha, P. H., Park, S. Y., Moon, M. W., Subhadra, B., Oh, T. K., Kim, E., Kim, J. F., & Lee, J. K. (2010). Characterization of an adenylate cyclase gene (*cyaB*) deletion mutant of *Corynebacterium glutamicum* ATCC 13032. *Appl Microbiol Biotechnol*, *85*(4), 1061-1068.

Conti, M., & Beavo, J. (2007). Biochemistry and physiology of cyclic nucleotide phosphodiesterases: essential components in cyclic nucleotide signaling. *Annu Rev Biochem*, *76*, 481-511.

Cook, W. H., Lipkin, D., & Markham, R. (1957). The formation of a cyclic dianhydro cyclic dianhydrodiadenylic acid (I) by the alkaline degradation of adenosine-5'-triphosphoric acid (II)1. *J Am Chem Soc*, *79*(13), 3607-3608.

Cotta, M. A., Whitehead, T. R., & Wheeler, M. B. (1998). Identification of a novel adenylate cyclase in the ruminal anaerobe, *Prevotella ruminicola* D31d. *FEMS Microbiol Lett*, *164*(2), 257-260.

Cotter, P. A., Chepuri, V., Gennis, R. B., & Gunsalus, R. P. (1990). Cytochrome *o* (*cyoABCDE*) and *d* (*cydAB*) oxidase gene expression in *Escherichia coli* is regulated by oxygen, pH, and the *fnr* gene product. *J Bacteriol*, *172*(11), 6333-6338.

Craig III, S. P., & Eakin, A. E. (2000). Purine phosphoribosyltransferases. *J Biol Chem*, *275*(27), 20231-20234.

D'Souza, C. A., & Heitman, J. (2001). Conserved cAMP signaling cascades regulate fungal development and virulence. *FEMS Microbiol Rev*, *25*(3), 349-364.

da Luz, J. A., Hans, E., Frank, D., & Zeng, A. P. (2017). Analysis of intracellular metabolites of *Corynebacterium glutamicum* at high cell density with automated sampling and filtration and assessment of engineered enzymes for effective L-lysine production. *Eng Life Sci*, *17*(5), 512-522.

Danchin, A. (1993). Phylogeny of adenylyl cyclases. *Adv Second Messenger Phosphoprotein Res*, *27*, 109-162.

Dass, B. K., Sharma, R., Shenoy, A. R., Mattoo, R., & Visweswariah, S. S. (2008). Cyclic AMP in mycobacteria: characterization and functional role of the Rv1647 ortholog in *Mycobacterium smegmatis*. *J Bacteriol*, *190*(11), 3824-3834.

Dautin, N., Karimova, G., & Ladant, D. (2002). *Bordetella pertussis* adenylate cyclase toxin: a versatile screening tool. *Toxicon*, *40*(10), 1383-1387.

de Crombrugghe, B., Busby, S., & Buc, H. (1984). Cyclic AMP receptor protein: role in transcription activation. *Science*, *224*(4651), 831-838.

Dessauer, C. W., Watts, V. J., Ostrom, R. S., Conti, M., Dove, S., & Seifert, R. (2017). International union of basic and clinical pharmacology. CI. structures and small molecule modulators of mammalian adenylyl cyclases. *Pharmacol Rev*, *69*(2), 93-139.

Eggeling, L., & Bott, M. (2015). A giant market and a powerful metabolism: L-lysine provided by *Corynebacterium glutamicum*. *Appl Microbiol Biotechnol*, *99*(8), 3387-3394.

Eggeling, L., Bott, M., & Marienhagen, J. (2015). Novel screening methods--biosensors. *Curr Opin Biotechnol*, *35*, 30-36.

El-Gebali, S., Mistry, J., Bateman, A., Eddy, S. R., Luciani, A., Potter, S. C., Qureshi, M., Richardson, L. J., Salazar, G. A., Smart, A., Sonnhammer, E. L. L., Hirsh, L., Paladin, L., Piovesan, D., Tosatto, S. C. E., & Finn, R. D. (2018). The Pfam protein families database in 2019. *Nucleic Acids Res*, *47*(D1), D427-D432.

Emmer, M., deCrombrugghe, B., Pastan, I., & Perlman, R. (1970). Cyclic AMP receptor protein of *E. coli*: its role in the synthesis of inducible enzymes. *Proc Natl Acad Sci U S A*, *66*(2), 480-487.

Endo, M. (2006). Calcium ion as a second messenger with special reference to excitation-contraction coupling. *J Pharmacol Sci*, *100*(5), 519-524.

Follmann, M., Ochrombel, I., Krämer, R., Trötschel, C., Poetsch, A., Rückert, C., Hüser, A., Persicke, M., Seiferling, D., Kalinowski, J., & Marin, K. (2009). Functional genomics of pH homeostasis in *Corynebacterium glutamicum* revealed novel links between pH response, oxidative stress, iron homeostasis and methionine synthesis. *BMC Genomics*, *10*, 621-621.

Francis, S. H., Blount, M. A., & Corbin, J. D. (2011). Mammalian cyclic nucleotide phosphodiesterases: molecular mechanisms and physiological functions. *Physiol Rev*, *91*(2), 651-690.

Francis, S. H., Turko, I. V., & Corbin, J. D. (2001). Cyclic nucleotide phosphodiesterases: relating structure and function. *Prog Nucleic Acid Res Mol Biol*, *65*, 1-52.

Gallagher, D. T., Smith, N. N., Kim, S. K., Heroux, A., Robinson, H., & Reddy, P. T. (2006). Structure of the class IV adenylyl cyclase reveals a novel fold. *J Mol Biol*, *362*(1), 114-122.

Gancedo, J. M. (2013). Biological roles of cAMP: variations on a theme in the different kingdoms of life. *Biol Rev Camb Philos Soc*, *88*(3), 645-668.

Gao, B., & Gupta, R. S. (2012). Phylogenetic framework and molecular signatures for the main clades of the phylum *Actinobacteria*. *Microbiol Mol Biol Rev*, *76*(1), 66-112.

Gazdik, M. A., Bai, G., Wu, Y., & McDonough, K. A. (2009). Rv1675c (*cmr*) regulates intramacrophage and cyclic AMP-induced gene expression in *Mycobacterium tuberculosis*-complex mycobacteria. *Mol Microbiol*, *71*(2), 434-448.

Gehring, C. (2010). Adenyl cyclases and cAMP in plant signaling - past and present. *Cell Commun Signal*, *8*, 15.

Georg, J., & Hess, W. R. (2011). *cis*-antisense RNA, another level of gene regulation in bacteria. *Microbiol Mol Biol Rev*, *75*(2), 286-300.

Goldenbaum, P. E., & Hall, G. A. (1979). Transport of cyclic adenosine 3',5'-monophosphate across *Escherichia coli* vesicle membranes. *J Bacteriol*, *140*(2), 459-467.

Görke, B., & Stülke, J. (2008). Carbon catabolite repression in bacteria: many ways to make the most out of nutrients. *Nat Rev Microbiol*, *6*(8), 613-624.

Gosset, G., Zhang, Z., Nayyar, S., Cuevas, W. A., & Saier, M. H., Jr. (2004). Transcriptome analysis of Crp-dependent catabolite control of gene expression in *Escherichia coli*. *J Bacteriol*, *186*(11), 3516-3524.

Guo, Z. P., Khoomrung, S., Nielsen, J., & Olsson, L. (2018). Changes in lipid metabolism convey acid tolerance in *Saccharomyces cerevisiae*. *Biotechnol Biofuels*, *11*, 297.

Hecker, M., & Völker, U. (2001). General stress response of *Bacillus subtilis* and other bacteria. *Adv Microb Physiol*, *44*, 35-91.

Heider, S. A., Wolf, N., Hofemeier, A., Peters-Wendisch, P., & Wendisch, V. F. (2014). Optimization of the IPP precursor supply for the production of lycopene, decaprenoxanthin and astaxanthin by *Corynebacterium glutamicum*. *Front Bioeng Biotechnol*, *20*, 2-28.

Henderson, P. J. (1993). The 12-transmembrane helix transporters. *Curr Opin Cell Biol*, *5*(4), 708-721.

Henke, N. A., Heider, S. A., Peters-Wendisch, P., & Wendisch, V. F. (2016). Production of the marine carotenoid astaxanthin by metabolically engineered *Corynebacterium glutamicum*. *Mar Drugs*, *14*(7), 124.

Hong, E. J., Park, J. S., Kim, Y., & Lee, H. S. (2014). Role of *Corynebacterium glutamicum sprA* encoding a serine protease in *glxR*-mediated global gene regulation. *PLoS One*, *9*(4), e93587.

Ikeda, M., & Nakagawa, S. (2003). The *Corynebacterium glutamicum* genome: features and impacts on biotechnological processes. *Appl Microbiol Biotechnol*, *62*(2), 99-109.

Imamura, R., Yamanaka, K., Ogura, T., Hiraga, S., Fujita, N., Ishihama, A., & Niki, H. (1996). Identification of the *cpdA* gene encoding cyclic 3',5'-adenosine monophosphate phosphodiesterase in *Escherichia coli*. *J Biol Chem*, *271*(41), 25423-25429.

Inui, M., Kawaguchi, H., Murakami, S., Vertès, A. A., & Yukawa, H. (2004). Metabolic engineering of *Corynebacterium glutamicum* for fuel ethanol production under oxygen-deprivation conditions. *J Mol Microbiol Biotechnol*, *8*(4), 243-254.

Jakob, K., Satorhelyi, P., Lange, C., Wendisch, V. F., Silakowski, B., Scherer, S., & Neuhaus, K. (2007). Gene expression analysis of *Corynebacterium glutamicum* subjected to long-term lactic acid adaptation. *J Bacteriol*, *189*(15), 5582-5590.

Jha, S. K., Sharma, M., & Pandey, G. K. (2016). Role of cyclic nucleotide gated channels in stress management in plants. *Curr Genomics*, *17*(4), 315-329.

Jolkver, E., Emer, D., Ballan, S., Kramer, R., Eikmanns, B. J., & Marin, K. (2009). Identification and characterization of a bacterial transport system for the uptake of pyruvate, propionate, and acetate in *Corynebacterium glutamicum*. *J Bacteriol*, *191*(3), 940-948.

Jungwirth, B., Emer, D., Brune, I., Hansmeier, N., Puhler, A., Eikmanns, B. J., & Tauch, A. (2008). Triple transcriptional control of the resuscitation promoting factor 2 *(rpf2*) gene of *Corynebacterium glutamicum* by the regulators of acetate metabolism RamA and RamB and the cAMP-dependent regulator GlxR. *FEMS Microbiol Lett*, *281*(2), 190-197.

Jungwirth, B., Sala, C., Kohl, T. A., Uplekar, S., Baumbach, J., Cole, S. T., Puhler, A., & Tauch, A. (2013). High-resolution detection of DNA binding sites of the global transcriptional regulator GlxR in *Corynebacterium glutamicum*. *Microbiology*, *159*(Pt 1), 12-22.

Kabus, A., Niebisch, A., & Bott, M. (2007). Role of cytochrome *bd* oxidase from *Corynebacterium glutamicum* in growth and lysine production. *Appl Environ Microbiol*, *73*(3), 861-868.

Kalinowski, J., Bathe, B., Bartels, D., Bischoff, N., Bott, M., Burkovski, A., Dusch, N., Eggeling, L., Eikmanns, B. J., Gaigalat, L., Goesmann, A., Hartmann, M., Huthmacher, K., Kramer, R., Linke, B., McHardy, A. C., Meyer, F., Mockel, B., Pfefferle, W., Puhler, A., Rey, D. A., Ruckert, C., Rupp, O., Sahm, H., Wendisch, V. F., Wiegrabe, I., & Tauch, A. (2003). The complete *Corynebacterium glutamicum* ATCC 13032 genome sequence and its impact on the production of L-aspartate-derived amino acids and vitamins. *J Biotechnol*, *104*, 5-25.

Kallscheuer, N., Vogt, M., Stenzel, A., Gatgens, J., Bott, M., & Marienhagen, J. (2016). Construction of a *Corynebacterium glutamicum* platform strain for the production of stilbenes and (2S)-flavanones. *Metab Eng*, *38*, 47-55.

Kamenetsky, M., Middelhaufe, S., Bank, E. M., Levin, L. R., Buck, J., & Steegborn, C. (2006). Molecular details of cAMP generation in mammalian cells: a tale of two systems. *J Mol Biol*, *362*(4), 623-639.

Kana, B. D., Weinstein, E. A., Avarbock, D., Dawes, S. S., Rubin, H., & Mizrahi, V. (2001). Characterization of the *cydAB*-encoded cytochrome *bd* oxidase from *Mycobacterium smegmatis*. *J Bacteriol*, *183*(24), 7076-7086.

Kasahara, M., Unno, T., Yashiro, K., & Ohmori, M. (2001). CyaG, a novel cyanobacterial adenylyl cyclase and a possible ancestor of mammalian guanylyl cyclases. *J Biol Chem*, *276*(13), 10564-10569.

Katcharava, N. (2015). Untersuchung einer *Corynebacterium glutamicum cyaB*-Deletionsmutante [Bachelor Thesis, Fachhochschule Aachen].

Kim, H. J., Kim, T. H., Kim, Y., & Lee, H. S. (2004). Identification and characterization of *glxR*, a gene involved in regulation of glyoxylate bypass in *Corynebacterium glutamicum*. *J Bacteriol*, *186*(11), 3453-3460.

Kim, T. H., Kim, H. J., Park, J. S., Kim, Y., Kim, P., & Lee, H. S. (2005). Functional analysis of *sigH* expression in *Corynebacterium glutamicum*. *Biochem Biophys Res Commun*, *331*(4), 1542-1547.

Kimura, Y., Yoshimi, M., & Takata, G. (2011). Enzymatic and mutational analyses of a class II 3',5'-cyclic nucleotide phosphodiesterase, PdeE, from *Myxococcus xanthus*. *J Bacteriol*, *193*(8), 2053-2057.

Kinoshita, S., Udaka, S., & Shimono, M. (1957). Studies on amino acid fermentation. Part 1. Production of L-glutamic acid by various microorganisms. *J Gen Appl Microbiol*, *3*, 193-205.

Kirsch, K. M. (2014). The impact of CO_2 on inorganic carbon supply and pH homeostasis in *Corynebacterium glutamicum*. urn:nbn:de:hbz:38-55451

Kishii, R., Falzon, L., Yoshida, T., Kobayashi, H., & Inouye, M. (2007). Structural and functional studies of the HAMP domain of EnvZ, an osmosensing transmembrane histidine kinase in *Escherichia coli*. *J Biol Chem*, *282*(36), 26401-26408.

Ko, E. M., & Oh, J. I. (2020). Induction of the *cydAB* operon encoding the *bd* quinol oxidase under respiration-inhibitory conditions by the major cAMP receptor protein MSMEG_6189 in *Mycobacterium smegmatis*. *Front Microbiol*, *11*, 608624.

Koch-Koerfges, A., Pfelzer, N., Platzen, L., Oldiges, M., & Bott, M. (2013). Conversion of *Corynebacterium glutamicum* from an aerobic respiring to an aerobic fermenting bacterium by inactivation of the respiratory chain. *Biochim Biophys Acta Bioenerg*, *1827*(6), 699-708.

Kohl, T. A., Baumbach, J., Jungwirth, B., Puhler, A., & Tauch, A. (2008). The GlxR regulon of the amino acid producer *Corynebacterium glutamicum*: *in silico* and *in vitro* detection of DNA binding sites of a global transcription regulator. *J Biotechnol*, *135*(4), 340-350.

Kohl, T. A., & Tauch, A. (2009). The GlxR regulon of the amino acid producer *Corynebacterium glutamicum*: Detection of the corynebacterial core regulon and integration into the transcriptional regulatory network model. *J Biotechnol*, *143*(4), 239-246.

Kolb, A., Busby, S., Buc, H., Garges, S., & Adhya, S. (1993). Transcriptional regulation by cAMP and its receptor protein. *Annu Rev Biochem*, *62*, 749-795.

Kopperud, R., Krakstad, C., Selheim, F., & Døskeland, S. O. (2003). cAMP effector mechanisms. Novel twists for an 'old' signaling system. *FEBS Lett*, *546*(1), 121-126.

Krulwich, T. A., Sachs, G., & Padan, E. (2011). Molecular aspects of bacterial pH sensing and homeostasis. *Nat Rev Microbiol*, *9*(5), 330-343.

Küberl, A., Fränzel, B., Eggeling, L., Polen, T., Wolters, D. A., & Bott, M. (2014). Pupylated proteins in *Corynebacterium glutamicum* revealed by MudPIT analysis. *Proteomics*, *14*(12), 1531-1542.

Laslo, T., von Zaluskowski, P., Gabris, C., Lodd, E., Rückert, C., Dangel, P., Kalinowski, J., Auchter, M., Seibold, G., & Eikmanns, B. J. (2012). Arabitol metabolism of *Corynebacterium glutamicum* and its regulation by AtlR. *J Bacteriol*, *194*(5), 941-955.

Lee, D. J., Minchin, S. D., & Busby, S. J. (2012). Activating transcription in bacteria. *Annu Rev Microbiol*, *66*, 125-152.

Letek, M., Valbuena, N., Ramos, A., Ordonez, E., Gil, J. A., & Mateos, L. M. (2006). Characterization and use of catabolite-repressed promoters from gluconate genes in *Corynebacterium glutamicum*. *J Bacteriol*, *188*(2), 409-423.

Leuchtenberger, W., Huthmacher, K., & Drauz, K. (2005). Biotechnological production of amino acids and derivatives: current status and prospects. *Appl Microbiol Biotechnol*, *69*(1), 1-8.

Leyval, D., Debay, F., Engasser, J., & Goergen, J. (1997). Flow cytometry for the intracellular pH measurement of glutamate producing *Corynebacterium glutamicum*. *J Microbiol Methods*, *29*(2), 121-127.

Lindahl, L., Genheden, S., Faria-Oliveira, F., Allard, S., Eriksson, L. A., Olsson, L., & Bettiga, M. (2017). Alcohols enhance the rate of acetic acid diffusion in *S. cerevisiae*: biophysical mechanisms and implications for acetic acid tolerance. *Microbial Cell*, *5*(1), 42-55.

Linder, J. U., Hammer, A., & Schultz, J. E. (2004). The effect of HAMP domains on class IIIb adenylyl cyclases from *Mycobacterium tuberculosis*. *Eur J Biochem*, *271*(12), 2446-2451.

Linder, J. U., & Schultz, J. E. (2003). The class III adenylyl cyclases: multi-purpose signalling modules. *Cell Signal*, *15*(12), 1081-1089.

Litsanov, B., Brocker, M., & Bott, M. (2012). Toward homosuccinate fermentation: metabolic engineering of *Corynebacterium glutamicum* for anaerobic production of succinate from glucose and formate. *Appl Environ Microbiol*, *78*(9), 3325-3337.

Litsanov, B., Kabus, A., Brocker, M., & Bott, M. (2012). Efficient aerobic succinate production from glucose in minimal medium with *Corynebacterium glutamicum*. *Microb Biotechnol*, *5*(1), 116-128.

Liu, C., Sun, D., Zhu, J., Liu, J., & Liu, W. (2020). The regulation of bacterial biofilm formation by cAMP-CRP: A Mini-Review. *Front Microbiol*, *11*, 802.

Lorenzo-Orts, L., Hohmann, U., Zhu, J., & Hothorn, M. (2019). Molecular characterization of CHAD domains as inorganic polyphosphate-binding modules. *Life Sci Alliance*, *2*(3), e201900385.

Lowrie, D. B., Aber, V. R., & Jackett, P. S. (1979). Phagosome-lysosome fusion and cyclic adenosine 3':5'-monophosphate in macrophages infected with *Mycobacterium microti*, *Mycobacterium bovis* BCG or *Mycobacterium lepraemurium*. *J Gen Microbiol*, *110*(2), 431-441.

Maathuis, F. J., & Sanders, D. (2001). Sodium uptake in Arabidopsis roots is regulated by cyclic nucleotides. *Plant Physiol*, *127*(4), 1617-1625.

Majors, J. (1975). Specific binding of CAP factor to lac promoter DNA. *Nature*, *256*(5519), 672-674.

Maurer, L. M., Yohannes, E., Bondurant, S. S., Radmacher, M., & Slonczewski, J. L. (2005). pH regulates genes for flagellar motility, catabolism, and oxidative stress in *Escherichia coli* K-12. *J Bacteriol*, *187*(1), 304-319.

Mbah, A. N. (2014). Application of hybrid functional groups to predict ATP binding proteins. *ISRN Comput Biol*, *2014*, 581245.

McCue, L. A., McDonough, K. A., & Lawrence, C. E. (2000). Functional classification of cNMP-binding proteins and nucleotide cyclases with implications for novel regulatory pathways in *Mycobacterium tuberculosis*. *Genome Res*, *10*(2), 204-219.

McDonough, K. A., & Rodriguez, A. (2011). The myriad roles of cyclic AMP in microbial pathogens: from signal to sword. *Nat Rev Microbiol*, *10*(1), 27-38.

McKnight, G. S. (1991). Cyclic AMP second messenger systems. *Curr Opin Cell Biol*, *3*(2), 213-217.

Mendoza-Vargas, A., Olvera, L., Olvera, M., Grande, R., Vega-Alvarado, L., Taboada, B., Jimenez-Jacinto, V., Salgado, H., Juárez, K., Contreras-Moreira, B., Huerta, A. M., Collado-Vides, J., & Morett, E. (2009). Genome-wide identification of transcription start sites, promoters and transcription factor binding sites in *E. coli*. *PLoS One*, *4*(10), e7526.

Miesenböck, G., De Angelis, D. A., & Rothman, J. E. (1998). Visualizing secretion and synaptic transmission with pH-sensitive green fluorescent proteins. *Nature*, *394*(6689), 192-195.

Milanesio, P., Arce-Rodríguez, A., Muñoz, A., Calles, B., & de Lorenzo, V. (2011). Regulatory exaptation of the catabolite repression protein (Crp)-cAMP system in *Pseudomonas putida*. *Environ Microbiol*, *13*(2), 324-339.

Mistry, J., Chuguransky, S., Williams, L., Qureshi, M., Salazar, G. A., Sonnhammer, E. L. L., Tosatto, S. C. E., Paladin, L., Raj, S., Richardson, L. J., Finn, R. D., & Bateman, A. (2020). Pfam: The protein families database in 2021. *Nucleic Acids Res*, *49*(D1), D412-D419.

Mizuno, Y., Nagano-Shoji, M., Kubo, S., Kawamura, Y., Yoshida, A., Kawasaki, H., Nishiyama, M., Yoshida, M., & Kosono, S. (2016). Altered acetylation and succinylation profiles in *Corynebacterium glutamicum* in response to conditions inducing glutamate overproduction. *Microbiologyopen*, *5*(1), 152-173.

Morosov, X., Davoudi, C. F., Baumgart, M., Brocker, M., & Bott, M. (2018). The copper-deprivation stimulon of *Corynebacterium glutamicum* comprises proteins for biogenesis of the actinobacterial cytochrome bc_1-aa_3 supercomplex. *J Biol Chem*, *293*(40), 15628-15640.

Mulder, N. J., & Apweiler, R. (2008). The InterPro database and tools for protein domain analysis. *Curr Protoc Bioinformatics*, *21*(1), 2.7.1-2.7.18.

Mustafi, N., Grünberger, A., Kohlheyer, D., Bott, M., & Frunzke, J. (2012). The development and application of a single-cell biosensor for the detection of L-methionine and branched-chain amino acids. *Metab Eng*, *14*(4), 449-457.

Nambi, S., Basu, N., & Visweswariah, S. S. (2010). cAMP-regulated protein lysine acetylases in mycobacteria. *J Biol Chem*, *285*(32), 24313-24323.

Nambi, S., Gupta, K., Bhattacharyya, M., Ramakrishnan, P., Ravikumar, V., Siddiqui, N., Thomas, A. T., & Visweswariah, S. S. (2013). Cyclic AMP-dependent protein lysine acylation in mycobacteria regulates fatty acid and propionate metabolism. *J Biol Chem*, *288*(20), 14114-14124.

Nambi, S., Gupta, K., Bhattacharyya, M., Ramakrishnan, P., Ravikumar, V., Siddiqui, N., Thomas, A. T., & Visweswariah, S. S. (2019). Correction: Cyclic AMP-dependent protein lysine acylation in mycobacteria regulates fatty acid and propionate metabolism. *J Biol Chem*, *294*(28), 11046.

Nishimura, T., Teramoto, H., Toyoda, K., Inui, M., & Yukawa, H. (2011). Regulation of the nitrate reductase operon *narKGHJI* by the cAMP-dependent regulator GlxR in *Corynebacterium glutamicum*. *Microbiology*, *157*(Pt 1), 21-28.

Notley-McRobb, L., Death, A., & Ferenci, T. (1997). The relationship between external glucose concentration and cAMP levels inside *Escherichia coli*: implications for models of phosphotransferase-mediated regulation of adenylate cyclase. *Microbiology*, *143*(6), 1909-1918.

Nystrom, T., & Neidhardt, F. C. (1992). Cloning, mapping and nucleotide sequencing of a gene encoding a universal stress protein in *Escherichia coli*. *Mol Microbiol*, *6*(21), 3187-3198.

Nystrom, T., & Neidhardt, F. C. (1993). Isolation and properties of a mutant of *Escherichia coli* with an insertional inactivation of the *uspA* gene, which encodes a universal stress protein. *J Bacteriol*, *175*(13), 3949-3956.

Okino, S., Noburyu, R., Suda, M., Jojima, T., Inui, M., & Yukawa, H. (2008). An efficient succinic acid production process in a metabolically engineered *Corynebacterium glutamicum* strain. *Appl Microbiol Biotechnol*, *81*(3), 459-464.

Okino, S., Suda, M., Fujikura, K., Inui, M., & Yukawa, H. (2008). Production of D-lactic acid by *Corynebacterium glutamicum* under oxygen deprivation. *Appl Microbiol Biotechnol*, *78*(3), 449-454.

Olson, E. R. (1993). Influence of pH on bacterial gene expression. *Mol Microbiol*, *8*(1), 5-14.

Omori, K., & Kotera, J. (2007). Overview of PDEs and their regulation. *Circ Res*, *100*(3), 309-327.

Oren, A., & Garrity, G. M. (2021). Valid publication of the names of forty-two phyla of prokaryotes. *Int J Syst Evol Microbiol*, *71*(10).

Orr, J. S., Christensen, D. G., Wolfe, A. J., & Rao, C. V. (2018). Extracellular acidic pH inhibits acetate consumption by decreasing gene transcription of the tricarboxylic acid cycle and the glyoxylate shunt. *J Bacteriol*, *201*(2), e00410-00418.

Padh, H., & Venkitasubramanian, T. A. (1976). Cyclic adenosine 3', 5'-monophosphate in mycobacteria. *Indian J Biochem Biophys*, *13*(4), 413-414.

Panhorst, M., Sorger-Herrmann, U., & Wendisch, V. F. (2011). The *pstSCAB* operon for phosphate uptake is regulated by the global regulator GlxR in *Corynebacterium glutamicum*. *J Biotechnol*, *154*(2-3), 149-155.

Park, S. Y., Moon, M. W., Subhadra, B., & Lee, J. K. (2010). Functional characterization of the *glxR* deletion mutant of *Corynebacterium glutamicum* ATCC 13032: involvement of GlxR in acetate metabolism and carbon catabolite repression. *FEMS Microbiol Lett*, *304*(2), 107-115.

Park, Y. H., Lee, B. R., Seok, Y. J., & Peterkofsky, A. (2006). *In vitro* reconstitution of catabolite repression in *Escherichia coli*. *J Biol Chem*, *281*(10), 6448-6454.

Passner, J. M., Schultz, S. C., & Steitz, T. A. (2000). Modeling the cAMP-induced allosteric transition using the crystal structure of CAP-cAMP at 2.1 Å resolution. *J Mol Biol*, *304*(5), 847-859.

Pauling, J., Röttger, R., Tauch, A., Azevedo, V., & Baumbach, J. (2012). CoryneRegNet 6.0-Updated database content, new analysis methods and novel features focusing on community demands. *Nucleic Acids Res*, *40*(D1), D610-D614.

Peng, X., Okai, N., Vertès, A. A., Inatomi, K.-I., Inui, M., & Yukawa, H. (2011). Characterization of the mannitol catabolic operon of *Corynebacterium glutamicum*. *Appl Microbiol Biotechnol*, *91*(5), 1375-1387.

Pfeifer-Sancar, K., Mentz, A., Ruckert, C., & Kalinowski, J. (2013). Comprehensive analysis of the *Corynebacterium glutamicum* transcriptome using an improved RNAseq technique. *BMC Genomics*, *14*, 888.

Phillips, A. T., & Mulfinger, L. M. (1981). Cyclic adenosine 3',5'-monophosphate levels in *Pseudomonas putida* and *Pseudomonas aeruginosa* during induction and carbon catabolite repression of histidase synthesis. *J Bacteriol*, *145*(3), 1286-1292.

Platzen, L. (2013). Modifikation der Atmungskette in *Corynebacterium glutamicum* und Rolle des Flävohämoproteins Hmp. ISBN 978-3-89336-931-7

Polen, T., Schluesener, D., Poetsch, A., Bott, M., & Wendisch, V. F. (2007). Characterization of citrate utilization in *Corynebacterium glutamicum* by transcriptome and proteome analysis. *FEMS Microbiol Lett*, *273*(1), 109-119.

Popovych, N., Tzeng, S. R., Tonelli, M., Ebright, R. H., & Kalodimos, C. G. (2009). Structural basis for cAMP-mediated allosteric control of the catabolite activator protein. *Proc Natl Acad Sci U S A*, *106*(17), 6927-6932.

Powell, S., Forslund, K., Szklarczyk, D., Trachana, K., Roth, A., Huerta-Cepas, J., Gabaldón, T., Rattei, T., Creevey, C., Kuhn, M., Jensen, L. J., von Mering, C., & Bork, P. (2014). eggNOG v4.0: nested orthology inference across 3686 organisms. *Nucleic Acids Res*, *42*(D1), D231-239.

Ren, Y. L., Garges, S., Adhya, S., & Krakow, J. S. (1990). Characterization of the binding of cAMP and cGMP to the CRP*598 mutant of the *E. coli* cAMP receptor protein. *Nucleic Acids Res*, *18*(17), 5127-5132.

Richet, E., Vidal-Ingigliardi, D., & Raibaud, O. (1991). A new mechanism for coactivation of transcription initiation: repositioning of an activator triggered by the binding of a second activator. *Cell*, *66*(6), 1185-1195.

Richter, W. (2002). 3',5' Cyclic nucleotide phosphodiesterases class III: members, structure, and catalytic mechanism. *Proteins*, *46*(3), 278-286.

Robert, X., & Gouet, P. (2014). Deciphering key features in protein structures with the new ENDscript server. *Nucleic Acids Res*, *42*(W1), W320-W324.

Robison, K., McGuire, A. M., & Church, G. M. (1998). A comprehensive library of DNA-binding site matrices for 55 proteins applied to the complete *Escherichia coli* K-12 genome. *J Mol Biol*, *284*(2), 241-254.

Saier, M. H., Jr., Feucht, B. U., & McCaman, M. T. (1975). Regulation of intracellular adenosine cyclic 3':5'-monophosphate levels in *Escherichia coli* and *Salmonella typhimurium*. Evidence for energy-dependent excretion of the cyclic nucleotide. *J Biol Chem*, *250*(19), 7593-7601.

Sass, P., Field, J., Nikawa, J., Toda, T., & Wigler, M. (1986). Cloning and characterization of the high-affinity cAMP phosphodiesterase of *Saccharomyces cerevisiae*. *Proc Natl Acad Sci U S A*, *83*(24), 9303-9307.

Sassone-Corsi, P. (2012). The cyclic AMP pathway. *Cold Spring Harb Perspect Biol*, *4*(12), a011148.

Savery, N. J., Lloyd, G. S., Kainz, M., Gaal, T., Ross, W., Ebright, R. H., Gourse, R. L., & Busby, S. J. (1998). Transcription activation at Class II CRP-dependent promoters: identification of determinants in the C-terminal domain of the RNA polymerase alpha subunit. *EMBO J*, *17*(12), 3439-3447.

Schaffer, S., Weil, B., Nguyen, V. D., Dongmann, G., Günther, K., Nickolaus, M., Hermann, T., & Bott, M. (2001). A high-resolution reference map for cytoplasmic and membrane-associated proteins of *Corynebacterium glutamicum*. *Electrophoresis*, *22*(20), 4404-4422.

Schendzielorz, G., Dippong, M., Grünberger, A., Kohlheyer, D., Yoshida, A., Binder, S., Nishiyama, C., Nishiyama, M., Bott, M., & Eggeling, L. (2014). Taking control over control: use of product sensing in single cells to remove flux control at key enzymes in biosynthesis pathways. *ACS Synth Biol*, *3*(1), 21-29.

Schubert, O. T., Mouritsen, J., Ludwig, C., Rost, H. L., Rosenberger, G., Arthur, P. K., Claassen, M., Campbell, D. S., Sun, Z., Farrah, T., Gengenbacher, M., Maiolica, A., Kaufmann, S. H. E., Moritz, R. L., & Aebersold, R. (2013). The Mtb proteome library: a resource of assays to quantify the complete proteome of *Mycobacterium tuberculosis*. *Cell Host Microbe*, *13*(5), 602-612.

Schulte, J., Baumgart, M., & Bott, M. (2017). Identification of the cAMP phosphodiesterase CpdA as novel key player in cAMP-dependent regulation in *Corynebacterium glutamicum*. *Mol Microbiol*, *103*(3), 534-552.

Sharma, R., Zaveri, A., Gopalakrishnapai, J., Srinath, T., Varshney, U., & Visweswariah, S. S. (2014). Paralogous cAMP receptor proteins in *Mycobacterium smegmatis* show biochemical and functional divergence. *Biochemistry*, *53*(49), 7765-7776.

Shenoy, A. R., Sivakumar, K., Krupa, A., Srinivasan, N., & Visweswariah, S. S. (2004). A survey of nucleotide cyclases in actinobacteria: unique domain organization and expansion of the class III cyclase family in *Mycobacterium tuberculosis*. *Comp Funct Genomics*, *5*(1), 17-38.

Shenoy, A. R., Sreenath, N., Podobnik, M., Kovacevic, M., & Visweswariah, S. S. (2005). The Rv0805 gene from *Mycobacterium tuberculosis* encodes a 3',5'-cyclic nucleotide phosphodiesterase: biochemical and mutational analysis. *Biochemistry*, *44*(48), 15695-15704.

Shenoy, A. R., & Visweswariah, S. S. (2006). Mycobacterial adenylyl cyclases: biochemical diversity and structural plasticity. *FEBS Lett*, *580*(14), 3344-3352.

Sismeiro, O., Trotot, P., Biville, F., Vivares, C., & Danchin, A. (1998). *Aeromonas hydrophila* adenylyl cyclase 2: a new class of adenylyl cyclases with thermophilic properties and sequence similarities to proteins from hyperthermophilic archaebacteria. *J Bacteriol*, *180*(13), 3339-3344.

Skorupski, K., & Taylor, R. K. (1997). Cyclic AMP and its receptor protein negatively regulate the coordinate expression of cholera toxin and toxin-coregulated pilus in *Vibrio cholerae*. *Proc Natl Acad Sci U S A*, *94*(1), 265-270.

Slonczewski, J. L., Fujisawa, M., Dopson, M., & Krulwich, T. A. (2009). Cytoplasmic pH measurement and homeostasis in bacteria and archaea. *Adv Microb Physiol*, *55*, 1-79, 317.

Smith, N. N., Kim, S. K., Reddy, P. T., & Gallagher, D. T. (2006). Crystallization of the class IV adenylyl cyclase from *Yersinia pestis*. *Acta Cryst*, *F62*, 200-204.

Sousa, M. C., & McKay, D. B. (2001). Structure of the universal stress protein of *Haemophilus influenzae*. *Structure*, *9*(12), 1135-1141.

Stapleton, M., Haq, I., Hunt, D. M., Arnvig, K. B., Artymiuk, P. J., Buxton, R. S., & Green, J. (2010). *Mycobacterium tuberculosis* cAMP receptor protein (Rv3676) differs from the *Escherichia coli* paradigm in its cAMP binding and DNA binding properties and transcription activation properties. *J Biol Chem*, *285*(10), 7016-7027.

Stolz, M., Peters-Wendisch, P., Etterich, H., Gerharz, T., Faurie, R., Sahm, H., Fersterra, H., & Eggeling, L. (2007). Reduced folate supply as a key to enhanced L-serine production by *Corynebacterium glutamicum*. *Appl Environ Microbiol*, *73*(3), 750-755.

Storz, G., Vogel, J., & Wassarman, K. M. (2011). Regulation by small RNAs in bacteria: expanding frontiers. *Mol Cell*, *43*(6), 880-891.

Subhadra, B., & Lee, J. K. (2013). Elucidation of the regulation of ethanol catabolic genes and *ptsG* using a *glxR* and adenylate cyclase gene (*cyaB*) deletion mutants of *Corynebacterium glutamicum* ATCC 13032. *J Microbiol Biotechnol*, *23*(12), 1683-1690.

Subhadra, B., Ray, D., Han, J. Y., Bae, K. H., & Lee, J. K. (2015). Identification of the regulators binding to the upstream region of *glxR* in *Corynebacterium glutamicum*. *J Microbiol Biotechnol*, *25*(8), 1216-1226.

Sun, Y., Fukamachi, T., Saito, H., & Kobayashi, H. (2012). Respiration and the F_1Fo-ATPase enhance survival under acidic conditions in *Escherichia coli*. *PLoS One*, *7*(12), e52577.

Sutherland, E. W., & Rall, T. W. (1958). Fractionation and characterization of a cyclic adenine ribonucleotide formed by tissue particles. *J Biol Chem*, *232*(2), 1077-1091.

Takahashi, M., Blazy, B., & Baudras, A. (1980). An equilibrium study of the cooperative binding of adenosine cyclic 3',5'-monophosphate and guanosine cyclic 3',5'-monophosphate to the adenosine cyclic 3',5'-monophosphate receptor protein from *Escherichia coli*. *Biochemistry*, *19*(22), 5124-5130.

Téllez-Sosa, J., Soberón, N., Vega-Segura, A., Torres-Márquez, M. E., & Cevallos, M. A. (2002). The *Rhizobium etli cyaC* product: characterization of a novel adenylate cyclase class. *J Bacteriol*, *184*(13), 3560-3568.

Tews, I., Findeisen, F., Sinning, I., Schultz, A., Schultz, J. E., & Linder, J. U. (2005). The structure of a pH-sensing mycobacterial adenylyl cyclase holoenzyme. *Science*, *308*(5724), 1020-1023.

Thomason, P. A., Traynor, D., Stock, J. B., & Kay, R. R. (1999). The RdeA-RegA system, a eukaryotic phospho-relay controlling cAMP breakdown. *J Biol Chem*, *274*(39), 27379-27384.

Thompson, J. D., Higgins, D. G., & Gibson, T. J. (1994). CLUSTAL W: improving the sensitivity of progressive multiple sequence alignment through sequence weighting, position-specific gap penalties and weight matrix choice. *Nucleic Acids Res*, *22*(22), 4673-4680.

Thomson, M., Nunta, K., Cheyne, A., liu, Y., Garza-Garcia, A., & Larrouy-Maumus, G. (2020). Modulation of the cAMP levels with a conserved actinobacteria phosphodiesterase enzyme reduces antimicrobial tolerance in mycobacteria. *bioRxiv*, 2020.2008.2026.267864.

Thomson, M., Liu, Y., Nunta, K., Cheyne, A., Fernandes, N., Williams, R., Garza-Garcia, A., & Larrouy-Maumus, G. (2022). Expression of a novel mycobacterial phosphodiesterase successfully lowers cAMP levels resulting in reduced tolerance to cell wall-targeting antimicrobials. *J Biol Chem*, *298*(8), 102151.

Townsend, P. D., Jungwirth, B., Pojer, F., Bussmann, M., Money, V. A., Cole, S. T., Puhler, A., Tauch, A., Bott, M., Cann, M. J., & Pohl, E. (2014). The crystal structures of apo and cAMP-bound GlxR from *Corynebacterium glutamicum* reveal structural and dynamic changes upon cAMP binding in CRP/FNR family transcription factors. *PLoS One*, *9*(12), e113265.

Toyoda, K., & Inui, M. (2016). Regulons of global transcription factors in *Corynebacterium glutamicum*. *Appl Microbiol Biotechnol*, *100*(1), 45-60.

Toyoda, K., Teramoto, H., Gunji, W., Inui, M., & Yukawa, H. (2013). Involvement of regulatory interactions among global regulators GlxR, SugR, and RamA in expression of *ramA* in *Corynebacterium glutamicum*. *J Bacteriol*, *195*(8), 1718-1726.

Toyoda, K., Teramoto, H., Inui, M., & Yukawa, H. (2009). Involvement of the LuxR-type transcriptional regulator RamA in regulation of expression of the *gapA* gene, encoding glyceraldehyde-3-phosphate dehydrogenase of *Corynebacterium glutamicum*. *J Bacteriol*, *191*(3), 968-977.

Toyoda, K., Teramoto, H., Inui, M., & Yukawa, H. (2011). Genome-wide identification of *in vivo* binding sites of GlxR, a cyclic AMP receptor protein-type regulator in *Corynebacterium glutamicum*. *J Bacteriol*, *193*(16), 4123-4133.

Tsirigos, K. D., Peters, C., Shu, N., Käll, L., & Elofsson, A. (2015). The TOPCONS web server for consensus prediction of membrane protein topology and signal peptides. *Nucleic Acids Res*, *43*(W1), W401-W407.

Udaka, S. (1960). Screening method for microorganisms accumulating metabolites and its use in the isolation of *Micrococcus glutamicus*. *J Bacteriol*, *79*, 754-755.

Valentini, M., & Filloux, A. (2016). Biofilms and cyclic di-GMP (c-di-GMP) signaling: Lessons from *Pseudomonas aeruginosa* and other bacteria. *J Biol Chem*, *291*(24), 12547-12555.

van Ooyen, J., Emer, D., Bussmann, M., Bott, M., Eikmanns, B. J., & Eggeling, L. (2011). Citrate synthase in *Corynebacterium glutamicum* is encoded by two *gltA* transcripts which are controlled by RamA, RamB, and GlxR. *J Biotechnol*, *154*(2-3), 140-148.

Vogt, M., Haas, S., Klaffl, S., Polen, T., Eggeling, L., van Ooyen, J., & Bott, M. (2014). Pushing product formation to its limit: metabolic engineering of *Corynebacterium glutamicum* for ʟ-leucine overproduction. *Metab Eng*, *22*, 40-52.

Vogt, M., Krumbach, K., Bang, W. G., van Ooyen, J., Noack, S., Klein, B., Bott, M., & Eggeling, L. (2015). The contest for precursors: channelling L-isoleucine synthesis in *Corynebacterium glutamicum* without byproduct formation. *Appl Microbiol Biotechnol*, *99*(2), 791-800.

Vollmer, A. C., & Bark, S. J. (2018). Twenty-five years of investigating the universal stress protein: function, structure, and applications. *Adv Appl Microbiol*, *102*, 1-36.

Waters, L. S., Sandoval, M., & Storz, G. (2011). The *Escherichia coli* MntR miniregulon includes genes encoding a small protein and an efflux pump required for manganese homeostasis. *J Bacteriol*, *193*(21), 5887-5897.

Weber, I. T., & Steitz, T. A. (1987). Structure of a complex of catabolite gene activator protein and cyclic AMP refined at 2.5 Å resolution. *J Mol Biol*, *198*(2), 311-326.

Weiss, A. A., Hewlett, E. L., Myers, G. A., & Falkow, S. (1984). Pertussis toxin and extracytoplasmic adenylate cyclase as virulence factors of *Bordetella pertussis*. *J Infect Dis*, *150*(2), 219-222.

Wendisch, V. F., Jorge, J. M. P., Pérez-García, F., & Sgobba, E. (2016). Updates on industrial production of amino acids using *Corynebacterium glutamicum*. *World J Microbiol Biotechnol*, *32*(6), 105.

Wiedmann, M., Arvik, T. J., Hurley, R. J., & Boor, K. J. (1998). General stress transcription factor SigmaB and its role in acid tolerance and virulence of *Listeria monocytogenes*. *J Bacteriol*, *180*(14), 3650-3656.

Wieschalka, S., Blombach, B., Bott, M., & Eikmanns, B. J. (2013). Bio-based production of organic acids with *Corynebacterium glutamicum*. *Microb Biotechnol*, *6*(2), 87-102.

Williams, S. B., & Stewart, V. (1999). Functional similarities among two-component sensors and methyl-accepting chemotaxis proteins suggest a role for linker region amphipathic helices in transmembrane signal transduction. *Mol Microbiol*, *33*(6), 1093-1102.

Wolf, N., Bussmann, M., Koch-Koerfges, A., Katcharava, N., Schulte, J., Polen, T., Hartl, J., Vorholt, J. A., Baumgart, M., & Bott, M. (2020). Molecular basis of growth inhibition by acetate of an adenylate cyclase-deficient mutant of *Corynebacterium glutamicum*. *Front Microbiol*, *11*(87).

Xu, N., Lv, H., Wei, L., Liang, Y., Ju, J., Liu, J., & Ma, Y. (2019). Impaired oxidative stress and sulfur assimilation contribute to acid tolerance of *Corynebacterium glutamicum*. *Appl Microbiol Biotechnol*, *103*(4), 1877-1891.

You, C., Okano, H., Hui, S., Zhang, Z., Kim, M., Gunderson, C. W., Wang, Y. P., Lenz, P., Yan, D., & Hwa, T. (2013). Coordination of bacterial proteome with metabolism by cyclic AMP signalling. *Nature*, *500*(7462), 301-306.

Zhang, G., Liu, Y., Ruoho, A. E., & Hurley, J. H. (1997). Structure of the adenylyl cyclase catalytic core. *Nature*, *386*(6622), 247-253.

Zhang, X., & Schleif, R. (1998). Catabolite gene activator protein mutations affecting activity of the *araBAD* promoter. *J Bacteriol*, *180*(2), 195-200.

Zheng, D., Constantinidou, C., Hobman, J. L., & Minchin, S. D. (2004). Identification of the CRP regulon using *in vitro* and *in vivo* transcriptional profiling. *Nucleic Acids Res*, *32*(19), 5874-5893.

Zheng, D. Q., Liu, T. Z., Chen, J., Zhang, K., Li, O., Zhu, L., Zhao, Y. H., Wu, X. C., & Wang, P. M. (2013) . Comparative functional genomics to reveal the molecular basis of phenotypic diversities and guide the genetic breeding of industrial yeast strains. *Appl Microbiol Biotechnol*, *97*(5), 2067-2076.

Zheng, Z., Zhu, M., He, Y., Li, N., Guo, T., Chen, Y., Wu, J., Ying, H., & Xie, J. (2013). Gene cloning, expression, and characterization of a cyclic nucleotide phosphodiesterase from *Arthrobacter* sp. CGMCC 3584. *Appl Biochem Biotechnol*, *169*(8), 2442-2456.

Danksagung

Ein besonderer Dank gilt Prof. Dr. Michael Bott für die Überlassung des spannenden Themas, die Ratschläge und die vielen hilfreichen Diskussionen, die den stetigen Fortschritt des Projekts ermöglicht haben.

Prof. Dr. Georg Groth danke ich für die freundliche Übernahme des Zweitgutachtens.

Dr. Meike Baumgart danke ich sehr herzlich für ihre Betreuung und Ihr Interesse am Fortlauf dieser Arbeit. Für die tolle Unterstützung der bioinformatische Analysen für dieses Projekt bedanke ich mich bei Dr. Andrei Filipchyk, Dr. Angela Kranz und Dr. Tino Polen.

Vielen Dank an Dr. Johannes Hartl und Prof. Dr. Julia Vorholt-Zambelli für die cAMP Messungen mittels LC-MS/MS und für die gelungene Zusammenarbeit an dem *cyaB*-Paper.

Mein Dank geht auch an alle Mitarbeitende des IBG-1 Instituts, insbesondere der Infrastruktur, die stets freundlich und hilfsbereit waren.

Der Arbeitsgruppe „Stoffwechselregulation und Metabolic Engineering“ danke ich für die stets sehr gute Arbeitsatmosphäre. Insbesondere meinen ehemaligen Kollegen Andy, Alina, Angela, Alexander, Brita, Cedric, Helga, Johanna, Kai, Karen, Kim, Lea, Lingfeng, Maike, Paul, Susana, und Yannik für ihre tolle Unterstützung im Labor und für die vielen spannenden Gespräche wissenschaftlicher und nicht-wissenschaftlicher Art. Ein besonderer Dank geht dabei an meine Labor- und Bürokollegin Tina. Bei Lukas bedanke ich mich für die Mitarbeit am Projekt in Form seiner Masterarbeit.

Darüber hinaus bedanke ich mich bei meinen Eltern, Geschwistern und Freunden für ihre Unterstützung in der gesamten Studien- und Doktorzeit. Ein besonderer Dank geht an meinen Mann, der mich in allem unterstützt hat.

Erklärung

Ich versichere an Eides Statt, dass die vorgelegte Dissertation von mir selbständig und ohne unzulässige fremde Hilfe unter Beachtung der „Grundsätze zur Sicherung guter wissenschaftlicher Praxis an der Heinrich-Heine-Universität Düsseldorf“ erstellt worden ist. Die Dissertation wurde in der vorgelegten oder in ähnlicher Form noch bei keiner anderen Institution eingereicht. Ich habe bisher keine erfolglosen Promotionsversuche unternommen.

____

Düsseldorf, 15.04.2023

Band / Volume 266
Dissecting iron and heme regulatory networks and adaptation to heme stress in *Corynebacterium glutamicum*
A. Krüger (2023), IV, 274 pp
ISBN: 978-3-95806-686-1

Band / Volume 267
Morphological and functional characterization of layer 5 neurons in rat medial prefrontal cortex, their synaptic microcircuitry and serotonin modulation
R. Rama (2023), 116 pp
ISBN: 978-3-95806-688-5

Band / Volume 268
Magnetic and transport studies of the parent and Fe doped Hexagonal-Mn_3Ge Weyl semimetal
V. Rai (2023), xviii, 156 pp
ISBN: 978-3-95806-695-3

Band / Volume 269
The complex inositol metabolism of *Corynebacterium glutamicum* and its application for the production of rare inositols
P. Ramp (2023), VI, 161 pp
ISBN: 978-3-95806-699-1

Band / Volume 270
Spin- and orbital-dependent band structure of unconventional topological semimetals
K. Hagiwara (2023), v, 115 pp
ISBN: 978-3-95806-701-1

Band / Volume 271
Neutron scattering
Experimental Manuals of the JCNS Laboratory Course held at Forschungszentrum Jülich and at the Heinz-Maier-Leibnitz Zentrum Garching
edited by T. Brückel, S. Förster, K. Friese, M. Kruteva, M. Zobel and R. Zorn (2023), ca 150 pp
ISBN: 978-3-95806-705-9

Band / Volume 272
Ab-initio investigation of the interplay between the hyperfine interaction and complex magnetism at the nanoscale
S. R. S. Shehada (2023), ix, xi, 119 pp
ISBN: 978-3-95806-718-9

Schriften des Forschungszentrums Jülich
Reihe Schlüsseltechnologien / Key Technologies

Band / Volume 273
Analysis of the signal transduction cascade tuning the 2-oxoglutarate dehydrogenase activity in *Corynebacterium glutamicum*
L. Sundermeyer (2023), VI, 119 pp
ISBN: 978-3-95806-722-6

Band / Volume 274
Multicellular defense against phage infection in *Streptomyces* – impact of secondary metabolites and mycelial development
L. Kever (2023), iv, 246 pp
ISBN: 978-3-95806-724-0

Band / Volume 275
Investigation of the electronic band structure of 2D transition metal dichalcogenides via angle-resolved photoemission spectroscopy
B. Parashar (2023), xvii, 156 pp
ISBN: 978-3-95806-725-7

Band / Volume 276
Strain- and process engineering for polyketides production with *Pseudomonas taiwanensis* VLB120 in two-phase cultivations
T. P. Schwanemann (2023), 230 pp
ISBN: 978-3-95806-726-4

Band / Volume 277
Quantitative atomic-level investigation of solid materials through multidimensional electron diffraction measurements
H. L. Lalandec-Robert (2024), xxi, 152 pp
ISBN: 978-3-95806-735-6

Band / Volume 278
Studies on the cAMP-responsive regulatory network of *Corynebacterium glutamicum*
N. Wolf (2024), iii, 122 pp
ISBN: 978-3-95806-736-3

Weitere ***Schriften des Verlags im Forschungszentrum Jülich*** unter
http://wwwzb1.fz-juelich.de/verlagextern1/index.asp

Schlüsseltechnologien / Key Technologies
Band / Volume 278
ISBN 978-3-95806-736-3

Mitglied der Helmholtz-Gemeinschaft

JÜLICH
Forschungszentrum